HISTONE DEMETHYLASE LSD1 RESTRICTS THE SIZE OF THE GERMLINE STEM CELL NICHE IN *DROSOPHILA* OVARIES

APPROVED BY SUPERVISORY COMMITTEE

_____
Michael Buszczak, Ph.D.

_____
Jin Jiang, Ph.D.

_____
Rueyling Lin, Ph.D.

_____
Eric Olson, Ph.D.

To my wonderful family

for their support and encouragement

ACKNOWLEDGEMENTS

I owe my deepest heartfelt gratitude to my mentor, Dr. Michael Buszczak for his encouragement and support throughout my graduate study. Without his guidance and training, I would not have come to this step in my career. Mike's enthusiasm and passion for science was infectious and inspired me every day to continue in science. He challenged me to always do my best and excel in my career.

I am grateful to my thesis committee members: Dr. Jin Jiang, Dr. Rueyling Lin and Dr. Eric Olson. Their advice was absolutely instrumental on the decisions and direction of my graduate research.

I thank the NIH for providing the financial support for three years.

I would like to thank all my lab colleagues who have made my experience in the lab fun and memorable. These five years have gone by fast. I would like to especially thank Nevine Shalaby, for teaching me everything she knew about the confocal, inspiring me to love that microscope and take beautiful pictures. I would like to thank Zhaohui Wang my fellow worker in the niche project without whose help I would not have isolated escort cells.

I cannot thank my family enough: My husband, Job Eliazer for being a constant moral support in my ups and downs, playing my role as a mom to the kids and without whose

help I would not have accomplished my dreams. My children Caleb and Calista for understanding me when I could not spend much time with them, helping me out as much as they could at home and at work, by plugging *Drosophila* food vials and labeling my stocks. My mom, Beulah Samuel for all her prayers, encouragement and good food which has upheld me and kept me going till the end. My dad, Dr. Sam Gnanamanickam, for initially seeding the thought of doing a Ph.D. and being a constant source of inspiration. Daddy, this is for you.

I want to thank my God and Savior Jesus Christ for the wisdom and perseverance that He has bestowed upon me, for blessing the work of my hands and helping me to succeed in everything I put my heart in. He has been true to His promise in Isaiah 41:13 “For I am the Lord, your God, who takes hold of your right hand and says to you, Do not fear; I will help you”.

HISTONE DEMETHYLASE LSD1 RESTRICTS THE SIZE OF THE GERMLINE STEM CELL NICHE IN *DROSOPHILA* OVARIES

by

SUSAN ELIAZER

DISSERTATION

Presented to the Faculty of the Graduate School of Biomedical Sciences

The University of Texas Southwestern Medical Center at Dallas

In Partial Fulfillment of the Requirements

For the Degree of

DOCTOR OF PHILOSOPHY

The University of Texas Southwestern Medical Center at Dallas

Dallas, Texas

August, 2012

HISTONE DEMETHYLASE LSD1 RESTRICTS THE SIZE OF THE GERMLINE STEM CELL NICHE IN *DROSOPHILA* OVARIES

SUSAN ELIAZER, Ph.D.

The University of Texas Southwestern Medical Center at Dallas, August 2012

MICHAEL BUSZCZAK, Ph.D.

Specialized microenvironments called niches keep stem cells in an undifferentiated and self-renewing state by producing a variety of factors. The size and signaling output of niches must be finely tuned to ensure proper tissue homeostasis. I use the *Drosophila* female germline as an excellent model system to study niche development and function. Five to seven somatic cap cells form the ovarian stem cell niche and produce dpp, a BMP homolog necessary for the maintenance of germline stem cells (GSCs). Mutations in *Lsd1,* a histone demethylase exhibit GSC-like tumor formation. Clonal analysis, cell-type specific knock down and rescue experiments demonstrate that

Lsd1 functions within the escort cells that reside immediately adjacent to cap cells (niche). Loss of *Lsd1* causes the escort cells to adopt an intermediate fate expressing both escort cell and cap cell markers and enables them to function as ectopic niches for the expanded stem cell population. Temporally restricted gene knock-down experiments suggest that Lsd1 functions both during development, to specify EC fate, and in adulthood, to prevent ECs from forming ectopic niches independent of changes in cell fate. Lsd1 specifically functions to repress *dpp*, the niche signal in the adult germaria. I have identified *engrailed* as a direct target of Lsd1 by performing Chromatin Immunoprecipitation (ChIP-seq) analysis in the escort cells of the *Drosophila* ovary. Engrailed is expressed in the cap cells of wild type germaria and in *Lsd1* mutants *engrailed* transcripts are misexpressed in the escort cells. Knocking down *engrailed* expression in the escort cells suppresses the *Lsd1* mutant phenotype. Moreover, ectopic expression of *engrailed* in the escort cells displays a GSC-tumor phenotype. Furthermore, I have shown that Engrailed functions upstream of *dpp*, and activates its expression in the cap cell niche.

TABLE OF CONTENTS

PRIOR PUBLICATIONS

Eliazer S, Buszczak M. "Finding a niche: studies from the *Drosophila* ovary" Stem Cell Res Ther. 2011; 2(6):45

Eliazer S., Shalaby NA., Buszczak M. "Loss of lysine-specific demethylase 1 nonautonomously causes stem cell tumors in the *Drosophila* ovary". *PNAS* 2011; 108(17):7064-9

Kroon E., Martinson LA., Kadoya K., Bang AG., Kelly OG., **Eliazer S.**, Young H., Richardson M., Smart NG., Cunningham J., Agulnick AD., D'Amour KA., Carpenter MK., Baetge EE. "Pancreatic endoderm derived from human embryonic stem cells generates glucose-responsive insulin-secreting cells in vivo". *Nature Biotechnology* 2008; 26(4):443-52

D'Amour KA., Bang AG., **Eliazer S.**, Kelly OG., Agulnick AD., Smart NG., Moorman MA., Kroon E., Carpenter MK., Baetge EE. "Production of pancreatic hormone-expressing endocrine cells from human embryonic stem cells". *Nature Biotechnology* 2006; 24(11):1392-401

D'Amour KA., Agulnick AD., **Eliazer S.**, Kelly OG., Kroon E., Baetge EE. "Efficient differentiation of human embryonic stem cells to definitive endoderm". *Nature Biotechnology* 2005; 23(12): 1534-41

Castillero-Trejo Y.*, **Eliazer S.***, Xiang L., Richardson JA., Ilaria RL. "Expression of the EWS/FLI-1 oncogene in murine primary bone-derived cells results in EWS/FLI-1 dependent, ewing sarcoma-like tumors". *Cancer Research* 2005; 65(19): 8698-705

(*co-first authors)

Eliazer S., Spencer J., Ye D., Olson E., Ilaria RL Jr. "Alteration of Mesodermal Cell differentiation by EWS/FLI-1, the Oncogene implicated in Ewing's Sarcoma"**.** *Molecular and Cellular Biology* 2003; 23(2): 482-492

Silvany, RE., **Eliazer S.**, Wolff, NC., and Ilaria, RL Jr. "Interference with the Constitutive Activation of ERK1 and ERK2 Impairs EWS/FLI-1-dependent Transformation". *Oncogene* 2000; 19:4523-4530

Spencer JA., **Eliazer S.**, Ilaria RL Jr., Richardson JA., Olson EN. "Regulation of Microtubule Dynamics and Myogenic Differentiation by MURF, a Striated Muscle RING-Finger Protein". *The Journal of Cell Biology* 2000; 150(4):771-784

LIST OF FIGURES

Chapter 1- Lysine Specific Demethylase 1: Introduction and Thesis Objectives

Chapter 2- Loss of Lysine Specific Demethylase 1 Nonautonomously causes Stem Cell Tumors in the *Drosophila* Ovary

Chapter 3- Lsd1 restricts the Size of the Germline Stem Cell Niche by silencing *Engrailed* in the Escort Cells of the *Drosophila* Ovary

Chapter 4- Screen for Chromatin Factors Functional in the Escort Cells of the *Drosophila* Ovary

LIST OF TABLES

Chapter 4- Screen for Chromatin Factors Functional in the Escort Cells of the *Drosophila* Ovary

LIST OF ABBREVIATIONS

ADP	Adenosine Diphosphate
AOL	Amine Oxidase Like
Arm	Armadillo
ATP	Adenosine Triphosphate
Bab	Bric-a-brac
bam	bag of marbles
BAPs	Brahma Associated Proteins
BMP	Bone Morphogenetic Protein
br	broad
Brat	Brain Tumor
brm	Brahma
Chip-seq	Chromatin Immunoprecipitation and Sequencing
COREST	Co-Repressor for Element-1 Silencing Transcription Factor
Crm	Cramped
Dad	Daughters against dpp
Dally	Division Abnormally Delayed
DBD	DNA Binding Domain
Dinr	Drosophila insulin receptor
DNA	Deoxyribonucleic Acid
Dom	Domino
Dpp	Decapentaplegic
E(z)	Enhancer of Zeste

EC	Escort Cell
ECM	Extra Cellular Matrix
EDTA	Ethylenediaminetetraacetic acid
Egf	Epidermal Growth Factor
Egfr	Epidermal Growth Factor Receptor
en	engrailed
FAD	Flavin Adenine Dinucleotide
Fe	Iron
Gbb	Glass bottom boat
Gh	Growth Hormone
GSC	Germline Stem Cells
HA	hemagglutinin
HDAC	Histone Deacetylase
hh	hedgehog
IGS	Inner Germarial Sheath
ISWI	Imitation SWI
JAK/STAT	Janus Kinase/Signal Transducers and Activator of Transcription
KDM1	Lysine Demethylase 1
Lhb	Luteinizing hormone β
LiCl	Lithium Chloride
LSD1	Lysine Specific Demethylase 1
Mad	Mothers against dpp
NaCl	Sodium Chloride

NLP	Nucleoplasmin
NuRD	Nucleosome Remodeling and Histone Acetylation
NURF	Nucleosome Remodeling Factor
PBS	Phosphate Buffered Saline
Pc	Polycomb
PcG	Polycomb Group proteins
PCR	Polymerase Chain Reaction
pERK	phosphorylated Extracellular signal Regulated Kinase
PGC	Primordial Germ cells
Ph	Polyhomeotic
Ph-p	Polyhomeotic Proximal
piRNA	piwi-interacting RNA
pMAD	phosphorylated Mothers Against Dpp
Pomcl	Pro-opiomelanocortin
PRC1	Polycomb Repressive Complex 1
PRC2	Polycomb Repressive Complex 2 (PRC2)
Psc	Posterior Sex Combs
RNA-Seq	RNA Sequencing
RT	Room Temperature
RT-PCR	Reverse Transcription- Polymerase Chain Reaction
RT-qPCR	Reverse Transcription- Quantitative Polymerase Chain Reaction
Sce	Sex Combs Extra
Shg	Shotgun

Ssrp	Structure Specific Recognition Protein
Stet	Stem cell tumor
Su(z)12	Suppressor of Zeste 12
SWI/SNF	SWItch/Sucrose NonFermentable
SWIRM	Swi3p/Rsc8p/Moira
TGFβ1	Transforming Growth Factor
Tkv	Thickveins
Trl	Trithorax
TrX	Trithorax Group
Tshb	Thyroid stimulating hormone β
ttk	Tramtrack
Vkg	Viking
Yb	female Sterile (1)Yb
αKG	α-Ketoglutarate

CHAPTER 1

LYSINE SPECIFIC DEMETHYLASE 1:

INTRODUCTION AND THESIS OBJECTIVES

CHROMATIN, THE GENETIC MATERIAL OF EUKARYOTES:

The transcription of DNA to RNA is a complex process involving basal and regulatory factors. In eukaryotes, this process of transcription is further complicated by the packaging of DNA into chromatin, a combination of histone proteins and DNA. A basic repeating unit of chromatin is the nucleosome (Kornberg 1974). The nucleosome consists of ~147 base pairs of DNA wrapped around an octamer, made of two molecules each of four core histone proteins, H2A, H2B, H3 and H4 (Kornberg and Thomas 1974; Kornberg 1977; Luger et al. 1997). The nucleosomes are interconnected by linker DNA that varies in length depending on the species and tissue. A fifth histone, H1 is associated with the linker DNA and stabilizes the DNA strands as they begin and end their paths around the octamer. The H1 histones interact with each other and further compacts the nucleosomes into higher order structures. (Bednar et al. 1998; Bustin et al. 2005).

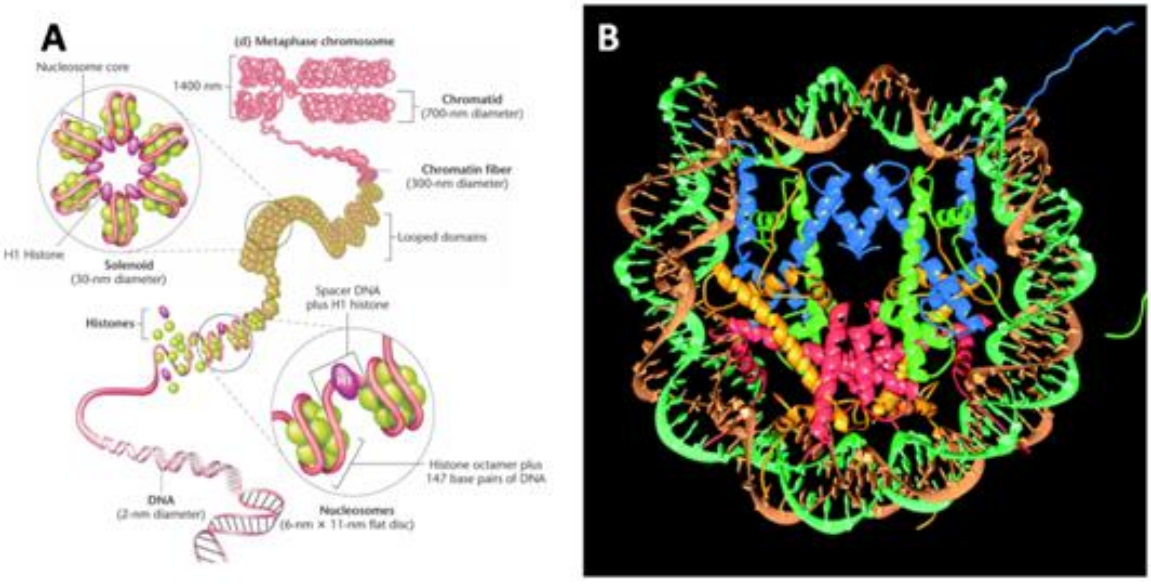

Figure 1. Nucleosome and Higher Order Chromatin Structure. (A) A 2-nm DNA double helix is wrapped around core histone proteins to form a nucleosome that is 11-nm in diameter. Linker histones H1 brings many nucleosomes together into a 30-nm

solenoid. The 30-nm fiber forms series of looped domains that condense into a 300-nm fiber that further coils into the chromatid arms (Adapted from http://bio3400.nicerweb.com). (B) Nucleosome Core Particle. Ribbon traces for the 147-bp of DNA phosphodiester backbone (brown and turquoise) and eight histone protein main chains (blue: H3; green: H4; yellow: H2A; red: H2B) (Adapted from Luger et al., 1997 (Luger et al. 1997))

The tight packaging of the DNA template into nucleosomes is known to impede transcription in vitro (Knezetic and Luse 1986; Lorch et al. 1987) and the deletion of histones or their basic tails have specific effects on gene expression in vivo (Han and Grunstein 1988). However, chromatin structure is very dynamic and continually changes in response to biological stimuli for purposes of transcription, repair, recombination and replication to occur.

In a non-dividing cell, chromatin is present in two functional states: euchromatin or heterochromatin. Within euchromatin, DNA is present in an open conformation and is easily accessible due to the relaxed state of nucleosomal arrangement. Euchromatin comprises of genes in an active and inactive transcriptional state (Koch et al. 2007). Some genes are ubiquitously expressed whereas others are developmentally regulated or stress induced. On the other hand, heterochromatin comprising more than 95% of the genome constitutes an area where the DNA is highly condensed and is inaccessible to transcription factors and chromatin associated proteins (Jenuwein and Allis 2001; Talbert and Henikoff 2006). Heterochromatin consists of non-coding and repetitive sequences and repressed genes associated with morphogenesis or differentiation (Feinberg and Tycko 2004; Reik 2007).

REGULATION OF CHROMATIN STRUCTURE

Chromatin conformation changes can occur globally at large chromatin domains or at the level of single nucleosomes. These changes have been linked to nucleosome remodeling complexes and covalent modifications on histone tails that regulate the transcriptional “on” and “off” states.

Compact chromatin fibers are continuously modified by ATP-dependent large nucleosome remodeling multi-protein complexes (SWI/SNF, ISWI, Mi2/NuRD, NURF families) (Peterson and Tamkun 1995; Tsukiyama and Wu 1995) that weakens the interaction between histones and DNA and repositions the nucleosomes. Pulse chase studies have suggested a high turnover of histones at the sites of active gene transcription (Clayton et al. 2006). Another study showed that histone H2B was rapidly exchanged in and out of the nucleosome relative to histone H3 and H4 (Kimura and Cook 2001).

The core histones H2A, H2B, H3 and H4 are small basic proteins that are highly conserved. Each of the core histones has a structured domain called the ‘histone fold domain’ made up of three α-helices and two loop regions. These histones have an unstructured amino-terminal tail of 25 to 40 amino acid residues that are rich in lysine and arginine residues making the protein highly basic. The residues are sites for post translational modifications such as acetylation, methylation, phosphorylation, sumoylation, ubiquitination and ADP-ribosylation (Peterson and Laniel 2004; Kouzarides 2007; Li et al. 2007; Ruthenburg et al. 2007).

Histone modifications can regulate the structure of the chromatin in various ways. First, these modifications, with the exception of methylation, alter the charge on histone tails, thereby changing DNA accessibility, protein-protein interactions and subsequently affect gene expression (Reinke and Horz 2003). Second, the protein modifications recruit other protein effector molecules that influence the chromatin structure and function (Strahl and Allis 2000; Jenuwein and Allis 2001). Third, the protein modifications can directly influence the higher order chromatin structure. For example, the acetylation of lysine residue on H4 histone tails (H4K16) inhibits the formation of 30nm compact chromatin fibers (Shogren-Knaak et al. 2006).

One of the major players in the regulation of gene activity is the methylation of histones. Histone methylation is the addition of one, two or three methyl groups on lysine and arginine residues of histone tails by enzymes called histone methyltransferases. Depending on the amino acid residue that is modified, methylation leads to gene activation or repression (Jenuwein and Allis 2001; Kouzarides 2002). In most cases, the methylation of H3K4, H3K36 and H3K79 correlates with gene activation, whereas methylation of H3K9, H3K27 and H4K20 leads to gene silencing.

For a long time, histone methylation was considered an irreversible epigenetic event until the first histone demethylase, Lsd1, was discovered in 2004 (Shi et al. 2004). In the subsequent years, additional histone demethylases were identified that were structurally different from Lsd1 and shared a common Jumonji C catalytic domain. Based on the mechanism of the demethylation reaction, the histone demethylases are classified

into two groups: The first group includes Lsd1, which demethylates histone substrates via an amine oxidation reaction using flavin adenine dinucleotide (FAD) as a cofactor. The second group contains histone demethylases containing the Jumonji C catalytic domain that use α-ketoglutarate (αKG) and iron (Fe) as cofactors to hydroxylate the methylated lysine substrates (Tian and Fang 2007).

LYSINE SPECIFIC DEMETHYLASE 1 (LSD1)

The first histone demethylase to be identified was Lysine Specific Demethylase 1 (Lsd1) also known as KDM1. This enzyme catalyzes the demethylation reaction of mono- and di-methylated lysine 4 on histone H3 tails (Shi et al. 2004). Lsd1 is highly conserved in organisms ranging from *Schizosaccharomyces pombe* to humans. Lsd1 has 3 major domains: an N-terminal SWIRM (Swi3p/Rsc8p/Moira) domain, a C-terminal AOL (amine oxidase like) domain and a central protruding tower domain (Chen et al. 2006). The SWIRM domain lies adjacent to the AOL domain and is important for the stability of Lsd1. The C-terminal AOL domain is the catalytic domain that shares high sequence homology to the family of FAD- dependent amine oxidases (Fraaije et al. 1998; Fraaije and Mattevi 2000). The AOL domain is subdivided into an FAD binding domain and a substrate binding domain (Chen et al. 2006). These two sub-domains create a large cavity with a catalytic center at their interface. The central tower domain, protrudes into the AOL domain, forms a helix-turn-helix structure and serves as a platform for binding to Lsd1 partners such as CoREST (Chen et al. 2006).

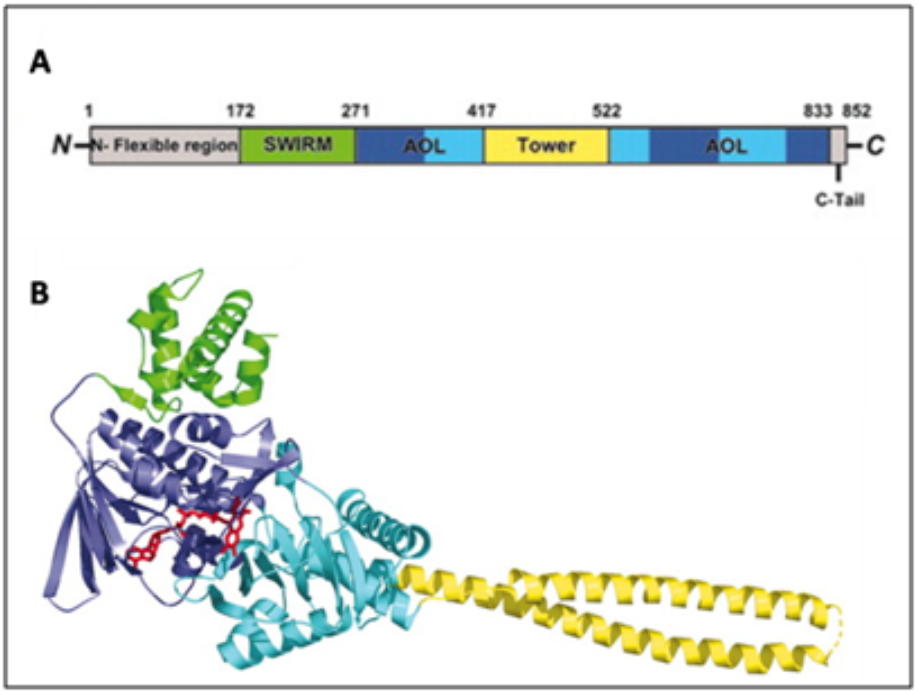

Figure 2. Structure of Lsd1. (A) Diagram of the structure of Lsd1. The SWIRM domain is shown in green, the AOL domain in blue (the FAD-binding subdomain) and cyan (the substrate-binding subdomain), and the Tower domain in yellow. The N-terminal flexible region and the C-terminal tail are colored in gray. (B) Ribbon diagram of the LSD1 structure. The molecule is colored as in A. FAD is in ball-and-stick representation and is colored in red. (Adapted from Chen Y., et al. (Chen et al. 2006))

Lsd1 acts on mono- and di- methylated lysine residue 4 by catalyzing the oxidation of these amine-containing substrates utilizing molecular oxygen as electron acceptor. The amine oxidation reaction is characterized by oxidative cleavage of the α-carbon bond of the amino group of the methylated lysine substrate to form an imine intermediate, which is the hydrolyzed to form an aldehyde and an amine via a non enzymatic process. The co-factor FAD is reduced to FADH2 and then is re-oxidized by oxygen to produce hydrogen peroxide (Binda et al. 2002). The enzymatic process of Lsd1 mediated demethylation requires the presence of a protonated methyl ε- ammonium group and therefore is unable to catalyze the demethylation of trimethylated lysine residues (Stavropoulos et al. 2006).

Lsd1 functions as a transcriptional repressor. *In vitro* luciferase reporter assays have shown that Hela cells transfected with human Lsd1 fused to the Gal4 DNA Binding Domain (DBD) can repress the luciferase reporter containing Gal4 binding sites. This repression is mediated by the amine oxidase domain as Lsd1 constructs lacking a large portion of the amine oxidase domain cannot repress the luciferase reporter (Shi et al. 2004). Lsd1 is found in a number of co-repressor complexes such as Nucleosome Remodeling and Histone Acetylation (NuRD), Co-Repressor for Element-1 Silencing Transcription factor (Co-REST) and a subset of Histone Deacetylase (HDAC) complexes (Tong et al. 1998; Humphrey et al. 2001; You et al. 2001; Hakimi et al. 2002; Shi et al. 2003). The C.elegans homolog of Lsd1, spr-5, functions as a transcriptional repressor by silencing the presenilin gene hop1 at early developmental stages (Eimer et al. 2002).

Lsd1, in some instances has also been shown to function as a transcriptional activator. In human prostrate, the androgen receptor changes the specificity of Lsd1 from lysine 4 to mono- and di-methyl groups on lysine 9, therefore functioning as a transcriptional activator rather than a repressor (Metzger et al. 2005; Wissmann et al. 2007). During pituitary organogenesis, Lsd1 functions both as a gene repressor and a gene activator of specific target genes at different developmental stages of development (Wang et al. 2007). The function of Lsd1 depends on its associated complex (Shi et al. 2005). However, it is not clearly understood how the interacting proteins change the specificity of Lsd1 from being a gene silencer to a gene activator.

Lsd1 is essential for mammalian development. Homozygous null Lsd1 mice generated by deleting a portion of the amine oxidase domain were lethal and no viable embryos were detected after E7.5 (Wang et al. 2007). Conditional deletion of Lsd1 during pituitary development resulted in reduced expression of pituitary hormones such as growth hormone (Gh), thyroid stimulating hormone β (Tshb), Luteinizing hormone β (Lhb) and pro-opiomelanocortin (Pomc1) (Wang et al. 2007) indicating that Lsd1 regulates specific developmental programs. Null mutants of *Drosophila Lsd1* generated by deleting a portion of the promoter region and SWIRM domain are sterile and display tissue specific defects (Di Stefano et al. 2007).

Dysfunction of Lsd1 plays a pathological role in diseases such as cancer. Lsd1 expression is highly upregulated in a number of cancers such as bladder carcinomas, lung cancer and ER negative breast cancer and is currently being used as a biomarker for the prediction of aggressive tumors (Lim et al. 2010; Hayami et al. 2011).

Lsd1 plays a functional role in uncontrolled cancer cell proliferation and metastasis. In human embryonic stem cells, Lsd1 plays a role in maintaining pluripotency by silencing the expression of several differentiation genes (Adamo et al. 2011). In this thesis, I present my investigations on the role of *Drosophila* Lsd1 in stem cells and their associated niches.

STEM CELLS AND THEIR NICHE

Stem cells are essential for tissue homeostasis, particularly in organs that exhibit high rates of cellular turnover such as the skin, intestine and hematopoietic system. Without the self-renewing capacity of stem cells, these tissues quickly cease to function properly, leading to various conditions including infertility, anemia and immunodeficiency. Overproliferation of stem cells is equally undesirable and can disrupt normal tissue homeostasis, possibly contributing to tumor formation and growth. Interestingly, cells within tumors often exhibit a hierarchy of malignant potential, giving rise to the notion that small populations of cancer stem cells may be responsible for propagating certain cancers (Bonnet and Dick 1997; O'Brien et al. 2010). Prospectively identifying these cells and determining how they differ from their normal stem cell counterparts will probably provide important insights into the origin and progression of malignancy.

Specialized microenvironments called niches help maintain stem cells in an undifferentiated and self-renewing state. The concept of the cellular niche represents one of the central paradigms in stem cell biology. First proposed by Schofield in 1978 (Schofield 1978), the niche hypothesis posits that specific locations or microenvironments within tissues prevent the maturation of resident stem cells. The niche model is consistent with many observations made in mammalian cell transplantation experiments, but difficulties in unequivocally identifying individual stem cells within their native environment prevented further testing of this hypothesis. Twenty years

following Schofield's seminal publication, Xie and Spradling provided compelling experimental evidence that a cellular niche supports the maintenance of germline stem cells (GSCs) in the *Drosophila* adult ovary (Xie and Spradling 2000). Shortly thereafter, similar findings were reported in the *Drosophila* testis (Kiger et al. 2001; Tulina and Matunis 2001).

In my thesis, I use the *Drosophila* ovary as a model system to study the function of histone demethylase, Lsd1, in stem cell biology. Stem cell and their daughters can be identified at single-cell resolution based on their location and through the use of morphological and molecular markers. The ability to distinguish individual cells within their native environment, coupled with the ability to genetically manipulate these cells, makes the *Drosophila* germarium a powerful platform with which to dissect the molecular mechanisms governing stem cell maintenance.

Organization of the adult *Drosophila* ovary

Drosophila females have two ovaries typically comprised of 16 to 21 tube-like structures called ovarioles. Each ovariole contains six to eight sequentially developing egg chambers, each of which is initially assembled in a structure at the tip of the ovariole called the germarium.

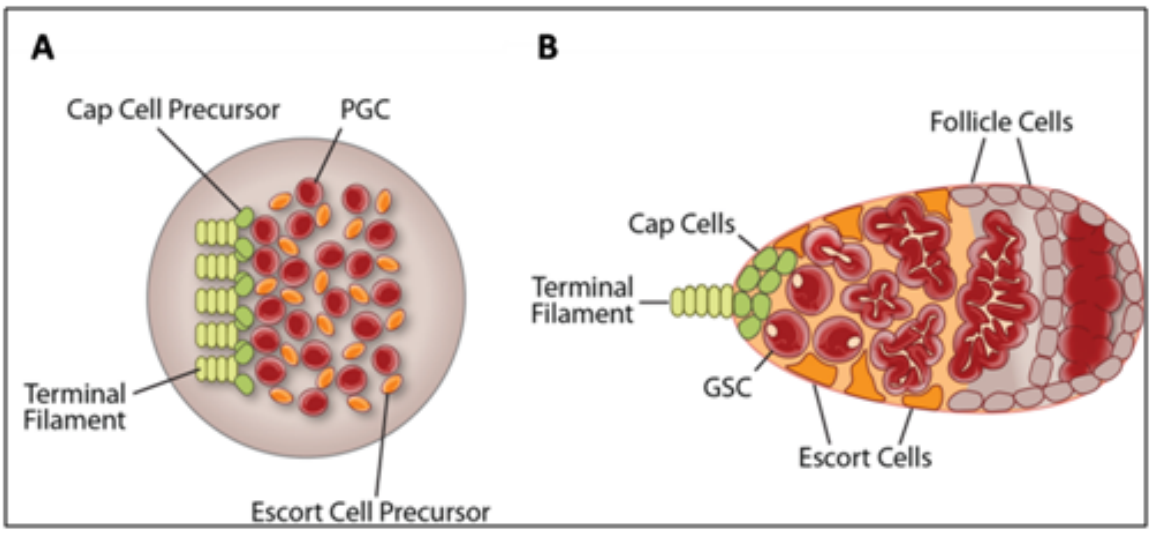

Figure 3. Organization of the developing female gonad and the adult germarium. (A) By the end of larval development, approximately 100 primordial germ cells (PGCs) (red) populate the gonad and associate with cap cell precursor (dark green) and escort cell precursor cells (orange). Terminal filament stacks (light green) begin to form and signal to adjacent somatic cells through the Delta–Notch pathway, inducing them to become cap cells. (B) The differentiation of adult germline cells (red) can be traced based on morphological changes in the fusome (beige), an endoplasmic reticulum-like organelle that appears round in the germline stem cells (GSCs) and becomes increasingly more branched as germline cysts develop. Adult GSCs reside in a niche formed by the terminal filament (light green) and cap cells (dark green). Escort cells (orange) help to guide developing cysts as they pass through the germarium. Eventually a single layer of follicle cells (grey) surrounds the germline cysts and these enveloped cysts bud off the germarium to form an egg chamber.

Two to three GSCs reside at the anterior tip of the germarium immediately adjacent to the niche, which includes a small cluster of five to seven cap cells attached to eight to ten terminal filament cells. GSCs typically undergo asymmetric self-renewing divisions, producing one daughter stem cell that remains associated with the cap cell niche and a second daughter that is displaced away from the niche and as a result differentiates. This newly formed cystoblast undergoes four incomplete mitotic divisions to form an interconnected 16-cell cyst. Escort cells, also called inner sheath cells or inner

germarium sheath cells, line the anterior region of the germarium and send extensions between germline cysts during the earliest stages of their differentiation. Recent live imaging experiments show that these escort cells help maturing germline cysts move posteriorly through the germarium (Morris and Spradling 2011). Eventually progeny of two follicle stem cells envelop the 16-cell germline cyst, and together this cluster of cells buds off from the germarium to form an egg chamber.

REVIEW OF THE FEMALE GERMLINE STEM CELL NICHE

Bone morphogenetic protein signaling in the adult germline stem cell niche

Significant progress has been made in defining the signaling events that promote GSC self-renewal (Figure 4). One of the principle ligands required for GSC maintenance is Decapentaplegic (Dpp), a member of the bone morphogenetic protein (BMP) superfamily of signaling molecules (Xie and Spradling 1998). Glass bottom boat (Gbb), a BMP5/6/7/8 homolog (Wharton et al. 1991), also functions to support GSC maintenance (Song et al. 2004). Disruption of either *dpp* or *gbb* results in GSC loss, while overexpression of *dpp*, but not *gbb*, causes a GSC tumor phenotype. BMP ligand produced by the cap cells at the anterior tip of the germarium transduces its effects through the type I receptors Thickveins and Saxophone and the type II receptor Punt.

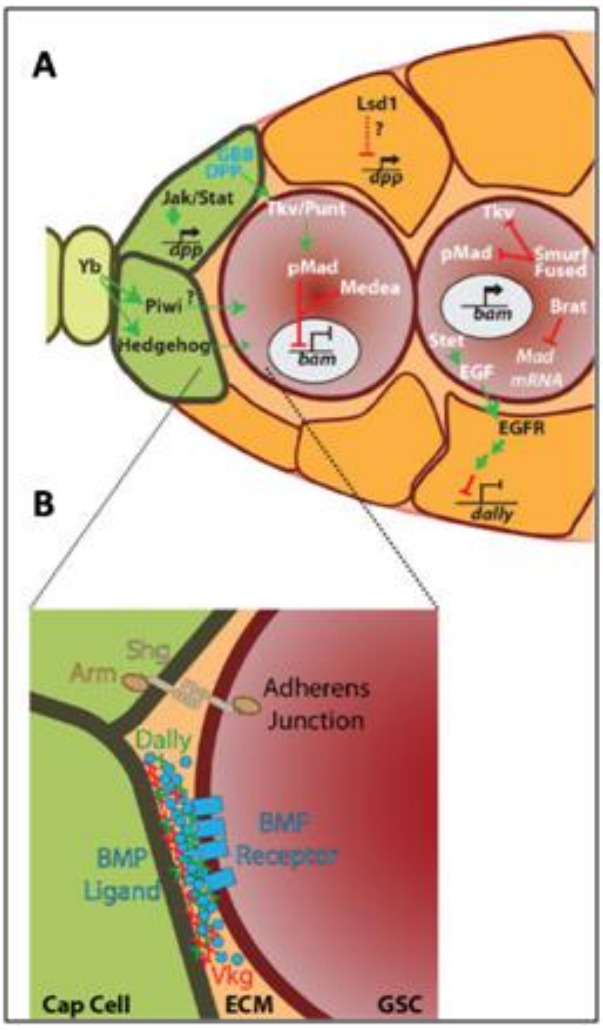

Figure 4. Signaling within the female germline stem cell niche. (A) Schematic illustrating that Decapentaplegic (Dpp) and Glass bottom boat (Gbb) produced in the anterior of the germarium binds to heterodimeric receptors on the surface of germline stem cells (GSCs). Activation of the receptor results in phosphorylation of Mad (pMad) which then partners with Medea and translocates into the nucleus, where it directly represses the transcription of *bag of marbles* (*bam*). This repression is relieved once a GSC daughter leaves the cap cell niche. Smurf, Fused, Brain tumor (Brat) and miR-184 all act to rapidly reduce bone morphogenetic protein (BMP) responsiveness within the cystoblast. Niche signaling is limited to the anterior of the germarium by Lsd1, which represses *dpp* expression outside the normal niche and by epidermal growth factor (Egf) signaling from the germline, which serves to limit *dally* expression in the escort cells. EGFR, epidermal growth factor receptor; JAK/STAT, Janus kinase/signal transducer and activator of transcription; pMad, phosphorylated Mothers Against Dpp; Tkv, Thickveins; YB, Female sterile (1) Yb. (B) Components of the extracellular matrix (ECM), including Viking (Vkg; red) and Division abnormally delayed (Dally; green) help to stabilize and limit BMP ligands (blue circles) within the anterior of the germarium. The adherens junction proteins Armadillo (Arm; brown) and Shotgun (Shg; grey) promote cell–cell adhesion between the cap cells (green) and GSCs (dark red).

Genetic mosaic experiments show that these receptors function autonomously in GSCs and are necessary for their maintenance (Xie and Spradling 1998). Activation of the receptor complex results in phosphorylation of Mothers Against Dpp (Mad), which then binds to its partner Medea (Hudson et al. 1998) and translocates into the nucleus.

Phosphorylated Mad and Medea associate with a specific silencer element in the promoter of the *bag of marbles* (*bam*) gene and repress its transcription (Chen and McKearin 2003a; Chen and McKearin 2003b; Song et al. 2004). Bam expression is both necessary and sufficient for germline differentiation (McKearin and Spradling 1990; McKearin and Ohlstein 1995; Ohlstein and McKearin 1997). Loss of *bam* results in germline tumors that contain undifferentiated cells that exist in a pre-cystoblast state, whereas misexpression of *bam* in GSCs results in their precocious differentiation. BMP pathway activation also results in high levels of *Daughters against dpp* (*Dad*) expression in GSCs (Kai and Spradling 2003; Casanueva and Ferguson 2004; Song et al. 2004). In GSC daughters displaced away from the cap cells, Dad expression decreases whereas *bam* transcription increases. Remarkably, this switch in *Dad* and *bam* expression occurs at one cell diameter away from the cap cells. Several studies have begun to describe some of the intrinsic mechanisms to ensure a very rapid downregulation of Dpp responsiveness in germline cells once they leave the niche (Podos et al. 2001; Casanueva and Ferguson 2004; Iovino et al. 2009; Xia et al. 2010; Harris et al. 2011).

Building upon the understanding of how the Dpp–Thickveins–phosphorylated Mad–Bam pathway controls GSC maintenance, the field is beginning to delve more deeply into how the ovarian niche first forms, how Dpp signaling from the niche is modulated and how the niche responds to environmental cues. Addressing these fundamental questions will provide a framework with which to better understand niches across species.

Formation of the ovarian niche

GSCs arise from primordial germ cells (PGCs) that first form at the posterior pole of the embryo. Through a series of migratory events, these PGCs make their way towards the gonadal mesoderm and eventually coalesce with a subpopulation of surrounding somatic cells to form the embryonic gonad (Starz-Gaiano and Lehmann 2001). Initially, about seven to 13 PGCs are incorporated into each gonad. This number expands to approximately 100 by the end of larval development. Cell–cell communication involving the epidermal growth factor (EGF) pathway helps to coordinate the expansion of the germline with the surrounding gonadal mesoderm (Gilboa and Lehmann 2006). Transformation of the primitive gonad into an adult ovary begins during late larval development, starting with the formation of terminal filaments (King et al. 1968) (Figure 1). These structures are composed of eight to 10 disc-shaped cells that demarcate individual ovarioles in the developing ovary. They arise from small clusters of cells that organize themselves into stacks. The actin-depolymerizing factor Cofilin/ADF, encoded by the *twinstar* gene, regulates the actin cytoskeletal rearrangements that drive the intercalation of presumptive terminal filament cells (Chen et al. 2001). Terminal filament formation occurs progressively, in a medial to lateral direction across the gonad (Sahut-Barnola et al. 1995). The steroid hormone ecdysone or its metabolites probably govern the timing of these morphogenic events, as mutations in the *ecdysone receptor* or its binding partner *ultraspiracle* result in heterochronic defects and malformation of these structures (Hodin and Riddiford 1998). While the mechanisms that designate specific somatic cell fates across the larval gonad remain unclear, enhancer trap screens revealed a small number of genes that exhibit high levels of expression in the developing terminal

filament (Sahut-Barnola et al. 1995). One of these genes, *bric-a-brac* (*bab*), encodes a BTB/POZ domain transcription factor (Godt and Laski 1995; Sahut-Barnola et al. 1995). The expression of *bab* is first observed in the female gonad during late larval development and continues to mark terminal filament cells through adulthood. Disruption of *bab* results in terminal filament defects accompanied by severe morphological defects in the adult ovary, revealing that the overall organization of the adult ovary depends on proper terminal filament formation. A second transcription factor Engrailed also marks terminal filaments and is necessary for their development (Bolivar et al. 2006). Identifying the transcriptional targets of Bab and Engrailed within the developing gonad remains important work for the future. Cap cells, which help form the functional GSC niche in the adult ovary, are specified as the terminal filament formation nears completion. Cap cells can be distinguished based on a number of morphological and molecular markers. They form immediately adjacent to the posterior tips of the terminal filaments and express *bab*, *engrailed*, *hedgehog* and high levels of Lamin C (Sahut-Barnola et al. 1995; Forbes et al. 1996a; Forbes et al. 1996b; Xie and Spradling 2000), but are not incorporated into the growing terminal filament stack. Several studies have shown that the Notch pathway helps to promote cap cell formation (Ward et al. 2006b; Song et al. 2007). Xie and colleagues showed that terminal filament cells express the Notch ligand Delta shortly after they begin to organize (Song et al. 2007). Delta activates Notch in adjacent somatic cells, inducing them to become cap cells. Overexpression of Delta or an activated form of Notch results in an accumulation of ectopic cap cells in the adult ovary. These extra cap cells are associated with ectopic GSCs, indicating that they act as functional niches. Heterozygous Notch mutant germaria carry a decreased number

of cap cells, suggesting that Notch signaling is both necessary and sufficient for cap cell formation in the developing gonad. The expression of the *E(spl)m7-LacZ* Notch target reporter suggests that Notch signaling remains active in adult cap cells. Indeed, disruption of Notch specifically in adults leads to a decrease of cap cells within adult germaria over time and a subsequent reduction in the number of GSCs (Song et al. 2007). Overexpression of activated Notch in adult escort cells does not convert them into cap cells or result in ectopic niche formation, indicating that escort cell identity becomes set during pupal development. The basis for the stabilization of this cell fate remains uncharacterized.

Stem cell capture by the niche

Of the approximately 100 PGCs that populate each larval gonad, only a subset become GSCs while the rest differentiate to form germline cysts. The hallmarks of GSC selection become evident during the larval to pupal transition and involve a number of mechanisms. While germline cells of the larval gonad do not express *bam*, they differentiate in response to ectopic *bam* expression (Zhu and Xie 2003; Gilboa and Lehmann 2004). Moreover, all PGCs exhibit phosphorylated Mad expression prior to terminal filament formation, suggesting that BMP signaling blocks *bam* expression in larval gonads as it does in adults (Zhu and Xie 2003; Gilboa and Lehmann 2004). Upon terminal filament formation, PGCs begin to exhibit spatially restricted changes in gene expression. In the posterior of the gonad, away from the terminal filaments, germline cells begin to express *bam* and show morphological signs of cyst development, while germline cells immediately adjacent to the terminal filament and newly established cap

cells remain undifferentiated and express markers of Dpp signal responsiveness (Zhu and Xie 2003). These cells, which probably give rise to adult GSCs, can undergo clonal expansion, giving rise to daughter GSCs that inhabit the same adult germarium. These findings suggest a simple model wherein PGCs immediately adjacent to cap cells receive BMP signals, continue to repress *bam* transcription and thus become incorporated into the maturing cap cell niche. Additional enhancer trap and cell transplantation experiments suggest there may be a bias in which PGCs associate with the nascent niche and ultimately become GSCs (Asaoka and Lin 2004). This mechanism appears flexible, however, as the same PGC can give rise to cells located both inside and outside the niche during its initial formation. How Dpp production and responsiveness become restricted during the transition from the larval/pupal gonad to the adult ovary and how PGCs home in on the newly formed niches remain unclear.

Modulation of adult niche signaling by the extracellular matrix

Recent work has begun to characterize how the extracellular matrix modulates BMP signaling in the adult ovarian niche. For example, type IV collagen – encoded by the *viking* gene – regulates the distribution of Dpp and helps foster interactions between BMP ligands and their receptors in the embryo (Wang et al. 2008b). Disruption of *viking* results in a modest GSC expansion phenotype, suggesting that this extracellular matrix component restricts the spread of Dpp, thereby creating a very localized source of ligand at the anterior tip of the germarium (Figure 4). The *division abnormally delayed* (*dally*) gene, a member of the glypican family of integral membrane heparin sulphate proteoglycans (Nakato et al. 1995), also plays a critical role in regulating the distribution

and stability of Dpp within the ovarian GSC niche. Dally, like other heparin sulphate proteoglycans, is a component of the extracellular matrix and covalently attaches to the plasma membrane by glycosylphosphatidylinositol linkage (Nakato et al. 1995). Heparin sulphate proteoglycans act as co-receptors for a variety of secreted proteins such as Wnts, Fibroblast Growth Factors, Transforming Growth Factor beta and Hedgehog (Kirkpatrick and Selleck 2007). In *Drosophila*, Dally promotes the stability and transport of Dpp (Akiyama et al. 2008). Dally is expressed in the cap cells, and *dally* mutants display a GSC loss phenotype accompanied by reduced Dpp signaling and premature expression of Bam within the germline (Guo and Wang 2009; Hayashi et al. 2009). In contrast, *dally* overexpression in somatic cells outside the niche results in an expansion of GSC-like cells (Guo and Wang 2009; Hayashi et al. 2009; Liu et al. 2010). While these findings show that the extracellular matrix modulates Dpp signaling within germaria, further work will be needed to elucidate the mechanisms that coordinate the deposition of extracellular matrix components within the niche and control their functions.

Pathways that regulate niche signaling

Several additional molecules function in the niche, either through or in parallel to Dpp signaling. The genes *female sterile (1) Yb* (*Yb*), *hedgehog* and *piwi* are expressed in somatic cells at the anterior tip of the germarium (Forbes et al. 1996a; Cox et al. 1998; King and Lin 1999; Cox et al. 2000; King et al. 2001). Loss of *Yb*, a large hydrophilic protein with limited homology to RNA helicases, disrupts the maintenance of both GSCs and follicle stem cells within the germarium (King and Lin 1999; King et al. 2001). Mutations in *piwi*, which encodes the founding member of a highly conserved family of

proteins that function in various small RNA pathways, also cause a significant GSC loss phenotype. Over expression of *piwi* within somatic cells of the germarium results in an expanded number of GSCs (Cox et al. 1998; Cox et al. 2000).

Hedgehog-mediated signaling primarily regulates follicle stem cells, but *hedgehog* mutants also exhibit a mild GSC loss phenotype (Forbes et al. 1996a; Forbes et al. 1996b; King et al. 2001). *Yb* mutants exhibit reduced *hedgehog* and *piwi* expression in terminal filament and cap cells (King et al. 2001). Further genetic evidence suggests that *Yb* regulates, through *piwi*-dependent and *hedgehog* dependent mechanisms, parallel pathways that control GSC and follicle stem cell maintenance, respectively. *piwi* appears to regulate GSCs in a *dpp*-independent manner (King et al. 2001), suggesting that additional unidentified GSC maintenance signals emanate from the cap cells.

Recent work shows that components of the Janus kinase/signal transducer and activator of transcription (Jak/Stat) pathway promote Dpp production by cap cells (Decotto and Spradling 2005; Lopez-Onieva et al. 2008; Wang et al. 2008a). Overexpression of the Jak/Stat ligands *unpaired* and *unpaired-2* in somatic cells results in GSC tumor formation, while mutations in pathway components cause a GSC loss phenotype (Decotto and Spradling 2005; Lopez-Onieva et al. 2008; Wang et al. 2008a). Stat reporters show activation of the pathway in somatic cells at the anterior tip of the germarium, and clonal analysis reveals that pathway activation in cap cells is critical for GSC maintenance. Disruption of the Jak/Stat pathway does not affect terminal filament or cap cell formation and, unlike the Notch pathway, overactivation of the Jak/Stat

pathway during development does not result in ectopic cap cells. Transcript analysis shows that the Jak/Stat pathway positively regulates *dpp* mRNA levels, providing a simple model for how this pathway promotes GSC self-renewal (Lopez-Onieva et al. 2008; Wang et al. 2008a). Several lines of evidence indicate that the germline itself can signal back to the surrounding somatic cells to regulate their signaling output. As described above, the EGF pathway functions to regulate PGC and somatic cell numbers in the developing gonad (Gilboa and Lehmann 2006). This pathway also functions in adult germaria. Disruption of the *stem cell tumor* gene results in the cell-autonomous failure of germline differentiation in both male and females (Schulz et al. 2002). Stem cell tumor protein shares sequence similarity with Rhomboid and proteins within this class act to cleave transmembrane EGF proteins in the Golgi, thereby creating a diffusible ligand. EGF ligands produced by germline cells in turn activate the EGF receptor–RAS–RAF–MEK–mitogen-activated protein kinase pathway in the surrounding somatic cells of the germarium. This activation of the EGF pathway limits the number of GSCs in germaria by repressing *dally* expression in escort cells (Liu et al. 2010). In contrast, disruption of EGF signaling causes an increase of *dally* expression outside the normal niche, presumably resulting in a broader distribution of stable Dpp (Liu et al. 2010). In effect, this feedback loop ensures that differentiating germline cysts experience lower levels of BMP signaling.

Cell adhesion and cell competition in the adult niche

Drosophila E-cadherin promotes stem cell maintenance by anchoring the GSCs to the cap cells (Song and Xie 2002). Encoded by the *shotgun* (*shg*) gene, E-cadherin is

highly enriched at the adherens junctions between the cap cells and GSCs. Armadillo, a β-catenin homolog, also localizes to these sites. The *shotgun* and *armadillo* mutant GSCs quickly leave the anterior of the germarium (Song and Xie 2002). The findings that *shotgun* and *armadillo* mutant PGCs within the developing gonad exhibit reduced interactions with newly formed cap cells (Song and Xie 2002) and the observation that E-cadherin contributes to the age-dependent decline of adult GSCs (Pan et al. 2007) highlight the importance of cell adhesion in promoting interactions between stem cells and their niches throughout life. Several studies have shown that individual GSCs compete for space within niches (Jin et al. 2008; Rhiner et al. 2009). Whether a particular stem cell is more or less competitive often depends on expression levels of E-cadherin (Jin et al. 2008). GSCs with relatively high levels of E-cadherin exhibit more competitiveness than neighboring cells and tend to have larger areas of contact with the cap cells. Bam, and its binding partner Benign gonial cell neoplasm (Ohlstein et al. 2000), negatively regulate E-cadherin. The *bam* and *benign gonial cell neoplasm* mutant GSC clones express high levels of E-cadherin and outcompete the neighboring wild-type GSCs for the niche (Jin et al. 2008). These results suggest that an important part of the GSC differentiation program may involve the rapid downregulation of genes involved in fostering cell–cell contacts between these stem cells and adjacent niche cells.

Insulin signaling influences the niche

Systemic factors that vary in response to diet and age play an important role in modulating niche output and stem cell responsiveness to niche signals. For example, insulin signaling contributes to the maintenance of the niche in adult ovaries. Activation

of the insulin pathway through inhibition of FOXO by phosphatidylinositol 3-kinase activates Notch signaling in the cap cells (Hsu and Drummond-Barbosa 2011). *Drosophila insulin receptor* (*dinr*) mutants have a time-dependent cap cell loss phenotype, leading to a reduction of GSCs over time (Hsu and Drummond-Barbosa 2009). *dinr* mutants exhibit severely reduced Notch signaling, and expressing an activated form of Notch rescues the *dinr* mutant cap cell and GSC loss phenotypes. Moreover, insulin signaling influences E-cadherin levels at the junction between cap cells and GSCs as *dinr* mutant cap cells display decreased levels of E-cadherin, independent of Notch signaling. Steroid hormones also contribute to the formation and regulation of GSC maintenance (Ables and Drummond-Barbosa 2010; Konig et al. 2011), suggesting that multiple systemic inputs impinge upon the niche during development and in adulthood.

Programming inside and outside the niche

Several studies have begun to reveal how epigenetic programming regulates the function and identity of somatic cells within the niche. For example, mutations in the gene encoding the chromatin-associated protein Corto suppress the GSC loss phenotype exhibited by *piwi* mutants (Smulders-Srinivasan et al. 2010). Disruption of *corto* also restores *hedgehog* expression in *Yb* mutant germaria. Corto protein interacts with both Polycomb and trithorax group proteins, suggesting that these chromatin-associated proteins may influence *Yb*, p*iwi* and *hedgehog*-mediated regulation of the niche. Piwi and small piwi-interacting RNAs (piRNAs) play an essential role in programming chromatin within the germarium and in defending the germline against unwanted transposable

element activity (Yin and Lin 2007; Brennecke et al. 2008; Lin and Yin 2008; Rangan et al. 2011).

THESIS OBJECTIVES

Loss of *Lsd1* in *Drosophila* results in small ovaries and an increased number of stem cells in the germarium. In this thesis, I characterized the germline phenotype of *Lsd1* mutants and found that Lsd1 functions in the escort cells of the germarium to silence *dpp*, the niche signal. Loss of *Lsd1* causes the escort cells to misexpress cap cell markers and possibly function as niches for the expanded stem cell population. Lsd1 is required both during development and in adults to silence niche signaling (described in Chapter 2: Loss of *Lysine Specific Demethylase 1* Nonautonomously causes Stem Cell Tumors in the *Drosophila* Ovary). I identified the direct targets of Lsd1 in escort cells by Chromatin Immunoprecipitation- sequencing (ChIP-seq) and determined the mechanism by which the niche signals are silenced (described in Chapter 3: Lsd1 Restricts the Size of the Germline Stem Cell Niche by silencing *engrailed* in the Escort Cells of the *Drosophila* Ovary). I performed a small-scale screen for identifying additional chromatin factors that play a functional role in the surrounding escort cells to limit niche signaling (Chapter 4: Screen for Chromatin Factors Functional in the Escort Cells of the *Drosophila* Ovary).

CHAPTER 2

LOSS OF LYSINE SPECIFIC DEMETHYLASE 1 NONAUTONOMOUSLY CAUSES STEM CELL TUMORS IN THE *DROSOPHILA* OVARY

INTRODUCTION

Many adult tissues such as the skin, intestine, and hematopoietic system experience constant cell turnover. The homeostasis and function of these organs depend on the self-renewing capacity of stem cells. Adult stem cells are often maintained in specialized microenvironments called niches (Ohlstein et al. 2004). The correct balance between stem cell self-renewal and stem cell daughter differentiation depends on the exquisite regulation of niche size and signaling output.

The germline stem cells (GSCs) of the *Drosophila* ovary have provided many insights into the functional relationships that exist between stem cells and their niches (Kirilly and Xie 2007). Ovaries are composed of tube-like structures known as ovarioles. Two to three GSCs reside at the tip of each ovariole in a structure called the germarium. Within each germarium, five to seven somatic cap cells form the functional GSC niche. These cells produce Decapentaplegic (Dpp), a bone morphogenetic protein-like molecule, which initiates a signal transduction cascade within GSCs that serves to repress the transcription of the differentiation factor *bag of marbles* (*bam*) (Xie and Spradling 1998; Xie and Spradling 2000; Chen and McKearin 2003a). Escort cells (ECs), also known as inner germarial sheath cells, lie adjacent to the cap cells and line the anterior region of germaria (Decotto and Spradling 2005). These cells do not normally express niche signals and are thought to support the early differentiation of germline cysts (Decotto and Spradling 2005). Ectopically expressing *dpp* throughout somatic cells blocks germline differentiation, resulting in the formation of GSC tumors (Xie and Spradling 1998).

Therefore, limiting the number of cells that produce dpp appears essential for the normal functional output of the ovary.

Recent work has shown that ectopic expression of activated Notch within somatic cells results in a marked increase in the number of cap cells (Ward et al. 2006a; Song et al. 2007). The increased number of cap cells subsequently leads to an expansion of the GSC population. Delta expressed by terminal filament cells of the developing gonad activates Notch in the adjacent somatic cells but not in the remaining somatic cells interspersed among the germ cells (Song et al. 2007). Activation of Notch within adult ECs does not cause these cells to adopt a cap cell fate, whereas overexpression of *dpp* alone in adult ECs in the absence of expanded Notch signaling supports GSC maintenance (Song et al. 2007). Thus, Notch controls cell fate decisions within the developing gonad.

Two additional pathways regulate *dpp* expression within adult ovaries. Disruption of the Janus kinase/Signal transducer and activator of transcription (Jak/Stat) pathway results in a GSC loss phenotype, whereas activation of the pathway within ECs leads to germline tumor formation marked by expanded Dpp responsiveness within germ cells (Lopez-Onieva et al. 2008; Wang et al. 2008a). The epidermal growth factor (EGF) pathway also acts to regulate the signaling output of the niche. Stet, an EGF-processing molecule, acts in germline cysts to promote the production of EGF receptor (EGFR) ligands, including Spitz, Keren, and Gurken (Liu et al. 2010). These molecules activate the RAS-RAF-MEK-MAPK pathway within surrounding somatic cells, which, in turn,

represses the transcription of *dally*, a factor that regulates Dpp transport and stability (Guo and Wang 2009; Hayashi et al. 2009). By repressing dally expression, the EGF pathway serves to restrict Dpp signaling to the most anterior region of the germarium (Liu et al. 2010). This pathway also plays a central role in a feedback loop that coordinates somatic cell survival and germ cell proliferation during development (Gilboa and Lehmann 2006).

Alterations within local chromatin environments likely underlie the coordinated specification of cell fate programs within the developing gonad and may help to regulate the homeostatic function of ovarian cells in adulthood. Here, I show that absence of lysine-specific demethylase 1 [Lsd1/Su(var)3-3/CG17149] results in GSC tumor formation attributable to an expansion of niche signaling. Further results indicate that Lsd1 acts to control niche size both during development and in adulthood.

MATERIALS AND METHODS

Drosophila Stocks

Drosophila stocks were maintained at room temperature on standard cornmeal-agar medium unless specified otherwise. The following fly strains were used in this study: w1118 was used as a control; $Lsd1^{\Delta N}$ and *UAS-Lsd1* were provided by N. Dyson (Massachusetts General Hospital Cancer Center, Charlestown, MA); *hs-bam* and *hs FLP; FRT2A histone GFP* were provided by D. McKearin (Howard Hughes Medical Institute, Chevy Chase, MD); *hh-gal4* was provided by J. Jiang (University of Texas Southwestern, Dallas, TX); dpp^{hr56}, *c587-gal4, Dad-LacZ,* and *CB03410* were provided by A. Spradling (Carnegie Institute for Science, Baltimore, MD); and *E(spl)mβ-CD2* was provided by D. Drummond–Barbosa (The Johns Hopkins School of Public Health, Baltimore, MD). dpp^{hr92}, N^{55e11}, *FRT2A,* and *UAS-GFP* as well as *UAS-dpp-RNAi* (BL-31530 and BL-31531) lines were obtained from the Bloomington Stock Center. *UAS-Lsd1- RNAi* was obtained from the National Institute of Genetics, Japan.

Immunostaining

Adult ovaries were dissected in Grace's medium and fixed in 4% (vol/vol) formaldehyde for 10min. The ovaries were washed with PBT (PBS, 0.5% BSA, and 0.3% Triton-X 100) and stained with primary antibody overnight at 4°C. The ovaries were washed and incubated in secondary antibody at room temperature for 5h. Ovaries were then washed again and mounted in Vectashield containing DAPI (Vector Laboratories).

The following primary antibodies were used: mouse anti-1B1 (Hts) (1:20) and mouse anti-Lamin C LC28.26 (1:20) (Developmental Studies Hybridoma Bank), goat anti-VASA (1:200) (Santa Cruz Biotechnology), rabbit anti-VASA (1:500) (gift from A. Spradling), mouse anti-BamC A7 (1:20) (gift from D. McKearin), rabbit anti-Nanos (gift from A. Nakamura, RIKEN, Kobe, Japan), rabbit anti-Spectrin (1:1,000) (gift from R. Dubreuil, University of Illinois at Chicago), mouse anti-β-galactosidase (1:1,000) (Promega), rabbit anti-GFP (1:1,000) (Invitrogen), guinea pig anti-Lsd1 antibody (1:5,000) and mouse anti-CD2 (1:20) (AbD Serotec), rabbit antiphosphorylated ERK1/2 (1:100) and rabbit anti-cleaved Caspase-3 (1:250) (Cell Signaling Technology), guinea pig anti-Traffic Jam (1:5,000) (gift from D. Godt, University of Toronto, Toronto, ON, Canada), and rabbit anti–phospho-histone H3 (1:250) (Upstate Cell Signaling Solutions). Fluorescence-conjugated secondary antibodies (Jackson Laboratories) were used at a dilution of 1:200. The Student t test was used (two-tail distribution and two-sample unequal variants; Microsoft Excel 2008) to compare the number of ovarioles with branched vs. round fusomes between genotypes.

Generation of Anti-Lsd1 Antibody

A sequence corresponding to 1–150 amino acids of Lsd1 protein was cloned into PROEX (Invitrogen) to produce His6-tagged protein. The protein was expressed in Escherichia coli and purified with Ni-NTA agarose (Invitrogen). Polyclonal antisera were generated in guinea pigs (Covance).

Generation of GSC and FSC Clones

FLP/FRT-mediated mitotic recombination was used to generate GSC and FSC clones. Adult females of the genotype *hs-FLP; FRT2A histone GFP/FRT2A, Lsd1*$^{\Delta N}$ were heat-shocked at 37 °C for 1h twice a day for 3 d. *hs-FLP; FRT2A histone GFP/FRT2A* flies were used as controls. The ovaries were dissected on days 7, 14, and 21 after induction of heat shock.

RNA Isolation and RT-PCR

RNA was isolated from *bamΔ86* and *Lsd1*$^{\Delta N}$ *bamΔ86* mutant ovaries using TRIzol (Invitrogen). The RNA was treated with DNase and subjected to RT-PCR reaction using the One Step RT-PCR kit (Qiagen).

The primers used to amplify *dpp* and *dally* mRNA are as follows:

dpp forward: 5’ -GGCTTCTACTCCTCGCAGTG

dpp reverse: 5’ -TGCTTTTGCTAATGCTGTGC

dally forward: 5’ -TGACTTGCACGAGGACTAC

dally reverse: 5’ -TAATACGACTCACTATAGGGTGAGGAGATGCAGTTTGCAC

RESULTS AND DISCUSSION

I sought to identify chromatin-associated factors that regulate adult GSC behavior. The histone demethylase Lsd1 emerged as a likely candidate based on its role in various developmental processes. In humans, loss of Lsd1 has been linked to several high risk cancers (Tsai et al. 2008; Schulte et al. 2009; Suikki et al. 2010) and Lsd1 has recently been shown to negatively regulate the transcription of *TGFβ1*, a Dpp homolog. (Wang et al. 2009b). Previous work has shown that *Drosophila Lsd1* mutants display male and female sterile phenotypes and defects in heterochromatin formation (Di Stefano et al. 2007; Rudolph et al. 2007). The earliest steps of germline cyst development appeared severely disrupted in $Lsd1^{\Delta N}$ null allele homozygotes, resulting in the formation of small ovaries (Di Stefano et al. 2007).

Lsd1 Mutants Display Small GSC Tumors

To characterize the *Lsd1* mutant ovarian phenotype further, I stained WT and $Lsd1^{\Delta N}$ mutant ovaries with the germline marker Vasa and the fusome marker Hts (Figure 1 A and B). The fusome is a specialized organelle that appears round in GSCs most of the time but becomes branched as GSC daughters move away from the niche and form multicellular cysts (Lin et al. 1994) (Lin and Spradling 1995; de Cuevas and Spradling 1998). In contrast to controls (average = 2, range: 1–3, n = 30 germaria), *Lsd1* mutant ovaries contained an increased number of single undifferentiated GSC-like cells with round fusomes (average = 26, range: 6–79, n = 79 germaria).

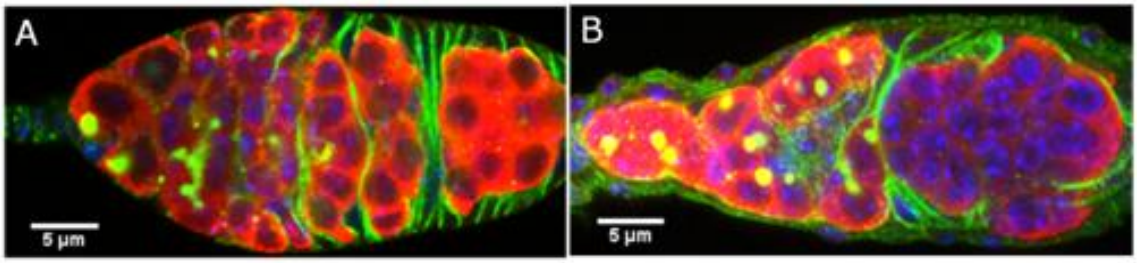

Figure 1. Disruption of *Lsd1* results in the formation of GSC-like tumors. Germaria immunostained for Hts (green), Vasa (red) and DNA (blue). (A) WT germaria contain two to three GSCs (B) $Lsd1^{\Delta N}$ mutants display an expanded number of GSC-like cells with single round fusomes.

These single cells underwent cell division as indicated by phospho- histone H3 staining (Figure 2A and B). The average overall size of these *Lsd1* mutant tumors did not increase over time, however, because of programmed cell death within the germline (Figure 2C and D).

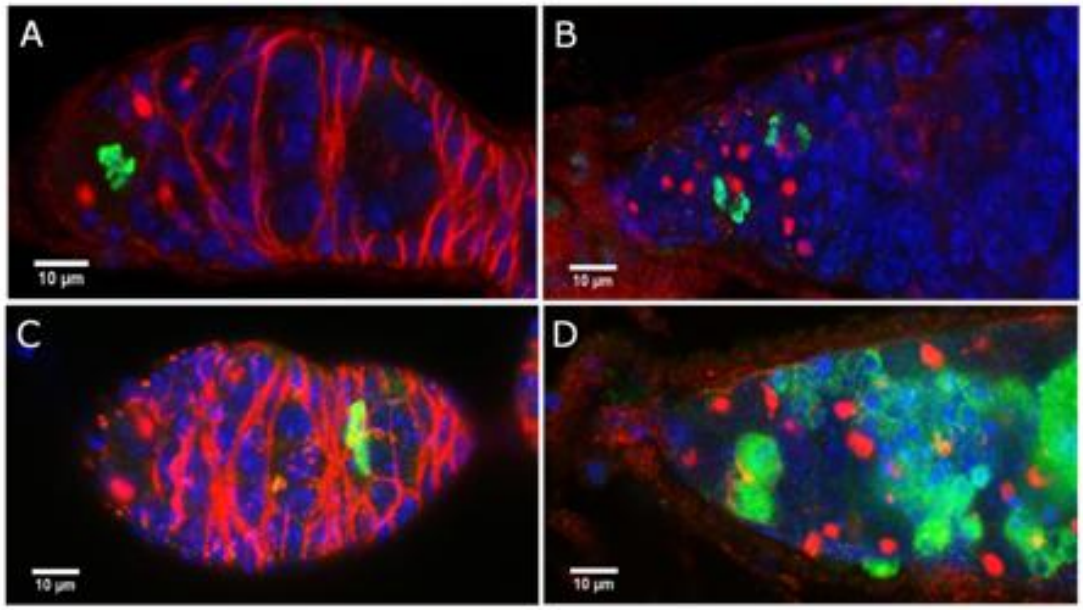

Figure 2. *Lsd1* mutant GSCs display increased cell division and undergo premature cell death. (A) WT and (B) $Lsd1^{\Delta N}$ germaria stained for phosphorylated histone H3 (red). Positive staining revealed that Lsd1 mutant GSC-like cells continue to divide. (C) WT and (D) $Lsd1^{\Delta N}$ mutant germaria stained using an antibody against activated Caspase 3 (red). Cells undergoing cell death are rarely observed in WT germaria but cell death occurs in *Lsd1* mutant samples. Germaria are stained for Hts (green) and DNA (blue).

Lsd1 Functions in a Nonautonomous Manner

To begin to evaluate the function of Lsd1 in the germarium, I generated a polyclonal antibody to the N terminus of the Lsd1 protein. This antibody revealed ubiquitous Lsd1 expression throughout the germarium (Figure 3B and C). As expected for a histone demethylase, the protein predominantly localized to the nuclei of all cells examined. Interestingly, Lsd1 expression appeared highest in the GSCs but was also clearly present in the ECs and follicle cells of the germarium.

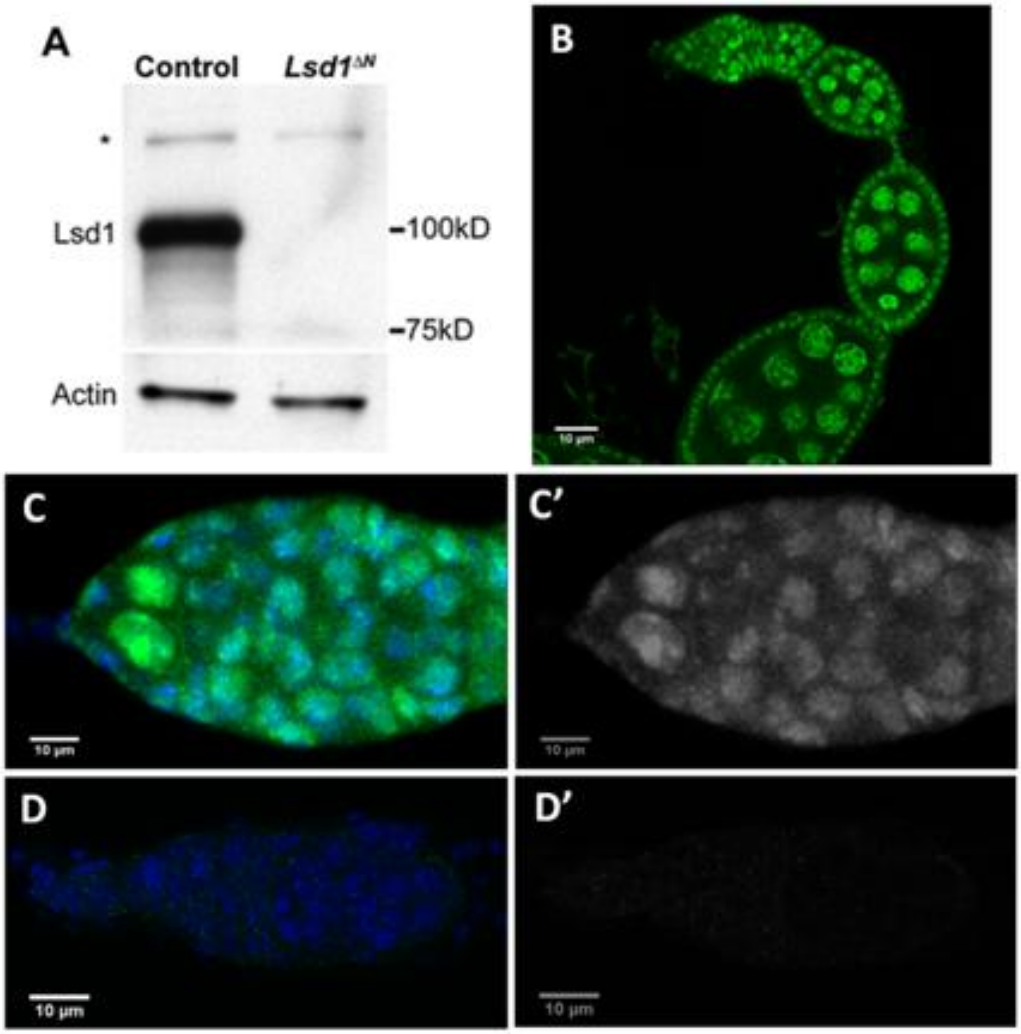

Figure 3. Lsd1 expression. (A) Western blot of whole-ovary extracts from *bamΔ86* (Control) and *Lsd1*$^{\Delta N}$ *bamΔ86* (*Lsd1*$^{\Delta N}$) double-mutant females using anti-Lsd1 antibody. The predicted size of Lsd1 is 100 kDa. This band disappears in the mutant sample. The antibody also recognizes a minor background band (asterisk). (B) Adult ovariole stained for Lsd1 (green). Lsd1 is expressed throughout this tissue and localizes to the nucleus. (C and C′) Adult germarium stained for Lsd1 (green) and DNA (blue). (D and D′) *Lsd1*$^{\Delta N}$ ovariole lacks detectable Lsd1 expression.

The GSC tumors within *Lsd1* mutant ovaries could be caused by defects in the intrinsic programming of GSCs or by extrinsic defects in the surrounding somatic cells. I performed clonal analysis and cell-specific rescue experiments to distinguish between these possibilities. First, I induced negatively marked *Lsd1* mutant clones in an otherwise heterozygous background in adults using FRT/FLP-mediated mitotic recombination (Figure 4). Interestingly, I found that negatively marked *Lsd1* mutant germline clones differentiated into morphologically normal egg chambers without any apparent block in differentiation, even over long periods of time (Figure 4A and B). Furthermore, *Lsd1*$^{\Delta N}$ GSC clones were maintained at levels similar to control clones (Figure 4D), demonstrating that Lsd1 was not required within the germline for GSC maintenance. Instead, these results suggest that Lsd1 acts within a different cell type (i.e., in a cell-non autonomous manner) to control germline differentiation.

I then examined *Lsd1* mutant follicle cell clones. These also appeared normal and were able to envelop germline cysts fully without any obvious defects (Figure 4C). The absence of *Lsd1* in the follicle cells did not result in an abnormal number of GSCs. Furthermore *Lsd1*$^{\Delta N}$ follicle stem cell (FSC) clones were maintained over long periods of time (Figure 4D). Together with the germline clone data, these experiments suggest that Lsd1 functions in either ECs or cap cells to limit the number of GSCs in the germarium.

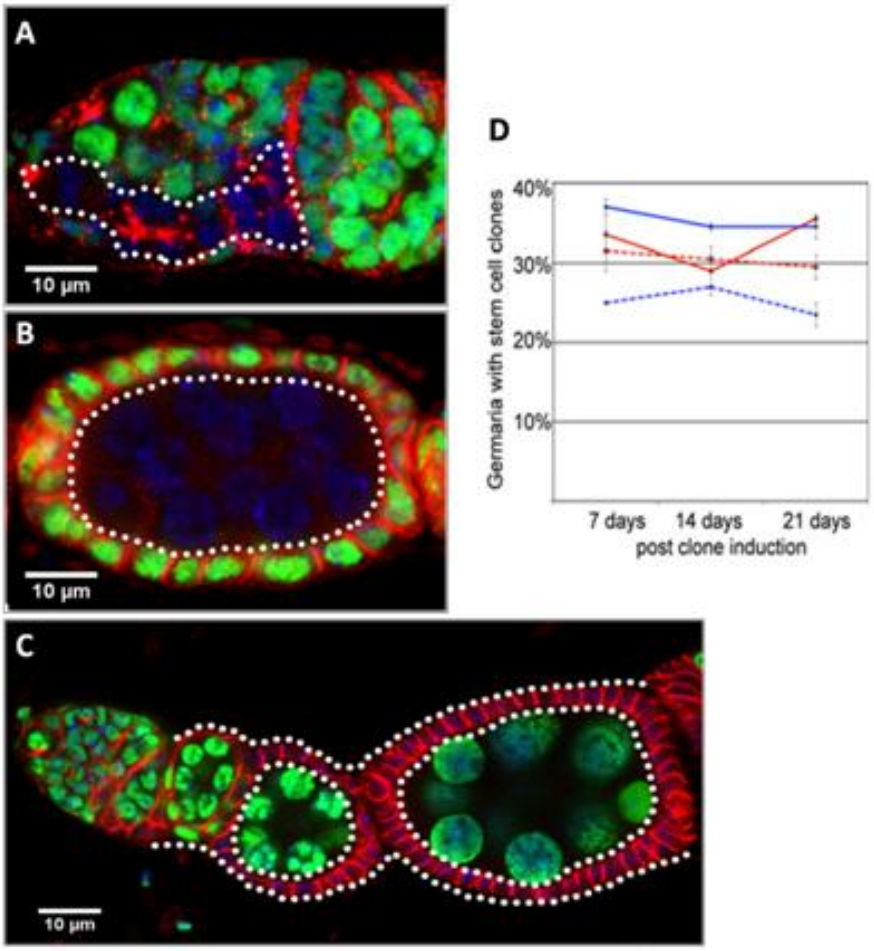

Figure 4. Germline and follicle cell clones of *Lsd1* do not exhibit a phenotype. (A and B) Negatively marked germline clones stained for GFP (green) and Hts (red). $Lsd1^{\Delta N}$ homozygous germline clones (dotted lines) differentiate to form cysts with branched fusomes and morphologically normal egg chambers. (C) $Lsd1^{\Delta N}$ homozygous follicle cells (dotted lines) do not exhibit a discernible phenotype. (D) Graph shows the percentage of control and *Lsd1* mutant stem cell clones maintained after clone induction. The solid red line refers to control germline clones, the dotted red line refers to $Lsd1^{\Delta N}$ germline clones, the solid blue line refers to control follicle cell clones, and the dotted blue line refers to $Lsd1^{\Delta N}$ follicle cell clones.

To distinguish between these two possibilities, I knocked down *Lsd1* expression using RNAi in a cell-specific manner (Brand and Perrimon 1993). Reducing *Lsd1* levels in cap cells and terminal filament cells using *Lsd1-RNAi* in combination with *hedgehog (hh) gal4* (Forbes et al. 1996a; Pan et al. 2007) did not disrupt the normal morphology of the germarium (Figure 5A).

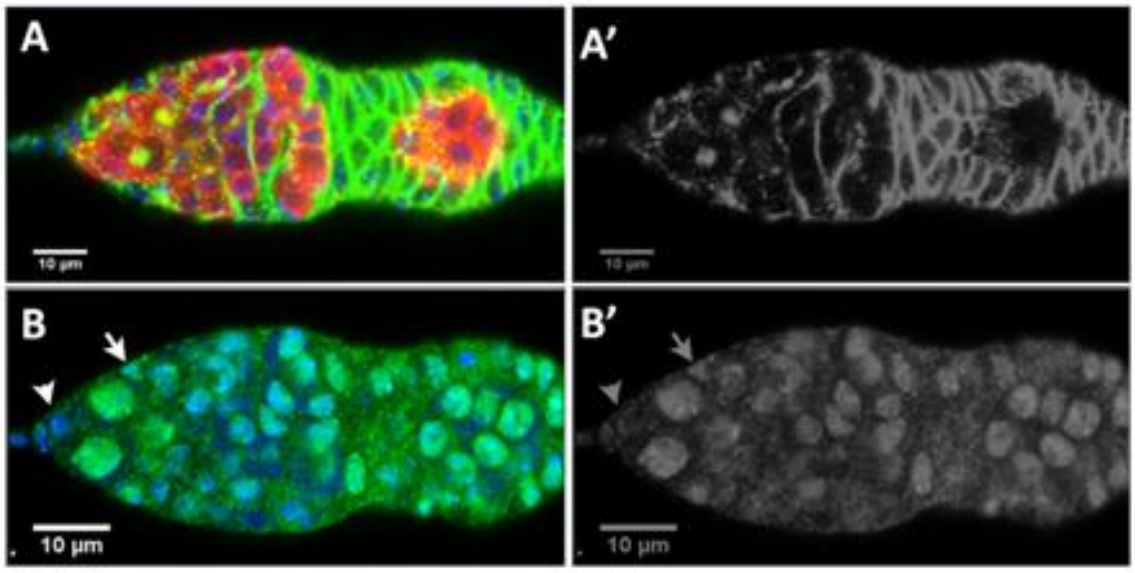

Figure 5. Knocking down *Lsd1* in cap cells does not have a phenotype. Germaria from *UAS-Lsd1RNAi/+; hh-gal4/+* females stained for (A and A') Hts (green), VASA (red) and DNA (blue) shows a normal germarium with no discernible phenotype. (B and B') Germaria stained for Lsd1 (green) and DNA (blue). Cap cells (arrowhead) exhibit reduced levels of Lsd1, but Lsd1 expression remains unaffected in ECs (arrow).

In contrast, *Lsd1-RNAi* driven by *c587-gal4*, which expresses GAL4 in most somatic cells in the developing gonad but becomes largely restricted to ECs and early follicle cells in adults (Zhu and Xie 2003; Song et al. 2004) (for Lsd1 expression, see Figure 6D'), phenocopied Lsd1 mutants (Figure 6A), resulting in the formation of GSC-like tumors within all examined germaria.

Furthermore, driving *Lsd1* WT transgenes with *c587-gal4* rescued the *Lsd1* null mutant phenotype so that the normal morphology of mutant germaria and ovarioles was fully restored in every female tested (Figure 6C). Given that reducing or eliminating *Lsd1* function within follicle cells (Figure 4C) or cap cells (Figure 5A) did not result in a phenotype, the knockdown and rescue experiments using *c587-gal4* strongly suggest that

Lsd1 functions within ECs to limit the number of GSCs. Interestingly, the fully mature eggs produced by *Lsd1* mutant females expressing rescuing transgenes remained sterile, suggesting that Lsd1 may also function outside of the ECs but in a manner unrelated to the expanded GSC phenotype. Perhaps *Drosophila* Lsd1 has an analogous function to its Caenorhabditis elegans homolog, which is required for germline maintenance over multiple generations (Katz et al. 2009). Regardless of this additional phenotype, the clonal loss-of-function and cell type specific knockdown and rescue experiments presented here clearly demonstrate that Lsd1 is required in somatic cells (likely ECs) for non autonomous control of the number of GSC-like cells within the germarium.

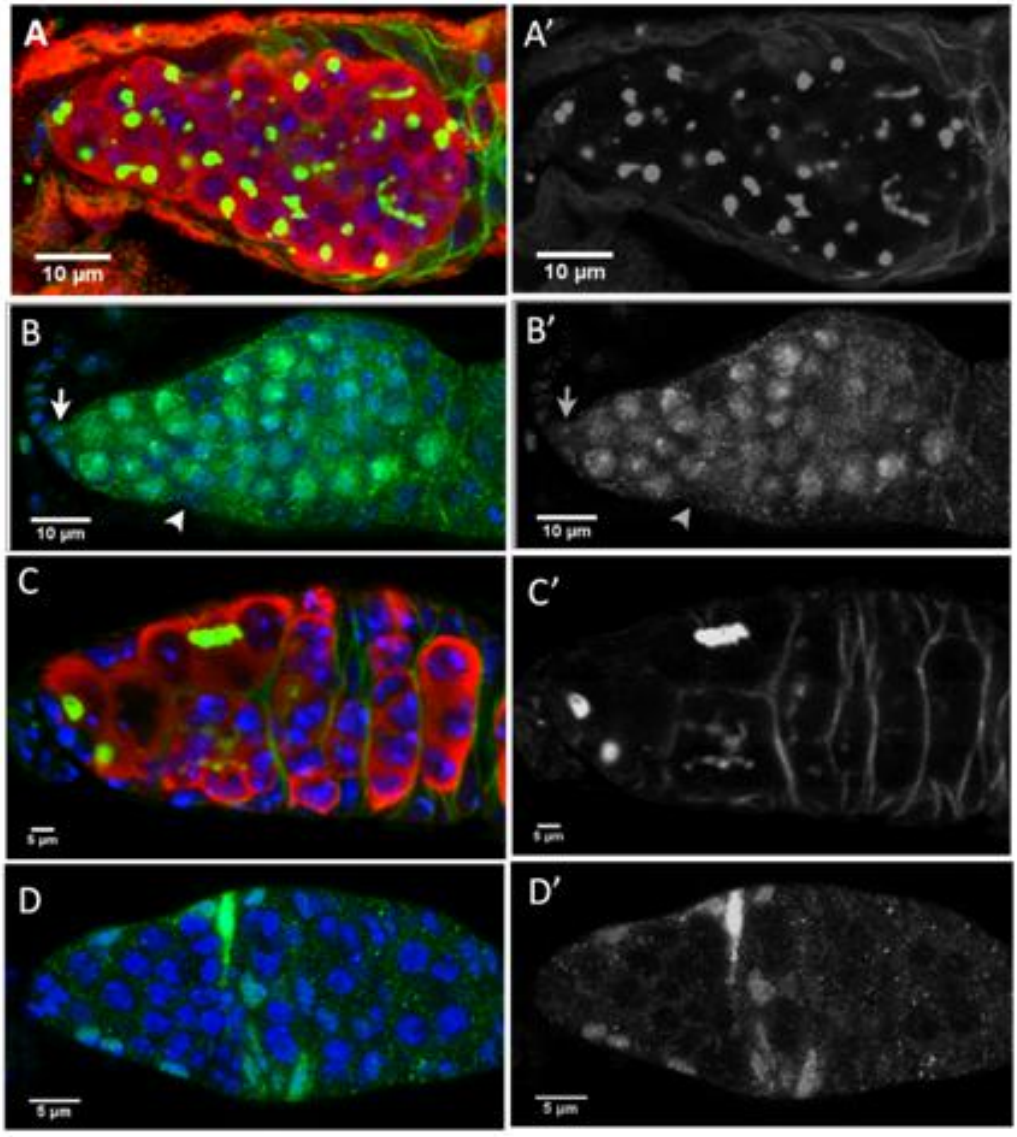

Figure 6. Lsd1 functions in a nonautonomous manner to regulate GSC numbers within the ovary. (A and A') Germarium from *c587-gal4/+; UAS-Lsd1RNAi/+* females stained for Hts (green), Vasa (red), and DNA (blue). Knocking down *Lsd1* in escort cells has an expanded population of GSC-like cells. (B and B′) Germarium from a *c587-gal4/+; UAS-Lsd1-RNAi/+* female stained for Lsd1 (green) and DNA (blue). ECs (arrowhead) exhibit reduced levels of Lsd1. Arrow points to cap cells. (C and C') Ovarian cells from *c587-gal4/+; UAS-Lsd1/+; $Lsd1^{\Delta N}/Lsd1^{\Delta N}$* females stained for Hts (green), Vasa (red), and DNA (blue) shows a rescue of the mutant phenotype. (D and D′) Germarium from a rescued *c587-gal4/+; UAS-Lsd1/+; $Lsd1^{\Delta N}/Lsd1^{\Delta N}$* female stained for Lsd1 (green) and DNA (blue). Lsd1 expression is observed in ECs (arrows) and early follicle cells but not in cap cells and the germline.

Lsd1 Limits Dpp Signaling Within the Germarium

I sought to understand further how Lsd1 regulated the differentiation of GSC daughters. GSCs express the translational repressor Nanos, a factor essential for GSC maintenance. On displacement away from the cap cell niche, GSC daughters express Bam, which represses the translation of nanos in differentiating cysts (Li et al. 2009). Costaining control and Lsd1 mutant germaria for Nanos and Bam revealed that less than 1.5% of Lsd1 mutant germaria expressed detectable levels of Bam (Figure 7B). Instead, most germline cells continued to express Nanos, indicating that loss of *Lsd1* prevents GSC daughters from differentiating into cystoblasts and multicellular cysts.

To test whether Lsd1 mutant germline cells were capable of forming multicellular cysts, I expressed *bam* in *Lsd1* mutant ovaries using an inducible transgene. Previous studies showed that bam expression is both necessary and sufficient for germ cell differentiation (McKearin and Spradling 1990; Ohlstein and McKearin 1997). Expression of bam in *Lsd1* mutants resulted in the formation of multicellular cysts that contained branched fusomes (Fig. 7E), indicating that *Lsd1* mutant germline cells can undergo differentiation and form multicellular cysts. This result strongly suggests that the tumorous phenotype exhibited by *Lsd1* mutants is caused by failure to initiate a proper differentiation program within GSC daughters.

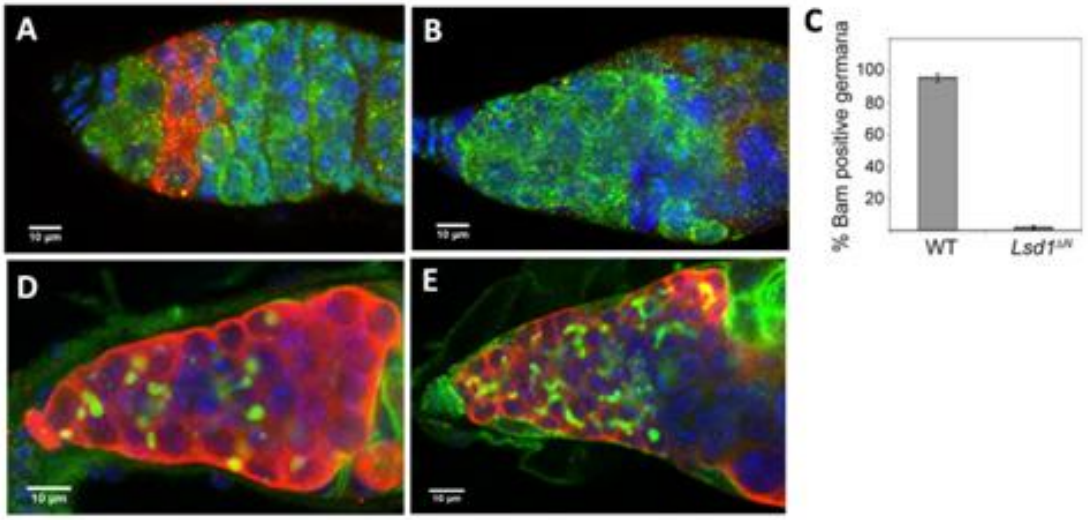

Figure 7: Bam expression is blocked in *Lsd1* mutants. (A) WT and (B) *Lsd1*$^{\Delta N}$ homozygous mutant germaria immunostained for Nanos (green) and Bam (red). (C) Graph comparing Bam expression in WT (n = 200) and *Lsd1*$^{\Delta N}$ homozygous (n = 244) germaria. Only 1.5% of *Lsd1*$^{\Delta N}$ mutant germaria express Bam. *hsbam/+; Lsd1*$^{\Delta N}$*/Lsd1*$^{\Delta N}$ germaria (D) before heat shock and (E) 2d after heat shock stained for Hts (green) and Vasa (red).

Given the previous findings that Dpp signaling represses *bam* expression in GSCs (Xie and Spradling 1998; Xie and Spradling 2000; Chen and McKearin 2003a), I considered the possibility that ectopic Dpp pathway activity might account for the absence of Bam expression in Lsd1 mutants.

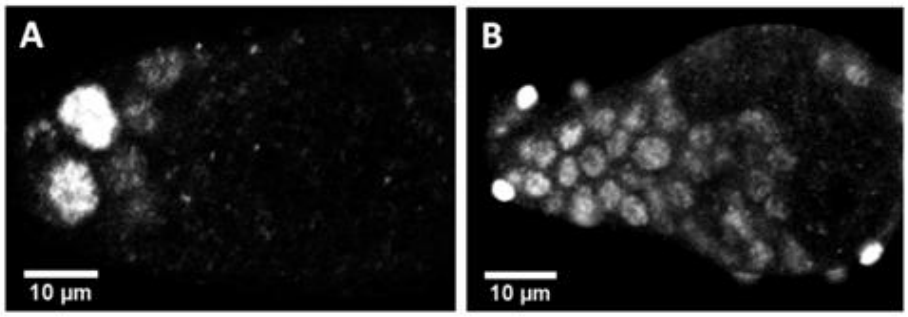

Figure 8. Loss of *Lsd1* results in expanded Dpp signaling. (A) High levels of *Dad-LacZ* (white) expression are normally restricted to GSCs in WT germaria. (B) *Lsd1* mutants exhibit expanded *Dad-LacZ* expression in germline cells.

To test this idea, I crossed a positive reporter of Dpp signaling, the *Dad-LacZ* enhancer trap, into the *Lsd1*$^{\Delta N}$ mutant background. Normally, high levels of *Dad-LacZ* expression are limited to the two to three GSCs immediately adjacent to the cap cells (Figure 8A). Although the overall levels of *Dad-LacZ* expression were not as high as in control GSCs, I found that the number of *Dad-LacZ*–positive cells was greatly expanded in *Lsd1* mutant germaria (100%, n >100 germaria) (Figure 8B), suggesting that greater Dpp signaling accounts for the increased number of GSC-like cells in *Lsd1* mutant ovaries. Consistent with this idea, two different dpp mutations partially suppressed the *Lsd1* phenotype (Figure 9A and B), resulting in an increased number of germline cysts with branched fusomes and maturing egg chambers (Figure 9C and D). Furthermore, the expression of two different dpp-RNAi transgenes strongly suppressed the *c587-gal4 > Lsd1-RNAi*-induced GSC tumor phenotype (Figure 9F and G).

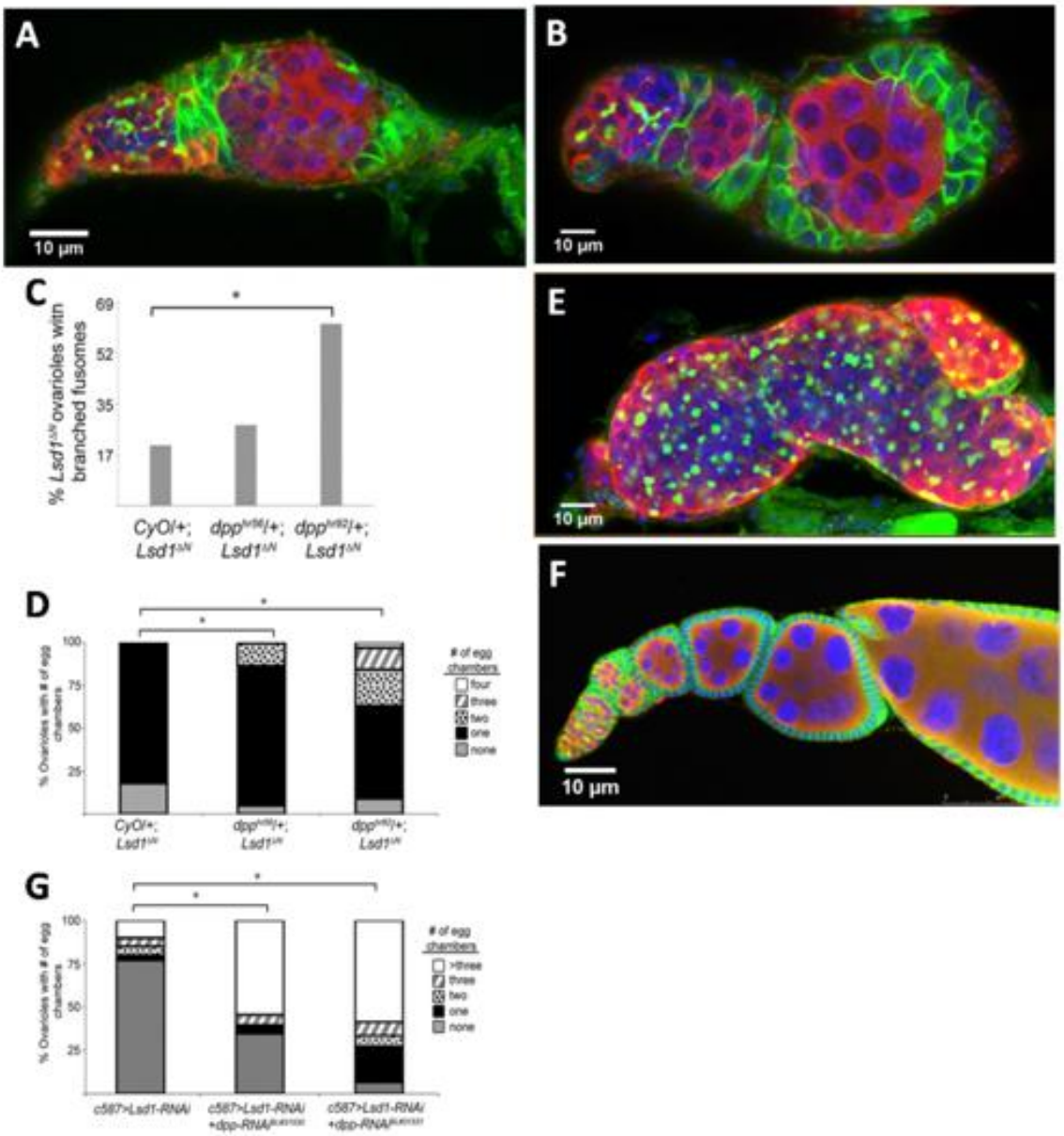

Figure 9. Knocking down *dpp* in Escort Cells suppresses the *Lsd1* mutant phenotype. (A) *dpp^{hr56}/+; Lsd1$^{\Delta N}$/Lsd1$^{\Delta N}$* and (B) *dpp^{hr92}/+; Lsd1$^{\Delta N}$/Lsd1$^{\Delta N}$* germaria stained for Hts (green), Vasa (red) and DNA (blue). Both *dpp* mutant alleles dominantly suppress the Lsd1 phenotype, leading to the appearance of cysts with branched fusomes (arrowheads). (C) Graph shows the percentage of ovarioles that contained multicellular germline cysts with branched fusomes for each given genotype. The difference between *Cyo/+; Lsd1$^{\Delta N}$/Lsd1$^{\Delta N}$* and *dpp^{hr92}/+; Lsd1$^{\Delta N}$/Lsd1$^{\Delta N}$* is significant (*P < 0.005). (D) Graph shows the percentage of ovarioles that contained a given number of developing egg chambers for each given genotype (*P < 0.005). Control (n = 63 ovarioles), *dpp^{hr56}/+; Lsd1$^{\Delta N}$/Lsd1$^{\Delta N}$* (n = 80 ovarioles), and *dpp^{hr92}/+; Lsd1$^{\Delta N}$/Lsd1$^{\Delta N}$* (n = 79 ovarioles). (E) Germaria from *c587-gal4/+; UAS-Lsd1-RNAi/+* and (F) *c587-gal4/+; UAS-Lsd1-RNAi/+; UAS-dpp-RNAi/+* females dissected 1 d after eclosion stained for Hts

(green), Vasa (red) and DNA (blue). Reduction of *dpp* expression by RNAi dramatically suppressed the tumorous phenotype induced by *Lsd1-RNAi*. (G) Graph shows the percentage of ovarioles that contained a given number of developing egg chambers for each given genotype 1 d after eclosion. Both *UAS-dpp-RNAi* lines tested suppressed the phenotype of *c587>Lsd1-RNAi* (*P < 0.005). *c587>Lsd1- RNAi* (n = 128), *c587>Lsd1-RNAi+dpp-RNAi* BL#31530 (n = 84), and *c587>Lsd1-RNAi+ dpp-RNAi* BL#31531 (n = 91).

Lsd1 Functions during Development to Specify Somatic Cell Fate

Loss of *Lsd1* did not appear to result in changes in somatic cell numbers within developing gonads or adult germaria. I considered the possibility that Lsd1 functioned in the somatic precursor cells of the developing gonad when ECs and cap cells are being specified. To test whether *Lsd1* mutant somatic cells adopt inappropriate fates, I compared the expression of several cap cell-specific markers. Cap cells and terminal filament cells express high levels of Lamin C and hh (Song et al. 2004; Song et al. 2007). *CB03410*, a previously identified protein trap line (Buszczak et al. 2007), is also expressed in adult cap cells and terminal filament cells. In *Lsd1* mutants, the expression of all three markers expanded to most of the somatic cells within the germarium (Figure 10A–F), indicating that *Lsd1* mutant ECs exhibit characteristics of cap cells. To determine whether *Lsd1* mutant ECs completely switch their identity, I examined *c587-gal4* expression within WT and *Lsd1* mutant adult ovaries (Figure 10G and H). Unlike WT adult germaria, which exhibited virtually exclusive expression of *c587-gal4* within ECs and early follicle cells, *Lsd1* mutants also displayed *c587-gal4* expression in cap cells. Thus, *Lsd1* mutant ECs and cap cells do not differentiate properly and display characteristics of both cell types in adult germaria.

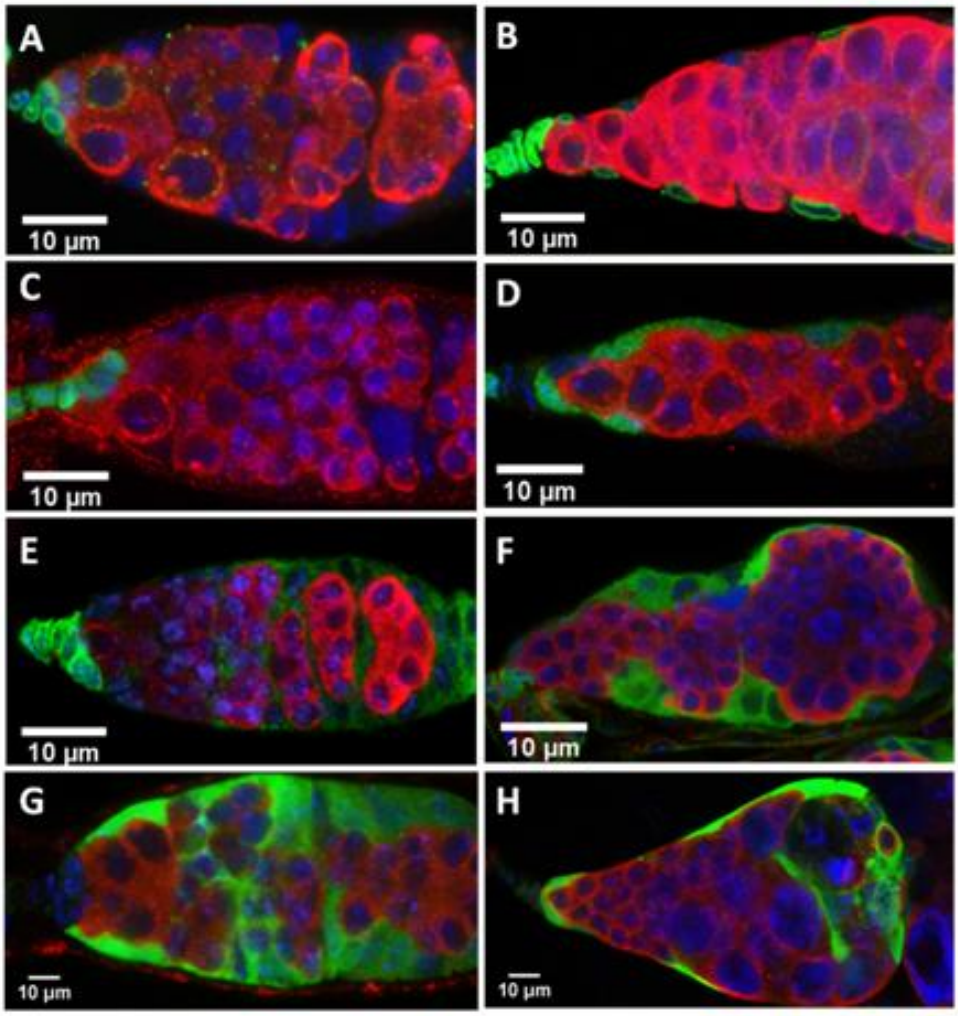

Figure 10. Loss of *Lsd1* results in somatic cell fate changes. (A) WT and (B) $Lsd1^{\Delta N}$ homozygous germaria stained for Lamin C (green). (C) *UAS-GFP; hh-gal4* and (D) *UAS-GFP; hh-gal4,* $Lsd1^{\Delta N}/Lsd1^{\Delta N}$ germaria stained for the expression of GFP (green). (E) *CB03410* and (F) *CB03410;* $Lsd1^{\Delta N}/Lsd1^{\Delta N}$ germaria stained for the expression of GFP (green). (G) *c587-gal4; UAS-GFP* and (H) *c587-gal4; UAS-GFP;* $Lsd1^{\Delta N}/Lsd1^{\Delta N}$ germaria stained for the expression of GFP (green). All germaria stained for VASA (red) and DNA (blue).

Several signaling pathways have been implicated in the formation and regulation of the GSC niche (Ward et al. 2006a; Song et al. 2007; Lopez-Onieva et al. 2008; Wang et al. 2008a; Guo and Wang 2009; Hayashi et al. 2009; Liu et al. 2010). For example, Delta from newly formed terminal filament cells activates Notch signaling and induces cap cell identity within a small number of somatic cells in the developing gonad (Song et

al. 2007). The EGFR pathway has also been implicated in regulating the development of the ovary and niche output in adults (Gilboa and Lehmann 2006; Liu et al. 2010). I did not observe genetic interactions between *Lsd1* and *Notch* (Figure 11A and B). Furthermore a transcriptional reporter of Notch activity, *E(spl)mβ-CD2* (de Celis and Bray 1997; Cooper and Bray 1999), exhibited a normal pattern of expression in Lsd1 pupal gonads, suggesting that loss of *Lsd1* does not result in inappropriate derepression of Notch target genes within the developing gonad (Figure 11C and D).

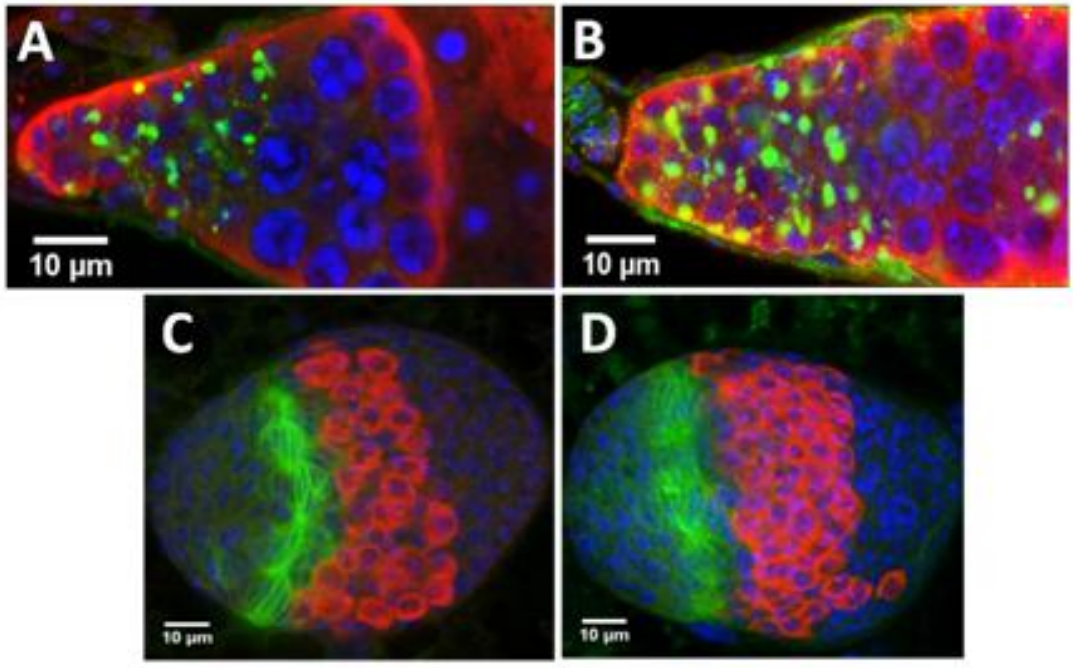

Figure 11. Loss of *Lsd1* does not affect Notch signaling in the adult ovary. (A) $Lsd1^{\Delta N}/Lsd1^{\Delta N}$ and (B) $N^{55e11}/+;\ Lsd1^{\Delta N}/Lsd1^{\Delta N}$ germaria stained for Hts (green), Vasa (red), and DAPI (blue).Removing one copy of *Notch* in an Lsd1 mutant does not improve the overall morphology of *Lsd1* mutant ovaries or reduce the number of GSC-like cells within the tumors. Late larval (C) WT and (D) $Lsd1^{\Delta N}$ homozygous female gonads stained for the *E(spl)mβ-CD2* reporter (green), VASA (red) and DNA (blue). There is no difference in the reporter staining in WT compared to $Lsd1^{\Delta N}$ mutants.

Likewise, I also found that activation of the EGFR-MAPK pathway does not change in *Lsd1* mutant gonads or in adult ovaries, based on the expression of phosphorylated extracellular signal-regulated kinase (pERK) (Figure 12). Therefore, Lsd1 does not appear to interact with or influence the activity of these signaling pathways within developing gonads.

Previous studies showed that the Jak/Stat pathway also regulates Dpp signaling in adults; however, unlike Lsd1, it does not have a developmental role in niche formation (Lopez-Onieva et al. 2008; Wang et al. 2008a). Despite these findings, I cannot rule out the possibility that *Lsd1* interacts with the Jak/Stat pathway at some level in adult germaria. My results suggest that Lsd1 directs EC cell formation and limits Dpp signaling through a previously unrecognized mechanism that does not involve the Notch and EGF pathways.

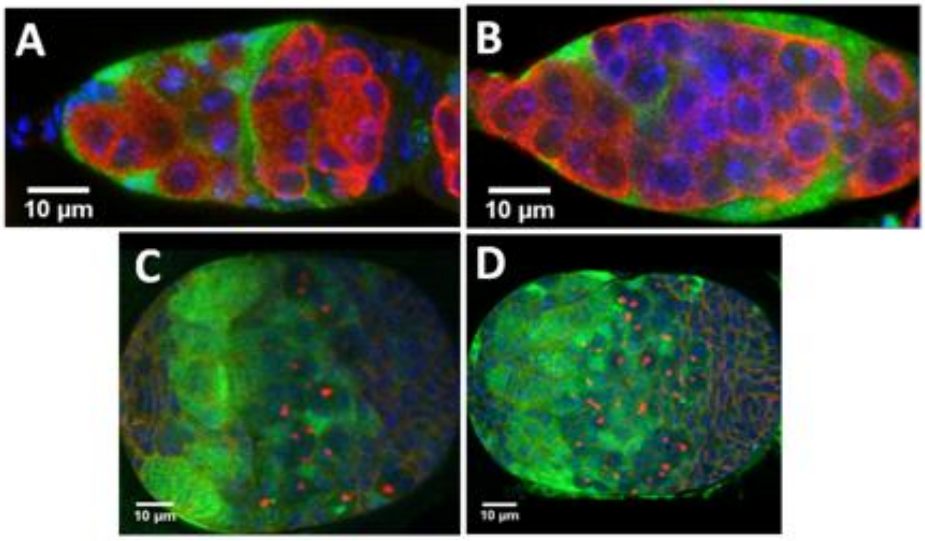

Figure 12. Loss of *Lsd1* does not affect EGFR signaling in the adult ovary. (A) WT and (B) $Lsd1^{\Delta N}/Lsd1^{\Delta N}$ adult germaria stained for pERK (green), VASA (red) and DNA

(blue). Late larval (C) WT and (D) *Lsd1*$^{\Delta N}$ homozygous female gonads stained for pERK (green), Hts (red) and DNA (blue). No dramatic differences are seen between the two samples.

Lsd1 Functions during Development and in Adults to Limit Niche Size

The role of Lsd1 in regulating EC fate does not preclude the possibility that this histone demethylase continues to restrict GSC number in adult ovaries independent of any developmental defects. To determine whether Lsd1 acts only during development, I took advantage of the temperature sensitivity of the C587 gal4 driver and performed a series of temperature shift experiments. In these experiments, *Lsd1* expression was specifically knocked down in somatic cells using *Lsd1 RNAi* driven by *c587-gal4* (Figure 13). First, females were raised at 29°C during larval and pupal development and then either kept at 29°C or shifted down to 18°C for 7d immediately after eclosion. Consistently, females raised and maintained at 29°C exhibited a pronounced GSC tumor phenotype with no signs of proper egg chamber development (Figure 13A). Females shifted down to 18°C for 7d displayed signs of germline differentiation, however. Ovaries from these females often contained ovarioles with a number of developing germline cysts that were fully encapsulated by follicle cells (Figure 13B). These results indicate that restoration of Lsd1 function during adulthood can rescue underlying developmental defects that result from the absence of Lsd1 during larval and pupal development.

If Lsd1 functions to limit the size of the GSC niche in adults, knocking down *Lsd1* expression in females specifically after they eclose would be predicted to result in a

GSC expansion phenotype. To test this possibility, I raised *c587-gal4; UAS-Lsd1-RNAi* females at 18°C. Ovaries from these females appeared normal and did not exhibit an expanded number of GSCs, even after 7d as adults (Figure 13C). I observed a striking GSC tumor phenotype when I shifted these females to 29°C for 7d after eclosion, however (Figure 13D). Lamin C staining showed that this phenotype was not accompanied by changes in EC identity (Figure 13F). These data demonstrate that Lsd1 functions to limit dpp signaling within germaria during adulthood.

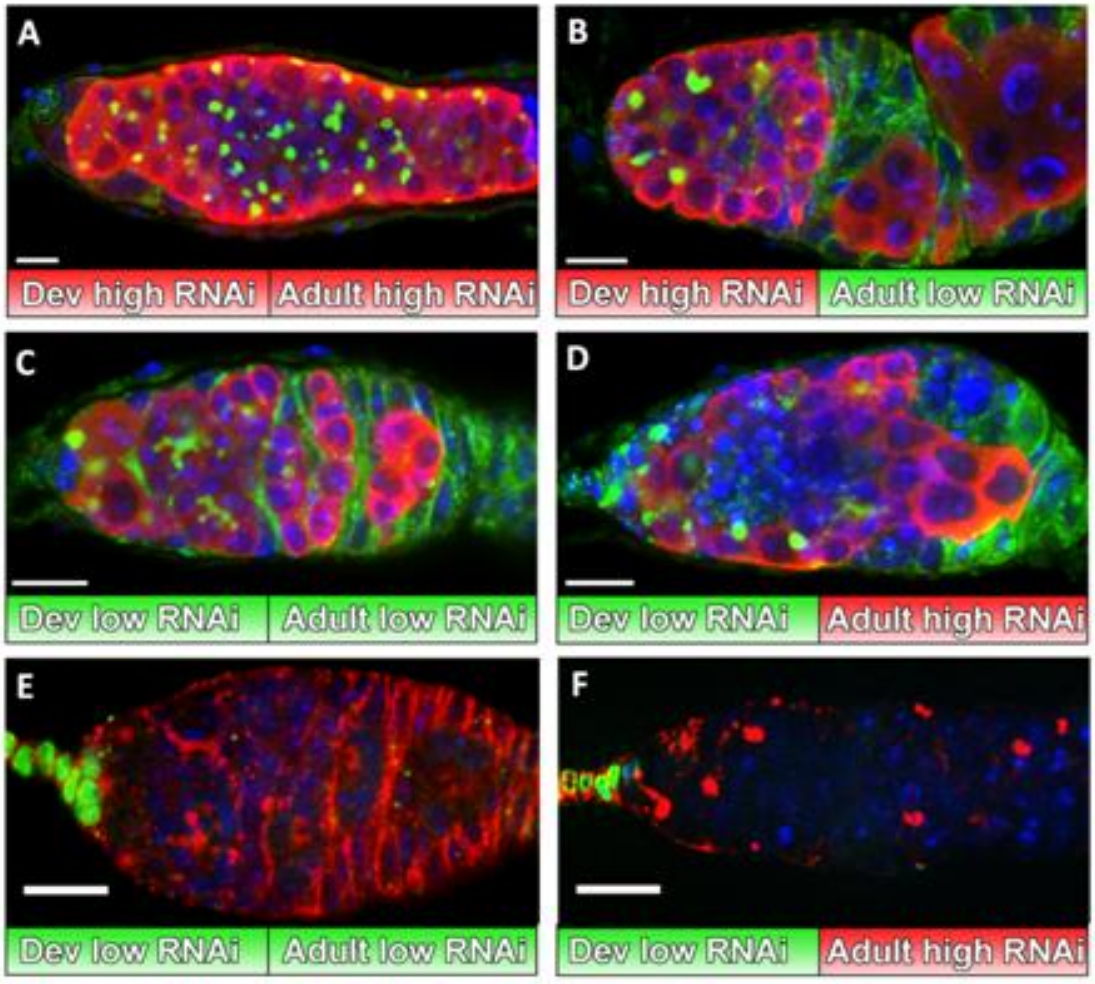

Figure 13. Lsd1 functions in adulthood to limit niche activity. (A–D) Germaria from *c587-gal4/+; UAS-Lsd1-RNAi/+* females raised at either 29°C (high RNAi) or 18°C (low

RNAi) and shifted after eclosion stained for Hts (green), Vasa (red), and DNA (blue). (E and F) *c587-gal4/+; UAS-Lsd1-RNAi/+* germaria stained for Lamin C (green), Spectrin (fusome and membranes; red), and DNA (blue). Both samples were from females raised at 18°C during development. Although one set of adults was kept at 18°C (E) and did not exhibit a phenotype, other adults were shifted to 29°C for 7d (F). These adults did not exhibit changes in Lamin C expression despite the formation of GSC-like tumors.

Loss of Lsd1 Results in Increased *dpp* but not *dally* Expression

Although my analysis of pERK suggests that loss of Lsd1 does not lead to obvious changes in EGFR signaling (Figure 12), this experiment does not rule out the possibility that Lsd1 influences the transcriptional output of the EGFR pathway. In adults, activation of the EGFR pathway limits Dpp signaling outside of the niche by repressing the transcription of *dally* (Liu et al. 2010), a glypican that facilitates Dpp transport and stability (Guo and Wang 2009; Hayashi et al. 2009). To determine whether Lsd1 specifically represses the expression of genes involved in promoting Dpp signaling, or perhaps dpp itself, I performed a number of RT-PCR–based experiments. To control for differences in the developmental state of the samples, I crossed the $Lsd1^{\Delta N}$ mutation into a *bamΔ86* mutant background. I observed no difference in *dally* mRNA levels between *bamΔ86* and $Lsd1^{\Delta N}$ *bamΔ86* double-mutant germaria, further suggesting that Lsd1 functions independent of the EGFR pathway (Figure 14A). In contrast, *dpp* mRNA levels were noticeably elevated in Lsd1 mutant adult germaria (Figure 14B). I also found that ectopic expression of *dpp* driven by *c587-gal4* during development resulted in the expanded expression of the cap cell marker Lamin C (Figure 14C). These observations suggest that misregulation of *dpp* itself accounts for the phenotypes observed in *Lsd1* mutants.

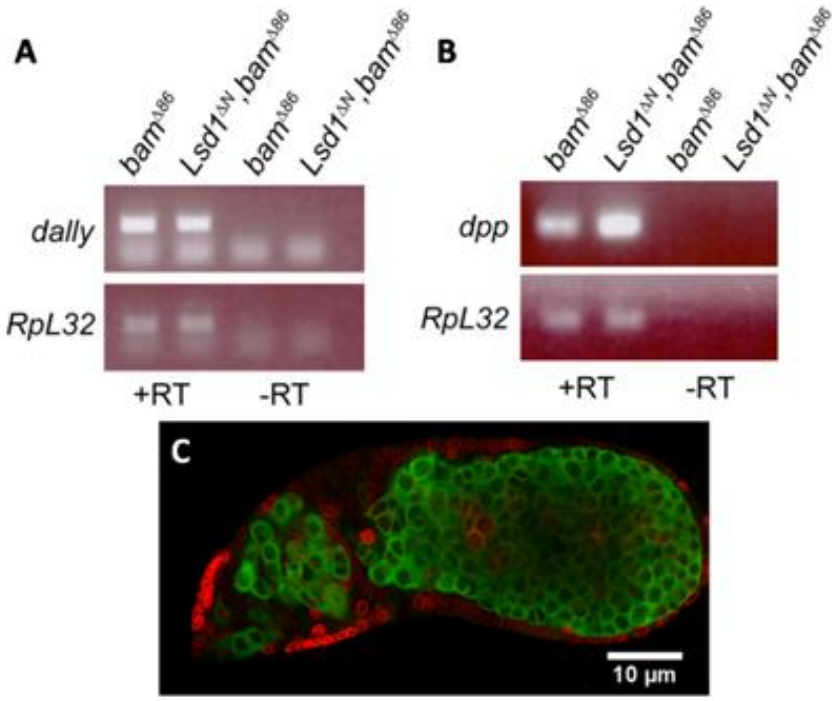

Figure 14. *Lsd1* mutant germaria display elevated levels of *dpp* mRNA. Ethidium bromide-stained gel shows the products of a RT-PCR on RNA isolated from *bamΔ86* and *Lsd1$^{\Delta N}$ bamΔ86* ovaries using (A) *dally*- or (B) *dpp*- specific primers. No difference in the levels of *dally* expression was observed, although *dpp* mRNA levels were clearly elevated in the absence of *Lsd1*. The presented gels are representative of three biological replicates. Germarium from *c587-gal4/+; UAS-dpp/+* females stained for Vasa (red) and Lamin C (green). Ectopic expression of *dpp* results in the expansion of cap cells.

The work presented here indicates that the conserved histone demethylase Lsd1 is functional in the somatic cells of the *Drosophila* ovary. Based on all the findings presented here, I favor a model in which Lsd1 represses *dpp* transcription outside the normal niche reiteratively during development and in adulthood. Within the developing gonad, loss of *Lsd1* results in expanded dpp expression leading to perturbations in normal cap cell and EC development. In other tissues, dpp expression is maintained through autoregulatory mechanisms (Yu et al. 1996; Chanut and Heberlein 1997; Hepker et al. 1999). Perhaps loss of *Lsd1* results in low levels of inappropriate dpp expression that

become reinforced through similar autoregulatory mechanisms. Restoration of normal Lsd1 activity in adults appears sufficient to block dpp activity outside of the normal niche caused by defects in EC differentiation, suggesting that Lsd1 function and the genes it targets for repression are likely to be the same in the developing gonad and in adults.

Previous work has focused on identifying signaling pathways that specify niche cell identity. Equally important in sculpting a fully functional stem cell microenvironment is preventing cells outside the normal niche from producing niche-specific signals in an inappropriate manner.

Recent studies show that mammalian Lsd1 directly targets TGF-β1 for transcriptional repression (Wang et al. 2009b) and has cell-autonomous roles in cancer (Tsai et al. 2008; Schulte et al. 2009; Wang et al. 2009a; Suikki et al. 2010). Given the possible links between cancer and stem cells (Feinberg et al. 2006) and the observation that Lsd1 has a conserved role in regulating intercellular signaling molecules, it will be important to determine whether Lsd1 and other chromatin factors have additional nonautonomous functions that contribute to stem cell maintenance, tumorigenesis, and metastasis.

CHAPTER 3

LSD1 RESTRICTS THE SIZE OF THE GERMLINE STEM CELL NICHE BY SILENCING ENGRAILED IN THE ESCORT CELLS OF THE *DROSOPHILA* OVARY

INTRODUCTION

Stem cells have the unique ability to self-renew themselves and the potential to differentiate into different cell types. During embryonic development, stem cells play an essential role in organogenesis. In adults, stem cells maintain tissue homeostasis, regenerating dying cells or cells lost due to injury. Throughout the life of an organism, there is an intricate balance between stem cell self renewal and differentiation which needs to be maintained. The stem cell characteristics of proliferation versus differentiation are directed by cell intrinsic genetic programs and by extrinsic environmental regulatory signals.

Stem cells reside in microenvironments called "niches" that produce signals to maintain the stem cells (Ohlstein et al. 2004). Niche size and signaling output must be tightly regulated to maintain stem cells and normal homeostasis (Zhang et al. 2003). Misregulation of the niche signaling can result in uncontrolled proliferation and cancer formation.

An excellent model to study the regulation of niche signaling is the germline stem cell niche of the *Drosophila* ovary as each cell type within the germarium can be identified in a single cell resolution. Two to three germline stem cells reside next to their somatic niche made of cap cells and terminal filament cells. Decapentaplegic (dpp), a BMP homologue from the cap cells, initiates a Smad signaling cascade in the germline stem cells that represses *bag of marbles* (*bam*) a key differentiation factor and maintains

the germline stem cells (McKearin and Spradling 1990; Xie and Spradling 1998; Chen and McKearin 2003a). Lining the anterior sides of the germarium, next to the cap cells are the inner germarial sheath cells (IGS) or escort cells (EC). These escort cells have thin cytoplasmic processes that envelop the differentiating cysts and are thought to support early germ cell differentiation (Decotto and Spradling 2005; Morris and Spradling 2011). Ectopic activation of *dpp* in the surrounding somatic cells results in an expansion of stem cells (Xie and Spradling 1998).

There are multiple mechanisms in place to ensure that the niche signal is silenced in the surrounding somatic cells. Dpp has been shown to be spatially restricted to the niche cells by the activation of EGFR-MAPK signaling pathway in the surrounding somatic cells (Liu et al. 2010). This signaling pathway represses *dally*, a glypican that is required for Dpp transport and stability within the niche (Guo and Wang 2009; Hayashi et al. 2009). Previously, we have shown that histone demethylase Lsd1 (Shi et al. 2004) functions to silence dpp signaling in the escort cells (Eliazer et al. 2011). Loss of Lsd1 in the escort cells results in an upregulation of Dpp signaling and exhibits a non-cell autonomous stem cell expansion phenotype in the germline.

Lsd1 is required for the differentiation of mouse embryonic stem cells by silencing genes that are important for self-renewal (Whyte et al. 2012). Here we show a similar conserved mechanism, where Lsd1 functions in the escort cells to silence the niche signals for normal tissue homeostasis to occur. For the first time, I have performed ChIP seq analysis on the small population of escort cells *in vivo* and show functional

targets of Lsd1 in the escort cell genome. I have identified *engrailed* (*en*), a homeodomain containing factor (Ades and Sauer 1994) as a direct target of Lsd1, which functions upstream of the niche signal Dpp.

MATERIALS AND METHODS:

Drosophila Stocks

Drosophila stocks were maintained at room temperature on standard cornmeal-agar medium unless specified otherwise. The following fly strains were used in this study: w1118 was used as a control; $Lsd1^{\Delta N}$ was provided by N. Dyson (Massachusetts General Hospital Cancer Center, Charlestown, MA); *hh-gal4* was provided by J. Jiang (University of Texas Southwestern, Dallas, TX); *c587-gal4* and *Dad-LacZ* were provided by A. Spradling (Carnegie Institute for Science, Baltimore, MD); *UAS- en GFP* (1608 and 1908) lines were provided by Florence Maschat (Institute of Human Genetics, France). en^{7}, en^{4}, en^{spt}, *UAS-mCD8 GFP*, *UAS-dpp RNAi* (BL-31172, BL-25782, BL-31530 and BL-31531) and *UAS-en RNAi* (BL-33715 and BL-26752) lines were obtained from the Bloomington Stock Center. *UAS-Lsd1- RNAi* (NIG 17149R-2) was obtained from the National Institute of Genetics, Japan.

Cloning of Tagged Transgenes

The HA tagged transgenes of Lsd1 was created using Gateway Cloning (Invitrogen). The open reading frame (ORF) of Lsd1 was cloned into pTHW and pPHW destination vectors. These constructs were injected into flies and transformed using φC31 integrase.

Immunostaining

Adult ovaries were dissected in Grace's medium and fixed in 4% (vol/vol) formaldehyde for 10 min. The ovaries were washed with PBT (PBS, 0.5% BSA, and 0.3% Triton-X 100) and stained with primary antibody overnight at 4°C. The ovaries were washed and incubated in secondary antibody at room temperature for 5h. Ovaries were then washed again and mounted in Vectashield containing DAPI (Vector Laboratories). The following primary antibodies were used: mouse anti-1B1 (Hts) (1:20), mouse anti-Lamin C LC28.26 (1:20), mouse engrailed 4D9 (1:20) and rat VASA (1:20) (Developmental Studies Hybridoma Bank), mouse anti-β-galactosidase (1:100) (Promega). Fluorescence-conjugated secondary antibodies (Jackson Laboratories) were used at a dilution of 1:200.

RNA Isolation and RT-PCR

RNA was isolated from *bamΔ86* and *Lsd1*$^{\Delta N}$ *bamΔ86* mutant ovaries using TRIzol (Invitrogen). The RNA was treated with DNase and subjected to RT-qPCR reaction using the Superscript III First-Strand Synthesis SuperMix (Invitrogen).

The primers used to amplify engrailed mRNA are as follows:

engrailed forward: 5' - GCCCGCCTGGGTGTACTG

engrailed reverse: 5' - CGCTTCTCGTCGTTGGTCTTG

Chromatin Immunoprecipitation and sequencing (ChIP-seq)

Ovaries were dissected and fixed in 1% formaldehyde at RT for 10 mins. The crosslinking is stopped by the addition of glycine solution at a final conc. of 0.125M. The

ovaries were washed three times with 1X cold PBS buffer and then sonicated in ChIP Sonication Buffer (1%Triton X-100, 0.1% Deoxycholate, 50mM Tris 8.1, 150mM NaCl, 5mM EDTA) to achieve a final DNA length of 100 to 600 base pairs. The sonicated sample is then blocked by adding Protein G agarose beads and incubating at 4^{o}C for one hour. The beads were removed. 1% of the sample is kept aside as INPUT and to the remaining sample 3ug rabbit-HA antibody (Abcam) was added and incubated overnight at 4^{o}C.

The next day protein agarose G beads were added and incubated for 3 hours at 4^{o}C. The beads are then washed well with ChIP Sonication Buffer, High Salt Wash Buffer (1% Triton X-100, 0.1% Deoxycholate, 50mM Tris 8.1, 500mM NaCl, 5mM EDTA), LiCl Immune Complex Wash Buffer and TE buffer. The protein bound to the beads is eluted using Elution Buffer (1% SDS, 0.1M $NaHCO_3$). The elution buffer was added to the INPUT samples and they were treated the same as the IP samples from this point. 20µl of 5M NaCl is added to 500µl of elution buffer and incubated at 65^{o}C overnight.

The third day, the sample is treated with RNase, Proteinase K and then DNA is isolated using Qiagen PCR Purification kit. The immunoprecipitated DNA and their INPUT were then sent to the Core facility to be prepared and sequenced. The initial bioinformatics after sequencing was done by the Core facility.

RNA-sequencing (RNA-seq)

The ovaries were dissected in Grace's medium containing 10% normal goat serum. The ovaries were then washed with cell dissociation buffer (Sigma) and digested with 4mg/ml elastase for 20 min at RT. The dissociated cells were filtered (50µM) and pelleted by centrifugation at 500 g for 5 min. The cell pellet was resuspended in PBS with 0.5% BSA and 2mM EDTA. 30 µl of CD8 magnetic beads were added to the cell suspension and rotated gently at 4°C for 15 min. The cells were centrifuged and resuspended in PBS with 0.5% BSA and 2mM EDTA. The cell suspension was then loaded onto the buffer-equilibrated magnetic column (through the filter). After the cell solution passed through, the column was washed with 1ml PBS plus 0.5%BSA, 2mM EDTA, three times. The column was removed from the MACS separator and using a plunger the cell fraction was eluted with 0.5 ml PBS plus 0.5% BSA, 2mM EDTA. The cell suspension was loaded onto a second column or (a third), washed and eluted as before. The cells were centrifuged and the cell pellet was resuspended in TRIzol (Invitrogen). RNA was isolated and sent to the core facility to be prepared and sequenced.

The RNA-seq reads were aligned to the genome using Bowtie. Cufflinks assembled the transcripts and the differential expression between the control and experimental samples was analyzed by Cuffdiff.

RESULTS AND DISCUSSION

Defining the targets of Lsd1 in escort cells:

To define the transcriptional targets of Lsd1 in the escort cells, I performed Chromatin Immunoprecipitation sequencing (ChIP-seq) analysis of Lsd1. I wanted to compare the binding sites of Lsd1 in the escort cell population to the binding sites in the cap cell population. Lsd1 is expressed by all the cells of the germarium in the *Drosophila* ovary (Eliazer et al. 2011), which made it impossible to use the Lsd1 antibody for immunoprecipitating from specific cell types. Therefore I made two different HA tagged transgenes of Lsd1; *pPHW-Lsd1* that expresses highly in the germline and less efficiently in the somatic cells and *pTHW-Lsd1* that expresses highly in the somatic cells. These HA tagged trangenes were expressed in the cap cells using *hh- gal4* (Forbes et al. 1996a; Pan et al. 2007) and in the escort cells using the *c587 gal4* driver (Zhu and Xie 2003; Song et al. 2004). ChIP was performed for the HA protein. The immunoprecipitated samples were compared to its INPUT as control. Model Based Analysis of ChIP-Seq data (MACS) was used to analyze the data and WIG files were generated (Zhang et al. 2008). These WIG files were used to view peaks of Lsd1 binding with the UCSC genome browser. I identified 109 unique binding sites for Lsd1 in the escort cells and 24 shared peaks in both the cap cell and escort cell population (Figure 1). It was surprising to observe that no unique Lsd1 binding site was seen in the cap cell population (The ChIP-seq data containing the Lsd1 binding sites in the cap cells and escort cells are presented in Appendix B).

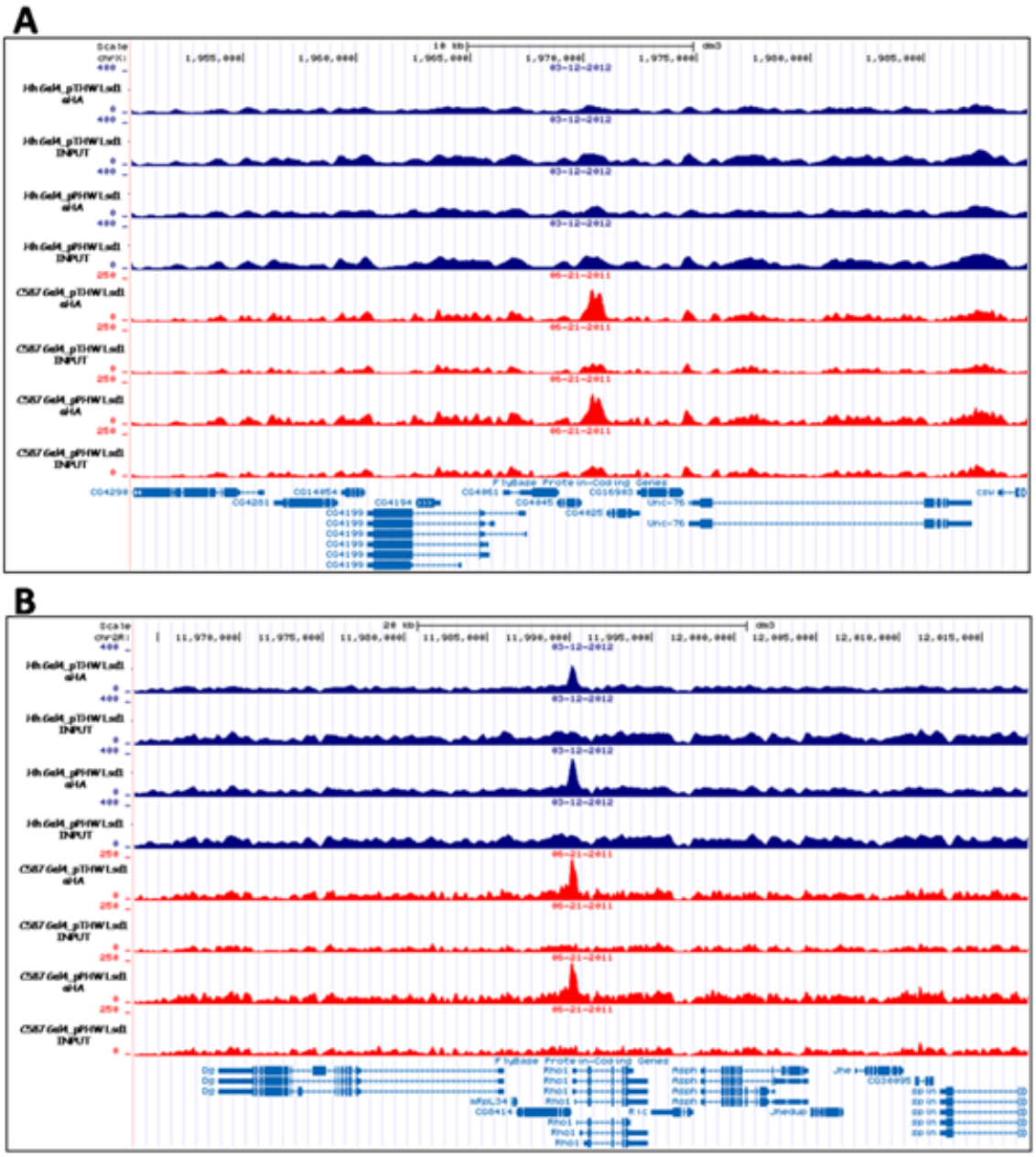

Figure 1. Screenshots of Lsd1 binding in the escort cell (red) and cap cell population (blue) (A) Screenshot of Lsd1 binding sites on coordinates chrX:1,950,083-1,989,589 showing an Lsd1 binding site only in the escort cells. (B) Screenshot of Lsd1 binding sites on coordinates chr2R:11,963,615-12,017,875 showing an Lsd1 binding site in both cap cell and escort cell population.

To functionally validate the Lsd1 ChIP-seq data in the escort cells, I performed RNA-sequencing (RNA-seq) analysis on wild type (WT) escort cells and on escort cells

where the expression of *Lsd1* is knocked down using an *Lsd1 RNAi*. The WT flies and *Lsd1 RNAi* flies were crossed to *c587 gal4; UAS-mCD8* flies to express the mouse CD8 antigen on the cell surface of escort cells and early follicle cells. These cells were isolated using mCD8 magnetic beads, RNA was isolated and the transcriptional profile of the WT cells and the Lsd1 knockdown cells were generated by RNA- sequencing. I observed the changes in gene expression of genes near the Lsd1 binding site (The RNA-seq data for genes that display significant differences between the WT and Lsd1 knockdown escort cells are presented in Appendix B). There were only 40 Lsd1 binding sites in the escort cells that caused significant changes in neighboring gene transcription between WT and *Lsd1* knockdown cells. This might be due to the reason that I used *Lsd1* knockdown escort cells instead of *Lsd1* null. I am not sure how much Lsd1 is still present in these cells even though the knockdown caused a stem cell expansion phenotype in the germ cells.

RNA-seq data of genes with significant differences revealed that Lsd1 mainly acts by silencing neighboring genes. In few instances such as seen in the binding to *tramtrack* (*ttk*) and *broad* (*br*) gene, Lsd1 binds to the first intron and functions as an activator of gene expression.

Engrailed is a target of Lsd1

One of the targets of Lsd1 is *engrailed*, a homeo domain transcription factor (Ades and Sauer 1994). Engrailed is expressed by the cap cells and terminal filament cells of the germarium. During the development of terminal filament cells, engrailed is

needed for the proper morphogenesis of these cells (Bolivar et al. 2006). In the cap cells, engrailed functions to maintain the germline stem cells (Rojas-Rios et al. 2012). Based on the ChIP seq data, Lsd1 binds to the 2kb region of the *engrailed* promoter in the escort cells but fails to bind in the cap cells (Figure 2A). I performed RNA RT-qPCR to look at the transcript levels of *engrailed* in Lsd1 mutants. I compared *bam* mutants to *bam-lsd1* double mutants as they are comparable in size. The *bam* mutants are blocked in differentiation and they have a stem cell expansion phenotype. The *engrailed* transcript levels are up-regulated 6 fold in *bam-lsd1* double mutants (Figure 2B). Also, I see *engrailed* transcript levels upregulated 4 fold in the *bam-lsd1* double mutants when compared to *bam* mutants by micro-array (Appendix A). I crossed in a transcriptional reporter en^{Xho25} that has 5.7 base pairs of promoter region fused to the lacZ reporter (Hama et al. 1990) in the *lsd1* mutants and looked at the β-galactosidase expression pattern in the mutants when compared to wild-type controls. I observed β-galactosidase staining only in the cap cells and terminal filament cells in the wild type germarium. Whereas in the *lsd1* mutant germaria, I noticed that the escort cells are expressing β-galactosidase, indicating that Lsd1 negatively regulates the expression of *engrailed* in the escort cells (Figure 2C and D).

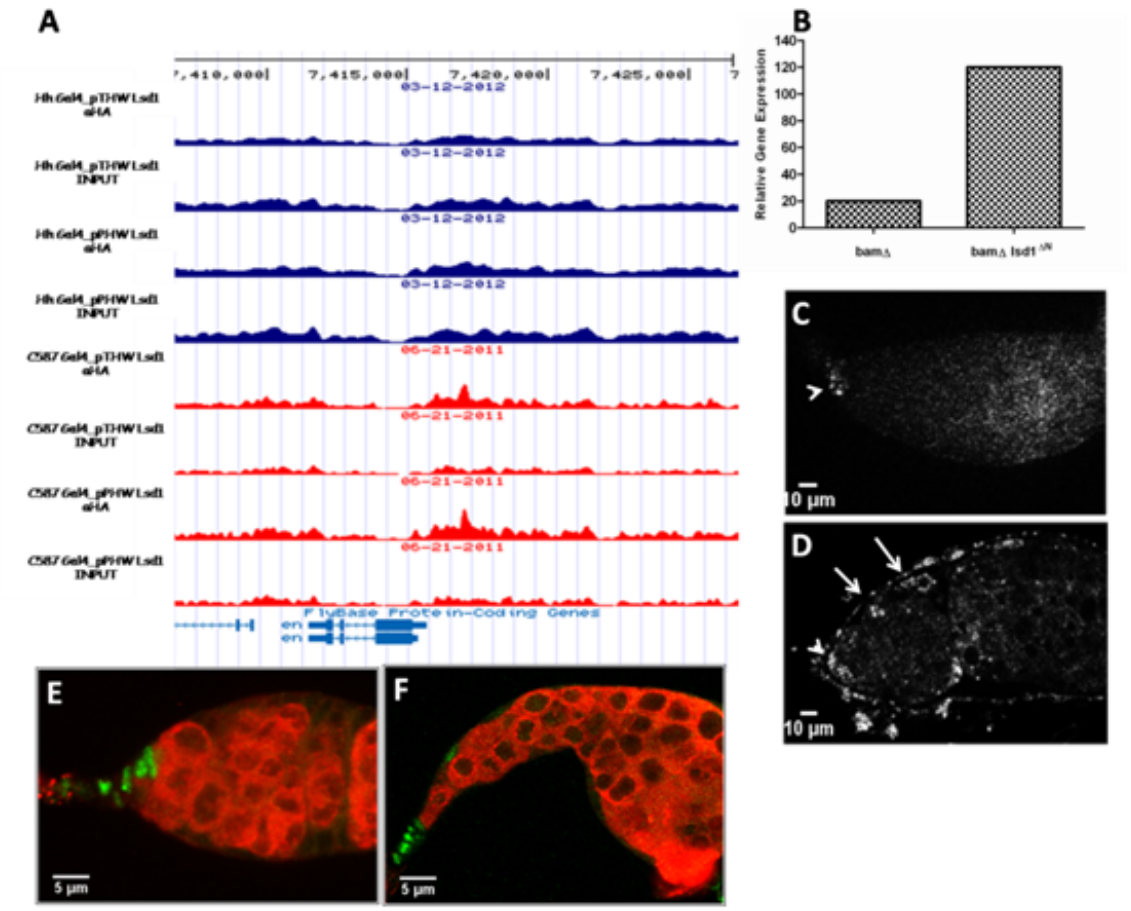

Figure 2. Lsd1 silences *engrailed* gene expression in the escort cells. (A) Screenshot of Lsd1 binding to the *engrailed* promoter in escort cells. (B) RNA RT-qPCR of *engrailed* transcripts comparing *bam*Δ mutants to *bam*Δ-*lsd1*$^{\Delta N}$ double mutants. (C, D) β-galactosidase staining (white) reporting the expression of 5.7kb of engrailed promoter fused to lacZ gene. (C) *en*^{Xho25} germaria and (D) *en*^{Xho25}*/+; Lsd1*$^{\Delta N}$*/Lsd1*$^{\Delta N}$ germaria. Arrows point to escort cells and arrowheads point to cap cells. (E) WT and (F) *Lsd1*$^{\Delta N}$*/Lsd1*$^{\Delta N}$ germaria stained with En (green) and VASA (red).

The protein expression of engrailed in wild type and *Lsd1* mutant ovarioles were analyzed by immunofluorescence staining. In the wild type ovarioles Engrailed is expressed in the cap cells and terminal filament cells (Bolivar et al. 2006; Rojas-Rios et al. 2012). In the *Lsd1* mutants I expected to see Engrailed expression in the escort cells as well, but on the contrary I observed very few ovarioles expressing high levels of Engrailed protein in the escort cells (Figure 2E and F). The high expressers of Engrailed

were the anterior most escort cells. This suggests that in the escort cells, Engrailed is also regulated at the translational level.

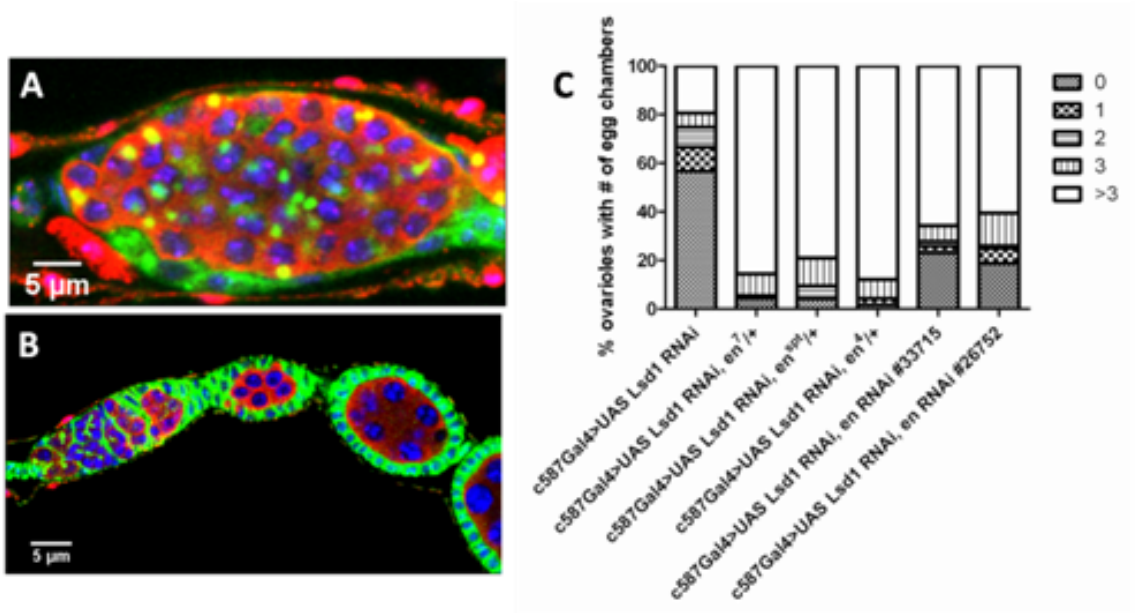

Figure 3. Knocking down *engrailed* in the escort cells suppresses an *Lsd1* RNAi phenotype. (A) *c587 gal4/+; UAS Lsd1 RNAi/+* (B) *c587 gal4/+; UAS Lsd1 RNAi/+; UAS En RNAi* BL 33715/+ germaria are stained with Hts (green), VASA (red) and DNA (blue). (C) Graph shows the percentage of ovarioles that contained a given number of developing egg chambers for each genotype. Reducing *engrailed* levels by *engrailed RNAi* and by one copy of *engrailed* mutants suppressed the *c587 gal4/+; UAS Lsd1 RNAi/+* phenotype. c*587 gal4/+; Lsd1 RNAi/+* (n=171); c*587 gal4/+; Lsd1 RNAi/ en*^{7} (n=90); *c587 gal4/+; Lsd1 RNAi/ en*^{spt} (n=95); *c587 gal4/+; Lsd1 RNAi/ en*^{4} (n=115); *c587 gal4/+; UAS Lsd1 RNAi/+; UAS En RNAi* BL 33715/+ (n=108); *c587 gal4/+; UAS Lsd1 RNAi/+; UAS En RNAi* BL 25752/+ (n=96).

Since the *engrailed* transcripts are upregulated in the lsd1 mutant escort cells, I knocked down the expression of engrailed in the lsd1 knockdown background. Normally, driving *Lsd1 RNAi* in the escort cells using the *c587 gal4* driver causes 50% of the ovarioles to have no egg chambers and the entire germarium is filled with stem cells (Figure 3A,C). Reducing the levels of *engrailed* using either one copy of *engrailed*

mutants or *engrailed RNAi* suppressed the mutant phenotype and resulted in the formation of more maturing egg chambers (Figure 3B,C).

Misexpression of *engrailed* in the escort cells has a stem cell expansion phenotype

To assess whether engrailed regulates germline stem cells, I expressed *engrailed* in the escort cells using the *c587 gal4* driver. Ectopic expression of *engrailed* displayed a stem cell expansion phenotype in the germarium (Figure 4B). The ovarioles did form egg chambers but the mutants failed to lay viable eggs. The stem cell expansion phenotype was only 50% penetrant as it is known that excessive Engrailed has a dominant negative effect (personal communication with Gary Struhl).

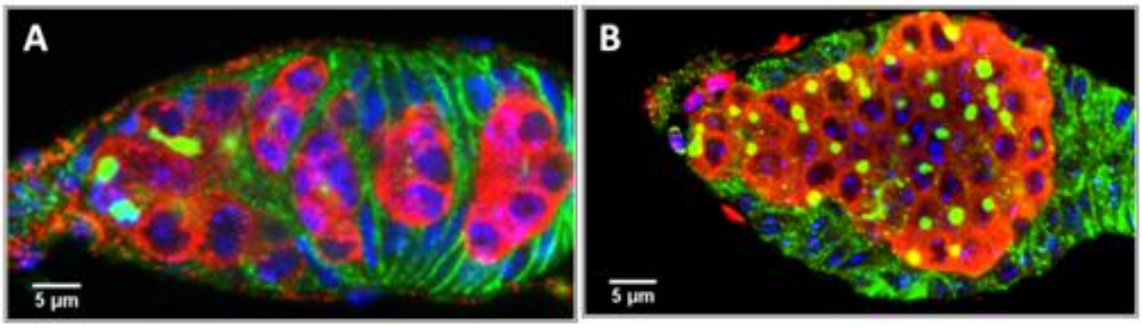

Figure 4. Ectopic expression of engrailed in the escort cells causes an expansion of stem cells in the germline. (A) WT and (B) *c587/+; UAS en/+* germaria stained with Hts (green), VASA (red) and DNA (blue). Misexpression of *engrailed* in the escort cells results in an increase in the number of stem cells.

Engrailed is upstream of dpp, the niche signal

In other tissues of *Drosophila* such as genital discs and wing discs, Engrailed positively regulates the expression of *dpp* through a hedgehog (hh) dependent pathway (Zecca et al. 1995; Emerald and Roy 1998). I wanted to see if Engrailed is upstream of

dpp in our model system. To verify if there is an expansion of Dpp signaling in the over-expression of *engrailed* ovarioles, I looked at Dad, a downstream target of Dpp. *Dad-lacZ* enhancer trap was used as a positive transcriptional reporter of Dad. In the control ovarioles, Dad is highly expressed in the stem cells and its expression is lowered in the differentiating cysts (Figure 5A). When *engrailed* is misexpressed in the escort cells, more cells in the germarium are positive for *Dad-lacZ*, indicating that there is an increase in Dpp signaling (Figure 5B).

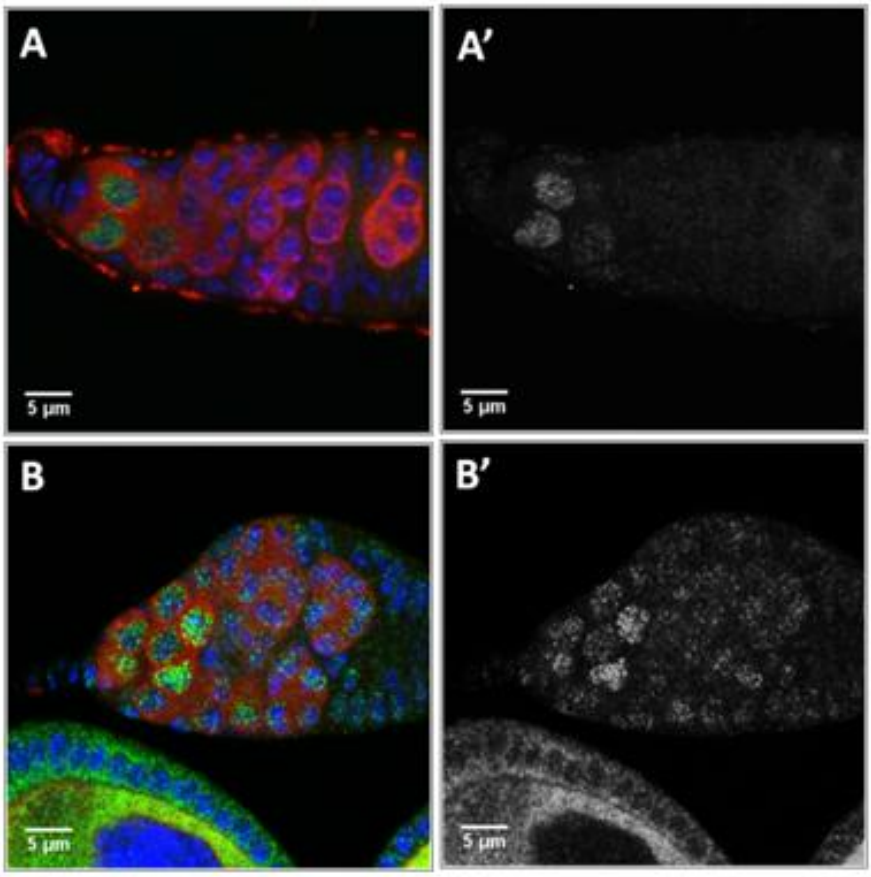

Figure 5. Overexpression of *engrailed* in the escort cells results in expanded Dpp signaling. (A, A') Control germaria and (B, B') Overexpression of *engrailed* germaria stained with *DAD-lacZ* (green), VASA (red) and DNA (blue). Overexpressing *en* results in expanded *Dad-lacZ* expression in germline cells.

I further knocked down the expression of *dpp* in the escort cells that are misexpressing *engrailed* using a *c587 gal4* driver and was able to suppress the phenotype (Figure 6). I was also able to rescue the sterility defect of the animals that ectopically expressed *engrailed*. This experiment suggest that engrailed functions upstream of dpp.

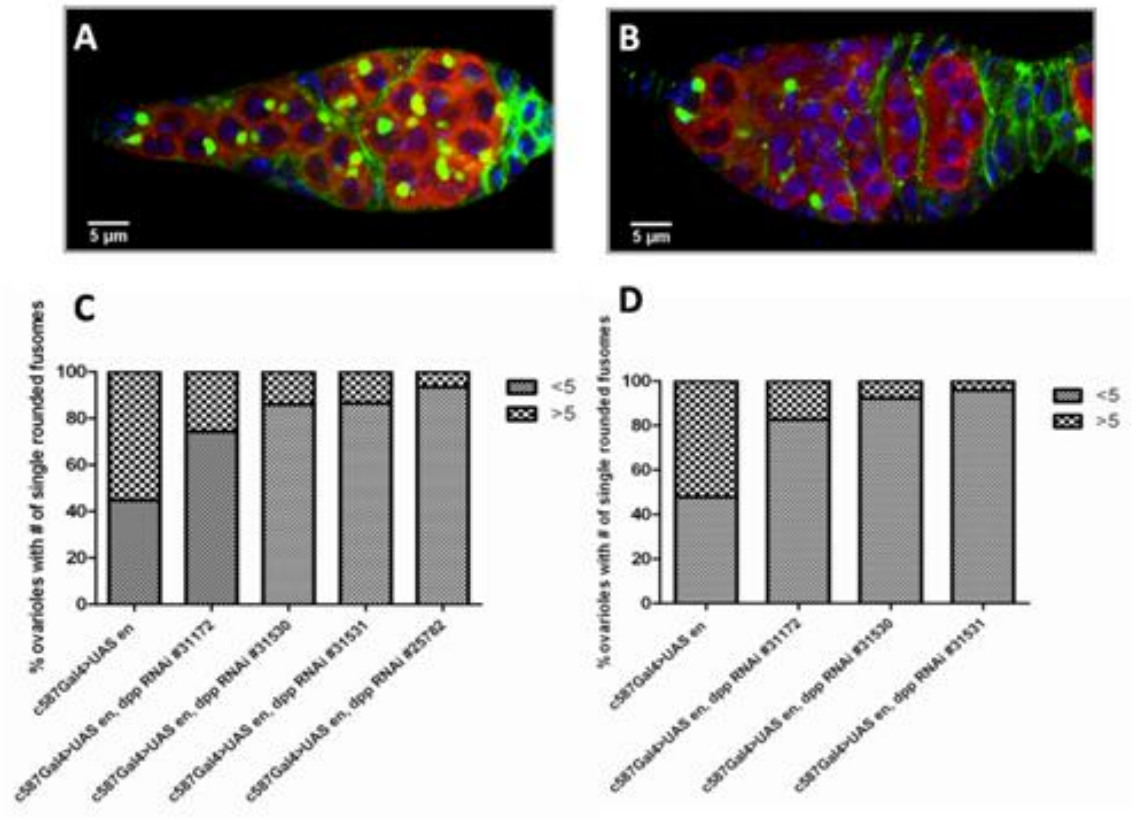

Figure 6. Knocking down *dpp* in the escort cells suppresses the overexpression of *engrailed* phenotype. (A) *c587 gal4/+; UAS en/+* (B) *c587 gal4/+; UAS en/+; UAS dpp RNAi* BL 31531/+ germaria are stained with Hts (green), VASA (red) and DNA (blue). (C, D) Graph shows the percentage of ovarioles that contained a given number of single rounded fusomes for each genotype. (C) Experiment is done with *UAS en 1608*: *c587 gal4/+; UAS en 1608/+* (n=47); *c587 gal4/+; UAS en/+; UAS dpp RNAi* BL 31172/+ (n=97); *c587 gal4/+; UAS en/+; UAS dpp RNAi* BL 31530/+ (n=57); *c587 gal4/+; UAS en/+; UAS dpp RNAi* BL 31531/+ (n=74); *c587 gal4/+; UAS en/+; UAS dpp RNAi* BL 25782/+ (n=76). (D) Experiment is done with *UAS en 1908*: *c587 gal4/+; UAS en 1908/+* (n=111); *c587 gal4/+; UAS en/+; UAS dpp RNAi* BL 31172/+ (n=46); *c587 gal4/+; UAS en/+; UAS dpp RNAi* BL 31530/+ (n=38); *c587 gal4/+; UAS en/+; UAS dpp RNAi* BL 31531/+ (n=120). Reducing *dpp* levels by using *dpp RNAi* suppressed the *c587 gal4/+; UAS en* phenotype.

I had previously showed that overexpression of *dpp* in the escort cells of the germarium results in a fate change where these escort cells are expressing cap cell markers such as Lamin C (Eliazer et al. 2011). I wanted to see if over-expressing *engrailed* in the escort cells led to the misexpression of cap cell markers. I stained the wild type and mutant ovarioles for Lamin C. Lamin C is normally expressed in the cap cells and terminal filament cells (Song et al. 2004; Song et al. 2007). I did not see Lamin C expressed in the escort cells of the mutant ovarioles. Overexpressing *engrailed* in the escort cells leads to an induction of dpp expression but there needs to be a threshold level of dpp expression for the escort cells to convert to a cap cell fate and express cap cell markers.

This study shows that Lsd1 functions in the escort cells to silence dpp, the niche signal from inappropriately being expressed in cells that are not niche cells. Lsd1 directly silences *engrailed*, a homeo domain factor that is upstream of dpp. In the cap cell population I have shown by ChIP-seq that Lsd1 is not recruited to the *engrailed* promoter and hence there is expression of engrailed in the cap cells and terminal filament cells. It has been shown that Polycomb Group Proteins bind to the conserved Polycomb Response Elements (PREs) in the *engrailed* promoter region and regulates its transcription (DeVido et al. 2008; Chen and Rasmuson-Lestander 2009). Also in Hela cells, Lsd1 interacts with E(z) and Su(z)12, that are components of the PRC2 complex of Polycomb genes (Tsai et al. 2010). I have shown that knockdown of *E(z)* and *Su(z)12* in the escort cells have a stem cell expansion phenotype (Chapter 4). I need to investigate this further and see if

Polycomb group proteins are required for recruiting Lsd1 to the *engrailed* promoter in the escort cells.

In summary, I have identified and functionally validated Lsd1's potential targets in the escort cell population of the *Drosophila* ovary. This comprehensive genome wide set of candidate genes will facilitate further studies of genes that need to be silenced or activated in the escort cells to enable differentiation of the daughter germline stem cells.

In vertebrates, Engrailed 1 and Engrailed 2 were identified based on their sequence similarity to *Drosophila* Engrailed. The Engrailed genes play an important role in development and dysfunction of these genes result in disease. Engrailed 1 mutant mouse dies soon after birth and exhibits multiple developmental defects (Wurst et al. 1994). Overexpression of Engrailed leads to cancer progression and metastasis (Bose et al. 2008; Morgan et al. 2011). In higher organisms, Lsd1 might have functional implications in silencing Engrailed and needs to be investigated further.

CHAPTER 4

SCREEN FOR CHROMATIN FACTORS FUNCTIONAL IN THE ESCORT CELLS OF THE *DROSOPHILA* OVARY

INTRODUCTION

In eukaryotes, meters of genomic DNA is compacted with histone proteins and packaged into the nucleus of a cell. The fundamental building block of chromatin structure are the nucleosomes (Kornberg 1974) that are made of ~147 base pairs of DNA wrapped around two molecules each of core histone proteins H2A, H2B, H3 and H4 (Kornberg and Thomas 1974; Kornberg 1977; Luger et al. 1997). The linker DNA between nucleosomes is stabilized by the presence of a linker histone H1. These H1 histones interact with each other and further condense the DNA into a complex higher order chromatin fibre (Bednar et al. 1998; Bustin et al. 2005). The extensive packaging of the DNA is thought to limit accessibility to basal and regulatory factors for the purposes of transcription, replication, repair and recombination. However, the chromatin structure is very dynamic and continuously changes in response to biological stimuli.

Alterations in the chromatin structure occur by two major mechanisms: The first mechanism is by post translational histone modifications and the second mechanism is by nucleosomal reorganization. The core histones H2A, H2B, H3 and H4 have N-terminal tails that are post translationally modified by methylation, acetylation, phosphorylation, ubiquitination and sumoylation. These modifications define the affinity between histones and their associated DNA. Nucleosomal reorganizations occur by ATP-dependent chromatin remodeling complexes that use the energy from ATP hydrolysis to weaken the interaction between histones and DNA and repositions the histones (Peterson and

Tamkun 1995; Tsukiyama and Wu 1995; Lusser and Kadonaga 2003; Martens and Winston 2003).

The modifications on histones and their positioning cause the genome to organize into a closed or open conformation, thus regulating the accessibility of DNA for gene transcription, replication and repair. Dysfunction of these enzymes that catalyze the post translational modifications and chromatin remodeling proteins results in an array of human diseases including cancer (Petrij et al. 1995; Gayther et al. 2000; Davis and Brackmann 2003).

In this study, I performed a small-scale screen to identify chromatin factors that play a role in restricting niche signaling in the *Drosophila* ovary. Decapentaplegic (Dpp), a BMP homolog from the cap cells initiates a signaling cascade in the germline stem cells (GSCs) that represses *bag of marbles* (*bam*), a key differentiation factor (Xie and Spradling 1998; Xie and Spradling 2000; Chen and McKearin 2003a). Ectopic expression of *dpp* in the surrounding somatic cells resulted in an expanded population of germline stem cells (Xie and Spradling 1998) and caused the escort cells to adopt a cap cell fate (Eliazer et al. 2011).

Previously, I had shown that Lysine Specific Demethylase 1 (Lsd1), a histone demethylase functions to limit niche signaling by silencing dpp in the escort cells. Loss of Lsd1 in the escort cells results in an inappropriate expression of dpp leading to a cell nonautonomous expansion of GSCs (Eliazer et al. 2011). I wanted to identify additional

chromatin factors that might play a role in restricting niche size and signaling output. The results of a screen for chromatin factors that are required in the escort cells and early follicle cells are summarized in this chapter.

MATERIALS AND METHODS

Drosophila Stocks:

Drosophila stocks are maintained at room temperature on standard cornmeal agar medium. The RNAi crosses were set at room temperature, 5 days later were moved to 29^{o}C and kept there till the progeny flies eclosed. The following fly strains were used in this study:

c587-gal4 flies were provided by A. Spradling;

Methyltransferases: **CG1868**- NIG 1868R-3; **Blimp1**- NIG 5249R-2; **pr-Set7**- NIG 3307R-3; **E(z)**- NIG 6502R-4; **Su(var)3-9**- NIG 6476R-1, NIG 6476R-2, NIG 6476R-2; **Set2**- BL 24108, BL 31355; **CG3353**- NIG 3353R-1, NIG 3353R-2, BL 28609; **dG9a**- BL 24107, BL 29541, BL 31630; **eggless**- NIG 12196R-1, NIG 12196R-4, BL 24106, BL 31352; **ash1**- BL 31050.

Histone Demethylases: **Lsd1**- NIG 17149R-2; **CG33182**- NIG 4037R-2; **Lid**- NIG 9088R-1, NIG 9088R-2, BL 27532, BL 28944; **CG7200**- NIG 7200R-3; **CG11033**- BL 31360; **CG2982**- NIG 2982R-1, NIG 2982R-6; **Jarid2**- NIG 3654-3R-3, BL 26184; **CG8165**- NIG 8165R-1.

Histone Acetyltransferases: **Tip60**- NIG 6121R-1, NIG 6121R-4; **mof**- NIG 3025R-2, NIG 3025R-3, BL 31401; **Chameau**- BL 27027; **Pcaf**- NIG 4107R-1; **Enok**- NIG 11290R-1.

Histone Deacetylases: **Sirt2**- NIG 5085R-3, NIG 5085R-5, BL 31613; **Sir2**- NIG 5216R-1, NIG 5216R-2, BL 31636; **Sirt4**- BL 31638; **Sirt6**- NIG 6284R-2, NIG 6284R-4, BL 31399; **Sirt7**- BL 31093; **HDAC3**- BL 31633; **Rpd3**- BL 31616; **HDAC4**- BL 28549; **HDAC6**- BL 31053; **HDACX**- NIG 31119R-2.

Ubiquitin Ligases: **Sex combs extra**- NIG 5595R-1, NIG 5595R-2, BL 31612; **Neuralized (neur)**- NIG 11988R-1, NIG 11988R-3, BL 26023; **NEDD4**- BL 31687; **DIAP1**- NIG 12284R-2; **Deltex**- NIG 3929R-1, NIG 3929R-2; **Suppressor of deltex**- NIG 4244R-2; **Sina Homologue**- NIG 13030R-3; **Seven in absentia**- NIG 9949R-1, NIG 9949R-2.

Trithorax: **Absent, Small or Homeotic discs 1**- BL 31050; **Absent, Small or Homeotic discs 2**- NIG 6677R-1; **Brahma**- BL 31712; **Osa**- NIG 7467R-1, NIG 7467R-3, BL 31266; **ISWI**- NIG 8625R-1, NIG 8625R-2, BL 31111; **Little Imaginal Discs**- NIG 9088R-1, NIG 9088R-2, BL 27532, BL 28944; **Lola Like**- BL 31632; **Trithorax**- BL 31092; **Trithorax like**- NIG 9343R-1, NIG 9343R-2; **Taranis**- NIG 6889R-1, NIG 6889R-2, BL 31634.

Brahma complex of trithorax group proteins: **Brahma (Brm)**- BL 31712; **Dalao**- NIG 7055R-3; **Domino (dom)**- NIG 9696R-1, NIG 9696R-3; **Eyelid (also called osa)**- NIG 7467R-1, NIG 7467R-3, BL 31266; **ISWI**- NIG 8625R-1, NIG 8625R-2, BL 31111; **Nurf-38**- NIG 4634R-2.

Brahma Associated Proteins: Brahma Associated Protein 55kD- NIG 6546R-1, BL 31708; **Brahma Associated Protein 60kD**- NIG 4303R-1; **Brahma Associated Protein 170kD**- BL 26308.

Polycomb: **Additional sex combs**- BL 31192; **Chameau**- BL 27027; **Cramped**- NIG 2714R-3; **Enhancer of Polycomb**- NIG 7776R-2, BL 28686; **Pipsqueak**- NIG 2368R-1, BL 28693; **Pleiohomeotic**- NIG 17743R-4, BL 31609; **Scm-related gene containing four mbt domains**- BL 28677; **Suppressor of zeste 2**- BL 31335, BL 31346.

PRC1 complex of Polycomb group proteins: **Polycomb**- NIG 32443R-1; **Polyhomeotic distal**- BL 31190; **Polyhomeotic proximal**- NIG 18414R-2; **Posterior sexcombs**- NIG 3886R-1, BL 31611; **Reptin**- NIG 9750R-2; **Sex combs extra**- NIG 5595R-1, NIG 5595R-2, BL 31612.

Esc-E(z) complex of Polycomb group proteins (PRC2): **Enhancer of zeste (E(z))**- NIG 6502R-4; **Extra sexcombs (Esc)**- NIG 14941R-2; **Suppressor of Zeste 12 (Su(z)12)**- BL 31191.

SAGA related complex: Ada2b- NIG 9638R-3; **Nipped-A**- NIG 2905R-3, BL 31255; **pCaf**- NIG 4107R-1; **Taf10**- NIG 2859R-5, NIG 2859R-6.

Suppressors and Enhancers of Variegation: Structure specific recognition protein (ssrp)- NIG 4817R-1; **Su(var)205 (HP1)**- NIG 8409R-4; **Suppressor of variegation 3-7**- NIG 8599R-3; **Suppressor of variegation 3-3 (Lsd1)**- NIG 17149R-2; **Suppressor of variegation 3-9**- NIG 6476R-1, NIG 6476R-2, BL 31619; **Suppressor of hairy wing**

Su(hw)- NIG 8573R-2, NIG 8573R-3; **Su(var)2/ HP2**- BL 25972; **Su(var)2-10**- BL 29448; **Su(var)3-1/JIL-1**- NIG 6297R-1, NIG 6297R-4; **E(var)3-9**- BL 31948.

Chromatin Remodeling Complexes:

Histone Chaperones: Nucleoplasmin (NLP)- NIG 7917R-3; **Nucleosome Assembly Protein-1 (dNap1)**- NIG 5330R-1, NIG 5330R-2; **Spt6**- NIG 12225R-3; **DEK**- BL 28696; **Anti silencing factor 1 (ASF1)**- NIG 9383R-1; **HirA (Histone regulatory Protein A)**- NIG 12153R-1, NIG 12153R-3.

Nucleosome Stabilizing factors: dre4 (spt16)- NIG 1828R-2, NIG 1828R-3; **Structure specific recognition protein (Ssrp)**- NIG 4817R-1; **Trithorax like (Trl)**- NIG 9343R-1, NIG 9343R-2.

ATP Utilizing Chromatin Assembly and Remodeling Factor (ACF) complex: ATP-dependent chromatin assembly factor large subunit (Acf1)- NIG 1966R-1, NIG 1966R-3, BL 31340; **ISWI**- NIG 8625R-1, NIG 8625R-2, BL 31111.

Chromatin Remodeling and Assembly Factor (CHRAC) complex: ATP-dependent chromatin assembly factor large subunit (Acf1)- NIG 1966R-1, NIG 1966R-3, BL 31340; **ISWI**- NIG 8625R-1, NIG 8625R-2, BL 31111; **CHRAC-14**- BL 31052.

Nucleosome Remodeling Factor (NURF) complex: Nurf-38- NIG 4634R-2; **ISWI**- NIG 8625R-1, NIG 8625R-2, BL 31111.

The BL lines were obtained from Bloomington Stock Center and NIG lines were obtained from National Institute of Genetics, Japan.

Immunofluorescence:

Adult ovaries were dissected in Grace's medium and fixed in 4% (vol/vol) formaldehyde for 10min. The ovaries were washed with PBT (PBS, 0.5% BSA, and 0.3% Triton-X 100) and stained with primary antibody overnight at 4°C. The ovaries were washed and incubated in secondary antibody at room temperature for 5h. Ovaries were then washed again and mounted in Vectashield containing DAPI (Vector Laboratories). The following primary antibodies were used: mouse anti-1B1 (Hts) (1:20) and rat anti-VASA (1:20) (Developmental Studies Hybridoma Bank). Fluorescence-conjugated secondary antibodies (Jackson Laboratories) were used at a dilution of 1:200.

RESULTS AND DISCUSSION

I performed a small-scale screen to knockdown the expression of various chromatin factors using RNAi. These lines were crossed to *c587-gal4* driver to reduce the expression specifically in escort cells and early follicle cells of the *Drosophila* ovary (Zhu and Xie 2003; Song et al. 2004). To see the expression pattern of this driver, refer to Chapter 2 Figure 6D. Using 151 RNAi lines I knocked down the expression of 127 genes belonging to different classes. This screen is not comprehensive and does not include all the chromatin factors in *Drosophila*. The results of the screen are summarized in this chapter.

Histone Methyltransferases:

This class comprises of enzymes that catalyze the addition of one, two or three methyl groups on lysine and arginine residues of histone tails. Depending on the residue that is modified, histone methylation causes gene activation or gene repression (Jenuwein and Allis 2001; Kouzarides 2002).

Lowering the expression of *E(z)*, the enzyme responsible for adding methylation marks on lysine 9 and 27 (H3K27) (Cao et al. 2002; Czermin et al. 2002) in escort cells and early follicle cells results in an expansion of stem cells in the germarium (Figure 1A). Knockdown of *E(z)* also has follicle cell defects. Normally the follicle cells surrounding the egg chamber are single layered but when the expression of *E(z)* is reduced, it results in multi layered follicle cells.

Knockdown of *eggless*, another histone methyltransferase that adds methyl marks on lysine 9 residues (H3K9) (Clough et al. 2007) results in an expansion of stem cells (Figure 1B).

Gene Name	CG#	Phenotype
CG1868	CG1868	No phenotype
Blimp1	CG5249	No phenotype
CG4565	CG4565	No phenotype
CG8378	CG8378	Not tested
Trithorax	CG8651	Not tested
pr-Set7	CG3307	No phenotype
E(z)	CG6502	Stem cell expansion; Follicle cell defect
CG11160	CG11160	Not tested
Su(var)3-9	CG6476	No phenotype
CG9642	CG9642	Not tested
Set2	CG1716	No phenotype
CG9007	CG9007	Not tested
CG3353	CG3353	No phenotype
dG9a	CG2995	No phenotype
dMES4	CG11301	No phenotype
eggless	CG12196	Stem cell expansion
grappa	CG10272	Not tested
ash1	CG8887	No phenotype

Table 1. Histone Methyltransferases and their phenotypes.

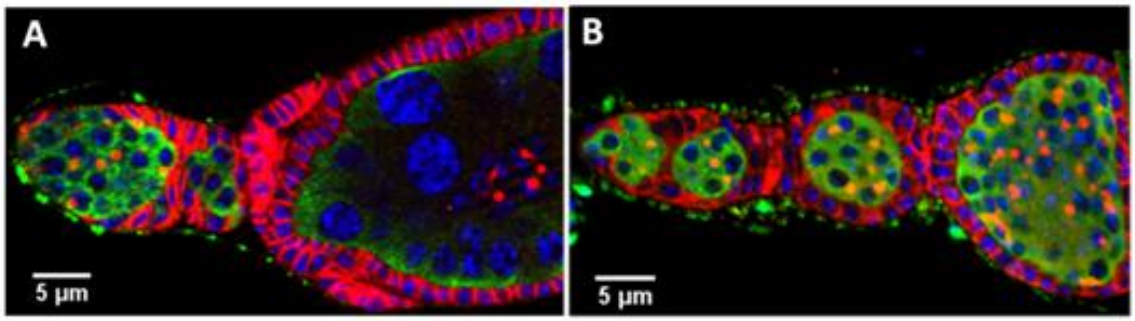

Figure 1. Knocking down histone methyltransferases results in a non-cell autonomous stem cell expansion phenotype. (A) *c587 gal4>UAS E(z) RNAi* (NIG 6502R-4) (B) *c587 gal4>UAS eggless RNAi* (BL 31352). The germaria are stained for Hts (red), VASA (green) and DNA (blue).

Histone Demethylases:

The removal of methylation marks from lysine residues is mediated by enzymes called histone demethylases. Depending on the methyl mark removed, it results in gene activation or gene repression. The one histone demethylase that had a phenotype when knocked down in the escort cells and early follicle cells is *Lsd1*, that removes mono- and di- methyl groups on lysine residue 4 (H3K4) (Figure 2).

Gene Name	CG#	Phenotype
Lsd1	CG17149	Stem cell expansion
CG33182	CG33182	No phenotype
CG15835	CG15835	Not tested
CG13902	CG13902	Not tested
Lid	CG9088	No phenotype
UTX	CG5640	No phenotype
CG5383	CG5383	No phenotype
CG10133	CG10133	Not tested
CG7200	CG7200	No phenotype
CG11033	CG11033	No phenotype
CG2982	CG2982	No phenotype
Jarid2	CG3654	No phenotype
CG8165	CG8165	No phenotype
CG12879	CG12879	Not tested

Table 2. Histone Demethylases and their phenotypes.

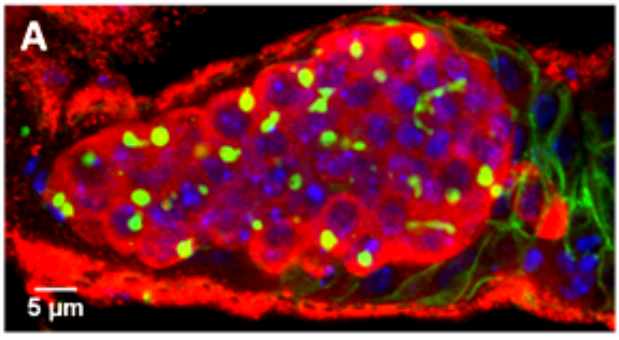

Figure 2. Knocking down histone demethylases results in a non-cell autonomous stem cell expansion phenotype. (A) *c587 gal4>UAS Lsd1 RNAi* (NIG 17149R-2). The germaria are stained for Hts (red), VASA (green) and DNA (blue).

Histone Acetyltransferases:

Histone acetyltransferases add acetyl marks on lysine residues. Histone acetylation is linked mainly to gene activation. Knocking down *Tip60* has a strong stem cell expansion phenotype, where the entire ovariole is filled with stem cells. *Enok RNAi* has a moderate phenotype, where the germarium is filled with stem cells. *Pcaf RNAi* has a very weak stem cell expansion phenotype.

Gene Name	CG#	Phenotype
CG2051	CG2051	Not tested
Tip60	CG6121	Stem cell expansion
mof	CG3025	No phenotype
Chameau (chm)	CG5229	No phenotype
Pcaf	CG4107	Stem cell expansion
Enok	CG11290	Stem cell expansion
CG1894	CG1894	Not tested
CBP	CG1435	Not tested

Table 3. Histone Acetyltransferases and their phenotypes.

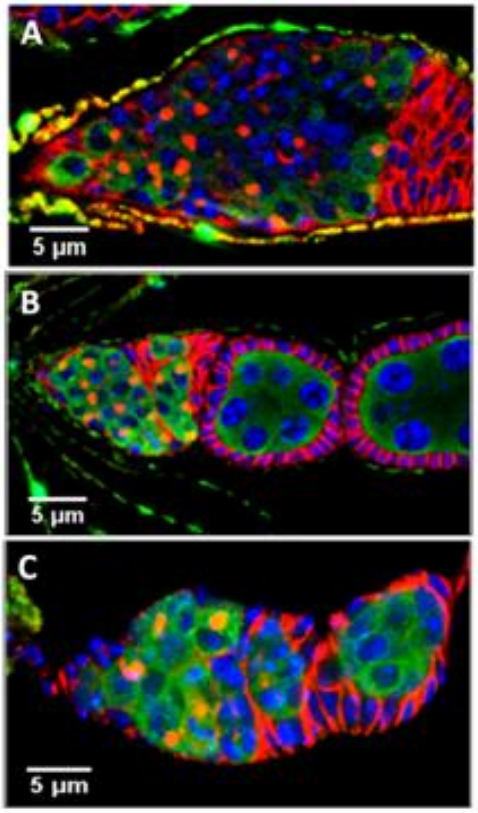

Figure 3. Knocking down histone acetyltransferases results in a non-cell autonomous stem cell expansion phenotype. (A) *c587 gal4>UAS Tip60 RNAi* (NIG 6121R-1) (B) *c587 gal4>UAS enok* RNAi (NIG 11290R-1) (C) *c587 gal4>UAS Pcaf1 RNAi* (NIG 4107R-1). The germaria are stained for Hts (red), VASA (green) and DNA (blue).

Histone deacetylases:

Histone deacetylases remove the acetyl mark from lysine residues and mediate gene repression. Knocking down *Rpd3* has follicle cell defects. An entire egg chamber is divided into two or three smaller egg chambers due to the invagination of follicle cells into an egg chamber (Figure 4A). Also, the ovarioles display counting defects where the number of nurse cells in an egg chamber is more than 15 (Figure 4B), the normal number of nurse cells in a wild type egg chamber. This defect could be caused by fusion of multiple egg chambers.

Gene Name	CG#	Phenotype
Sirt2	CG5085	No phenotype
Sir2	CG5216	No phenotype
Sirt4	CG3187	No phenotype
Sirt6	CG6284	No phenotype
Sirt7	CG11305	No phenotype
HDAC3	CG2128	No phenotype
Rpd3	CG7471	egg chamber counting and fusion defects
HDAC4	CG1770	No phenotype
HDAC6	CG6170	No phenotype
HDACX	CG31119	No phenotype

Table 4. Histone Deacetylases and their phenotypes.

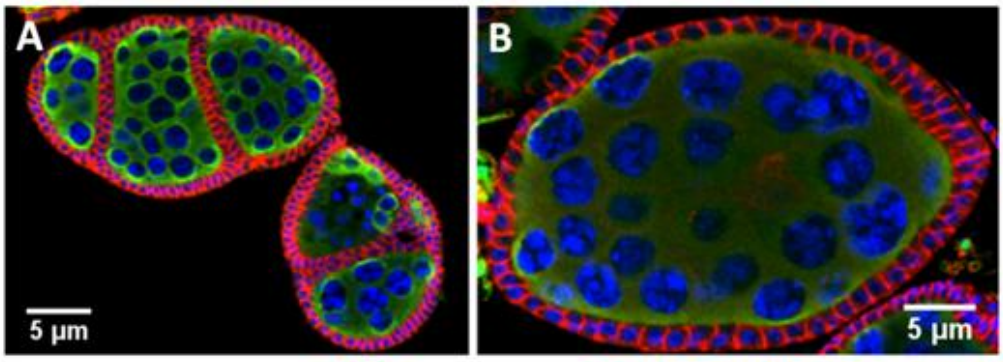

Figure 4. Knocking down histone deacetylases results in a cell autonomous follicle cell defect. (A, B) *c587 gal4>UAS Rpd3 RNAi* (BL 31616). The germaria are stained for Hts (red), VASA (green) and DNA (blue).

Ubiquitin Ligases:

Ubiquitin Ligases also called E3 Ubiquitin Ligases attach ubiquitin molecules on Lysine residues. *Sex Combs Extra (Sce) RNAi* expressed at 29^{o}C caused the flies to be lethal. The RNAi crossed to the gal4 driver and kept at room temperature resulted in a strong stem cell expansion phenotype. Also, the ovarioles displayed egg chamber fusion defects (Figure 5A). *Nedd4*, an ubiquitin ligase displayed a weak stem cell expansion phenotype (Figure 5B).

Gene Name	CG#	Phenotype
Sex combs extra (sce) (also known as ring1)	CG5595	stem cell expansion; egg chamber fusion defect
Bre1	CG10542	Not tested
Mind Bomb 1 (mib1)	CG5841	Not tested
Neuralized (neur)	CG11988	No phenotype
NEDD4	CG42279	Stem cell expansion
DIAP1 (also called thread)	CG12284	No phenotype
Deltex (dx)	CG3929	No phenotype
Suppressor of deltex (su(dx))	CG4244	No phenotype
Sina Homologue (Sinah)	CG13030	No phenotype
Seven in absentia (Sina)	CG9949	No phenotype
Roc1a	CG16982	Not tested

Table 5. Ubiquitin Ligases and their phenotypes.

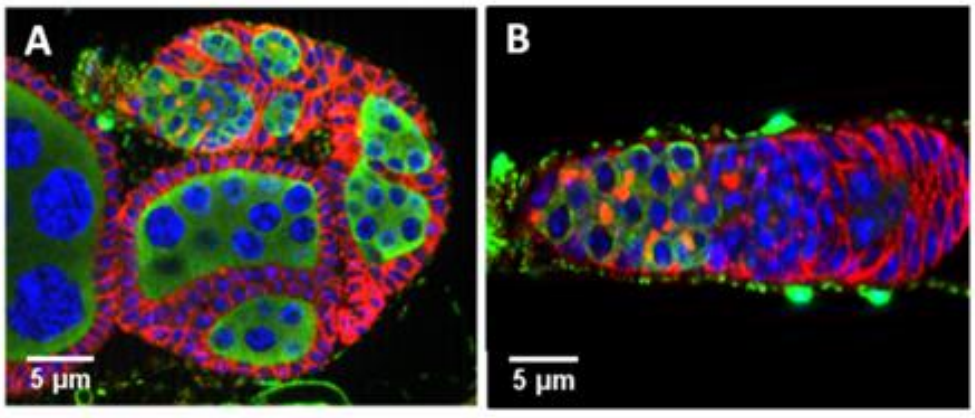

Figure 5. Knocking down Ubiquitin Ligases results in a non-cell autonomous stem cell expansion phenotype. (A) *c587 gal4>UAS Sce RNAi* at 25^{o}C (NIG 5595R-2) (B)

c587 gal4>UAS Nedd4 RNAi (BL 31687). The germaria are stained for Hts (red), VASA (green) and DNA (blue).

Trithorax Group Proteins:

Trithorax Group (TrX) genes are involved in the positive regulation of gene transcription. These trithorax group proteins bind to conserved Trithorax Response Elements (TRE) and stably activate genes (Ringrose et al. 2003). Brahma, a member of the trithorax group gene is a part of a large protein complex and was initially identified as a suppressor of Polycomb (Tamkun et al. 1992). Knocking down *Brahma* (*brm*) in the escort cells results in a strong stem cell expansion phenotype (Figure 6A). *Trithorax* (*Trl*) had a weak phenotype (Figure 6C)

Different components of the Brahma complex displayed phenotypes: *Dalao RNAi* (Figure 6D) and *Nurf38 RNAi* (Figure 6F) have a strong stem cell expansion phenotype, *ISWI* (Figure 6B) and *Domino* (Figure 6E) had a moderate stem cell expansion phenotype.

Different Brahma Associated Proteins (BAPs) displayed phenotypes. Lowering the expression of *BAP60* had a strong stem cell expansion phenotype and counting defects with more nurse cells than normal in the egg chambers (Figure 6H). *BAP170* also had a strong stem cell expansion phenotype and multi layered stalk cells (Figure 6G).

Gene Name	CG#	Phenotype
Absent, Small or Homeotic discs 1 (ash1)	CG8887	No phenotype
Absent, Small or Homeotic discs 2 (ash2)	CG6677	No phenotype
Brahma (Brm)	CG5942	Stem cell expansion
Osa	CG7467	No phenotype
Female Sterile (1) homeotic (fs(1)h)	CG2252	Not tested
Imitation SWI (ISWI)	CG8625	Stem cell expansion
Kismet	CG3696	Not tested
Little Imaginal Discs (LID)	CG9088	No phenotype
Lola Like (lolal)	CG5738	No phenotype
Modifier of mdg4	CG32491	Not tested
Moira (MOR)	CG18740	Not tested
Snf5 related 1 (Snr1)	CG1064	Not tested
Trithorax (Trx)	CG8651	No phenotype
Trithorax like (Trl)	CG33261	Stem cell expansion
Ultrabithorax (Ubx)	CG10388	Not tested
Taranis (Tara)	CG6889	No phenotype
Zeste (z)	CG7803	Not tested
Brahma complex of trithorax group proteins		
Brahma (Brm)	CG5942	Stem cell expansion
Polybromo	CG11375	Not tested
Dalao	CG7055	Stem cell expansion
Domino (dom)	CG9696	Stem cell expansion
Enhancer of Bithorax (E(bx))	CG32346	Not tested
Eyelid (also called osa)	CG7467	No phenotype
ISWI	CG8625	Stem cell expansion
Moira	CG18740	Not tested
Nucleosome remodeling factor 38kd (Nurf	CG4634	Stem cell expansion
Snf5 related 1 (Snr1)	CG1064	Not tested
Brahma Associated Proteins		
Brahma Associated Protein 55kD (Bap55)	CG6546	No phenotype
Brahma Associated Protein 60kD (Bap60)	CG4303	Stem cell expansion
Brahma Associated Protein 170kD (Bap170	CG3274	Stem cell expansion; Follicle cell defects

Table 6. Trithorax Group Proteins and their phenotypes.

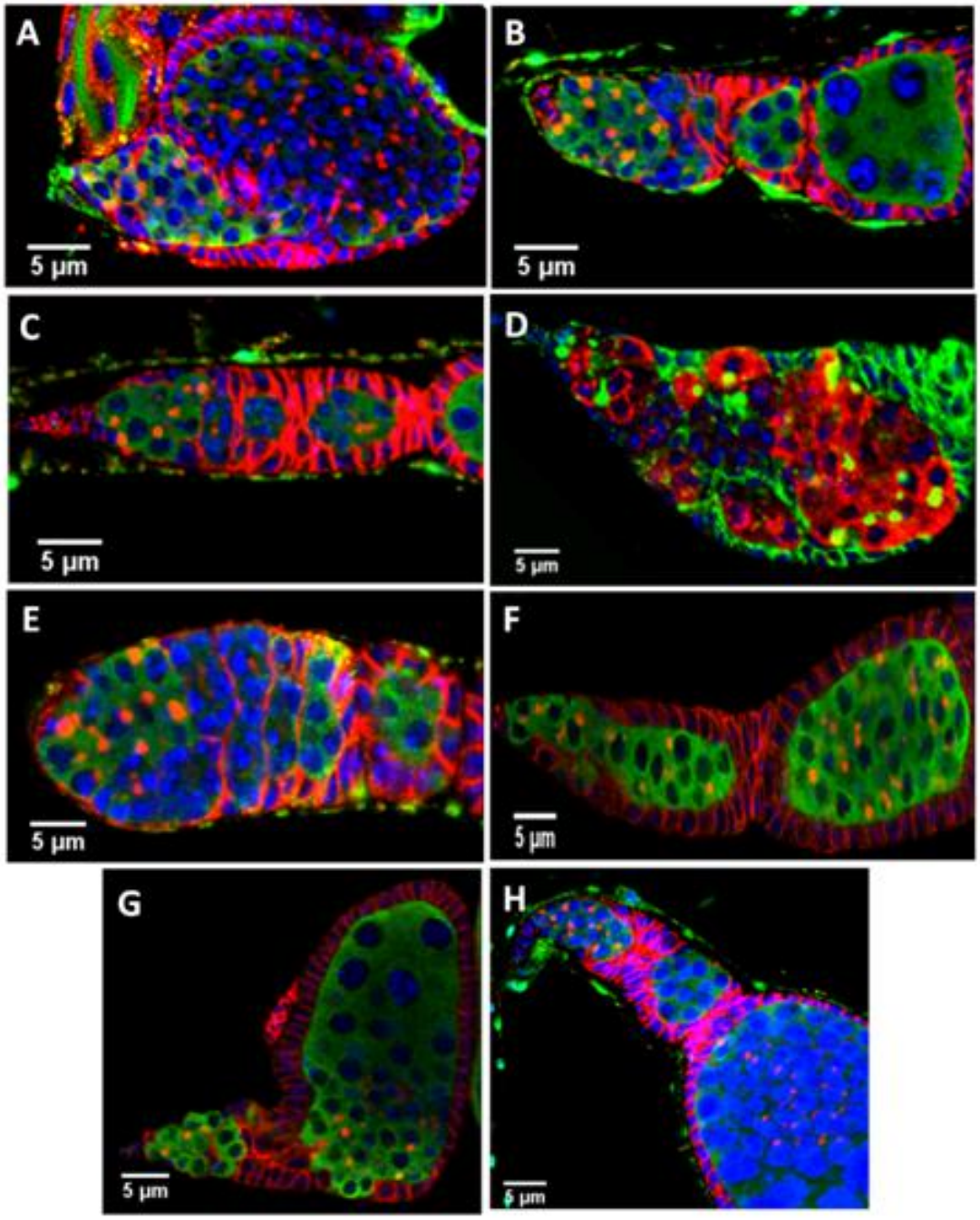

Figure 6. Knocking down Trithorax Group Genes results in a non-cell autonomous stem cell expansion phenotype. (A) *c587 gal4>UAS Brahma RNAi* (BL 31712) (B) *c587 gal4>UAS ISWI RNAi* (NIG 8625R-2) (C) *c587 gal4>UAS Trl RNAi* (NIG 9343R-4) (D) *c587 gal4>UAS Dalao RNAi* (NIG 7055R-3) (E) *c587 gal4>UAS Domino RNAi* (NIG 9696R-3) (F) *c587 gal4>UAS Nurf38 RNAi* (NIG 4634R-2) (G) *c587 gal4>UAS Bap170 RNAi* (BL 26308) (H) *c587 gal4>UAS Bap60 RNAi* (NIG 4303R-1). The germaria are stained for Hts (red), VASA (green) and DNA (blue).

Polycomb Group Proteins:

Polycomb Group (PcG) proteins assemble together to form large multi-protein complexes that function by silencing gene transcription. They were first identified as regulators of homeotic genes in *Drosophila* (Kennison 1995). The polycomb genes are recruited to specific DNA sequences called Polycomb Response Elements (PRE) and silence neighboring genes (Chan et al. 1994; Sengupta et al. 2004). The polycomb gene that displayed phenotypes is Cramped (Crm) that exhibited a moderate stem cell expansion (Figure 7E).

There are two complexes of PcG genes: Polycomb Repressive Complex 1 (PRC1) includes Polycomb (Pc), Posterior Sex Combs (Psc), Polyhomeotic (Ph) and dRing (Satijn et al. 1997; Shao et al. 1999). The PRC1 complex members that display phenotypes are: *Polyhomeotic Proximal* (*Ph-p*) (Figure 7A), *Reptin* (Figure 7B) and *Sce* (Figure 5A) have strong stem cell expansion phenotypes. *Sce* in addition has an egg chamber fusion defect (Figure 5A). *Polycomb* (*Pc*) has a moderate stem cell expansion phenotype and counting defect in the egg chamber (Figure 7D).

The Polycomb Repressive Complex 2 (PRC2) includes E(z), a histone methyltransferase that trimethylates lysine 9 and 27 residue on histone H3 tails (Cao et al. 2002; Czermin et al. 2002). The methylation activity of E(z) is required for the stable silencing of the Polycomb complex (Rastelli et al. 1993). *E(z) RNAi* exhibited a moderate stem cell expansion phenotype and follicle cell defects (Figure 1A). *Su(z)12*, another

histone methyltransferase, responsible for methylating lysine 27 residues on histone H3 tails (Chen et al. 2008) displayed a strong stem cell expansion phenotype (Figure 7C).

Gene Name	CG#	Phenotype
Polycomb		
Additional sex combs (Asx)	CG8787	No phenotype
Chameau (Chm)	CG5229	No phenotype
Cramped (crm)	CG2714	Stem cell expansion
Enhancer of Polycomb E(Pc)	CG7776	No phenotype
Pipsqueak (Psq)	CG2368	No phenotype
Pleiohomeotic (Pho)	CG17743	No phenotype
Scm-related gene containing four mbt domains (sfmbt)	CG16975	No phenotype
Suppressor of zeste 2 (Su(z)2)	CG3905	Stem cell expansion
PRC1 complex of Polycomb group proteins		
Polycomb (Pc)	CG32443	Stem cell expansion; egg chamber counting defect
Polyhomeotic distal (ph-d)	CG3895	No phenotype
Polyhomeotic proximal (ph-p)	CG18412	Stem cell expansion
Posterior sexcombs (Psc)	CG3886	No phenotype
Reptin (rept)	CG9750	Stem cell expansion
Sex combs extra (sce) (also known as ring1)	CG5595	stem cell expansion; egg chamber fusion defect
Esc-E(z) complex of Polycomb group proteins (PRC2)		
Chromatin Assembly Factor1 (CAF1) also called Nurf55	CG4236	Not tested
Enhancer of zeste (E(z))	CG6502	Stem cell expansion; Follicle cell defect
Extra sexcombs (Esc)	CG14941	No phenotype
Suppressor of Zeste 12 (Su(z)12)	CG8013	Stem cell expansion

Table 7. Polycomb Group Proteins and their phenotypes.

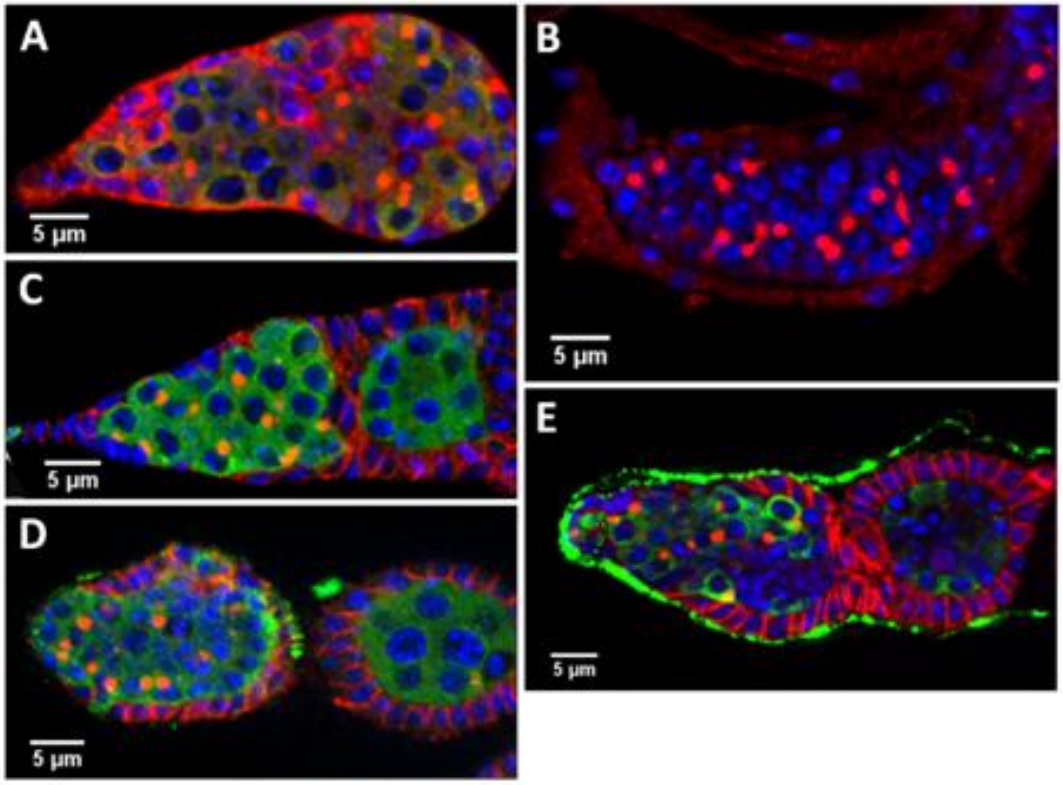

Figure 7. Knocking down Polycomb Group Genes results in a non-cell autonomous stem cell expansion phenotype. (A) *c587 gal4>UAS ph-p RNAi* (NIG 18414R-2) (B) *c587 gal4>UAS Reptin RNAi* (NIG 9750R-2) (C) *c587 gal4>UAS Su(z)12 RNAi* (BL 31191) (D) *c587 gal4>UAS Pc RNAi* at 25^{o}C (NIG 32443R-1) (E) *c587 gal4>UAS Crm RNAi* (NIG 2714R-3). The germaria are stained for Hts (red), VASA (green) and DNA (blue).

Suppressors and Enhancers of Variegation:

In *Drosophila*, variegated phenotypes result due to altered chromosomal rearrangements. A heterochromatic region placed in the vicinity of a transcriptionally active gene can cause silencing of the gene as spreading of the heterochromatin can take place. There are genes that act as dominant modifiers (enhancers and suppressors) of the variegated phenotype indicating that they are components of the chromatin involved in regulating its structure and function (Reuter and Spierer 1992; Wallrath and Elgin 1995).

The different suppressors and enhancers of variegation that exhibit phenotypes are: Loss of *Ssrp*, *Lsd1*, *Su(var)205/HP1*, *Su(var)2/HP2* and *Su(var)2-10* display strong stem cell tumors and *Su(hw)* displays a weak GSC expansion phenotype.

Gene Name	CG#	Phenotype
Structure specific recognition protein (ssrp)	CG4817	Stem cell expansion
Su(var)205 (HP1)	CG8409	Stem cell expansion
Suppressor of variegation 3-7	CG8599	No phenotype
Suppressor of variegation 3-3 (lsd1)	CG17149	Stem cell expansion
Suppressor of variegation 3-9	CG6476	No phenotype
Suppressor of hairy wing Su(hw)	CG8573	Stem cell expansion
Su(var)2/ HP2	CG12864	Stem cell expansion
Su(var)2-10	CG8068	Stem cell expansion; egg chamber counting defect
Su(var)3-1/JIL-1	CG6297	No phenotype
E(var)3-9	CG11971	No phenotype

Table 8. Enhancers and Suppressors of Variegation and their phenotypes.

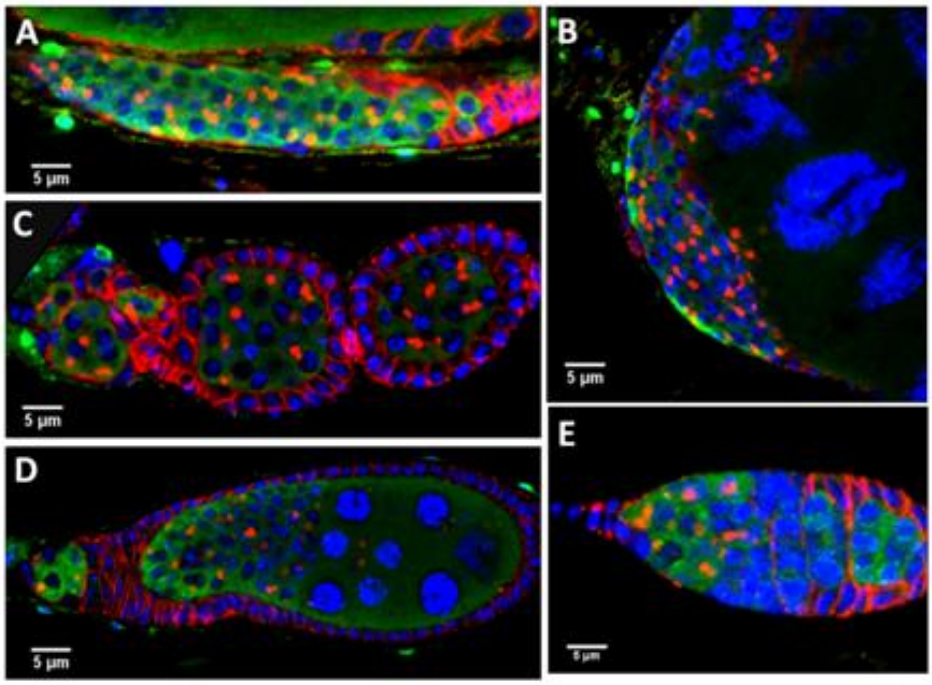

Figure 8. Knocking down Suppressors and Enhancers of Variegation results in a non-cell autonomous stem cell expansion phenotype. (A) *c587 gal4>UAS Ssrp* (NIG

4817R-1) (B) *c587 gal4>UAS HP1 RNAi* (NIG 8409R-4) (C*) c587 gal4>UAS Su(var)2-10* at 25^{o}C (BL 29448) (D) *c587 gal4>UAS Su(var)2 RNAi* (BL 25972) (E) *c587 gal4>UAS Su(Hw) RNAi* (NIG 8573R-2). The germaria are stained for Hts (red), VASA (green) and DNA (blue).

Chromatin Remodeling Complexes:

Chromatin remodeling factors utilize the energy of ATP hydrolysis to weaken the interaction between DNA and histone proteins, to move the histone octamers in cis and in trans and to increase the accessibility of the nucleosomal DNA to transcription factors (Peterson and Tamkun 1995; Tsukiyama and Wu 1995).

Drosophila Imitation SWI (ISWI), a highly conserved, common component of different chromatin remodeling complexes such as NuRF, Acf and CHRAC complexes is the ATPase subunit of the complex (Deuring et al. 2000). *ISWI RNAi* results in stem cell expansion phenotype (Figure 6B).

Histone Chaperones are factors that bind histones and are responsible for histone transport, transfer and storage (De Koning et al. 2007). Histone Chaperones that display phenotypes are *Nucleoplasmin* (*Nlp*) *RNAi* that has a moderate stem cell expansion phenotype (Figure 9A) and *Spt6* that has a strong stem cell expansion phenotype (Figure 9B).

Nucleosome stabilizing factors such as *Ssrp* (Figure 8A) and *Trl* (Figure 6C) display stem cell tumor phenotypes when knocked down.

Gene Name	CG#	Phenotype
Histone Chaperones		
Nucleoplasmin (NLP)	CG7917	Stem cell expansion
Nucleosome Assembly Protein-1 (dNap1)	CG5330	No phenotype
Chromatin Assembly Factor1 (CAF1) also called Nurf55	CG4236	Not tested
Spt6	CG12225	Stem cell expansion
DEK	CG5935	No phenotype
Anti silencing factor 1 (ASF1)	CG9383	No phenotype
HirA (Histone regulatory Protein A)	CG12153	No phenotype
Nucleosome Stabilizing factors		
dre4 (spt16)	CG1828	No phenotype
Structure specific recognition protein (ssrp)	CG4817	Stem cell expansion
Trithorax like (Trl)	CG33261	Stem cell expansion
ATP Utilizing Chromatin Assembly and Remodeling Factor (ACF) complex		
ATP-dependent chromatin assembly factor large subunit (Acf1)	CG1966	No phenotype
Imitation SWI (ISWI)	CG8625	Stem cell expansion
Chromatin Remodeling and Assembly Factor (CHRAC) complex		
ATP-dependent chromatin assembly factor large subunit (Acf1)	CG1966	No phenotype
Imitation SWI (ISWI)	CG8625	Stem cell expansion
CHRAC-14	CG13399	No phenotype
CHRAC-16	CG15736	Not tested
Nucleosome Remodeling Factor (NURF) complex		
Enhancer of bithorax (Nurf301)	CG32346	Not tested
Chromatin Assembly Factor1 (CAF1) also called Nurf55	CG4236	Not tested
Nucleosome remodeling factor 38kd (Nurf-38)	CG4634	Stem cell expansion
Imitation SWI (ISWI)	CG8625	Stem cell expansion

Table 9. Chromatin Remodeling Complexes and their phenotypes.

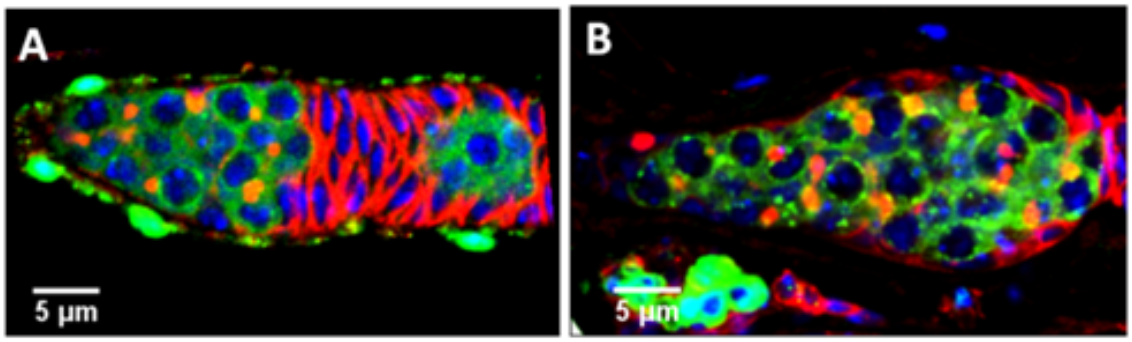

Figure 9. Knocking down Histone Chaperones results in a non-cell autonomous stem cell expansion phenotype. (A) *c587 gal4>UAS NLP RNAi* (NIG 7917R-3) (B) *c587 gal4>UAS spt6 RNAi* (NIG 12225R-3). The germaria are stained for Hts (red), VASA (green) and DNA (blue).

The knockdown of 122 different chromatin factors using *c587 gal4* driver that expresses the RNAi specifically in the escort cells and early follicle cells resulted in 29 genes having a non-cell autonomous phenotype in the germline with an expansion of stem cells. These phenotypes ranged from strong, where there are a large number of stem cells resulting in huge germline tumors and a block in differentiation to moderate phenotype, where the germarium has an increased number of stem cells and differentiation is still occurring with the formation of egg chambers to weak phenotype, where there are two or three more stem cells than normal away from the niche.

This screen also provided information on chromatin factors that are required in the follicle cells as the Gal4 driver is also expressed in early follicle cells. The follicle cell defects ranged from egg chamber fusion defects to multi-layered stalk cells.

Genes involved in activation such as Tip60, Enok and Trithorax complex members exhibit stem cell expansion phenotype similar to the genes that are involved in silencing such as Lsd1, eggless, HP1 and Polycomb Group members. Further investigation needs to be done to determine if the chromatin factors that are involved in gene activation function in signaling pathways that activate genes in the surrounding somatic cells for differentiation to occur in the germline.

The chromatin screen has opened up a number of questions: Do these genes work together with Lsd1 in silencing niche signaling? Do these genes regulate Dpp expression? Do the loss of these chromatin factors cause a change in cell fate? Are these genes important both during development and in adulthood?

This small-scale RNAi screen for chromatin factors has identified post translational modifiers of histone tails, polycomb and trithorax genes and chromatin remodelers that are functional in the escort cells of the *Drosophila* ovary for differentiation to occur. The stepwise mechanism of histone modifications and nucleosomal reorganization needs to be worked out and the *Drosophila* niche cells present an excellent *in vivo* model to study the genome regulation of the niche cells.

CHAPTER 5

CONCLUSIONS AND FUTURE DIRECTIONS

Histone demethylase Lsd1 plays an important role in development. Loss of mammalian Lsd1 results in embryonic mouse lethality (Wang et al. 2007; Foster et al. 2010). Conditional knockout of Lsd1 shows pituitary gland developmental defects (Wang et al. 2007). In *Drosophila*, loss of Lsd1 does not cause lethality, although the viability of the animals is reduced. Null mutants of Lsd1 are sterile and display tissue specific defects (Di Stefano et al. 2007).

In this thesis, I have identified a novel mechanism for Lsd1 in the *Drosophila* fermale germline. The ovaries are very small when compared to wild type and results in the formation of stem cell tumors in the germarium. My results indicate that Lsd1 acts nonautonomously to limit GSC numbers within the *Drosophila* ovary. These conclusions are based on several lines of experimental evidence. Clonal analyses demonstrate that Lsd1 does not function within the germline or in follicle cells in regard to the regulation of GSC number or GSC daughter differentiation. Furthermore *Lsd1* mutant GSCs and FSCs are maintained for long periods of time, indicating that Lsd1 is not required within stem cells for their maintenance in the ovary. Strikingly, RNAi knockdown of *Lsd1* within ECs phenocopies the expanded GSC phenotype of Lsd1 null mutants. In addition, independent *Lsd1* transgenes rescue the $Lsd1^{\Delta N}$ tumorous phenotype when expressed in the escort cells that line the anterior region of the germarium. These data indicate that Lsd1 functions within the escort cells of the germarium to limit the size of the functional GSC niche.

Lsd1 functions in escort cells to repress the expression of niche-specific signals. Undifferentiated germ cells in *Lsd1* mutants exhibit increased Dpp signaling as seen by the expansion of Dad expressing cells and by the increase of *dpp* transcripts by RT-PCR. Reducing *dpp* levels within escort cells suppresses the Lsd1 phenotype. By ChIP-seq analysis on the escort cell population, I have identified Lsd1 directly binds to regulate the expression of *engrailed,* a homeodomain factor. Engrailed is an upstream target of dpp and misexpressing *engrailed* in the escort cells exhibits a GSC tumor phenotype. Lsd1 silences dpp in the escort cells indirectly by repressing *engrailed* expression.

The loss of Lsd1 during development results in the misexpression of cap cell markers in escort cells. The finding that escort cells can potentially express cap cell markers and *vice versa* suggests that these two cell populations might arise from a common precursor within the developing gonad. Lsd1 might play a role earlier in development to establish cap cell and escort cell fate and limit the size of the cap cell niche.

Lsd1 activity is spatially limited even though the expression of Lsd1 is ubiquitous in the germarium. ChIP-seq analyses on the escort cell and cap cell population indicates that there are unique Lsd1 binding sites in the escort cells that are not present in the cap cell genome. Lsd1 binds to the *engrailed* gene promoter region in the escort cells but fails to bind to the same promoter region in the cap cells. This suggests that Lsd1 could be recruited to specific sites by other proteins that have more cell-specific expression patterns.

Lsd1 homologs regulate heterochromatin formation and gene expression across species (Chosed and Dent 2007; Di Stefano et al. 2007; Rudolph et al. 2007; Hu et al. 2009; Katz et al. 2009; Wang et al. 2009b; Amente et al. 2010). From the ChIP-seq analysis on the cap cell and escort cell genome, we did not see any Lsd1 binding peaks in the heterochromatic region. This could be due to the reason that the parameters applied during the initial bioinformatics analysis to identify reads on the genome does not encompass the heterochromatic region. We will revisit the data and see if we can find any Lsd1 binding peaks in that region.

Additional Chromatin factors play an important role in restricting the size of the GSC niche. Small-scale RNAi screen for chromatin factors identified post translational modifiers of histone tails, polycomb and trithorax genes and chromatin remodelers that are required to silence niche signals. The stepwise mechanism of histone modifications and nucleosome reorganization needs to be worked out and the *Drosophila* niche cells present an excellent *in vivo* model to study the genome regulation of the niche cells.

This functional characterization of Lsd1 in escort cells reveals that the active repression of niche-specific signals outside the normal microenvironment may be essential for proper tissue homeostasis. Recent studies show that mammalian Lsd1 directly targets TGF-β1 for transcriptional repression (Wang et al. 2009b) and has cell-autonomous roles in cancer (Tsai et al. 2008; Schulte et al. 2009; Wang et al. 2009b; Suikki et al. 2010). Given the possible links between cancer and stem cells (Feinberg et al. 2006) and the observation that Lsd1 has a conserved role in regulating intercellular

signaling molecules, it will be important to determine whether Lsd1 and other chromatin factors have additional nonautonomous functions that contribute to stem cell maintenance, tumorigenesis, and metastasis.

APPENDIX

APPENDIX A

MICROARRAY COMPARISON BETWEEN

BAMΔ AND BAMΔ-LSD1$^{\Delta}$ MUTANTS

To identify genes differentially regulated by Lsd1, I performed microarray analysis on *lsd1*$^{\Delta N}$-*bam*Δ double mutants comparing them to *bam*Δ mutants. The *bam*Δ mutant ovaries were used as controls as they are comparable in size to the *lsd1*$^{\Delta N}$-*bam*Δ double mutant ovaries. Ovaries were dissected and total RNA isolated using the standard Trizol protocol. The cDNA was synthesized using the T7 oligo (dT) primer. The cDNA was then subjected to in vitro transcription reaction to generate multiple copies of aRNA (antisense RNA), during which biotinylated nucleotides label the RNA. The labeled RNA was then hybridized to *Drosophila* 2.0 gene chips from Affymetrix. Partek genomic suite was used to analyze the gene expression data.

I determined 495 genes that were upregulated 2 fold and higher in *lsd1*$^{\Delta N}$-*bam*Δ double mutants and 374 genes that were down regulated 0.5 fold and less.

In this experiment, the change in transcript levels is not limited to the somatic cells but also includes the germline cells as all the cells are null for lsd1 in these double mutant ovaries. Since Lsd1 functions in the escort cells of the germarium, a better experiment would be to knock down *Lsd1* using RNAi specifically in the escort cells of the *bam*Δ mutants and compare the ovaries to control *bam*Δ mutants.

Another caveat of this experiment is, if the gene is expressed in both germline and somatic cells minor changes in gene expression in the somatic cells will not be visible as the signal from the many germ cells will dampen any signal from the few somatic cells surrounding them.

Table 1. Upregulated Genes Due to the Loss of lsd1 by Microarray

lsd1ΔN-bamΔ/bamΔ Fold Change	Identifier	Description
37.49	NA	AJ000387/FEA=transposon
29.02	NA	AJ000387/FEA=transposon
26.73	NA	RE44040/FEA=sim4/SEG=chr2R:+502122,506228
21.42	NA	FEA=transposon
19.98	CG8768	CG8768-RA
18.90	Fat body protein 1 (Fbp1)	CG17285-RA
18.21	Cyp4p2	CG1944-RA
15.73	Fat body protein 2 (Fbp2)	CG3763-RA
15.50	Odorant-binding protein 99b (Obp99b)	CG7592-RA
15.43	NA	S.CX002471/FEA=fgenesh/SEG=chrX:+21609546,21651619
14.82	Larval serum protein 1γ (Lsp1γ)	CG6821-RA
14.76	NA	AF364549/FEA=transposon
14.07	CG8563	CG8563-RA
13.64	NA	HDC08273/FEA=HDP/SEG=chr3L:-3464539,3465249
13.05	CG12441	CG12441-RB
12.68	CG16965	CG16965-RA
12.55	Neither inactivation nor after potential D (ninaD)	CG31783-RA
12.10	GNBP-like	CG13422-RA
11.63	Odorant-binding protein 56d (Obp56d)	CG11218-RA
11.50	Neuropeptide-like precursor 3 (Nplp3)	CG13061-RA
10.98	NA	S.C2L001254/FEA=fgenesh/SEG=chr2L:+9283639,9283894
10.95	Transferrin 1 (Tsf1)	CG6186-RB
10.49	CG32834	CG32834-RA
10.29	CG3526	CG3526-RB
10.20	CG9897	CG9897-RA
9.95	CG12441	CG12441-RB
9.83	CG16704	CG16704-RA
9.65	CG32105	CG32105-RB
9.41	Troponin C at 25D (TpnC25D)	CG6514-RA
9.35	NA	HDC20215/FEA=HDP/SEG=chr3h:+1425613,1426037
9.08	Spatzle Processing Enzyme (SPE)	CG16705-RA
8.98	Homeodomain Protein 2.0 (H2.0)	CG11607-RA
8.92	Ance-4	CG8196-RA
8.79	NA	AJ010298/FEA=transposon
8.75	CG13129	CG13129-RA
8.59	CG8586	CG8586-RA
8.41	CG33458	CG33458-RA
8.22	CG6018	CG6018-RA
8.16	PGRP-SD	CG7496-RA
8.11	CG31681	CG31681-RA
7.99	CG31775	CG31775-RA
7.82	CG31766	CG31766-RA
7.55	NA	AB022762/FEA=transposon
7.43	CG31769	CG31769-RA
7.38	Photoreceptor dehyrogenase (Pdh)	CG4899-RA
7.29	CG15065	CG15065-RA
7.17	Hand	CG18144-RA

lsd1ΔN-bamΔ/bamΔ Fold Change	Identifier	Description
7.14	CG13962	CG13962-RA
7.09	CG5791	CG5791-RA
7.09	CG8501	CG8501-RA
7.07	Ionotropic receptor 76a (Ir76a)	CG8533-RB
7.06	CG17350	CG17350-RA
7.05	CG10031	CG10031-RA
7.03	Immune induced molecule 1 (IM1)	CG18108-RA
6.95	CG11668	CG11668-RA
6.90	CG14661	CG14661-RA
6.89	CG30371	CG30371-RA
6.86	CG30287	CG30287-RA
6.86	CG16736	CG16736-RA
6.86	CG9899	CG9899-RA
6.81	CG3246	CG3246-RA
6.71	Chitin deacetylase-like 4 (Cda4)	CG32499-RA
6.67	CG30090	CG30090-RA
6.61	forkhead domain 102C (fd102C)	CG11152-RA
6.56	α-Esterase-1 (a-Est-1)	CG1031-RA
6.48	CG14439	CG14439-RA
6.45	CG5945	CG5945-RA
6.39	NA	AE003485/FEA=transposon
6.34	NA	FEA=transposon
6.34		CG32919-RA
6.32	CG4462	CG4462-RA
6.30	NA	S.CX000659/FEA=fgenesh/SEG=chrX:-5939655,5940217
6.21	nimrod C4 (nimC4)	CG16876-RA
6.17	NA	FEA=transposon
6.14	CG32187	CG32187-RA
5.97	CG16756	CG16756-RA
5.76		CG40142-RC
5.73	Jonah 74E (Jon 74E)	CG6298-RA
5.72	CG6639	CG6639-RA
5.70	CG9989	CG9989-RA
5.64	CG2444	CG2444-RA
5.60	Pheromone-binding protein-related protein 5 (Pbprp5)	CG6641-RA
5.49	Tektin C (Tektin-C)	CG10541-RA
5.47	CG12674	CG12674-RA
5.44	nimrod B1 (nimB1)	CG33119-RA
5.39	NA	HDC20166/FEA=HDP/SEG=chrU:-1131685,1132661
5.36	CG14949	CG14949-RA
5.29	CG18003	CG30019-RB
5.21	CG9780	CG9780-RA
5.13	CG3699	CG3699-RA
5.09	CG6495	CG6495-RA
5.04	short neuropeptide F receptor (sNPF-R)	CG7395-RA
5.01	CG43155	CG1756-RA
4.99	CG40339	CG40339-RA
4.99	CG7409	CG7409-RA
4.97	CG3604	CG3604-RA

lsd1ΔN-bamΔ/bamΔ Fold Change	Identifier	Description
4.97	CG18635	CG18635-RA
4.95	CG31606	CG31606-RB
4.88	pericardin (prc)	CG5700-RB
4.87	retinal degeneration C (rdgC)	CG6571-RA
4.85	Cuticular protein 67B (Cpr67B)	CG3672-RA
4.79	CG13215	CG13215-RA
4.75	CG3597	CG3597-RA
4.73	NA	FEA=transposon
4.70	CG9380	CG9380-RA
4.64	CG13285	CG13285-RA
4.62	CG13794	CG13794-RA
4.61	CG30091	CG30091-RA
4.59	CG5895	CG5895-RA
4.58	CG40485	CG40485-RA
4.58	NA	HDC03722/FEA=HDP/SEG=chr3h:+983270,983583
4.57	CG4525	CG4525-RA
4.55	Cuticular protein 49Ae (Cpr49Ae)	CG8505-RA
4.53	CG30083	CG30083-RA
4.52	CG10660	CG10660-RA
4.48	CG3635	CG3635-RA
4.46	Ser7	CG2045-RA
4.46	CG18284	CG18284-RA
4.46	NA	CT39784/FEA=sim4/SEG=chr2h:-668024,668345
4.43	CG4335	CG4335-RA
4.42	complexin (cpx)	CG32490-RG
4.40	CG31685	CG31685-RA
4.40	CG40139	CG40139-RA
4.40	CG17244	CG17244-RA
4.39	Larval serum protein 1 beta (Lsp1beta)	CG4178-RA
4.38	CG5493	CG5493-RA
4.37	Cyp309a2 (Cyp309a2)	CG18559-RA
4.37	CG18609	CG18609-RA
4.37	Immune induced molecule 23 (IM23)	CG15066-RA
4.34	CG11592	CG11592-RA
4.27	Cyp4ac1	CG14032-RA
4.27	NA	HDC11307/FEA=HDP/SEG=chr3L:+21174031,21175931
4.25	NA	CT33755/FEA=sim4/SEG=chr3L:-10580743,10580996
4.24	CG17478	CG17478-RA
4.24	CG13618	CG13618-RA
4.24	pannier (pnr)	CG3978-RB
4.23	Immune induced molecule 2 (IM2)	CG18106-RA
4.22	CG17239	CG17239-RA
4.21	Glutamine:fructose-6-phosphate aminotransferase 1 (Gfat1)	CG12449-RA
4.19	CG40484	CG40484-RA
4.15	Heat shock protein cognate 1 (Hsc70-1)	CG8937-RB
4.14	NA	HDC20537/FEA=HDP/SEG=chrU:-2779000,2781237
4.12	Dichaete (D)	CG5893-RA
4.12	CG1124	CG1124-RA
4.10	Phosphoribosylamidotransferase 2 (Prat2)	CG10078-RB

lsd1ΔN-bamΔ/bamΔ Fold Change	Identifier	Description
4.02	NA	FEA=transposon
4.02	NA	CT32418/FEA=sim4/SEG=chr2R:+7228689,7228900
4.00	NA	HDC03384/FEA=HDP/SEG=chrU:-2143308,2144592
4.00	CG10657	CG10657-RA
3.99	NA	HDC20167/FEA=HDP/SEG=chrU:-1132994,1134467
3.99	CG3955	CG3955-RA
3.98	CG7900	CG7900-RA
3.98	CG1213	CG1213-RB
3.94	engrailed (en)	CG9015-RB
3.90		CG33318-RA
3.90	Cyp28d1	CG10833-RA
3.90	CG4847	CG4847-RA
3.89	Wake-up-call (wuc)	CG12442-RA
3.86	taxi (tx)	CG5441-RA
3.86	CG11226	CG11226-RA
3.86	Cecropin A1 (CecA1)	CG4740-RA
3.86	Casein kinase II beta2 subunit (CkIIbeta2)	CG8914-RA
3.84	NA	HDC20229/FEA=HDP/SEG=chr2h:+495716,497098
3.79	Osiris 24 (Osi24)	CG15589-RA
3.76	elongase F (eloF)	CG16905-RA
3.75	CG13318	CG13318-RA
3.75	CG14321	CG14321-RA
3.74	CG8654	CG8654-RA
3.70	CG4721	CG4721-RA
3.69	CG2816	CG2816-RA
3.67	NA	HDC19504/FEA=HDP/SEG=chrX:-17860662,17861717
3.66	NA	CT35721/FEA=sim4/SEG=chrX:+15421863,15422091
3.63	CG8785	CG8785-RA
3.63	CG11756	CG11756-RA
3.62	NA	HDC20523/FEA=HDP/SEG=chrU:+559846,560728
3.62	Odorant-binding protein 57c (Obp57c)	CG13421-RA
3.62	NA	CT33154/FEA=sim4/SEG=chr3L:-18018725,18018994
3.60	GV1	CG12023-RA
3.59	NA	FEA=transposon
3.58	FLASH ortholog (FLASH)	CG4616-RA
3.58	CG8564	CG8564-RA
3.58	Rh50	CG7499-RA
3.56	CG1299	CG1299-RA
3.56	GV1	CG12023-RB
3.55	Scavenger receptor class C, type II (Sr-CII)	CG8856-RA
3.53	Esterase Q (Est-Q)	CG7529-RA
3.52	CG9812	CG9812-RB
3.51	CG17217	CG17217-RA
3.50	Histamine-gated chloride channel subunit 1 (HisCl1)	CG14723-RA
3.50	CG7738	CG7738-RA
3.47	CG10051	CG10051-RA
3.46	Cuticular protein 49Ac (Cpr49Ac)	CG8502-RC
3.46	Cyp9h1	CG17577-RA
3.44	NA	M12927/FEA=transposon

lsd1ΔN-bamΔ/bamΔ Fold Change	Identifier	Description
3.44	CG17839	CG17839-RA
3.43	CG9396	CG9396-RA
3.42	Drosocin (Dro)	CG10816-RA
3.42	NA	FEA=transposon
3.40	CG7201	CG7201-RA
3.39	CG16898	CG16898-RA
3.38	NA	FEA=transposon
3.38	complexin (cpx)	CG32490-RE
3.37	CG10361	CG10361-RA
3.35	Immune induced molecule 4 (IM4)	CG15231-RA
3.35	CG3328	CG3328-RA
3.31	CG16772	CG16772-RA
3.29	NA	HDC07622/FEA=HDP/SEG=chr3h:+1373421,1374096
3.29	CG7560	CG7560-RA
3.27	faulty attraction (frac)	CG7526-RA
3.26	Neprilysin 1 (Nep1)	CG5905-RB
3.23	CG11550	CG11550-RA
3.23	nimrod B5 (nimB5)	CG16873-RA
3.22	CG4408	CG4408-RA
3.22	NA	CT35452/FEA=sim4/SEG=chr2L:+2947414,2947891
3.21	CG7442	CG7442-RA
3.21	CG40142	CG40142-RC
3.19	CG1468	CG1468-RA
3.18	CG32277	CG32277-RA
3.17	CG10508	CG10508-RC
3.16	CG14695	CG14695-RA
3.15	beta-Tubulin at 85D (betaTub85D)	CG9359-RA
3.15	spookier (spok)	CG40123-RA
3.14	Esterase 6 (Est-6)	CG6917-RA
3.13	Rab-protein 3 (Rab3)	CG7576-RA
3.12	CG9780	CG9780-RA
3.11	CG6415	CG6415-RA
3.10	golden goal (gogo)	CG32227-RA
3.10	NA	HDC07680/FEA=HDP/SEG=chrU:-6338857,6339265
3.09	CG31778	CG31778-RA
3.09	axotactin (axo)	CG13717-RA
3.09	CG8401	CG8401-RA
3.08	CG8738	CG8738-RA
3.07	CG7735	CG7735-RA
3.05	NA	AL035631/FEA=transposon
3.03	CG34380	CG31640-RA
3.03	Heat shock protein cognate 1 (Hsc70-1)	CG8937-RB
3.02	IA-2 ortholog (IA-2)	CG31795-RB
3.02	CG14314	CG14314-RA
3.02	CG40378	CG40378-RA
2.99	CG10232	CG10232-RA
2.98	CG7408	CG7408-RB
2.98	NA	RH05583/FEA=sim4/SEG=chr2R:+10684936,10688513
2.97	CG9631	CG9631-RA

lsd1ΔN-bamΔ/bamΔ Fold Change	Identifier	Description
2.96	CG14153	CG14153-RA
2.96	CG12402	CG12402-RA
2.96	CG10352	CG10352-RA
2.96	CG16904	CG16904-RA
2.95	CG30289	CG30289-RA
2.95	CG30148	CG30148-RA
2.95	CG3568	CG3568-RA
2.95	CG16778	CG16778-RA
2.92	CG4577	CG4577-RA
2.92	CG14762	CG14762-RA
2.92	Excitatory amino acid transporter 1 (Eaat1)	CG3747-RB
2.91	CG30379	CG30379-RA
2.91		CG32605-RA
2.91	Obp44a	CG2297-RA
2.91	Serotonin transporter (SerT)	CG4545-RA
2.90	Nutrient Amino Acid Transporter 1 (NAAT1)	CG3252-RA
2.89	Transferrin 1 (Tsf1)	CG6186-RA
2.89	CG15674	CG15674-RA
2.89	boule (bol)	CG4760-RB
2.88	CG9649	CG9649-RA
2.88	CG40164	CG40164-RA
2.87	CG2269	CG2269-RC
2.86	thoc6	CG5632-RA
2.85	Peroxiredoxin 2540-2 (Prx2540-2)	CG11765-RA
2.85	NA	S.C2R000100/FEA=fgenesh/SEG=chr2R:-1481739,1508980
2.85	GV1	CG12023-RB
2.84	CG13594	CG13594-RA
2.84	CG18563	CG18563-RA
2.84	CG8129	CG8129-RB
2.84	CG7203	CG7203-RA
2.83	juvenile hormone acid methyltransferase (jhamt)	CG17330-RA
2.83	CG15460	CG15460-RA
2.82	Adenosine deaminase-related growth factor D (Adgf-D)	CG9621-RA
2.82	CG7368	CG7368-RA
2.81	beta galactosidase (Gal)	CG9092-RA
2.81	CG40115	CG40115-RB
2.81	Listericin	CG9080-RA
2.80	inebriated (ine)	CG15444-RB
2.80	CG8317	CG8317-RA
2.79	CG3213	CG3213-RA
2.78	CG30046	CG30046-RB
2.78	CG18284	CG18284-RA
2.77	C-type lectin 27kD (Clect27)	CG3244-RA
2.76	BBS8	CG13691-RA
2.75	CG13077	CG13077-RA
2.75	NA	HDC20187/FEA=HDP/SEG=chrU:-729405,729742
2.74	Cuticular protein 78Ca (Cpr78Ca)	CG11310-RA
2.74	CG5773	CG5773-RA
2.74	CG7214	CG7214-RA

lsd1ΔN-bamΔ/bamΔ Fold Change	Identifier	Description
2.73	CG15892	CG32918-RA
2.73	CG4927	CG4927-RA
2.72	CG14642	CG14642-RB
2.72	CG3121	CG3121-RA
2.72	Cyp311a1	CG1488-RA
2.70	CG14523	CG14523-RA
2.70	NA	CT39116/FEA=sim4/SEG=chr2h:-1169125,1172070
2.69	NA	HDC03535/FEA=HDP/SEG=chr2L:+21066932,21068472
2.68	CG15067	CG15067-RA
2.67	CG9689	CG9689-RA
2.67	CG11842	CG11842-RA
2.67	CG11263	CG11263-RA
2.67	CG15695	CG15695-RA
2.67	Imaginal disc growth factor 5 (Idgf5)	CG5154-RA
2.66	CG40138	CG40138-RA
2.66	CG8519	CG8519-RA
2.65	CG5389	CG5389-RA
2.65	CG13283	CG13283-RA
2.65	NA	S.C3L001763/FEA=fgenesh/SEG=chr3L:-13735493,13744464
2.65	Gram-negative bacteria binding protein 2 (GNBP2)	CG4144-RB
2.64	CG15828	CG15828-RA
2.63	NA	HDC09471/FEA=HDP/SEG=chr3L:-10650343,10650652
2.63	NA	S.C3L002302/FEA=fgenesh/SEG=chr3L:-18035574,18036076
2.63	fat-spondin	CG6953-RA
2.63	skpB	CG8881-RA
2.63	Hexokinase C (Hex-C)	CG8094-RA
2.62	CG13793	CG13793-RA
2.62	Immune induced molecule 3 (IM3)	CG16844-RA
2.62	CG15185	CG15185-RA
2.60	CG3829	CG3829-RA
2.60	Deoxyribonuclease II (DNaseII)	CG7780-RA
2.60	Protein phosphatase 1 at 13C (Pp1-13C)	CG9156-RA
2.58	CG6034	CG6034-RA
2.58	NA	AY180918/FEA=transposon
2.57	Ance-5	CG10142-RA
2.56	yellow-b	CG17914-RA
2.55	Cytochrome P450-6a2 (Cyp6a2)	CG9438-RA
2.55	NA	GH06606/FEA=sim4/SEG=chr2R:-9953073,9956759
2.54	Carbonic anhydrase 2 (CAH2)	CG6906-RA
2.54	CG13551	CG13551-RC
2.53	CG15293	CG15293-RA
2.53	CG7299	CG7299-RA
2.53	CG10186	CG10186-RA
2.53	CG3713	CG3713-RA
2.52	lin-28	CG17334-RA
2.52	CG9068	CG9068-RA
2.52	NA	RH42808/FEA=sim4/SEG=chr3R:-13725074,13727325
2.51	methuselah-like 7 (mthl7)	CG7476-RB
2.49	CG17018	CG17018-RA

lsd1ΔN-bamΔ/bamΔ Fold Change	Identifier	Description
2.49	Serine pyruvate aminotransferase (Spat)	CG3926-RA
2.48	TweedleE (TwdlE)	CG14534-RA
2.48	yellow-emperor (ymp)	CG12250-RB
2.48	CG13488	CG13488-RA
2.48	Hemese (He)	CG31770-RB
2.48	CG10680	CG10680-RA
2.47	Olig family (Oli)	CG5545-RA
2.47	CG4133	CG4133-RA
2.45	NA	FEA=stencil/SEG=chr2R:+7401699,7402254
2.45	CG31300	CG31300-RA
2.45	CG6788	CG6788-RA
2.45	dusky (dy)	CG9355-RA
2.44	CG9394	CG9394-RA
2.44	CG10566	CG10566-RA
2.44	Cyp4p3	CG10843-RA
2.42	NA	FEA=stencil/SEG=chr2R:+8476483,8477383
2.41	CG30083	CG30008-RA
2.40	CG14357	CG14357-RA
2.40	Fad2	CG7923-RA
2.39	CG32695	CG32695-RA
2.39	Elastin-like (Ela)	CG7021-RA
2.39	CR33221	CG12260-RB
2.39		CG40134-RA
2.39	CG10131	CG10131-RA
2.38	NA	AF365402/FEA=transposon
2.38	CG7607	CG7607-RA
2.38	farinelli (fan)	CG7919-RA
2.38	CG8795	CG8795-RA
2.37	CG8358	CG8358-RA
2.36	CG31704	CG31704-RA
2.36	Rim	CG7321-RA
2.36	CG33459	CG33459-RA
2.35	CG33282	CG15407-RB
2.33	CG6723	CG6723-RA
2.33	lectin-33A	CG16834-RA
2.32	Odorant-binding protein 57a (Obp57a)	CG30141-RA
2.32	CG9928	CG9928-RA
2.32	CG31100	CG31100-RA
2.32	CG17560	CG17560-RA
2.32	ninaG	CG6728-RA
2.31	fondue (fon)	CG15825-RB
2.30	CG8630	CG8630-RA
2.29	CG32647	CG32647-RB
2.29	CG6067	CG6067-RA
2.29	CG13928	CG13928-RA
2.28	CG7294	CG7294-RA
2.28	Gonadotropin-releasing hormone receptor (GRHR)	CG11325-RB
2.28	nimrod B4 (nimB4)	CG33115-RA
2.27	CG14323	CG14323-RA

lsd1ΔN-bamΔ/bamΔ Fold Change	Identifier	Description
2.27	Diptericin B (DptB)	CG10794-RA
2.27	drumstick (drm)	CG10016-RB
2.27	CG10132	CG10132-RA
2.27	male sterile (3) K81 (ms(3)K81)	CG14251-RA
2.26	Flavin-containing monooxygenase 2 (Fmo-2)	CG3174-RA
2.26	CG34437	CG16918-RA
2.26	msta	CG32800-RA
2.26	Cytochrome b5-related (Cyt-b5-r)	CG13279-RA
2.25	NA	FEA=stencil/SEG=chr2L:-13949638,13950078
2.25	CG5687	CG5687-RA
2.24	CG13833	CG13833-RA
2.24	Glutactin (Glt)	CG9280-RC
2.24	CG7202	CG7202-RA
2.24	Serine protease 7 (Sp7)	CG3066-RA
2.24	CG11327	CG11327-RB
2.23	CG14870	CG14870-RA
2.23	CG3775	CG3775-RA
2.23	CG15930	CG15930-RA
2.22	CG42370	CG9511-RA
2.22	CG42492	CG17761-RA
2.22	CG9380	CG9380-RB
2.21	Tetraspanin 42Eo (Tsp42Eo)	CG12838-RA
2.21	CG10562	CG10562-RA
2.21	Ribosomal protein S7 (RpS7)	CG1883-RB
2.21	CG12926	CG12926-RA
2.21	spaghetti-squash activator (sqa)	CG1776-RA
2.20	Tetraspanin 42Eh (Tsp42Eh)	CG12844-RA
2.20	CG6834	CG6834-RA
2.20	Metallothionein D (MtnD)	CG33192-RA
2.20	CG12656	CG12656-RA
2.19	CG5613	CG5613-RA
2.19	NA	AY180916/FEA=transposon
2.18	Odorant-binding protein 99c (Obp99c)	CG7584-RA
2.18	Ionotropic receptor 31a (Ir31a)	CG31718-RA
2.18	CG32850	CG32850-RA
2.18	CG5322	CG5322-RA
2.18	CG6553	CG6553-RA
2.18	CG12581	CG12581-RB
2.17	NA	S.C3R002919/FEA=fgenesh/SEG=chr3R:-21311373,21316702
2.17	Major Facilitator Superfamily Transporter 3 (MFS3)	CG4726-RA
2.17	CG30151	CG30151-RA
2.17	Calcineurin B (CanB)	CG4209-RA
2.16	Sox21b	CG32139-RA
2.16	CG10440	CG10440-RA
2.16	katanin p60-like 1 (kat-60L1)	CG1193-RA
2.16	CG40295	CG40295-RA
2.16	CG32115	CG32115-RA
2.16	NA	HDC10707/FEA=HDP/SEG=chr3L:-17594492,17595319
2.16	highwire (hiw)	CG32592-RA

lsd1ΔN-bamΔ/bamΔ Fold Change	Identifier	Description
2.16	NA	AF541948/FEA=transposon
2.16	NA	HDC20591/FEA=HDP/SEG=chrU:+3650950,3655088
2.16	CG14227	CG14227-RA
2.16	CG32679	CG32679-RA
2.15	NA	RH17774/FEA=sim4/SEG=chr3R:-25256243,25257327
2.14	Ras-related protein (Rala)	CG2849-RB
2.14	CG13795	CG13795-RA
2.14	Adenylyl cyclase 78C (Ac78C)	CG10564-RA
2.14	CG14628	CG14628-RA
2.13	CG8083	CG8083-RA
2.13	CG12766	CG12766-RA
2.13	yellow-d	CG9889-RA
2.12	rosy (ry)	CG7642-RA
2.12	Cad96Ca	CG10244-RA
2.12	NA	S.C3R001979/FEA=fgenesh/SEG=chr3R:-14547742,14548261
2.12	Cyp6g1	CG8453-RA
2.12	CG30438	CG30438-RA
2.11	CG6426	CG6426-RA
2.11	NA	S.C2R002534/FEA=fgenesh/SEG=chr2R:+17986294,17988668
2.11	Imaginal disc growth factor 3 (Idgf3)	CG4559-RA
2.11	CG40006	CG40006-RC
2.10	Henna (Hn)	CG7399-RA
2.10	CG13032	CG13032-RA
2.09	CG30099	CG30099-RA
2.09	CG5697	CG5697-RA
2.08	CG3556	CG3556-RA
2.08	odd skipped (odd)	CG3851-RA
2.08	NA	HDC10357/FEA=HDP/SEG=chr3L:-15800630,15801182
2.08	Glutathione S transferase D5 (GstD5)	CG12242-RA
2.07	UDP-glycosyltransferase 35b (Ugt35b)	CG6649-RA
2.07	NA	HDC07622/FEA=HDP/SEG=chr3h:+1373421,1374096
2.06	Gr43b	CG1339-RA
2.06	NA	HDC20116/FEA=HDP/SEG=chr3h:+50015,55787
2.06	CG8713	CG8713-RA
2.06	CG40124	CG40124-RA
2.06	CG14275	CG14275-RA
2.06	Dromyosuppressin (Dms)	CG6440-RA
2.06	CG13577	CG13577-RA
2.06	Ornithine decarboxylase 1 (Odc1)	CG8721-RA
2.06	NA	FEA=transposon
2.05	CG31686	CG31686-RA
2.05	Rgk3	CG15663-RA
2.05	Tetraspanin 42En (Tsp42En)	CG12839-RA
2.05	(6-4)-photolyase (phr6-4)	CG2488-RA
2.04	Shaker cognate w (Shaw)	CG2822-RB
2.04	pou domain motif 3 (pdm3)	CG14755-RA
2.03	Cyp6a20	CG10245-RA
2.03	CG4676	CG4676-RA
2.02	persephone (psh)	CG6367-RA
2.02	CG7433	CG7433-RB
2.02	CG13894	CG13894-RA
2.01	Band4.1 inhibitor LRP interactor (Bili)	CG11848-RA
2.01	CG14423	CG14423-RA
2.00	NA	GM08552_revcomp/FEA=sim4/SEG=chrU:+2387881,2389317
2.00	CG10799	CG10799-RA
2.00	Larval serum protein 2 (Lsp2)	CG6806-RA

Table 2. Downregulated Genes Due to the Loss of lsd1 by Microarray

lsd1$^{\Delta N}$-bamΔ/bamΔ Fold Change	Identifier	Description
0.50	CG10702	CG10702-RB
0.50	CR31044	CG31044-RA
0.50	Cht6	CG15313-RA
0.50	CG10933	CG10933-RA
0.50	E(spl) region transcript m3 (HLHm3)	CG8346-RA
0.50	stoned B (stnB)	CG40306-RA
0.50	CG31176	CG31176-RA
0.50	CG17816	CG17816-RA
0.50	CG9505	CG9505-RA
0.50	CG6830	CG6830-RA
0.49	Netrin-A (NetA)	CG18657-RA
0.49	CG1632	CG1632-RA
0.49	polychaetoid (pyd)	CG31349-RE
0.49	NA	FEA=stencil/SEG=chr3R:-3683910,3685174
0.49	Heat shock gene 67Bc (Hsp67Bc)	CG4190-RA
0.49	midgut expression 1 (mex1)	CG7936-RA
0.49	NA	GH04518/FEA=sim4/SEG=chrX:+12390121,12391302
0.49	CG31619	CG31619-RA
0.48	Met75Cb (Met75Cb)	CG18064-RA
0.48	NA	FEA=stencil/SEG=chrX:-13627658,13631239
0.48	Abl tyrosine kinase (Abl)	CG4032-RA
0.48	fruitless (fru)	CG14307-RC
0.48	decay	CG14902-RA
0.48	Sox102F	CG11153-RA
0.48	NA	X15469/FEA=transposon
0.48	CG17698	CG17698-RA
0.48	CG14131	CG14131-RA
0.48	CG5853	CG5853-RA
0.48	shotgun (shg)	CG3722-RA
0.48	nicotinic Acetylcholine Receptor beta 96A (nAcRbeta-96A)	CG6798-RA
0.48	stripe (sr)	CG7847-RA
0.47	Delta (Dl)	CG3619-RB
0.47	Cecropin C (CecC)	CG1373-RA
0.47	nautilus (nau)	CG10250-RA
0.47	CG12974	CG12974-RA
0.47	laccase 2	CG30437-RA
0.47	Wnt oncogene analog 4 (Wnt4)	CG4698-RA
0.47	Wnt oncogene analog 2 (Wnt2)	CG1916-RA
0.47	Jupiter	CG31363-RB
0.47	CG9317	CG9317-RB
0.46	Cdep	CG31536-RC
0.46	NA	HDC05924/FEA=HDP/SEG=chr2R:-7229834,7230347
0.46	CG4570	CG4570-RA
0.46	sugar free floating (sff)	CG6114-RA
0.46	NA	CT33523/FEA=sim4/SEG=chr2L:-20081522,20082140
0.46	CG13075	CG13075-RA
0.46	Calcium activated protein for secretion (Caps)	CG18026-RA
0.46	CG3397	CG3397-RA
0.46	Fasciclin 3 (Fas3)	CG5803-RA

lsd1$^{\Delta N}$-bamΔ/bamΔ Fold Change	Identifier	Description
0.46	Heat shock gene 67Ba (Hsp67Ba)	CG4167-RA
0.45	2mit	CG10148-RA
0.45	Ac3	CG1506-RA
0.45	CG10650	CG10650-RA
0.45	CG15270	CG15270-RA
0.45	starry night (stan)	CG11895-RA
0.45	Organic cation transporter 2 (Orct2)	CG13610-RA
0.45	lazaro (laza)	CG11440-RA
0.45	CG3502	CG3502-RA
0.45	windbeutel (wbl)	CG7225-RA
0.45	Adenosine deaminase-related growth factor A (Adgf-A)	CG5992-RA
0.44	CG17684	CG40260-RA
0.44	CG18598	CG18598-RA
0.44	NMDA receptor 1 (Nmdar1)	CG2902-RA
0.44	terribly reduced optic lobes (trol)	CG12497-RA
0.44	CG3104	CG3104-RA
0.44	CG13921	CG13921-RA
0.43	CG32568	CG32568-RA
0.43	CG14795	CG14795-RB
0.43	spalt major (salm)	CG6464-RA
0.43	CG5707	CG5707-RA
0.43	NA	HDC07605/FEA=HDP/SEG=chr2h:+1622739,1623448
0.43	CG13737	CG13737-RA
0.43		CG40213-RA
0.43	dawdle (daw)	CG16987-RB
0.43	dachsous (ds)	CG17941-RA
0.43	CG7402	CG7402-RA
0.43	NA	CT33684/FEA=sim4/SEG=chr3L:-19388980,19389370
0.43	CG9411	CG9411-RA
0.43	polyhomeotic distal (ph-d)	CG3895-RA
0.43	CG30017	CG30017-RA
0.42	CG43729	CG12958-RA
0.42	alpha methyl dopa-resistant (amd)	CG10501-RB
0.42	pebbled (peb)	CG12212-RA
0.42	CG17470	CG17470-RA
0.42	Epidermal growth factor (Egfr)	CG10079-RA
0.42	CG16959	CG16959-RA
0.42	NA	S.C2R000437/FEA=fgenesh/SEG=chr2R:+3680066,3680399
0.42	slowdown (slow)	CG7447-RA
0.42	CG30377	CG30377-RA
0.42	ZnT35C	CG3994-RA
0.42	alpha-Tubulin at 67C (alphaTub67C)	CG8308-RA
0.42	CG11659	CG11659-RA
0.42	NA	S.C3L001530/FEA=fgenesh/SEG=chr3L:-11792794,11794240
0.42	CG6023	CG6023-RA
0.41	nervy (nvy)	CG3385-RA
0.41	CG13840	CG13840-RA
0.41	alphaPS4	CG16827-RA
0.41	CG5361	CG5361-RA

0.41	CG11378	CG11378-RA
0.40	acyl-Coenyme A oxidase at 57D distal (Acox57D-d)	CG9709-RA
0.40	reduced ocelli (rdo)	CG15151-RA
0.40	midline (mid)	CG6634-RA
0.40	CG31760	CG31760-RA
0.40	NA	CT33798/FEA=sim4/SEG=chrX:+18756086,18757017
0.40	Glucose transporter 4 enhancer factor (Glut4E)	CG12802-RA
0.40	CG12824	CG12824-RA
0.40	hedgehog (hh)	CG4637-RA
0.39	CG42249	CG1961-RA
0.39	E(spl) region transcript mbeta (HLHmbeta)	CG14548-RA
0.39	CG31530	CG31530-RA
0.39	twin of eyeless (toy)	CG11186-RB
0.39	Osiris 19 (Osi19)	CG15189-RA
0.39	sevenless (sev)	CG18085-RA
0.39	CG4998	CG4998-RA
0.39	CG14502	CG14502-RA
0.39	CG4619	CG4619-RA
0.38	net	CG11450-RA
0.38	CG12418	CG12418-RA
0.38	CG16886	CG16886-RA
0.38	CG32447	CG32447-RA
0.38	CG43729	CG8179-RA
0.38	Lipase 4 (Lip4)	CG6113-RA
0.37	CG11878	CG11878-RA
0.37	frizzled (fz)	CG17697-RB
0.37	CG15422	CG15422-RA
0.37	CG30440	CG30440-RA
0.37	echinus (ec)	CG2904-RA
0.37	CG10924	CG10924-RA
0.37	biniou (bin)	CG18647-RA
0.37	CG30485	CG30485-RA
0.37	Six4	CG3871-RA
0.37	defective proventriculus (dve)	CG5799-RA
0.36	oskar (osk)	CG10901-RB
0.36	CG4797	CG4797-RB
0.36	Antigen 5-related (Ag5r)	CG9538-RA
0.36	outsiders (out)	CG8062-RA
0.36	CG32107	CG32107-RA
0.36	CG4666	CG4666-RA
0.36	Edem1	CG3810-RC
0.36	Metallothionein B (MtnB)	CG4312-RA
0.36	NA	CT33783/FEA=sim4/SEG=chr3L:+9510675,9510921
0.35	CG32639	CG32639-RA
0.35	CG11353	CG11353-RA
0.35	CG14072	CG14072-RA
0.35		CG32805-RA
0.35	Lin29	CG2052-RB
0.35	Heat shock gene 67Bb (Hsp67Bb)	CG32041-RA

lsd1$^{\Delta N}$-bamΔ/bamΔ Fold Change	Identifier	Description
0.35	p24-related-2 (p24-2)	CG33105-RA
0.35	NA	LD48030/FEA=sim4/SEG=chrX:-4177601,4178554
0.35	CG12768	CG12768-RA
0.34	CG4325	CG4325-RA
0.34	Cytochrome P450-18a1 (Cyp18a1)	CG6816-RB
0.34	CG4783	CG4783-RA
0.34	CG11889	CG33091-RA
0.33	CG32249	CG32249-RA
0.33	CG32642	CG32642-RC
0.33	CG3987	CG3987-RA
0.33	Nuclear factor I (NfI)	CG2380-RA
0.33	TAR DNA-binding protein-43 homolog (TBPH)	CG10327-RC
0.33	knickkopf (knk)	CG6217-RA
0.32	Mucin related 2B (Mur2B)	CG14796-RA
0.32	pan gu (png)	CG11420-RA
0.32	CG42336	CG13210-RA
0.32	Cad99C	CG31009-RA
0.32	Follistatin (Fs)	CG12956-RA
0.31	CG13813	CG13813-RA
0.31	unplugged (unpg)	CG1650-RA
0.31	CG16727	CG16727-RA
0.31	CG7881	CG7881-RA
0.31	Glutathione S transferase D2 (GstD2)	CG4181-RA
0.31	CG18519	CG18519-RA
0.31	CG31759	CG31759-RB
0.31	spook (spo)	CG10594-RA
0.30	oskar (osk)	CG10901-RA
0.30	Dual oxidase (Duox)	CG3131-RA
0.30	Organic anion transporting polypeptide 58Db (Oatp58Db)	CG3382-RA
0.30	lectin-37Da (lectin-37Da)	CG9978-RA
0.30	CG18508	CG4015-RA
0.30	CG9815	CG9815-RA
0.30	wunen-2 (wun2)	CG8805-RA
0.30	Cyp6a18 (Cyp6a18)	CG13977-RA
0.30	CG9837	CG9837-RA
0.30	CG15035	CG15035-RA
0.29	wrapper	CG10382-RA
0.29	CG9314	CG9314-RA
0.29	CG11951	CG11951-RA
0.29	CG12780	CG12780-RA
0.29	CG30385	CG30385-RA
0.29	Serotonin receptor 2 (5-HT2)	CG1056-RA
0.29	CG30076	CG30076-RA
0.29	CG6739	CG6739-RA
0.29	Twin of m4 (Tom)	CG5185-RA
0.29	maternal gene required for meiosis (mamo)	CG11072-RA
0.28	kekkon-2 (kek2)	CG4977-RA
0.28	CG1942	CG1942-RA
0.28	CG9747	CG9747-RA

lsd1$^{\Delta N}$-bamΔ/bamΔ Fold Change	Identifier	Description
0.28	Monocarboxylate transporter 1 (Mct1)	CG3456-RA
0.28	Cad88C	CG3389-RA
0.28	NA	HDC15003/FEA=HDP/SEG=chr3R:-18263657,18263902
0.28	CG31267	CG31267-RA
0.28	CG17322	CG17322-RD
0.27	NA	HDC06000/FEA=HDP/SEG=chr2R:+7523305,7523900
0.27	CG13003	CG13003-RA
0.27	CG9673	CG9673-RA
0.27	CG3884	CG3884-RB
0.27	Rapgap1	CG6682-RA
0.26	cut (ct)	CG11387-RB
0.26	CG6908	CG6908-RA
0.26	CG15155	CG15155-RA
0.26	scarecrow (scro)	CG17594-RA
0.26	CG8245	CG8245-RA
0.26	CG43332	CG32972-RB
0.26	CG17169	CG17169-RA
0.26	NA	HDC19639/FEA=HDP/SEG=chrX:+18724149,18725680
0.25	yellow-g	CG5717-RA
0.25	CG17732	CG17732-RA
0.25	CG9164	CG9164-RC
0.25	kekkon4 (kek4)	CG9431-RA
0.25	CG11380	CG11380-RA
0.25	timeless (tim)	CG3234-RC
0.25	thisbe (ths)	CG12443-RA
0.25	CG13227	CG13227-RA
0.25	CG8964	CG8964-RA
0.25	CG31601	CG31601-RA
0.25	CG15546	CG15546-RA
0.24	CG31343	CG31343-RA
0.24	Chorion protein a at 7F (Cp7Fa)	CG15348-RA
0.23	CG11320	CG11320-RA
0.23	biniou (bin)	CG18647-RA
0.23	CG33296	CG33296-RA
0.23	Guanine nucleotide exchange factor GEF64C (Gef64C)	CG32239-RA
0.23	Chitin deacetylase-like 5 (Cda5)	CG31973-RA
0.23	NA	LD19629/FEA=sim4/SEG=chr3R:+16103035,16104902
0.23	CG31661	CG31661-RA
0.22	E(spl) region transcript m2 (m2)	CG6104-RA
0.22	Ecdysone-induced protein 75B (Eip75B)	CG8127-RB
0.22	CG15822	CG15822-RC
0.22	CG6125	CG6125-RB
0.21	Synapsin (Syn)	CG3985-RB
0.21	NA	FEA=ncRNA/SEG=chr3R:-8958150,8981405
0.21	fruitless (fru)	CG14307-RD
0.21	CG5921	CG5921-RA
0.21	CG12206	CG12206-RA
0.21	CG10396	CG10396-RA
0.21	Lysozyme X (LysX)	CG9120-RA

lsd1$^{\Delta N}$-bamΔ/bamΔ Fold Change	Identifier	Description
0.21	Sodium-dependent multivitamin transporter (Smvt)	CG2191-RA
0.20	shade (shd)	CG13478-RA
0.20	CG16995	CG16995-RA
0.20	CG10086	CG10086-RA
0.20	Jon65Aiii	CG6483-RA
0.20	Chorion protein 18 (Cp18)	CG6517-RA
0.20	apterous (ap)	CG8376-RB
0.19	CG17681	CG17681-RA
0.19	CG10912	CG10912-RA
0.19	CG14834	CG14834-RA
0.19	Vesicular monoamine transporter (Vmat)	CG6139-RB
0.18	Cytochrome P450-4d8 (Cyp4d8)	CG4321-RA
0.18	CG9568	CG9568-RA
0.18	CG43366	CG14470-RA
0.18	CG6602	CG6602-RA
0.18	CG7675	CG7675-RA
0.18	CG6753	CG6753-RA
0.18	CG10257	CG10257-RA
0.18	CG18673	CG18673-RA
0.18	salty dog (salt)	CG2196-RA
0.17	CG31004	CG31004-RA
0.17	CG31926	CG31926-RA
0.17	Cuticular protein 47Ee (Cpr47Ee)	CG13222-RA
0.17	CG14499	CG14499-RA
0.17	CG12540	CG12540-RA
0.17	CG8628	CG8628-RA
0.17	NA	FEA=ncRNA/SEG=chr2R:-620172,622359
0.16	CG32024	CG32024-RA
0.16	CG9259	CG9259-RA
0.16	CG5804	CG5804-RA
0.16	CG9449	CG9449-RA
0.16	CG31272	CG31272-RA
0.16	CG31157	CG31157-RA
0.16	Insulin-like peptide 6 (Ilp6)	CG14049-RA
0.15	pipe (pip)	CG9614-RA
0.15	CG2837	CG2837-RB
0.15	CG9220	CG9220-RA
0.15	Mucin 4B (Muc4B)	CG32774-RA
0.15	CG42747	CG14911-RA
0.15	off-track (otk)	CG8967-RA
0.15	CG9449	CG9449-RB
0.15	CG6337	CG6337-RA
0.15	CG34347	CG15566-RA
0.14	HES-related (Her)	CG5927-RA
0.14	CG13311	CG13311-RA
0.14	white (w)	CG2759-RA
0.14	Organic anion transporting polypeptide 58Dc (Oatp58Dc)	CG3380-RA
0.13	CG9503	CG9503-RA
0.13	CG17475	CG17475-RA

lsd1$^{\Delta N}$-bamΔ/bamΔ Fold Change	Identifier	Description
0.13	neverland (nvd)	CG40050-RA
0.13	NA	CT33922/FEA=sim4/SEG=chr3R:-14728195,14728525
0.13	NA	FEA=stencil/SEG=chrX:-13636195,13639537
0.13	CG31714	CG31714-RA
0.12	CG8303	CG8303-RA
0.12	Cytochrome P450-18a1 (Cyp18a1)	CG6816-RA
0.12	CG14059	CG14059-RA
0.12	NA	AM01350/FEA=sim4/SEG=chrX:+2090943,2091368
0.12	CG13309	CG13309-RA
0.12	veil	CG4827-RA
0.12	Chorion protein c at 7F (Cp7Fc)	CG15351-RA
0.12	Ugt36Ba	CG13270-RA
0.12	shroud (sro)	CG12068-RA
0.11	doublesex cognate 73A (dsx-c73A)	CG32159-RB
0.11	CG32798	CG32798-RA
0.11	CG31262	CG31262-RA
0.10	CG13905	CG13905-RA
0.10	CG42826	CG6640-RA
0.10	CG13113	CG13113-RA
0.10	prolyl-4-hydroxylase-alpha PV (PH4alphaPV)	CG31015-RA
0.10	CG13616	CG13616-RA
0.10	sickle (sick)	CG13701-RA
0.10	Mucin 12Ea (Muc12Ea)	CG32602-RA
0.09	CG13084	CG13084-RA
0.09	traffic jam (tj)	CG10034-RA
0.09	CG10175	CG10175-RA
0.09	CG13403	CG13403-RA
0.09	phantom (phm)	CG6578-RA
0.09	cln3	CG5582-RA
0.09	CG13321	CG13321-RA
0.09	castor (cas)	CG2102-RA
0.09	prominin (prom)	CG30165-RA
0.09	cad74A	CG6445-RB
0.09	defective chorion 1 (dec-1)	CG2175-RA
0.09	CG14187	CG14187-RA
0.08	Urate oxidase (Uro)	CG7171-RA
0.08	CG10163	CG10163-RA
0.08	CG5506	CG5506-RA
0.08	stall (stl)	CG3622-RB
0.08	CG32204	CG32204-RA
0.08	CG31198	CG31198-RA
0.08	CG31809	CG31809-RA
0.08	Ionotropic receptor 7c (Ir7c)	CG15324-RA
0.07	CG3290	CG3290-RA
0.07	Chorion protein 16 (Cp16)	CG6533-RA
0.07	CG15570	CG15570-RA
0.07	Chorion protein 19 (Cp19)	CG6524-RA
0.07	CG13636	CG13636-RB
0.07	CG10911	CG10911-RA

lsd1$^{\Delta N}$-bamΔ/bamΔ Fold Change	Identifier	Description
0.07	CG13992	CG13992-RA
0.07	CG13114	CG13114-RA
0.07	CG1077	CG1077-RA
0.06	Sulfotransferase 4 (St4)	CG6704-RA
0.06	Vitelline membrane 26Ab (Vm26Ab)	CG9046-RA
0.06	CG15721	CG15721-RA
0.06	yellow-k	CG7463-RA
0.06	Odorant-binding protein 19c (Obp19c)	CG15457-RA
0.06	innexin 7 (inx7)	CG2977-RB
0.06	Chorion protein a at 7F (Cp7Fa)	CG15349-RA
0.06	Chorion protein b at 7F (Cp7Fb)	CG15350-RA
0.06	CG15571	CG15571-RA
0.06	Chorion protein 15 (Cp15)	CG6519-RA
0.06	yellow-g2	CG13804-RA
0.05	Femcoat	CG15573-RB
0.05	CG13083	CG13083-RA
0.05	CG33258	CR33258-RA
0.05	Vitelline membrane 26Aac (Vm26Ac)	CG13997-RA
0.05	Chorion protein 36 (Cp36)	CG1478-RA
0.05	CG12398	CG12398-RA
0.05	Mucin related 29B (Mur29B)	CG31901-RA
0.05	CG5326	CG5326-RB
0.04	Vitelline membrane 32E (Vm32E)	CG16874-RA
0.04	Suppressor of variegation 3-3 (Su(var)3-3)	CG17149-RA
0.04	CG11381	CG11381-RA
0.04	CG5326	CG5326-RA
0.04	CG4009	CG4009-RA
0.03	palisade (psd)	CG9050-RA
0.03	Vitelline membrane 34Ca (Vm34Ca)	CG9271-RA
0.03	Vitelline membrane 26Aa (Vm26Aa)	CG9048-RA
0.02	Chorion protein 38 (Cp38)	CG11213-RA

APPENDIX B

CHIP-SEQ DATA FOR LSD1

IDENTIFYING TRANSCRIPTIONAL TARGETS OF LSD1 IN ESCORT CELLS

RNA-SEQ TO FUNTIONALLY VALIDATE CHIP-SEQ

Binding Sites of Lsd1 on Chromosome X

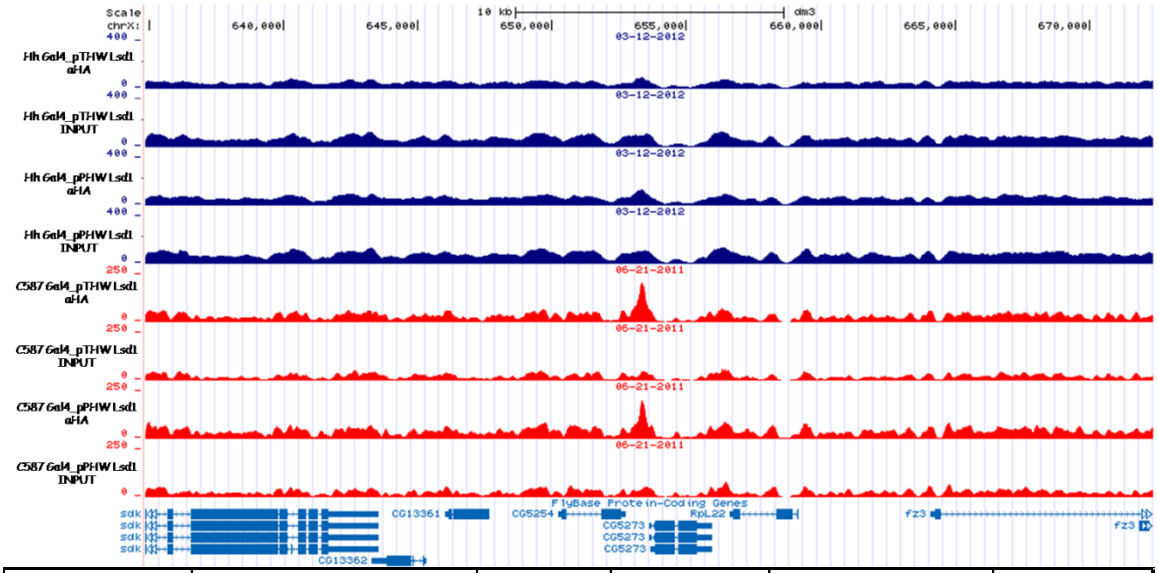

gene	locus	WT_EC	Lsd1 KD_EC	log2(fold_change)	significant
CG5273	chrX:653627-655972	6.98134	37.8018	2.43688	yes

Figure 1. Screenshot of Lsd1 binding sites on coordinates chrX:634,868-672,367 and RNA seq data for genes that exhibit significant difference between WT escort cells and Lsd1 knockdown escort cells

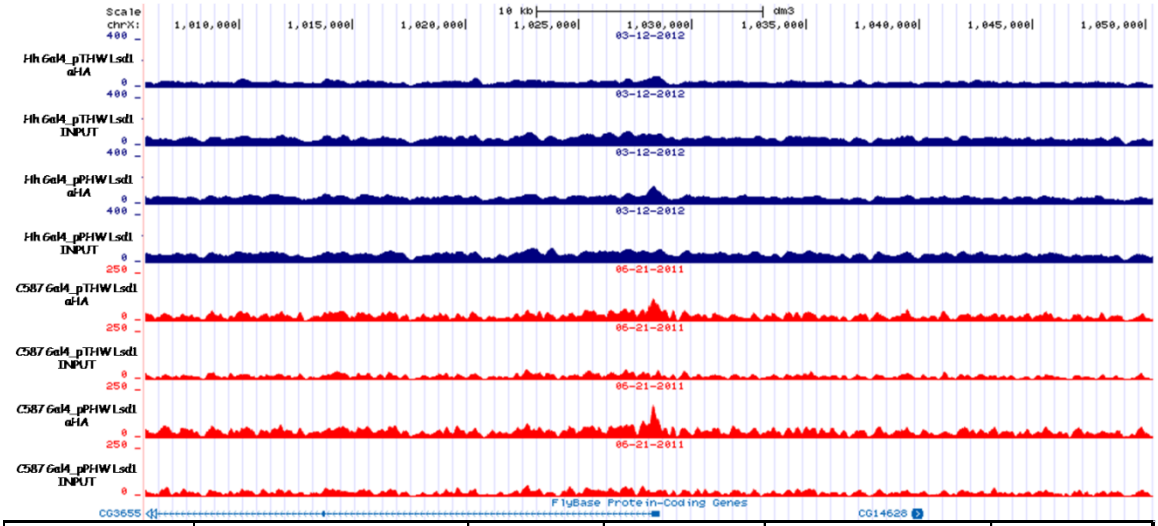

gene	locus	WT_EC	Lsd1 KD_EC	log2(fold_change)	significant
CG3655	chrX:967936-1028547	3.76089	14.6348	1.96025	yes

Figure 2. Screenshot of Lsd1 binding sites on coordinates chrX:1,005,878-1,050,322 and RNA seq data for genes that exhibit significant difference between WT escort cells and Lsd1 knockdown escort cells

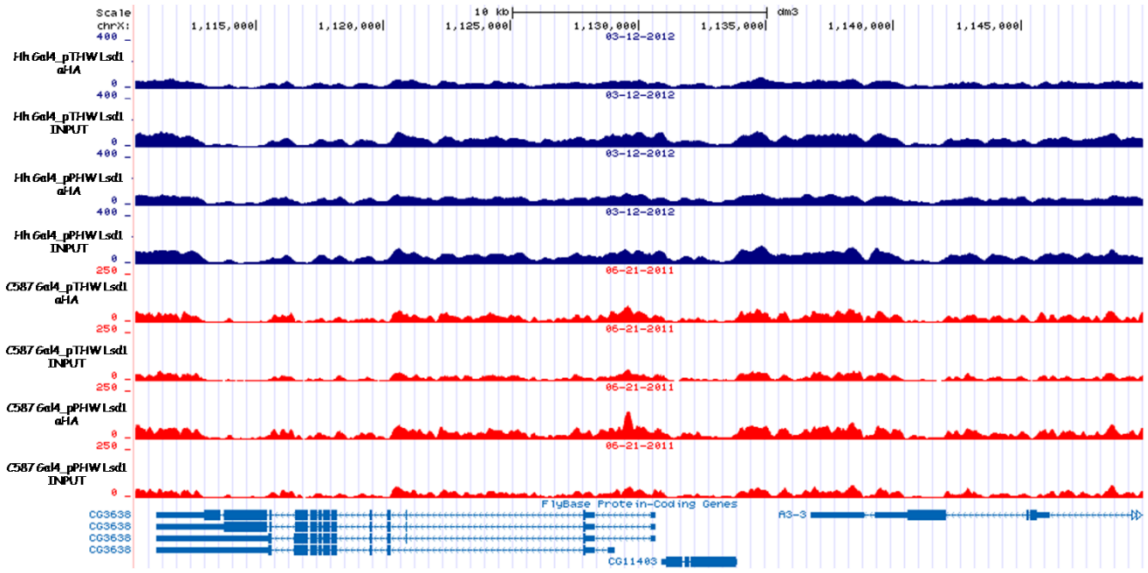

Figure 3. Screenshot of Lsd1 binding sites on coordinates chrX:1,110,281-1,149,787

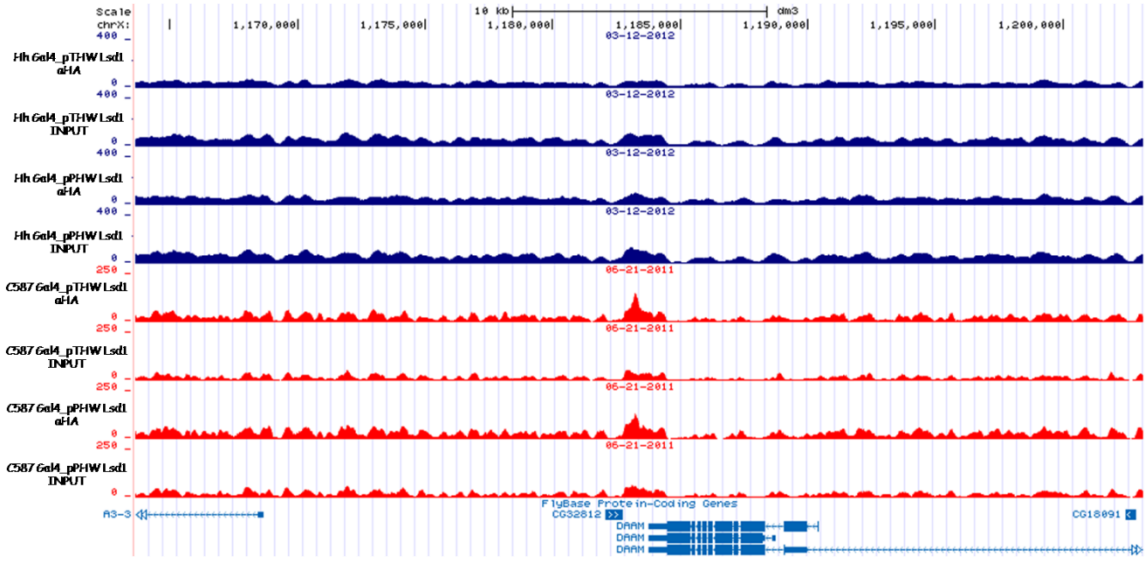

gene	locus	WT_EC	Lsd1 KD_EC	log2(fold_change)	significant
CG32812	chrX:1181322-1182978	0.0932121	0.704005	2.917	yes
DAAM	chrX:1183745-1216427	1.77194	11.7848	2.73353	yes

Figure 4. Screenshot of Lsd1 binding sites on coordinates chrX:1,163,635-1,203,141 and RNA seq data for genes that exhibit significant difference between WT escort cells and Lsd1 knockdown escort cells

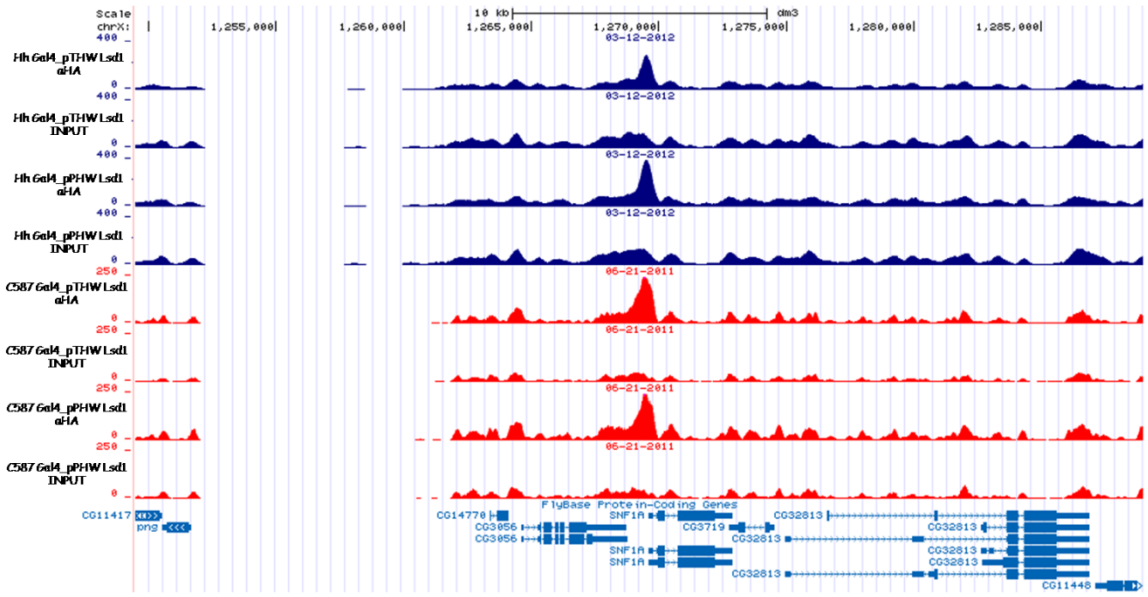

Figure 5. Screenshot of Lsd1 binding sites on coordinates chrX:1,249,473-1,288,979

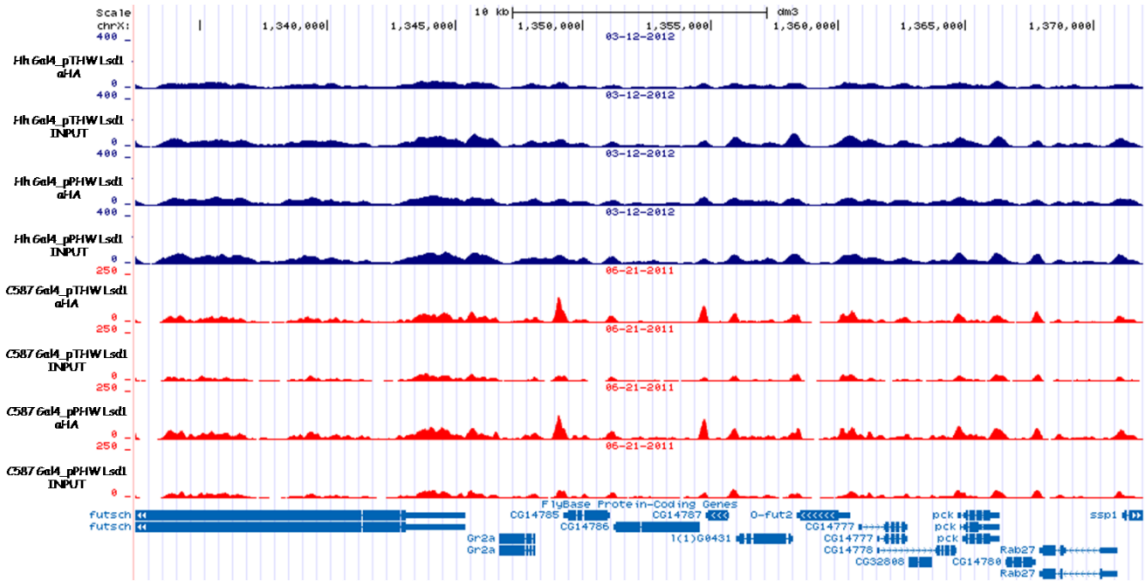

Figure 6. Screenshot of Lsd1 binding sites on coordinates chrX:1,332,458-1,371,964

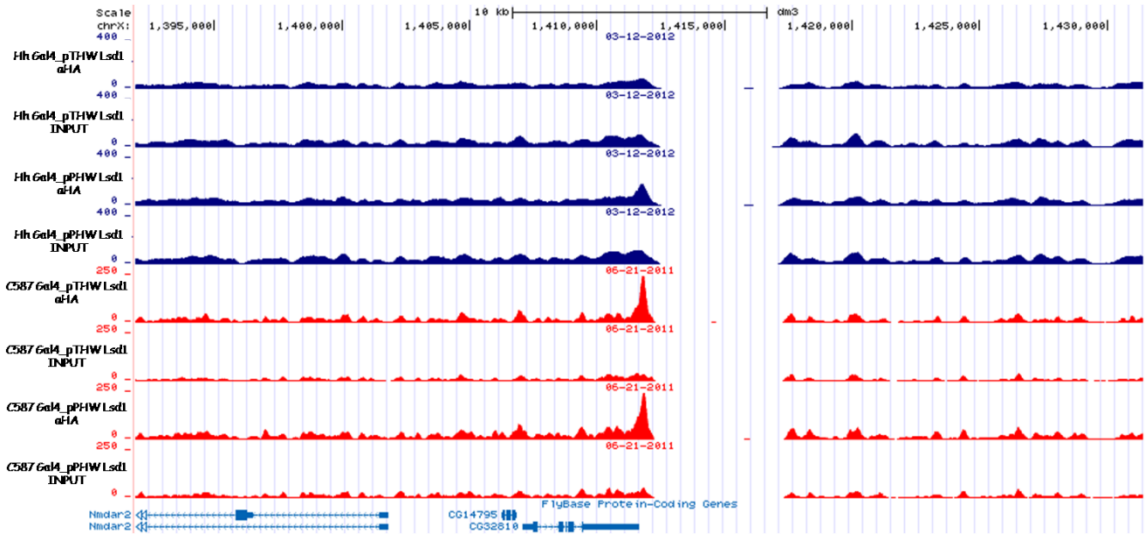

Figure 7. Screenshot of Lsd1 binding sites on coordinates chrX:1,391,903-1,431,409

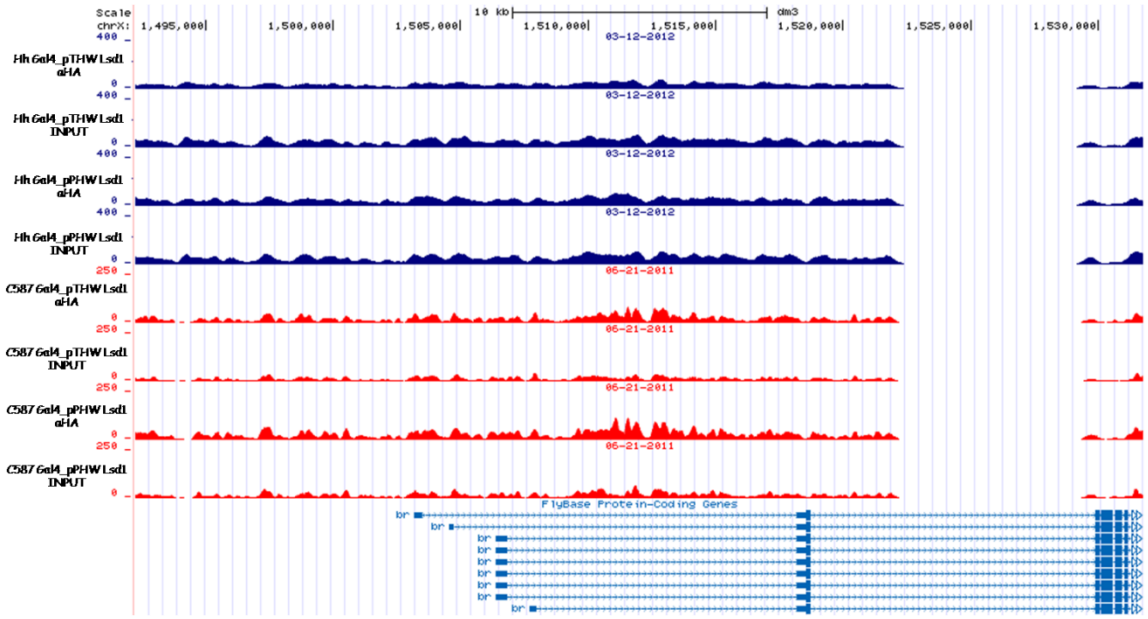

gene	locus	WT_EC	Lsd1 KD_EC	log2(fold_change)	significant
br	chrX:1417932-1553962	62.5562	32.4519	-0.946848	yes

Figure 8. Screenshot of Lsd1 binding sites on coordinates chrX:1,492,248-1,531,754 and RNA seq data for genes that exhibit significant difference between WT escort cells and Lsd1 knockdown escort cells

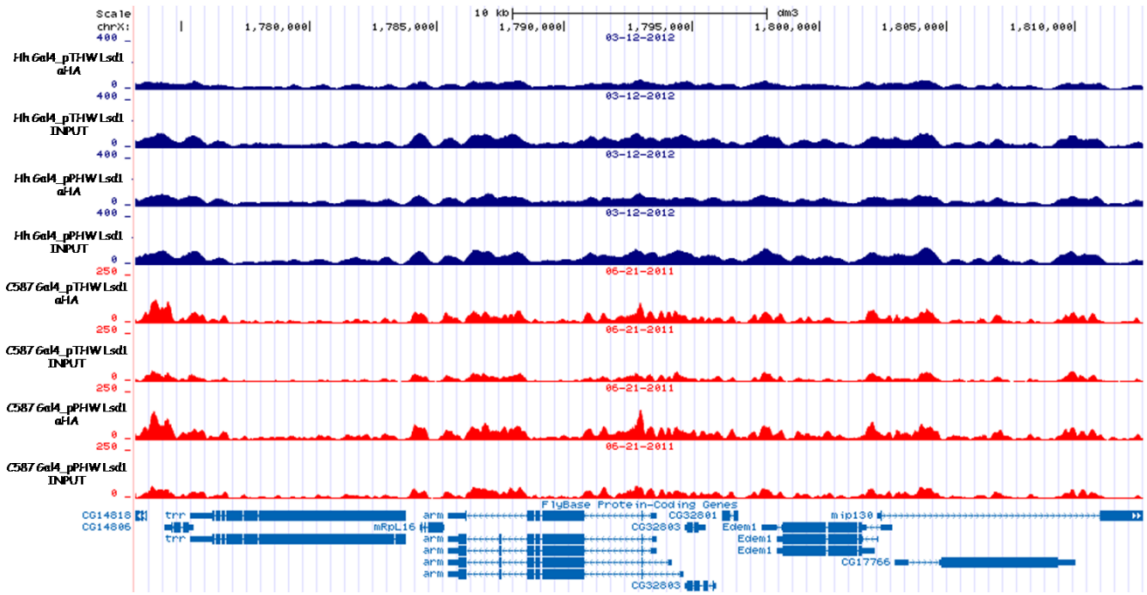

Figure 9. Screenshot of Lsd1 binding sites on coordinates chrX:1,773,186-1,812,692

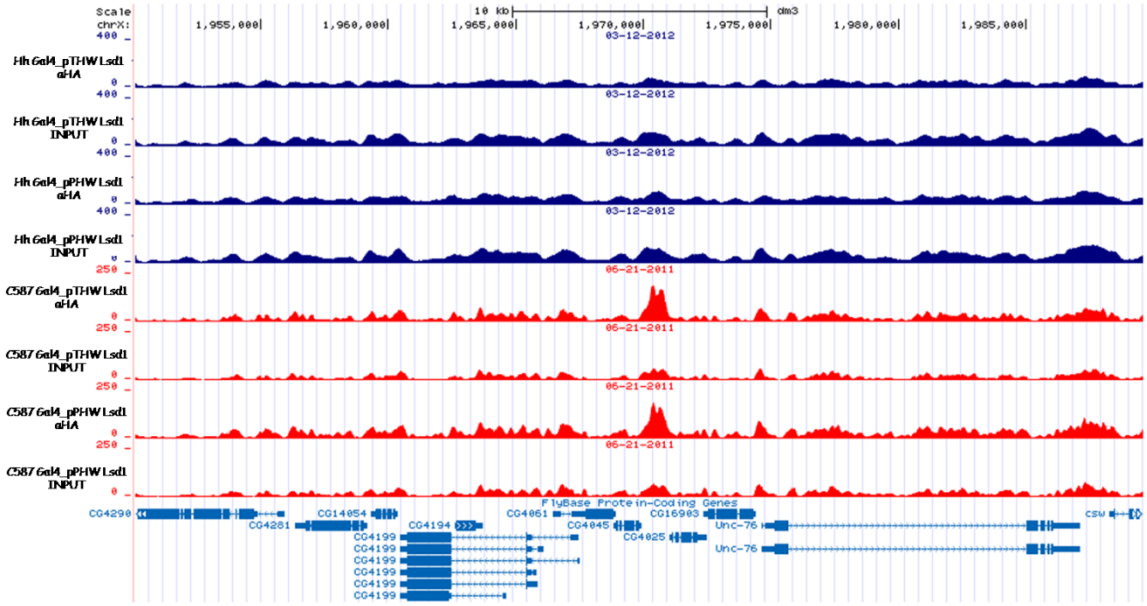

gene	locus	WT_EC	Lsd1 KD_EC	log2(fold_change)	significant
CG4199	chrX:1960467-1969933	12.8581	50.6479	1.97783	yes
Unc-76	chrX:1974644-1987129	10.8341	27.8607	1.36266	yes

Figure 10. Screenshot of Lsd1 binding sites on coordinates chrX:1,950,083-1,989,589 and RNA seq data for genes that exhibit significant difference between WT escort cells and Lsd1 knockdown escort cells

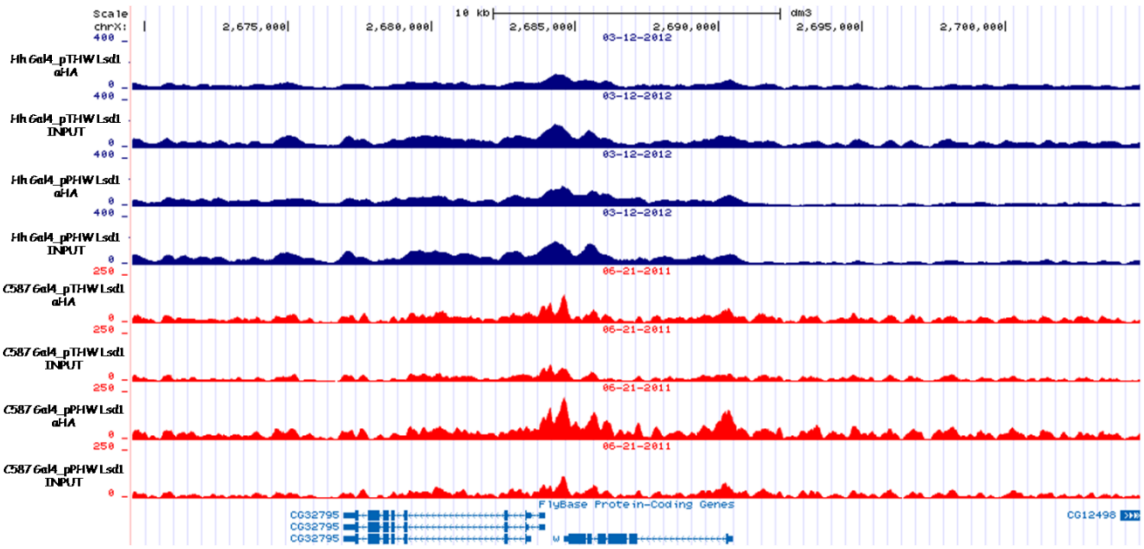

Figure 11. Screenshot of Lsd1 binding sites on coordinates chrX:2,669,578-2,704,694

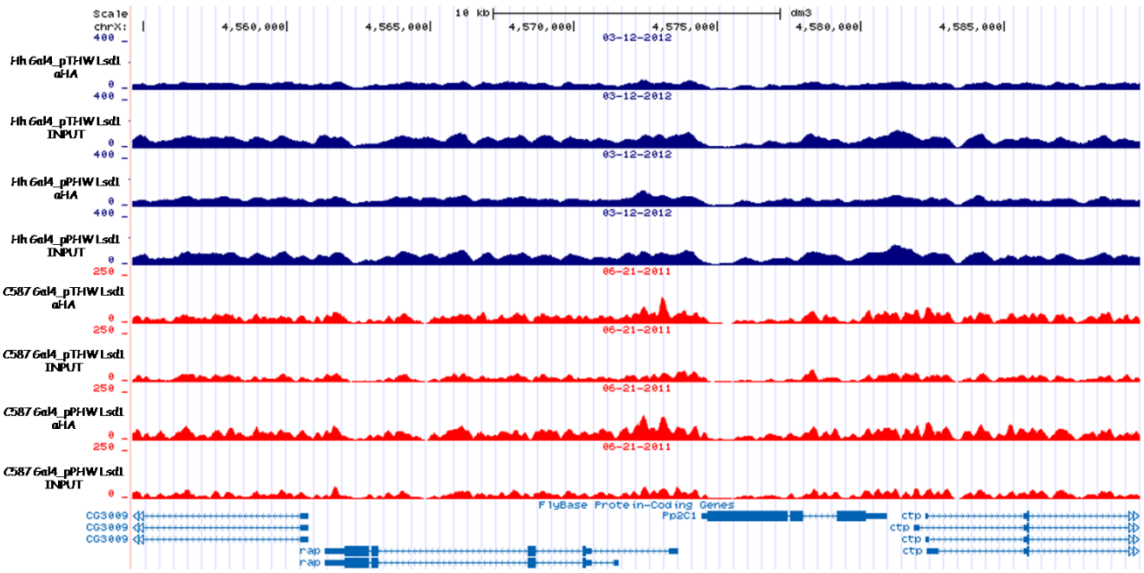

Figure 12. Screenshot of Lsd1 binding sites on coordinates chrX:4,554,610-4,589,726

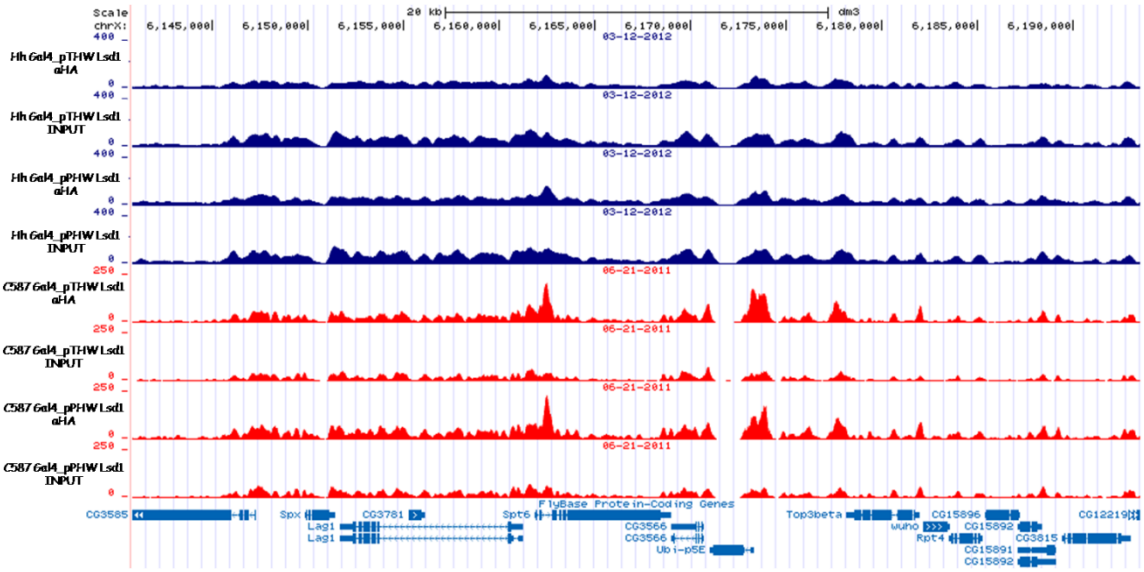

Figure 13. Screenshot of Lsd1 binding sites on coordinates chrX:6,140,834-6,193,509

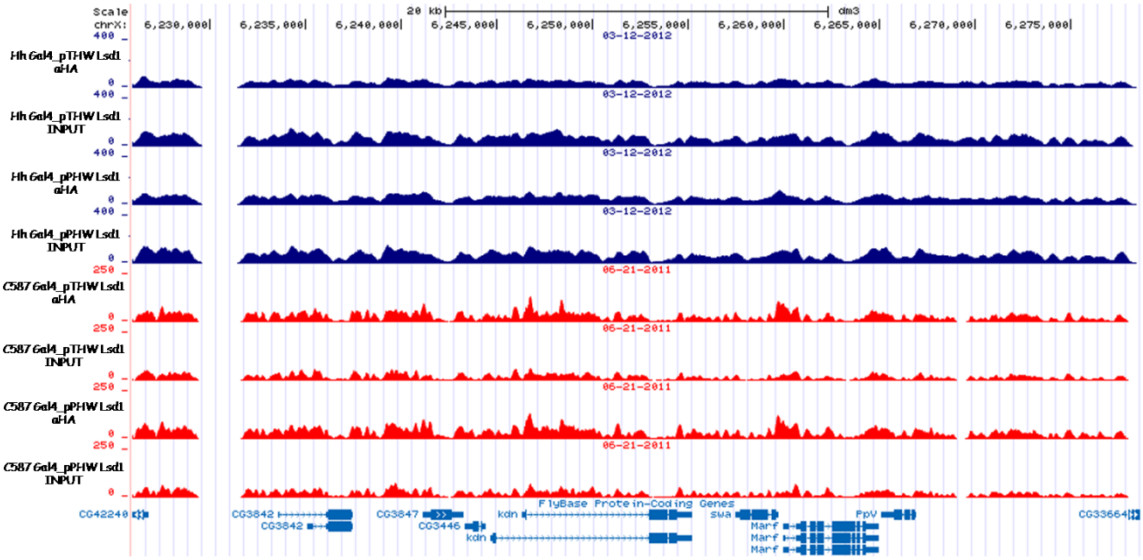

gene	locus	WT_EC	Lsd1 KD_EC	log2(fold_change)	significant
swa	chrX:6257450-6259742	0.178713	2.98536	4.06219	yes

Figure 14. Screenshot of Lsd1 binding sites on coordinates chrX:6,225,952-6,278,627 and RNA seq data for genes that exhibit significant difference between WT escort cells and Lsd1 knockdown escort cells

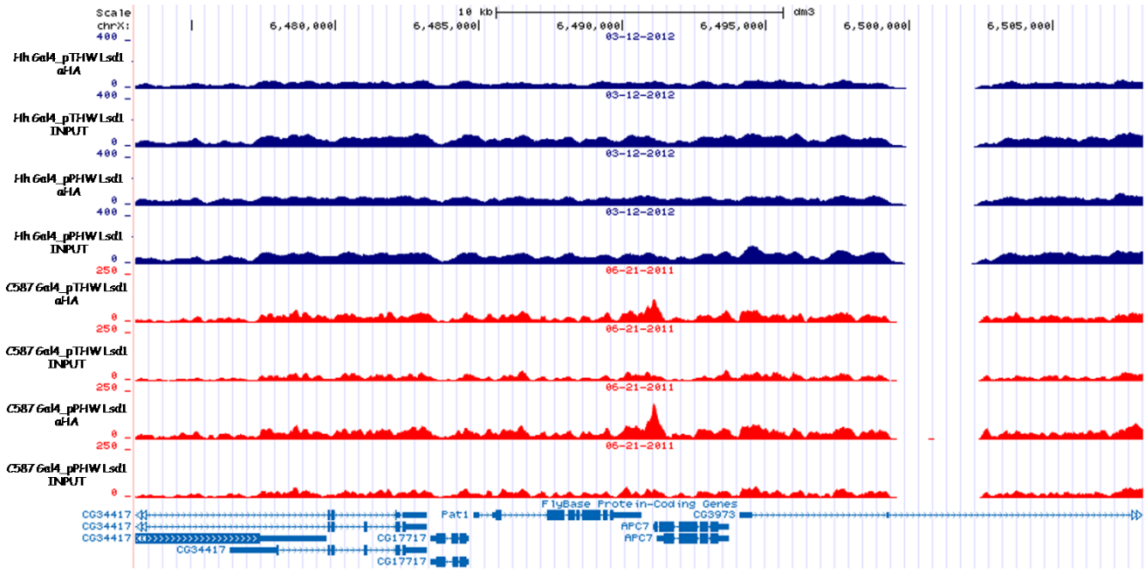

gene	locus	WT_EC	Lsd1 KD_EC	log2(fold_change)	significant
Apc7	chrX:6491077-6493733	0.10088	2.10375	4.38225	yes

Figure 15. Screenshot of Lsd1 binding sites on coordinates chrX:6,473,038-6,508,154 and RNA seq data for genes that exhibit significant difference between WT escort cells and Lsd1 knockdown escort cells

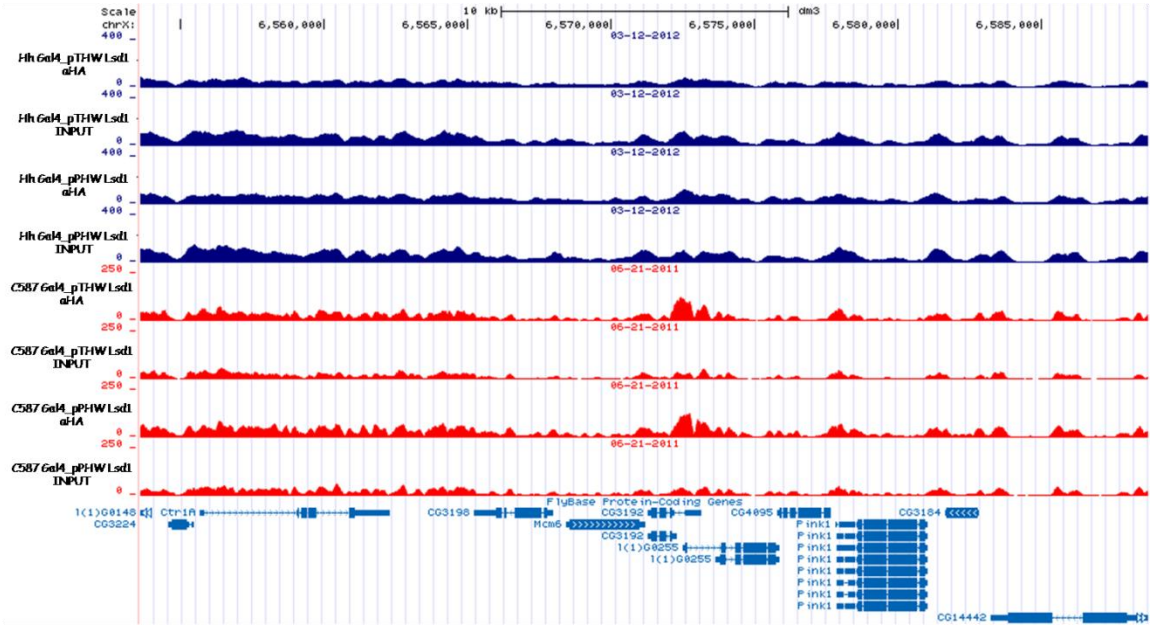

Figure 16. Screenshot of Lsd1 binding sites on coordinates chrX:6,553,600-6,588,716

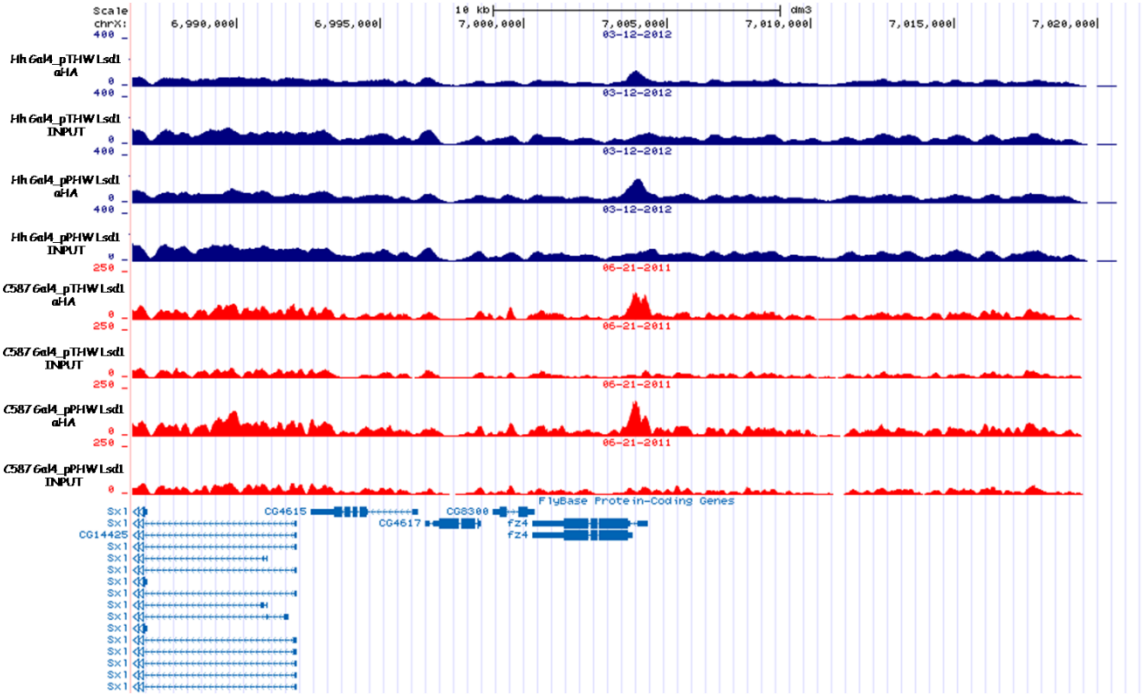

Figure 17. Screenshot of Lsd1 binding sites on coordinates chrX:6,986,373-7,021,489

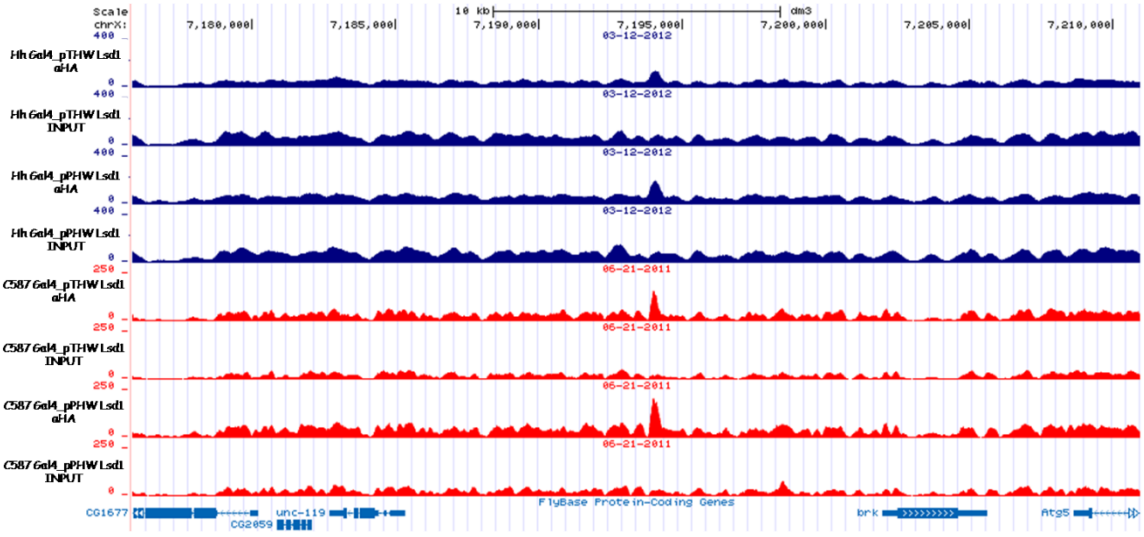

Figure 18. Screenshot of Lsd1 binding sites on coordinates chrX:7,175,834-7,210,950

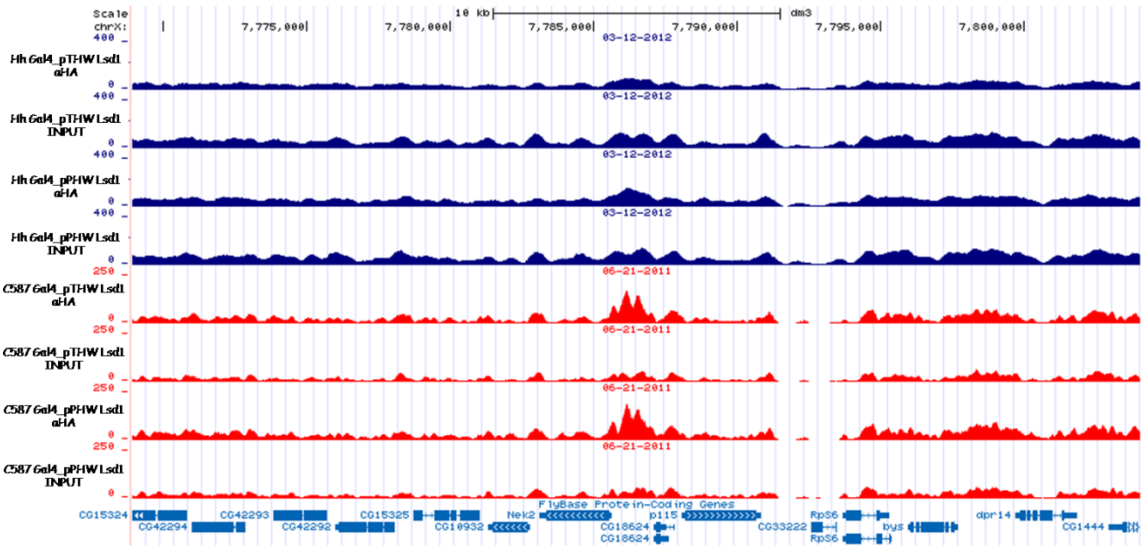

Figure 19. Screenshot of Lsd1 binding sites on coordinates chrX:7,768,911-7,804,027

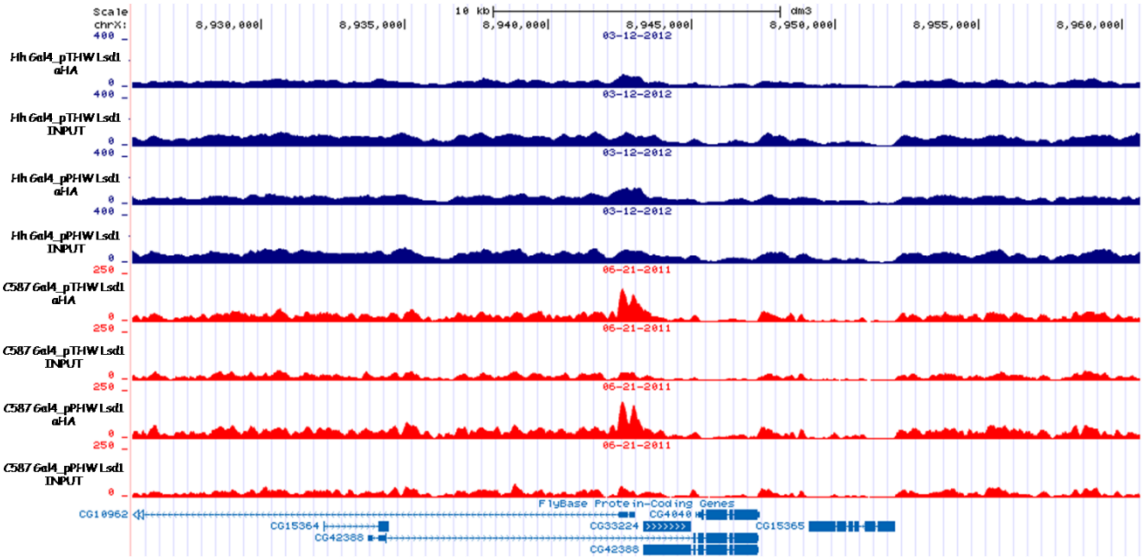

gene	locus	WT_EC	Lsd1 KD_EC	log2(fold_change)	significant
CG10962	chrX:8801100-8947352	0.683804	4.11841	2.59043	yes

Figure 20. Screenshot of Lsd1 binding sites on coordinates chrX:8,925,508-8,960,624 and RNA seq data for genes that exhibit significant difference between WT escort cells and Lsd1 knockdown escort cells

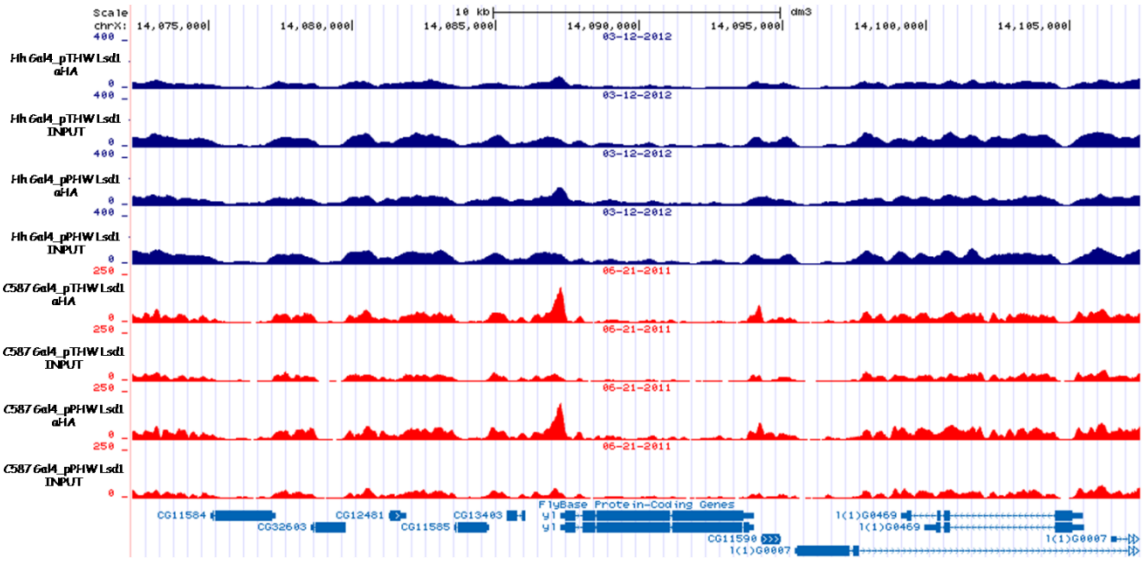

Gene	Locus	WT_EC	Lsd1 KD_EC	log2(fold_change)	significant
CG13403	chrX:14085247-14086019	0.235558	27.14	6.8482	yes
yl	chrX:14087251-14093996	0.627055	7.23697	3.52872	yes

Figure 21. Screenshot of Lsd1 binding sites on coordinates chrX:14,072,337-14,107,453 and RNA seq data for genes that exhibit significant difference between WT escort cells and Lsd1 knockdown escort cells

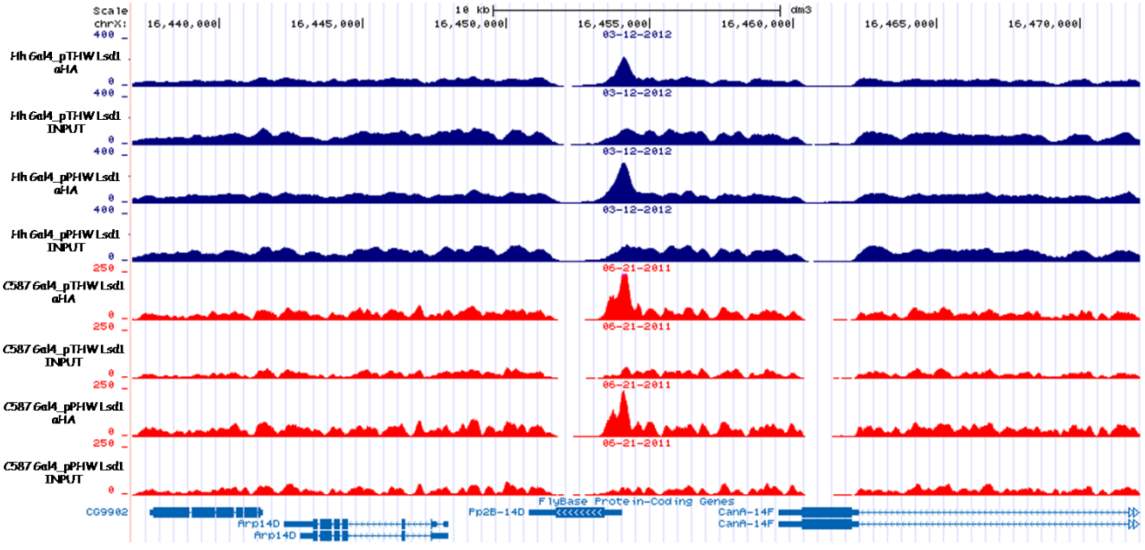

Figure 22. Screenshot of Lsd1 binding sites on coordinates chrX:16,436,978-16,472,094

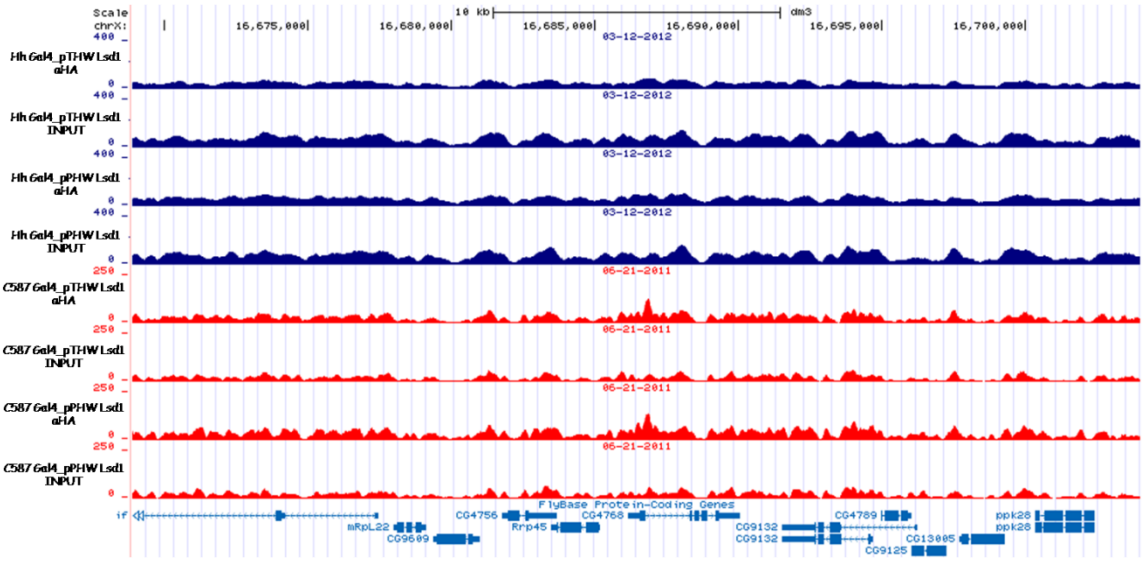

Figure 23. Screenshot of Lsd1 binding sites on coordinates chrX:16,668,900-16,704,016

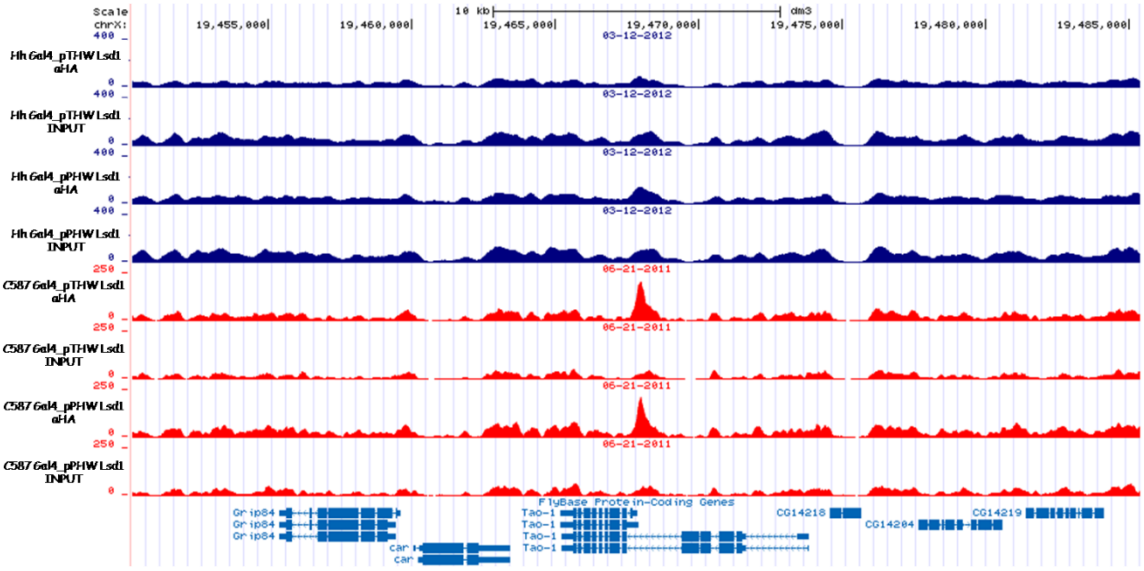

Figure 24. Screenshot of Lsd1 binding sites on coordinates chrX:19,450,264-19,485,380

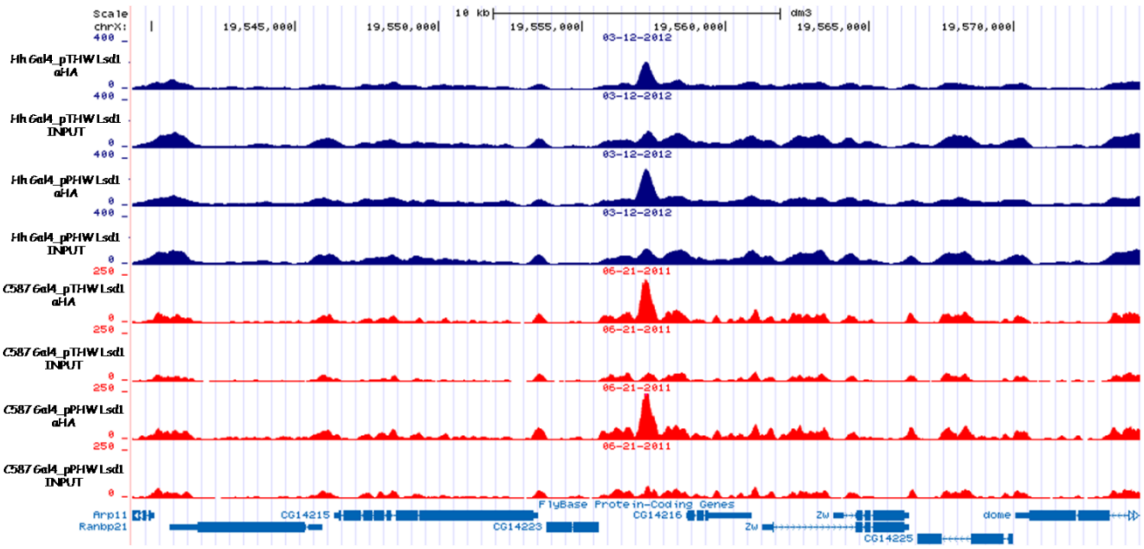

Figure 25. Screenshot of Lsd1 binding sites on coordinates chrX:19,539,314-19,574,430

Binding Sites of Lsd1 on Chromosome 2L

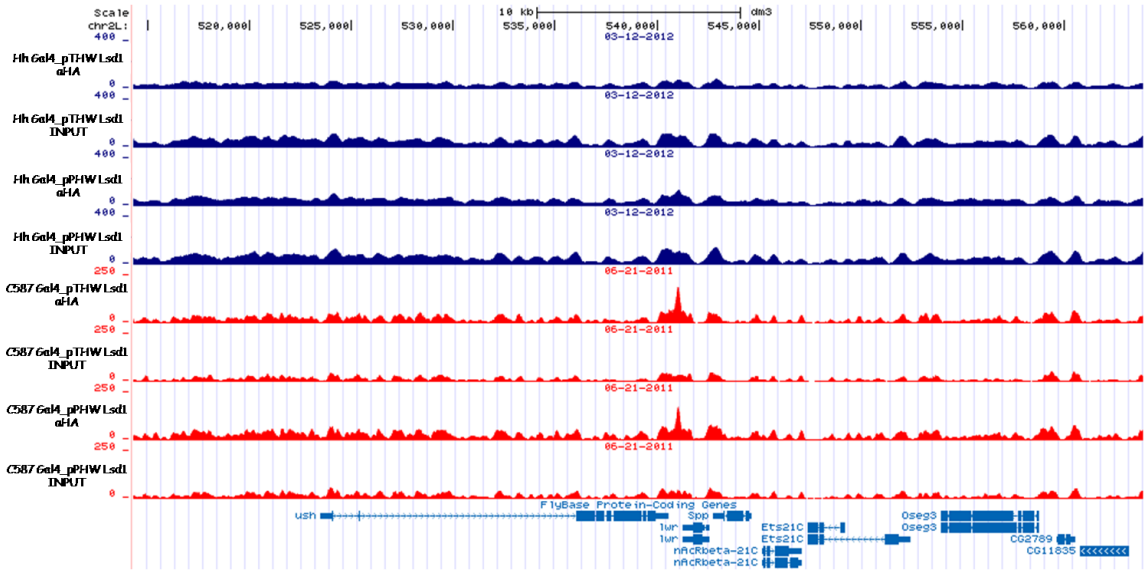

Gene	Locus	WT_EC	Lsd1 KD_EC	log2(fold_change)	significant
nAcRbeta-21C	chr2L:545147-547096	3.36685	14.7846	2.13463	yes

Figure 26. Screenshot of Lsd1 binding sites on coordinates chr2L:514,290-563,864 and RNA seq data for genes that exhibit significant difference between WT escort cells and Lsd1 knockdown escort cells

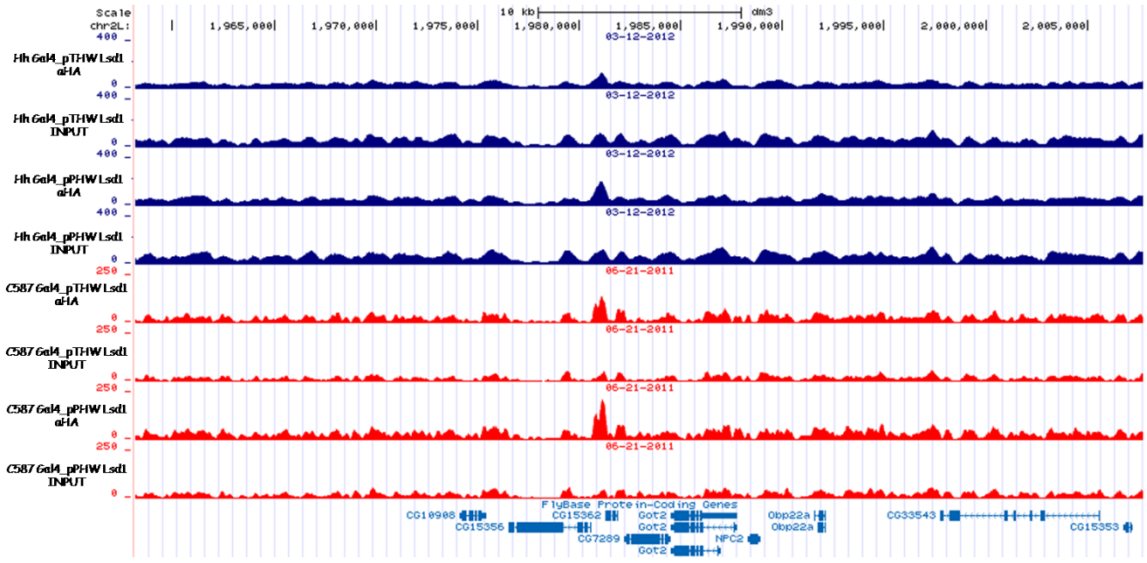

Figure 27. Screenshot of Lsd1 binding sites on coordinates chr2L:1,958,169-2,007,743

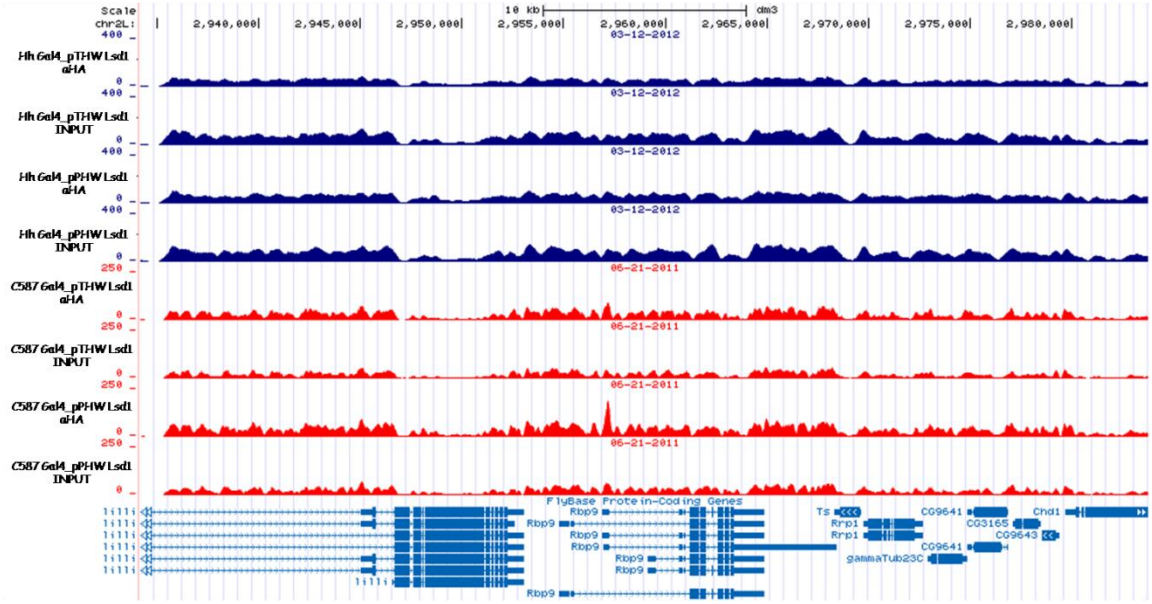

Figure 28. Screenshot of Lsd1 binding sites on coordinates chr2L:2,934,180-2,983,754

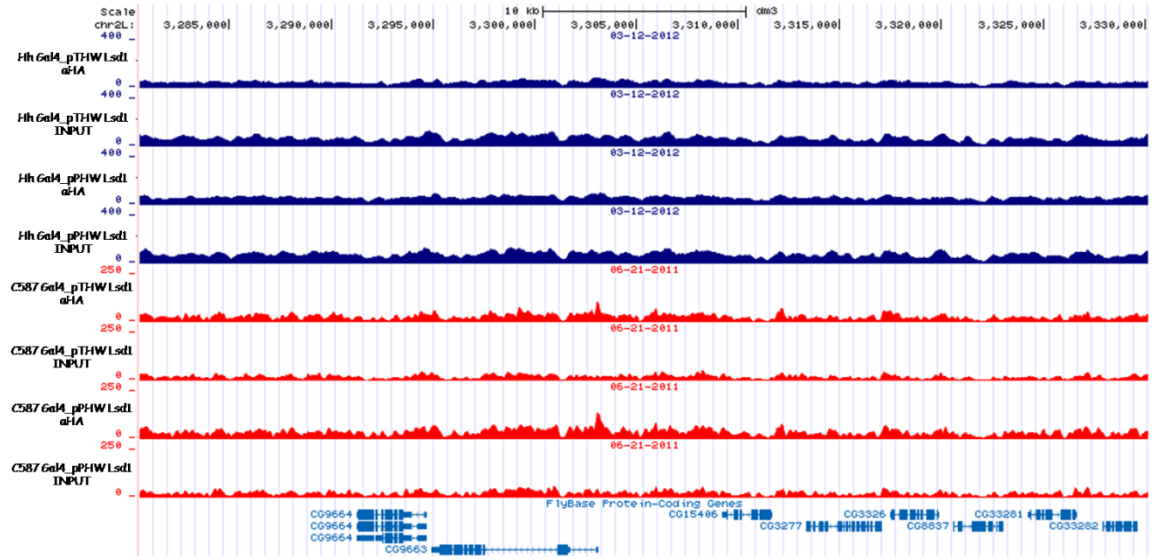

Figure 29. Screenshot of Lsd1 binding sites on coordinates chr2L:3,280,586-3,330,160

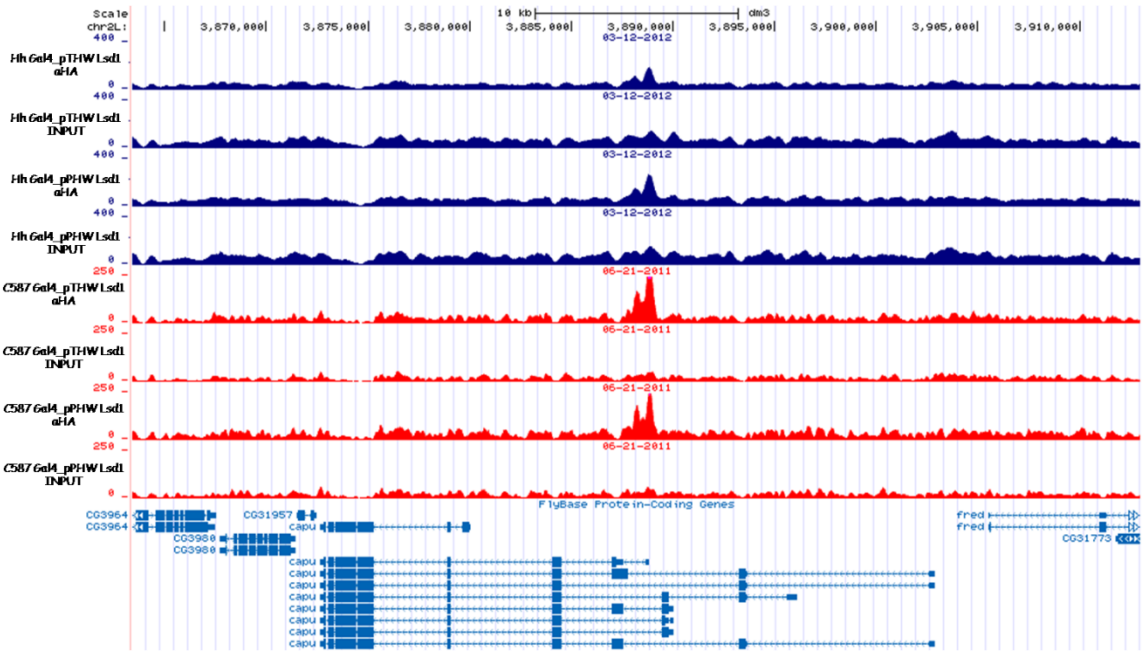

Figure 30. Screenshot of Lsd1 binding sites on coordinates chr2L:3,863,404-3,912,978

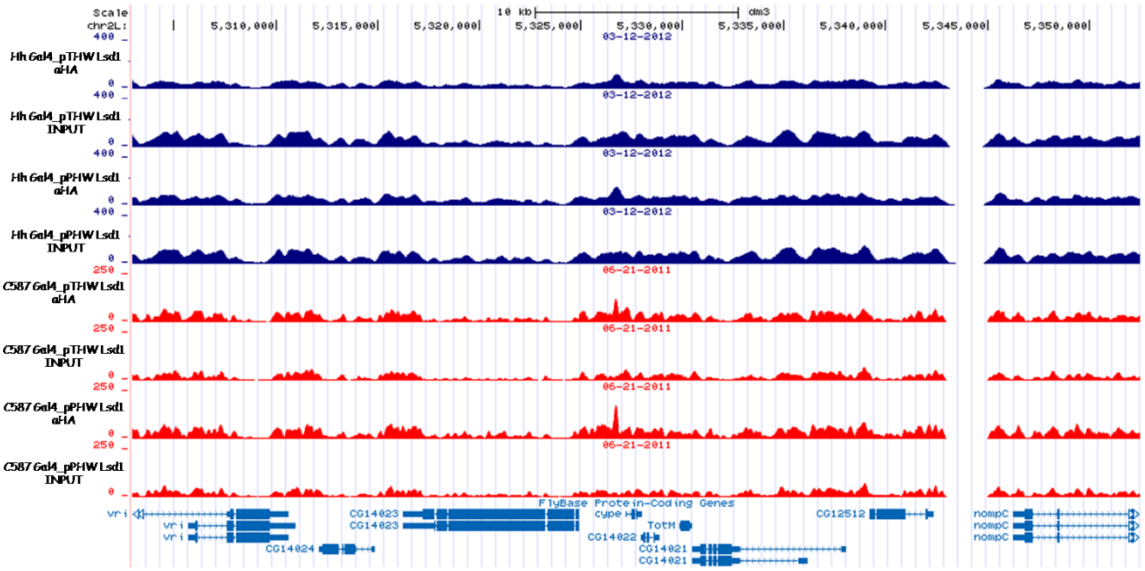

Figure 31. Screenshot of Lsd1 binding sites on coordinates chr2L:5,302,942-5,352,516

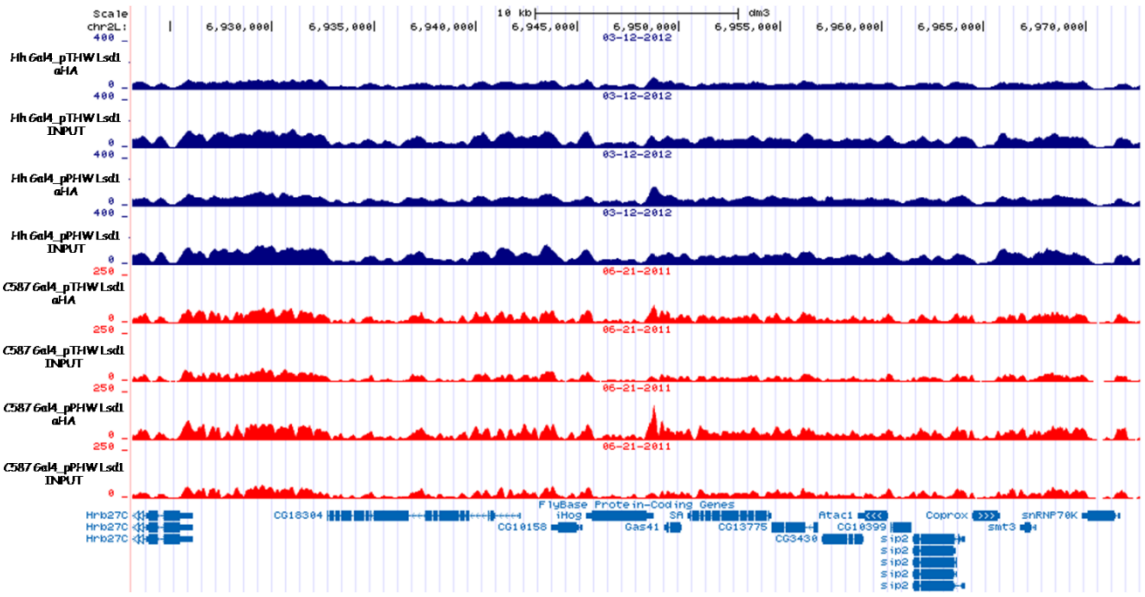

Figure 32. Screenshot of Lsd1 binding sites on coordinates chr2L:6,923,122-6,972,696

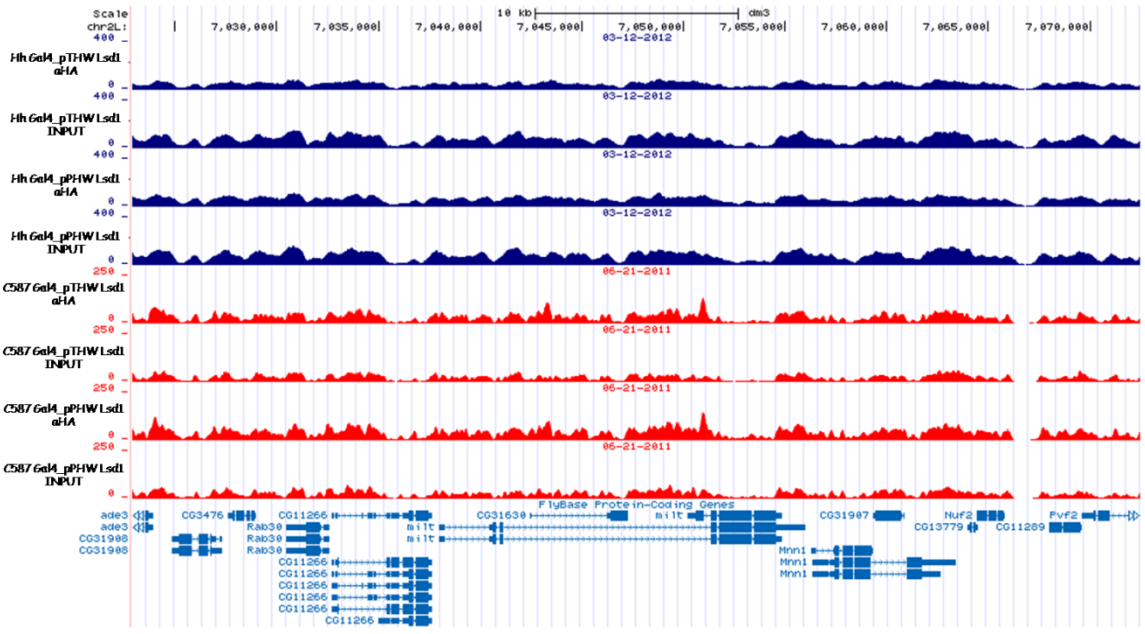

Figure 33. Screenshot of Lsd1 binding sites on coordinates chr2L:7,022,892-7,072,466

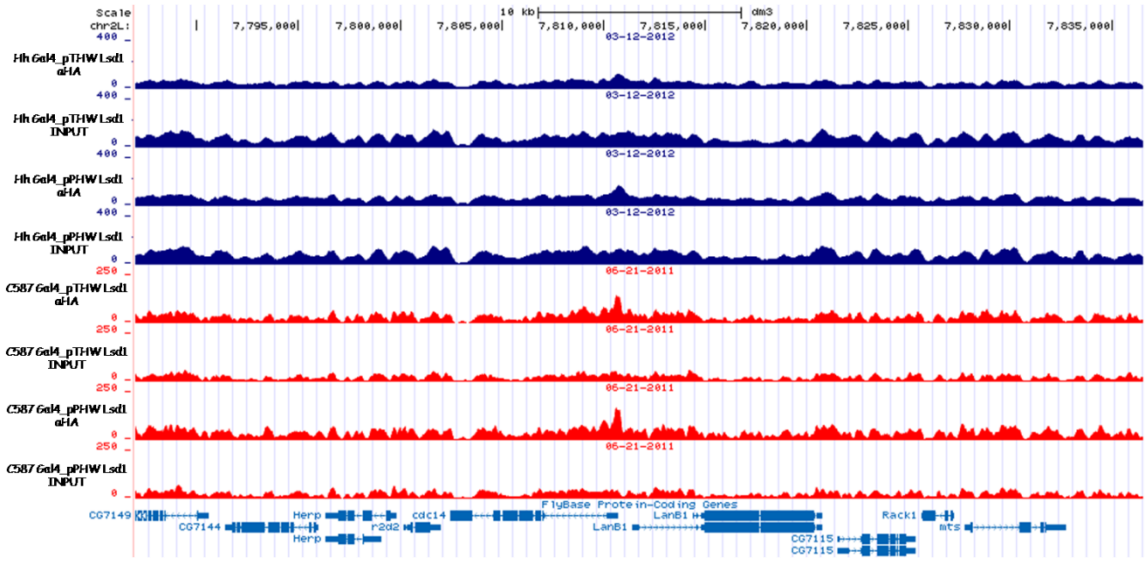

Figure 34. Screenshot of Lsd1 binding sites on coordinates chr2L:7,786,969-7,836,543

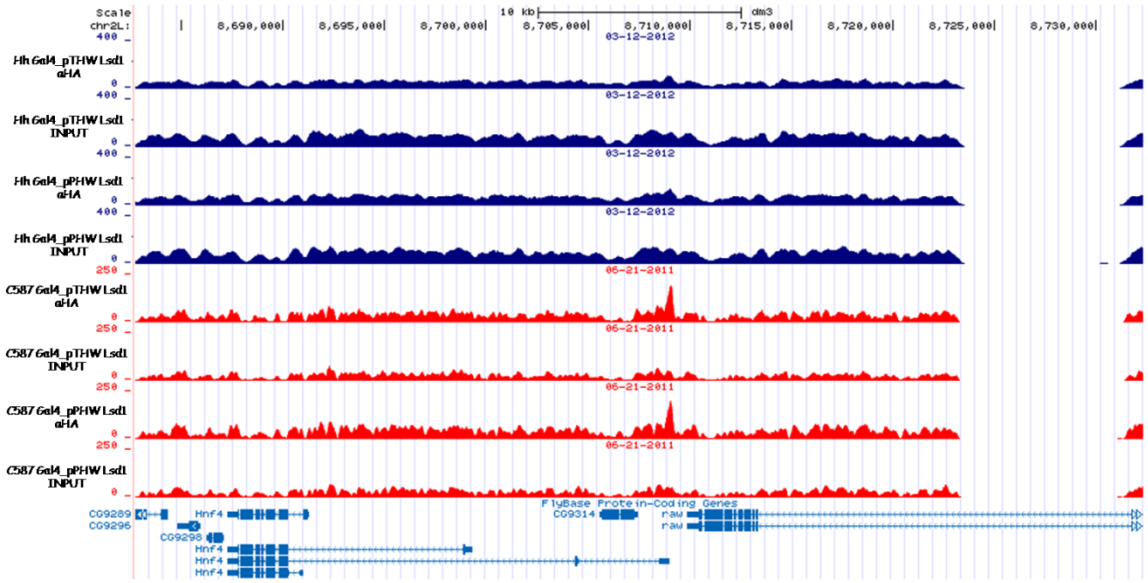

gene	locus	WT_EC	Lsd1 KD_EC	log2(fold_change)	significant
CG9314	chr2L:8687280-8709038	0.388981	4.03714	3.37556	yes
raw	chr2L:8709879-8740660	16.8517	39.4874	1.22849	yes

Figure 35. Screenshot of Lsd1 binding sites on coordinates chr2L:8,682,731-8,732,305 and RNA seq data for genes that exhibit significant difference between WT escort cells and Lsd1 knockdown escort cells

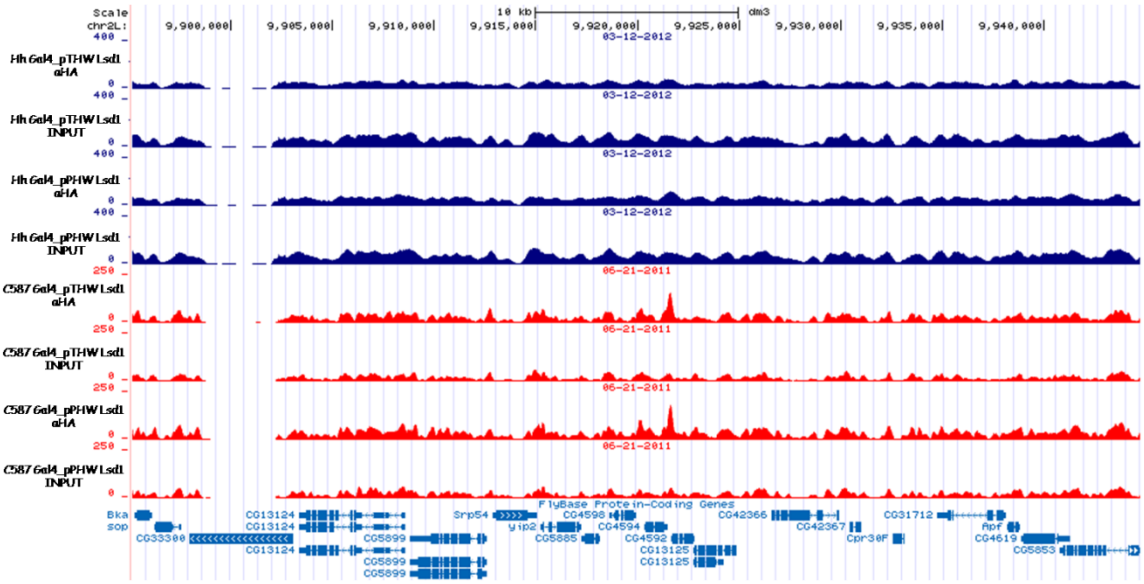

Figure 36. Screenshot of Lsd1 binding sites on coordinates chr2L:9,895,154-9,944,728

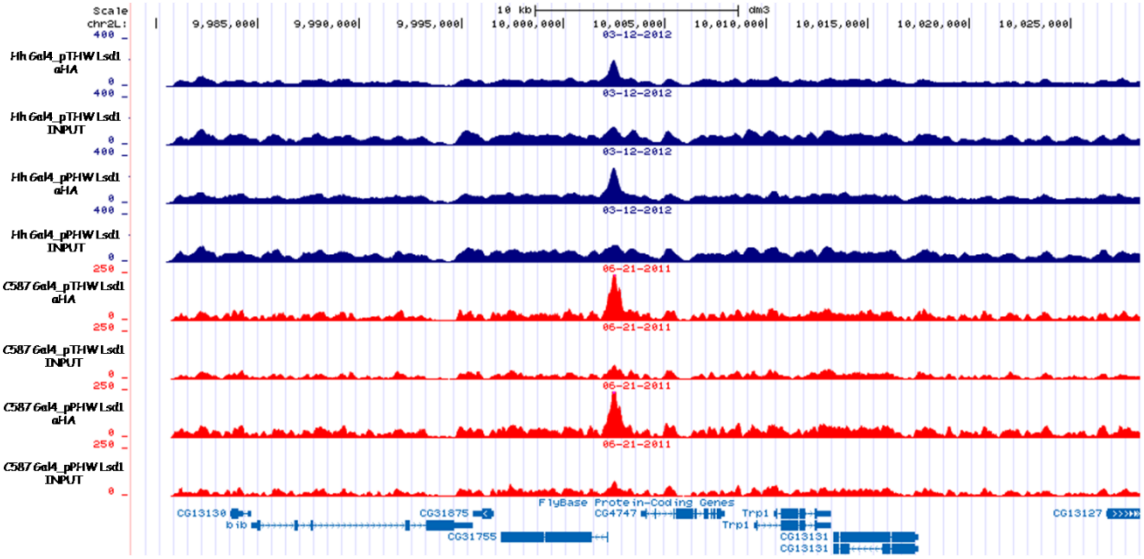

Figure 37. Screenshot of Lsd1 binding sites on coordinates chr2L:9,978,813-10,028,387

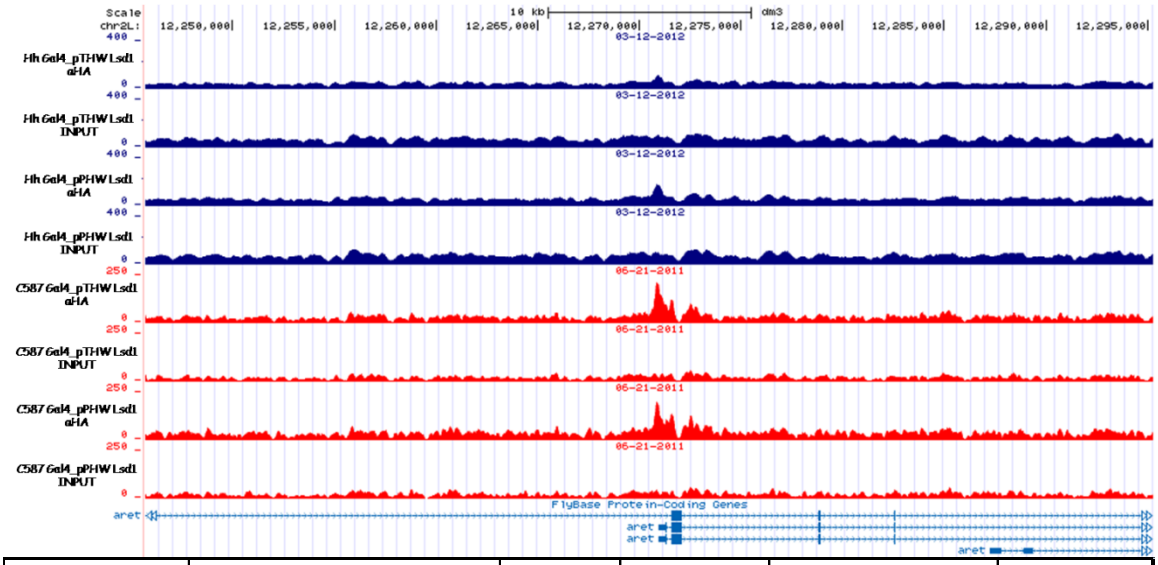

gene	locus	WT_EC	Lsd1 KD_EC	log2(fold_change)	significant
aret	chr2L:12205842-12312795	1.24687	7.86297	2.65676	yes

Figure 38. Screenshot of Lsd1 binding sites on coordinates chr2L:12,245,702-12,295,276 and RNA seq data for genes that exhibit significant difference between WT escort cells and Lsd1 knockdown escort cells

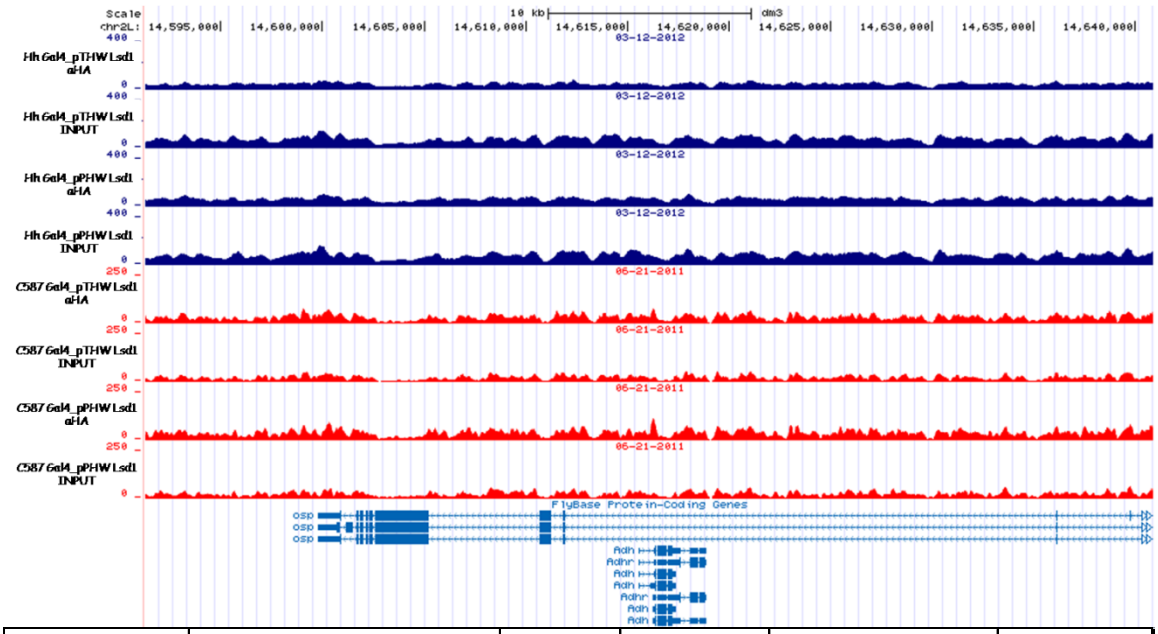

gene	locus	WT_EC	Lsd1 KD_EC	log2(fold_change)	significant
Adh	chr2L:14599775-14689325	2.48418	26.3739	3.40827	yes

Figure 39. Screenshot of Lsd1 binding sites on coordinates chr2L:14,591,287-14,640,861 and RNA seq data for genes that exhibit significant difference between WT escort cells and Lsd1 knockdown escort cells

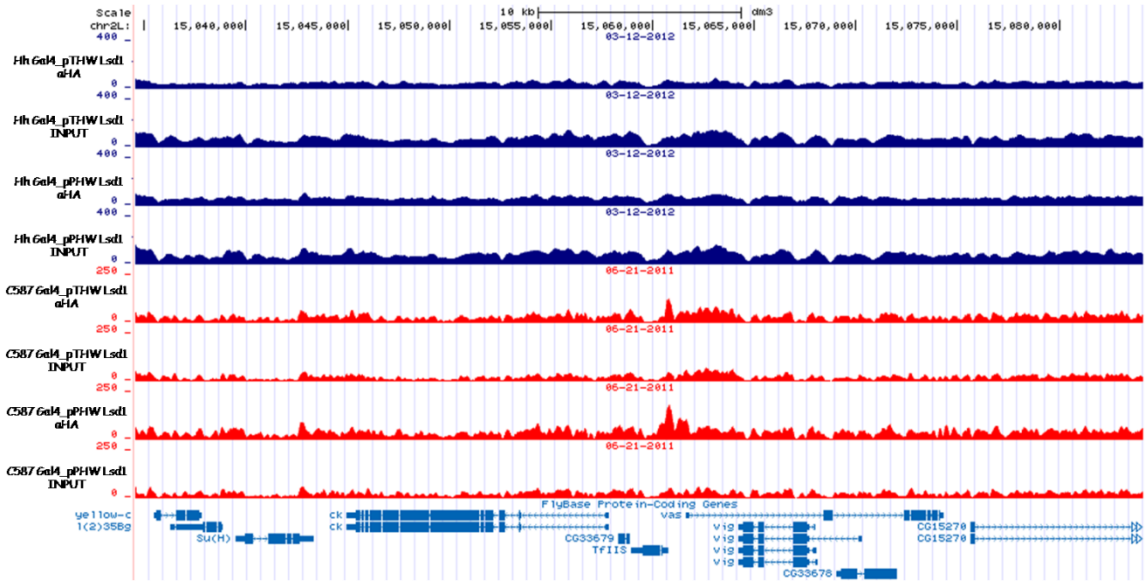

Figure 40. Screenshot of Lsd1 binding sites on coordinates chr2L:15,034,553-15,084,127

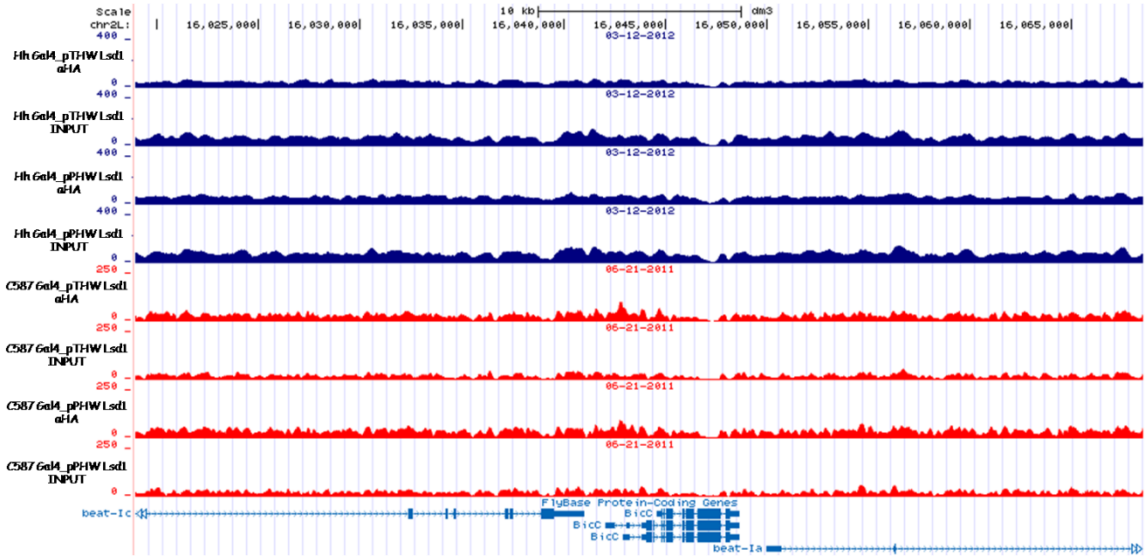

gene	locus	WT_EC	Lsd1 KD_EC	log2(fold_change)	significant
BicC	chr2L:16042031-16048626	0.483356	3.02322	2.64493	yes

Figure 41. Screenshot of Lsd1 binding sites on coordinates chr2L:16,018,931-16,068,505 and RNA seq data for genes that exhibit significant difference between WT escort cells and Lsd1 knockdown escort cells

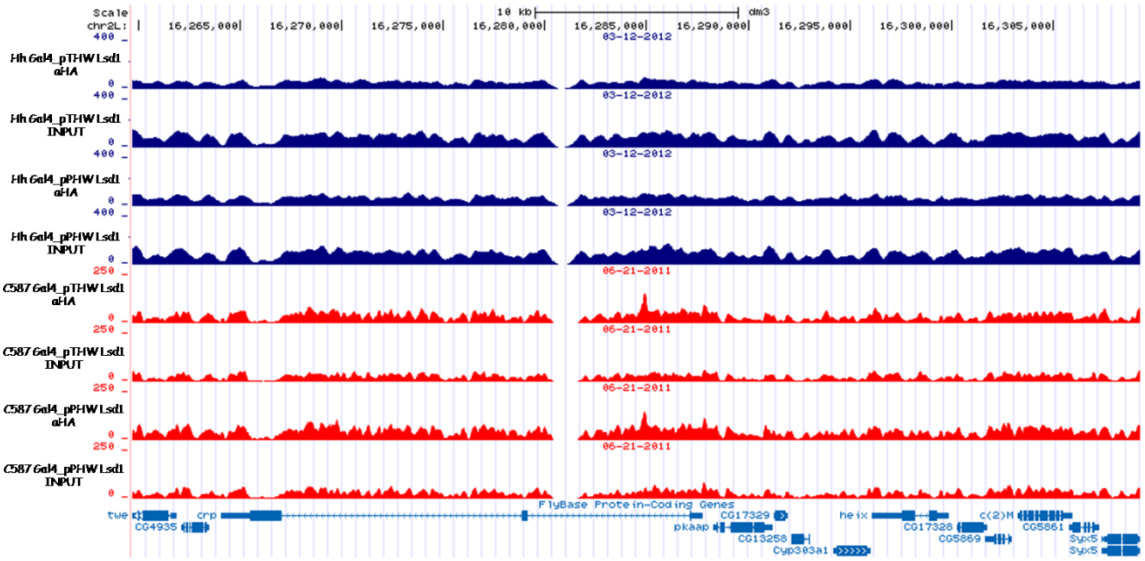

Figure 42. Screenshot of Lsd1 binding sites on coordinates chr2L:16,259,699-16,309,273

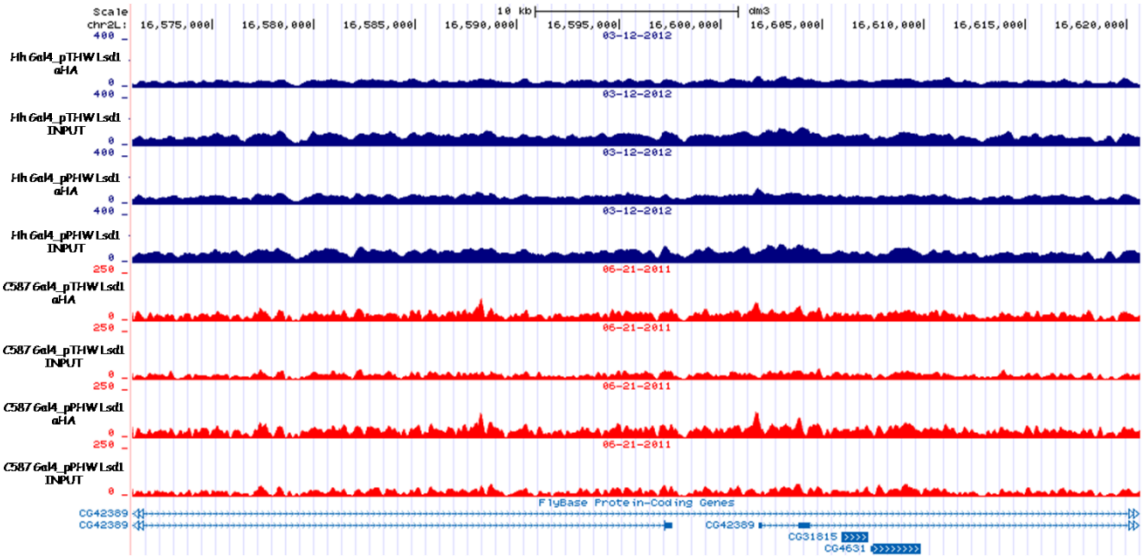

Figure 43. Screenshot of Lsd1 binding sites on coordinates chr2L:16,571,074-16,620,648

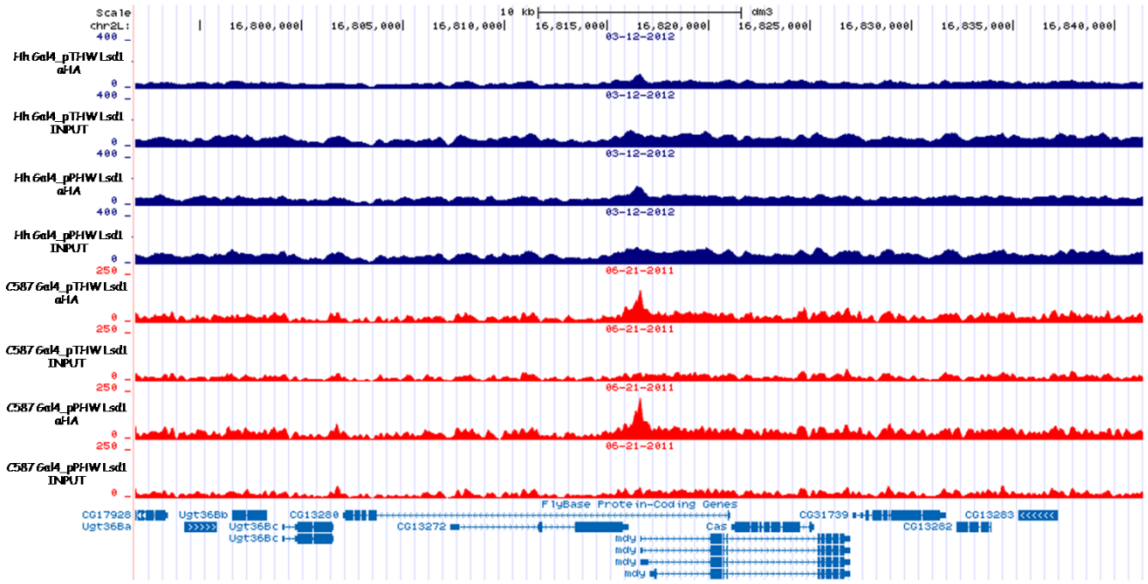

Gene	Locus	WT_EC	Lsd1 KD_EC	log2(fold_change)	significant
Cas	chr2L:16802020-16826991	7.79389	29.7927	1.93454	yes

Figure 44. Screenshot of Lsd1 binding sites on coordinates chr2L:16,791,815-16,841,389 and RNA seq data for genes that exhibit significant difference between WT escort cells and Lsd1 knockdown escort cells

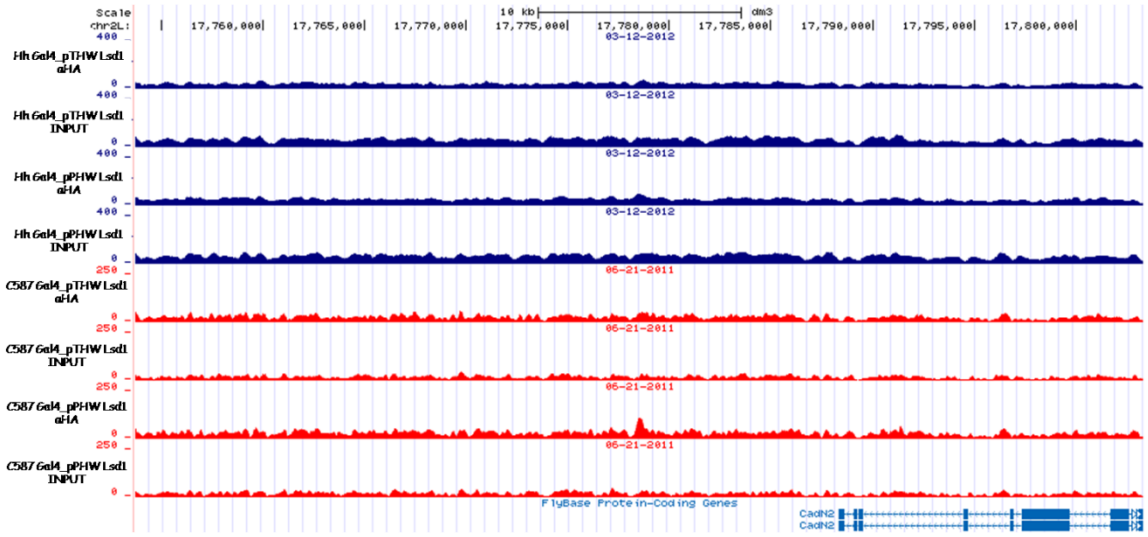

Figure 45. Screenshot of Lsd1 binding sites on coordinates chr2L:17,753,732-17,803,306

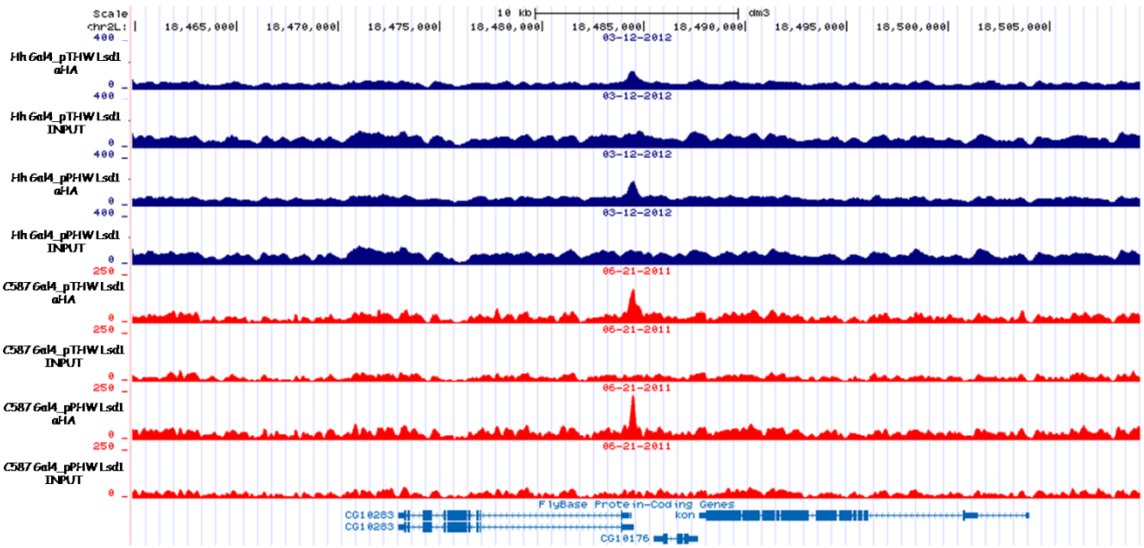

Figure 46. Screenshot of Lsd1 binding sites on coordinates chr2L:18,459,855-18,509,429

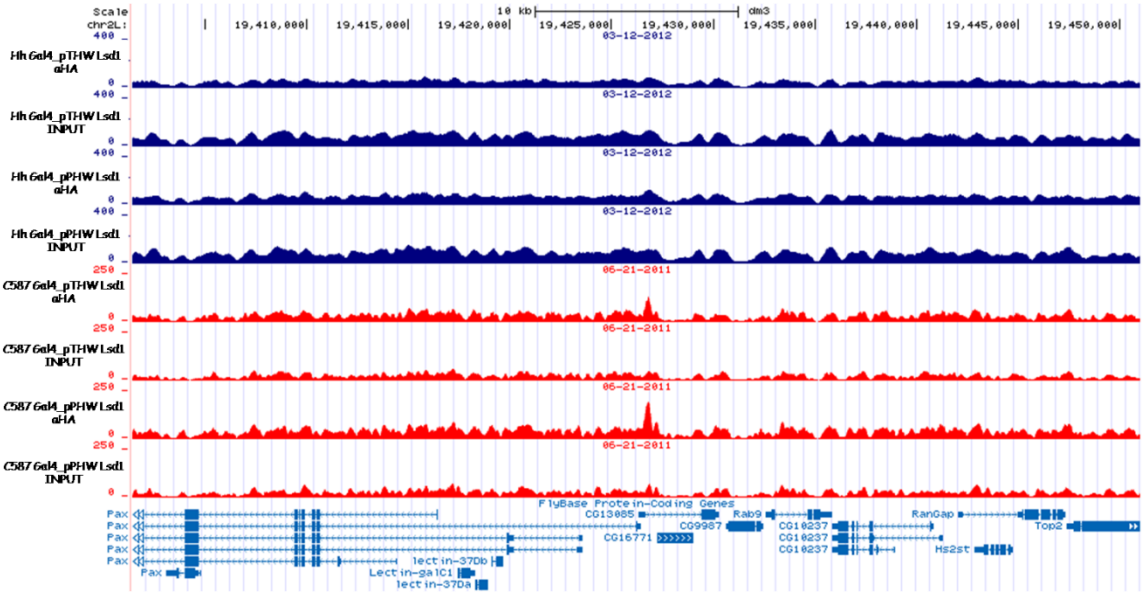

gene	locus	WT_EC	Lsd1 KD_EC	log2(fold_change)	significant
CG16771	chr2L:19400780-19430270	2.77718	15.1943	2.45184	yes

Figure 47. Screenshot of Lsd1 binding sites on coordinates chr2L:19,401,426-19,451,000 and RNA seq data for genes that exhibit significant difference between WT escort cells and Lsd1 knockdown escort cells

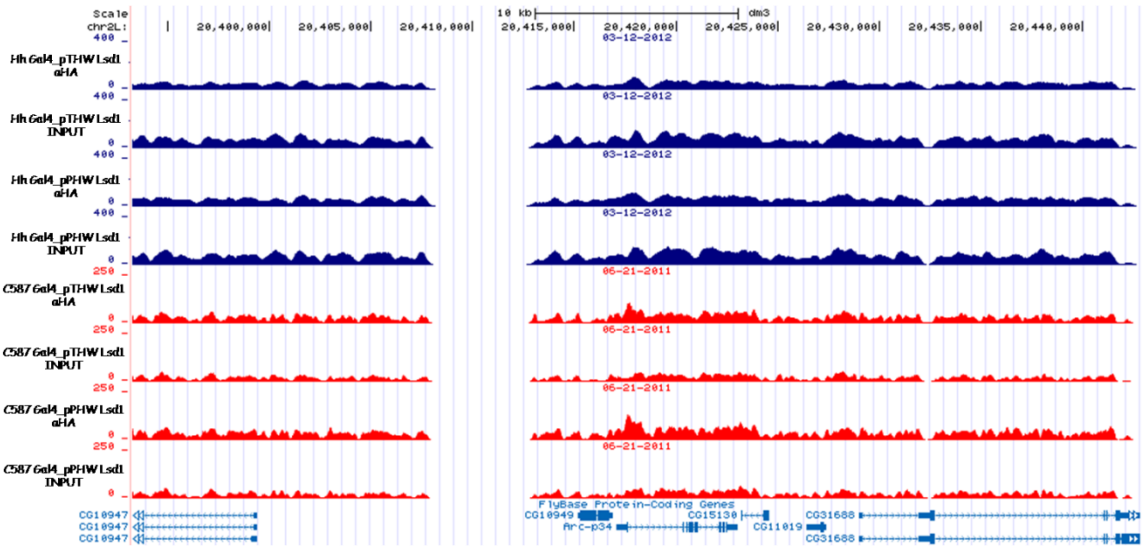

Figure 48. Screenshot of Lsd1 binding sites on coordinates chr2L:20,393,261-20,442,835

Binding Sites of Lsd1 on Chromosome 2R

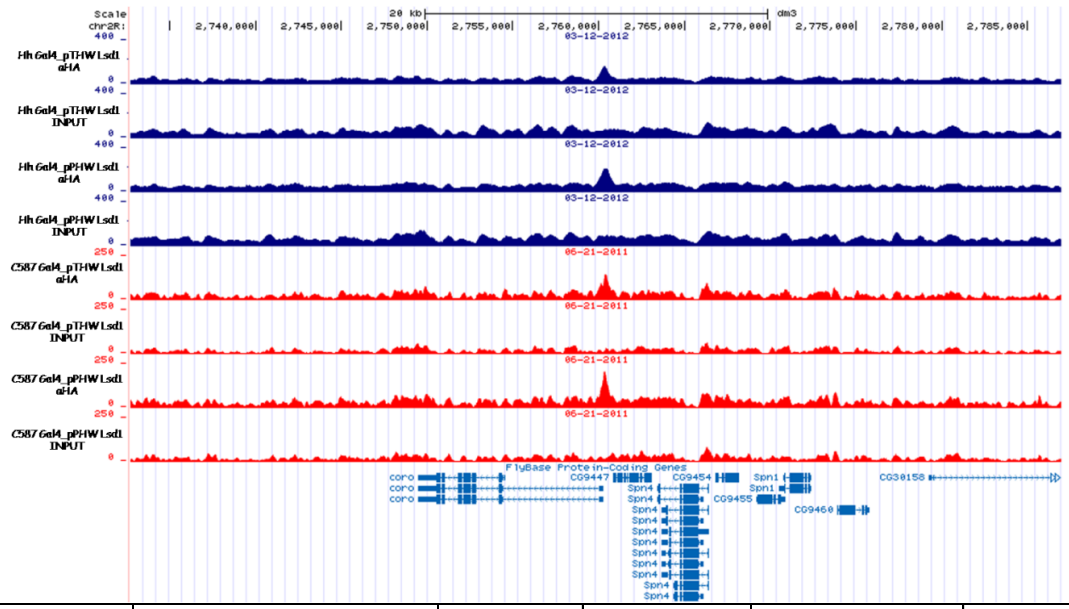

Gene	Locus	WT_EC	Lsd1 KD_EC	log2(fold_change)	significant
Spn4	chr2R:2763408-2766428	22.8254	65.0001	1.5098	yes

Figure 49. Screenshot of Lsd1 binding sites on coordinates chr2R:2,732,711-2,786,971 and RNA seq data for genes that exhibit significant difference between WT escort cells and Lsd1 knockdown escort cells

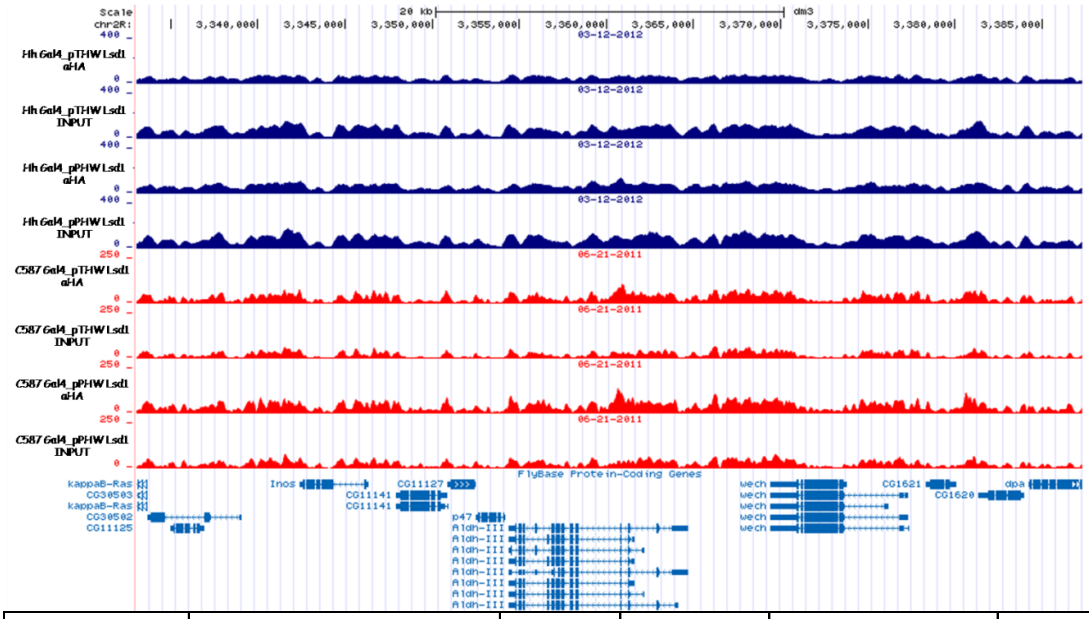

gene	locus	WT_EC	Lsd1 KD_EC	log2(fold_change)	significant
wech	chr2R:3369380-3377368	2.49565	7.26261	1.54107	yes

Figure 50. Screenshot of Lsd1 binding sites on coordinates chr2R:3,333,044-3,387,304 and RNA seq data for genes that exhibit significant difference between WT escort cells and Lsd1 knockdown escort cells

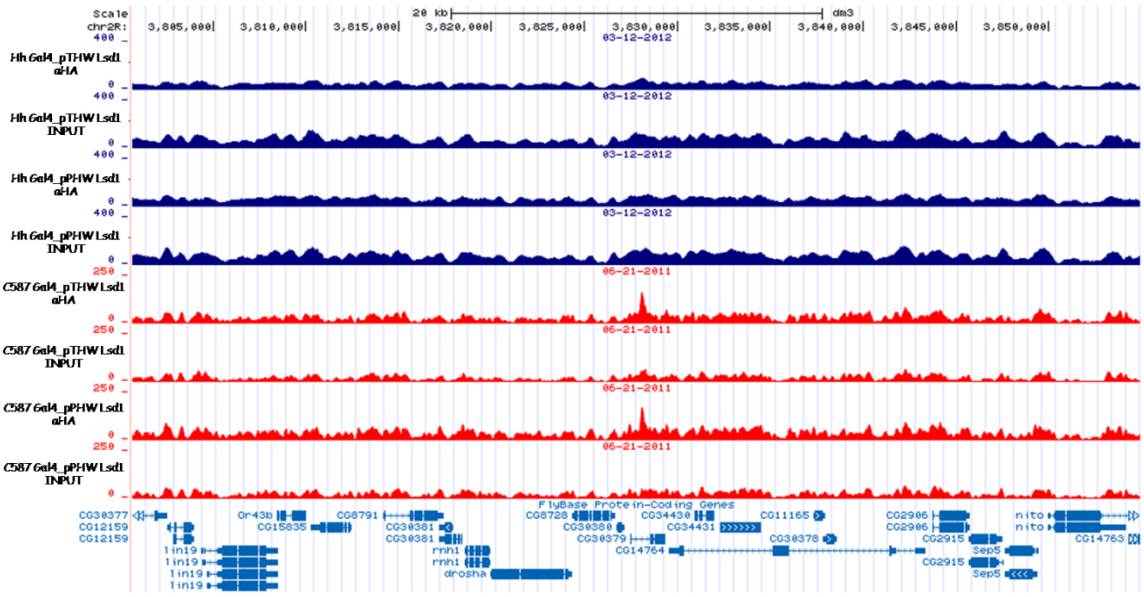

Figure 51. Screenshot of Lsd1 binding sites on coordinates chr2R:3,800,662-3,854,922

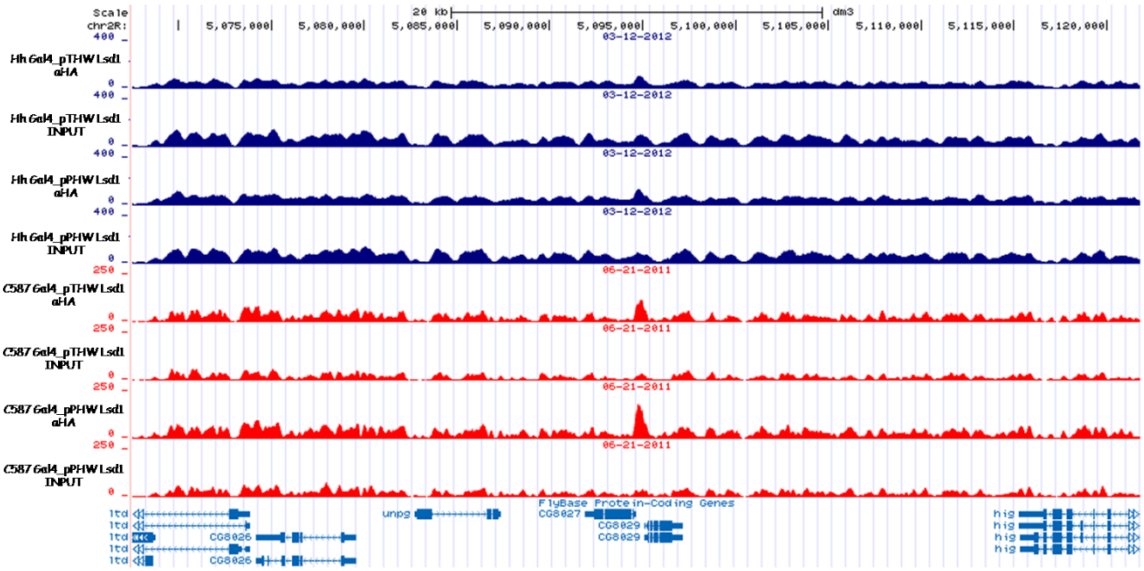

Figure 52. Screenshot of Lsd1 binding sites on coordinates chr2R:5,067,526-5,121,786

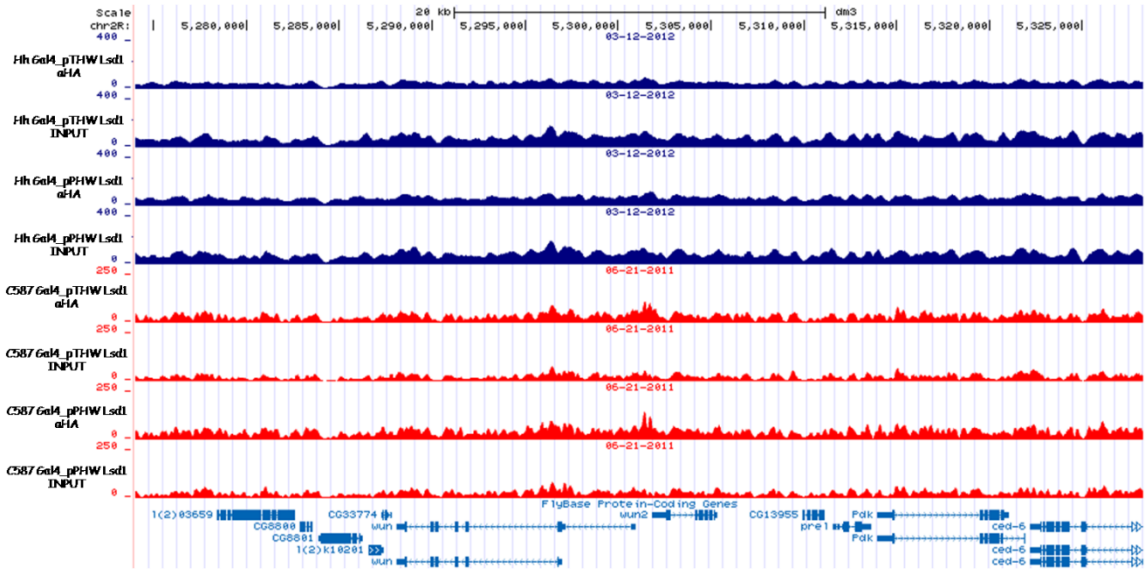

Figure 53. Screenshot of Lsd1 binding sites on coordinates chr2R:5,274,015-5,328,275

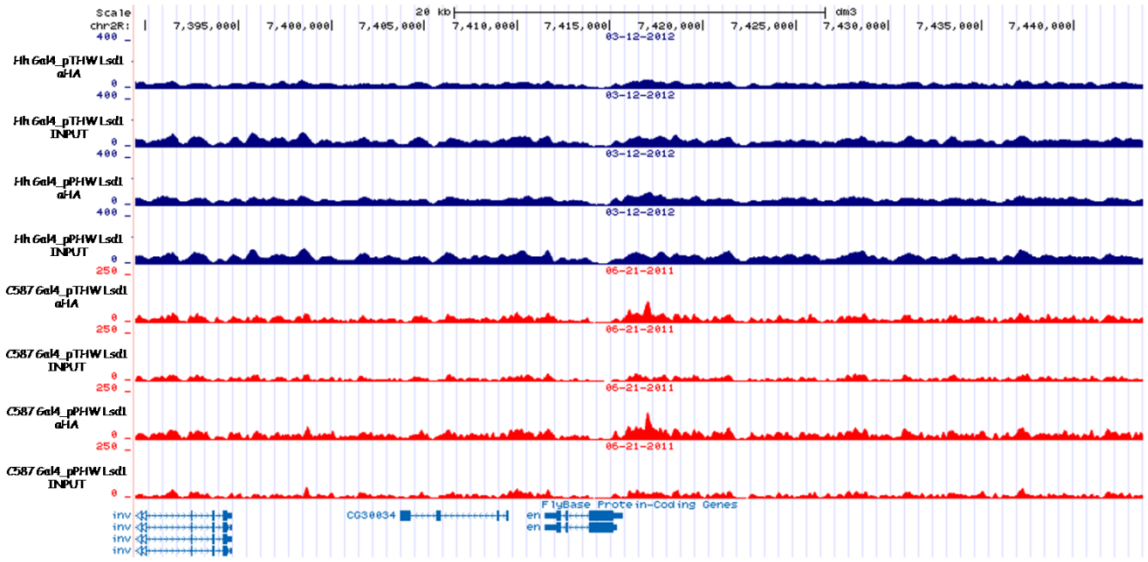

Figure 54. Screenshot of Lsd1 binding sites on coordinates chr2R:7,389,447-7,443,707

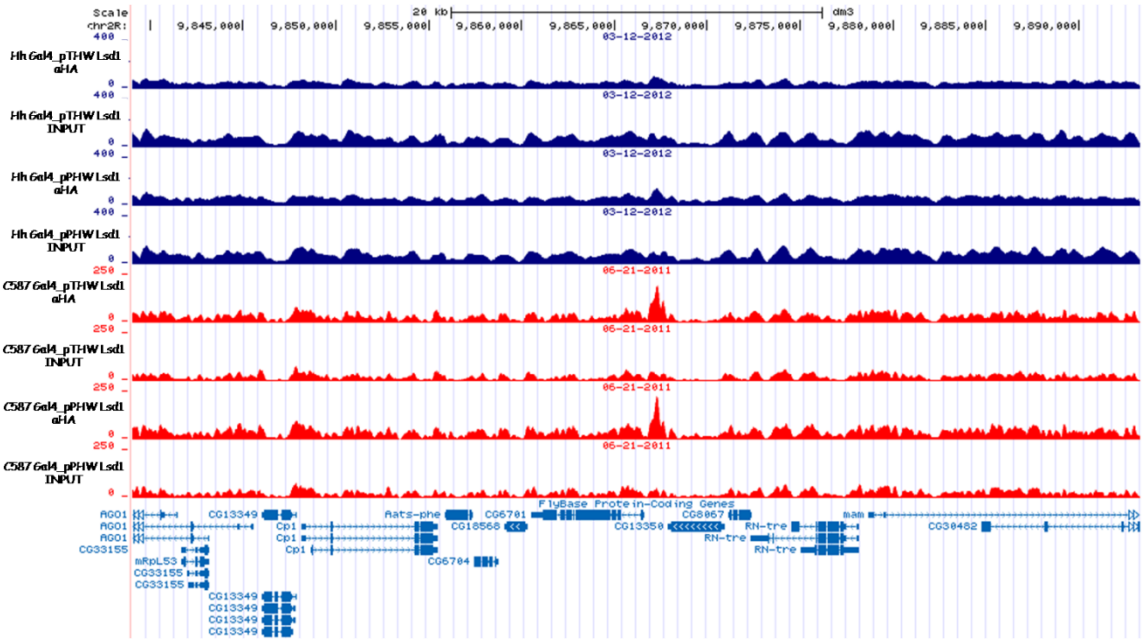

Figure 55. Screenshot of Lsd1 binding sites on coordinates chr2R:9,839,047-9,893,307

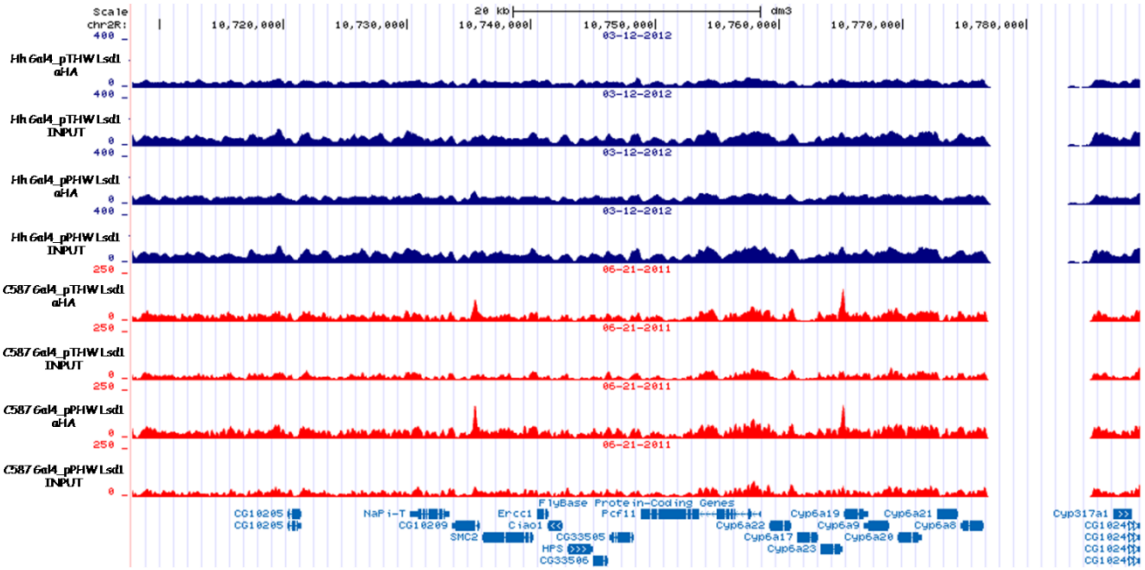

Figure 56. Screenshot of Lsd1 binding sites on coordinates chr2R:10,707,790-10,789,181

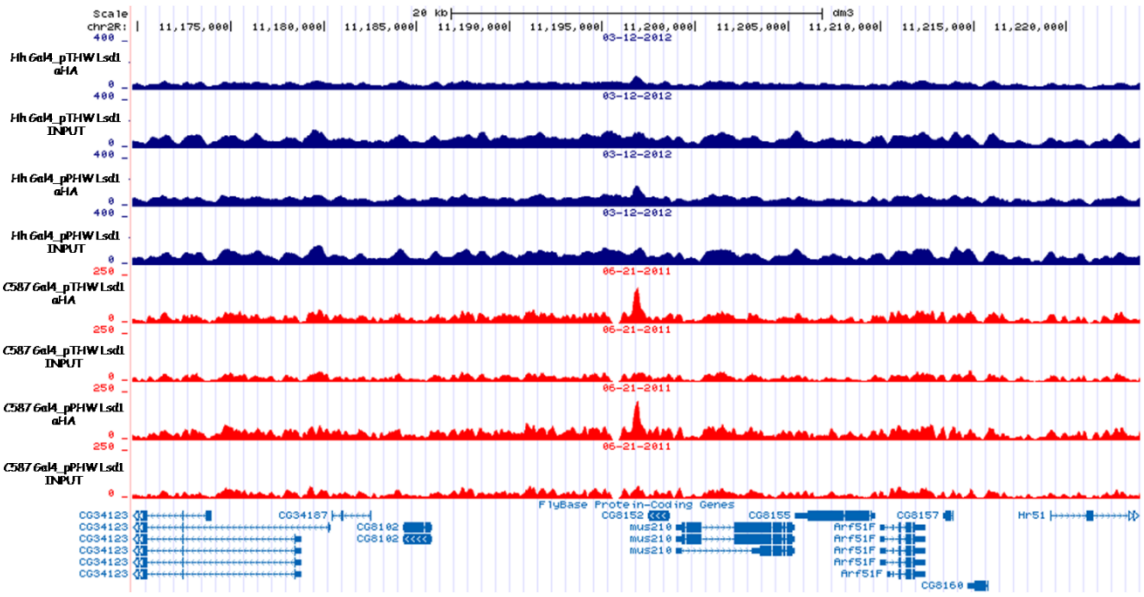

gene	locus	WT_EC	Lsd1 KD_EC	log2(fold_change)	significant
mus210	chr2R:11198990-11205347	5.06177	18.0068	1.83083	yes

Figure 57. Screenshot of Lsd1 binding sites on coordinates chr2R:11,169,697-11,223,957 and RNA seq data for genes that exhibit significant difference between WT escort cells and Lsd1 knockdown escort cells

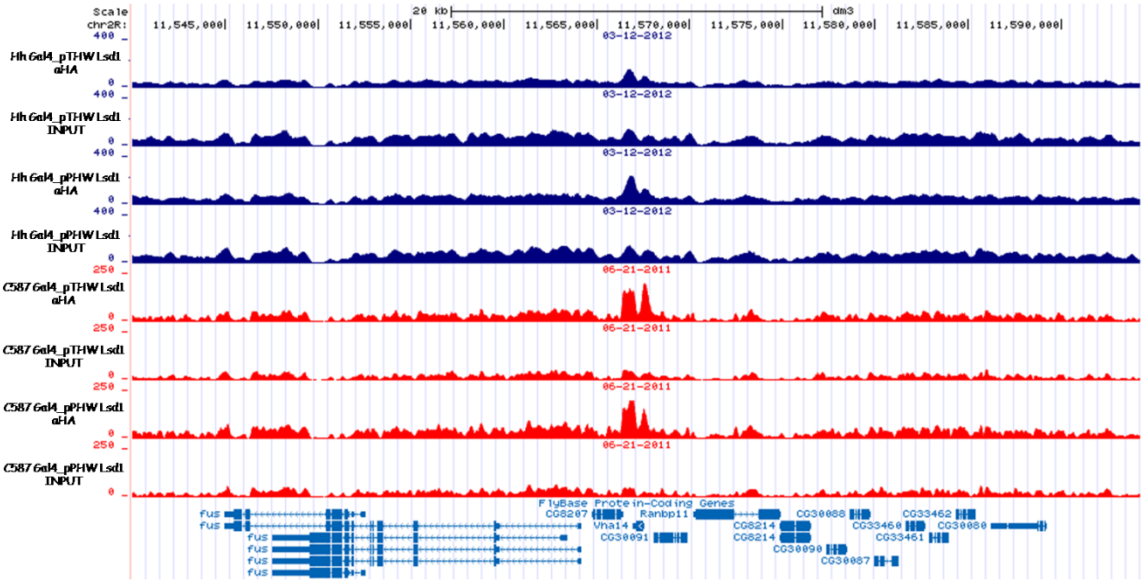

Figure 58. Screenshot of Lsd1 binding sites on coordinates chr2R:11,540,004-11,594,264

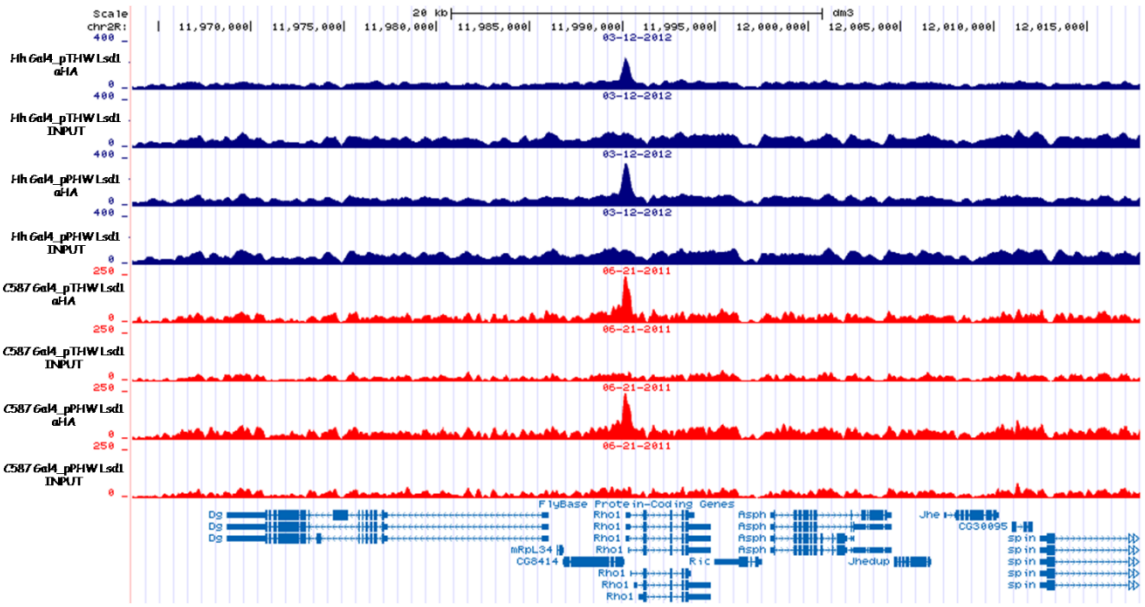

Figure 59. Screenshot of Lsd1 binding sites on coordinates chr2R:11,963,615-12,017,875

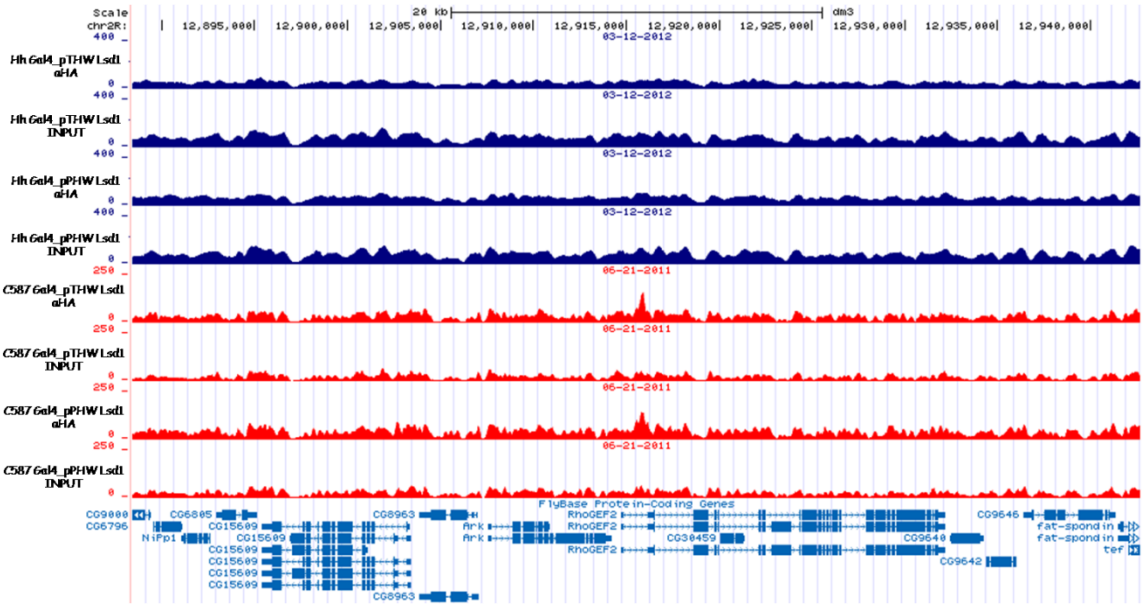

Figure 60. Screenshot of Lsd1 binding sites on coordinates chr2R:12,888,409-12,942,669

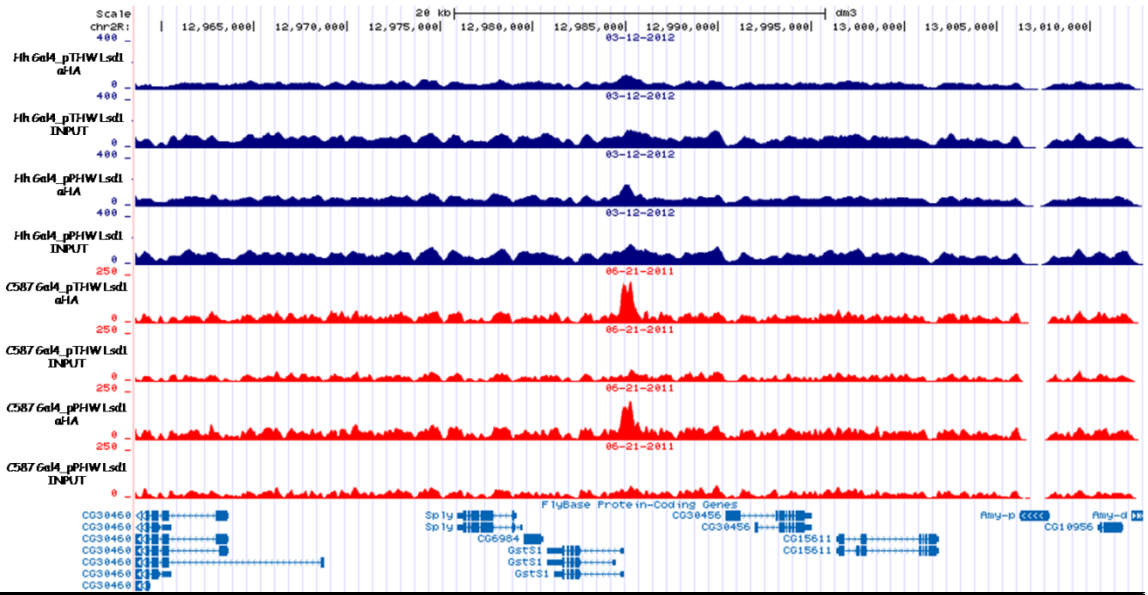

Gene	Locus	WT_EC	Lsd1 KD_EC	log2(fold_change)	significant
GstS1	chr2R:12980757-12984935	115.31	313.691	1.44382	yes

Figure 61. Screenshot of Lsd1 binding sites on coordinates chr2R:12,958,609-13,012,869 and RNA seq data for genes that exhibit significant difference between WT escort cells and Lsd1 knockdown escort cells

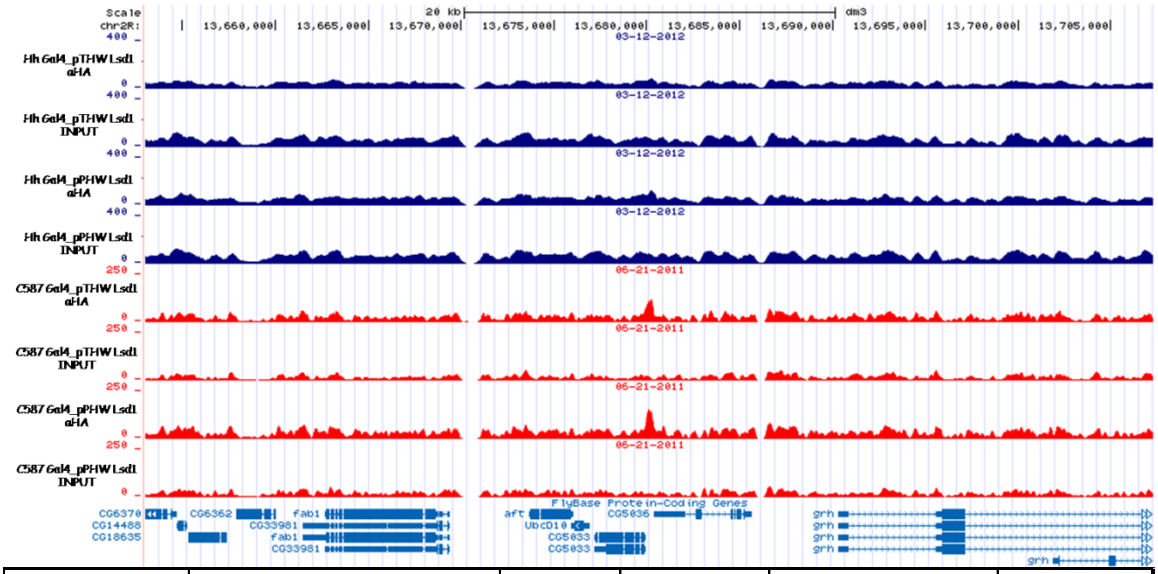

gene	locus	WT_EC	Lsd1 KD_EC	log2(fold_change)	significant
CG5036	chr2R:13680386-13685633	0.195757	1.38065	2.81822	yes

Figure 62. Screenshot of Lsd1 binding sites on coordinates chr2R:13,653,003-13,707,263 and RNA seq data for genes that exhibit significant difference between WT escort cells and Lsd1 knockdown escort cells

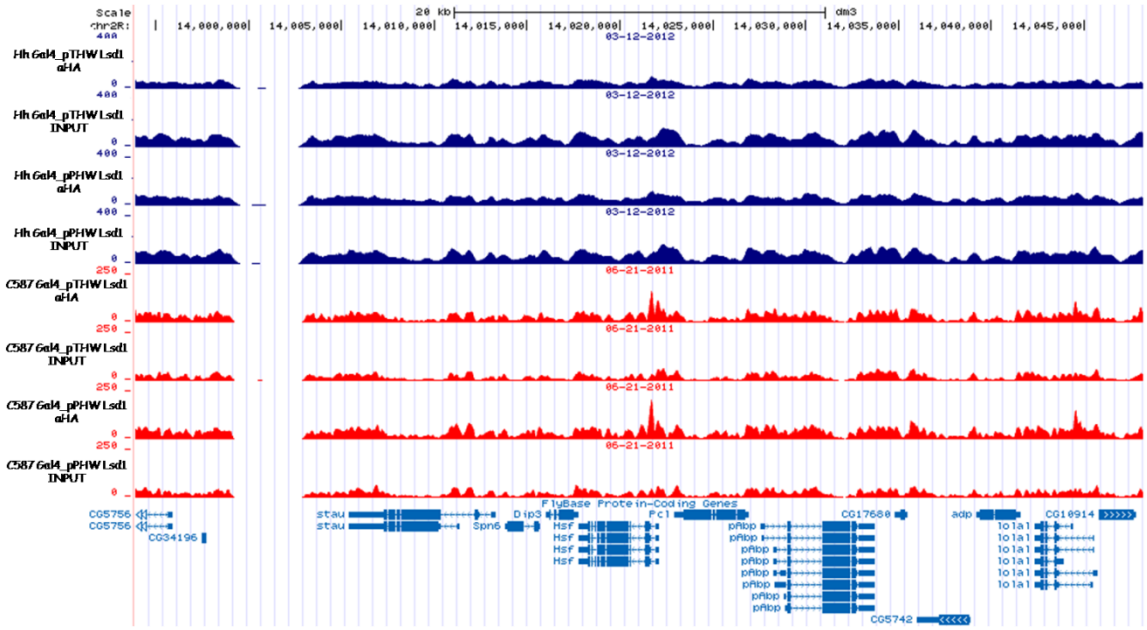

Figure 63. Screenshot of Lsd1 binding sites on coordinates chr2R:13,993,909-14,048,169

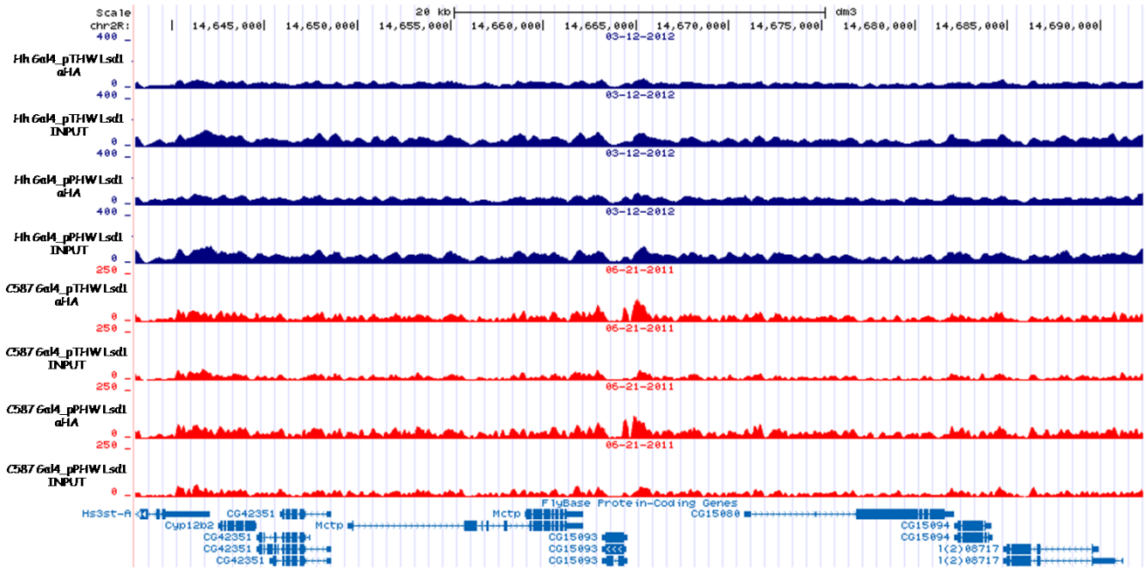

Figure 64. Screenshot of Lsd1 binding sites on coordinates chr2R:14,638,043-14,692,303

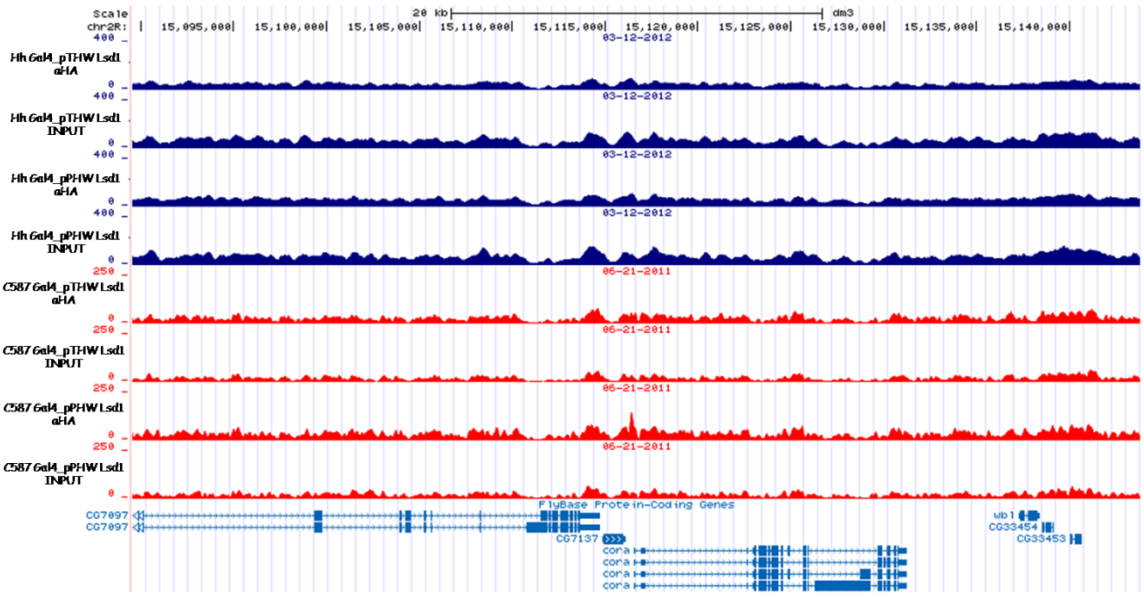

Figure 65. Screenshot of Lsd1 binding sites on coordinates chr2R:15,089,548-15,143,808

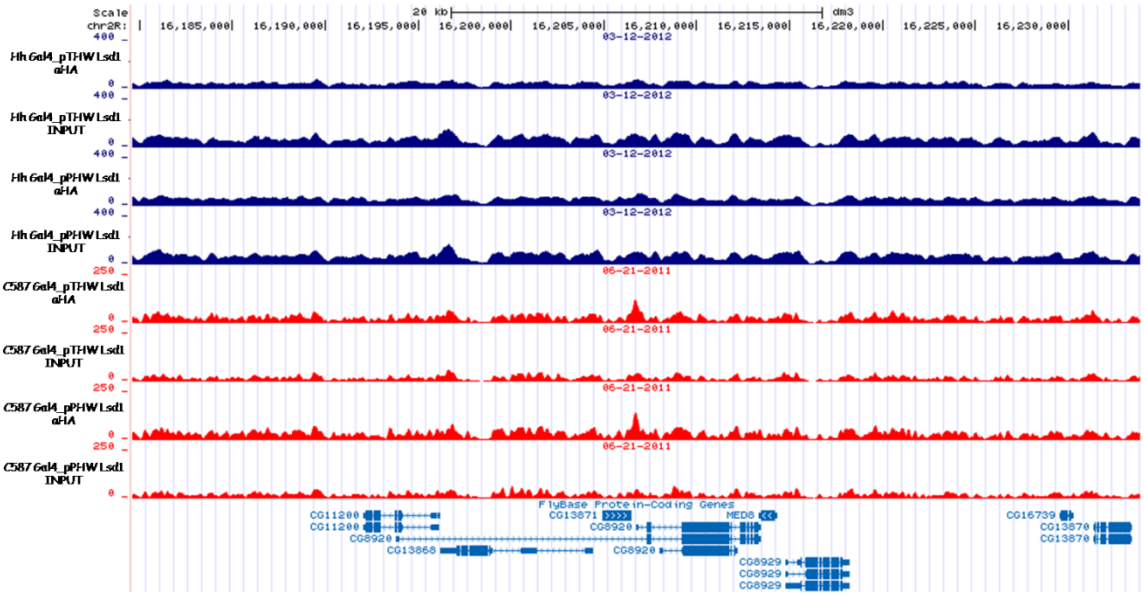

Figure 66. Screenshot of Lsd1 binding sites on coordinates chr2R:16,179,606-16,233,866

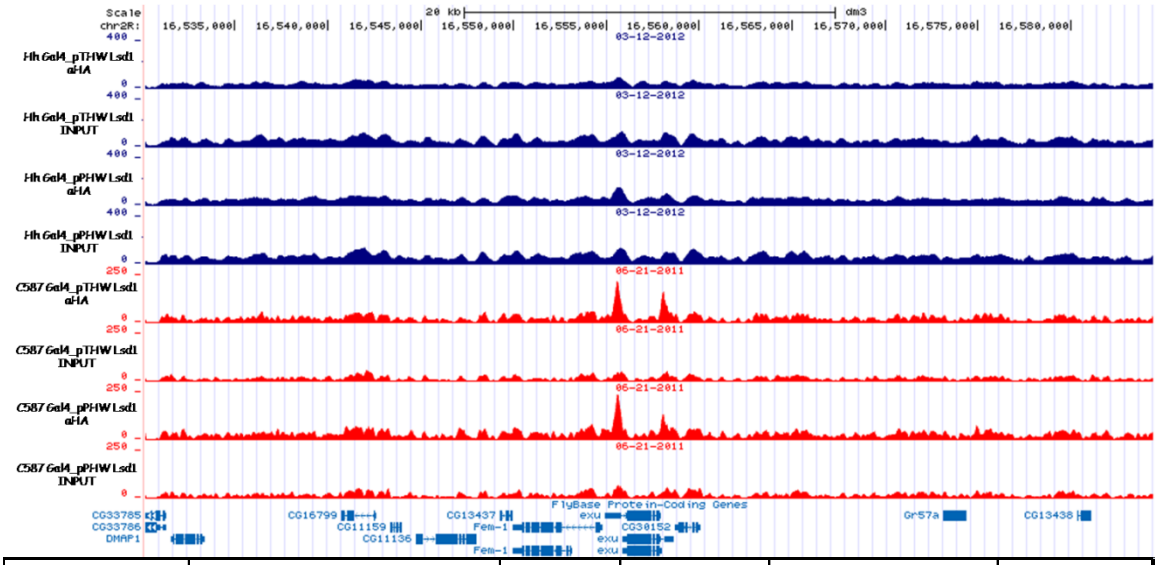

gene	locus	WT_EC	Lsd1 KD_EC	log2(fold_change)	significant
exu	chr2R:16554923-16558379	0.521328	3.1136	2.57832	yes

Figure 67. Screenshot of Lsd1 binding sites on coordinates chr2R:16,530,176-16,584,436 and RNA seq data for genes that exhibit significant difference between WT escort cells and Lsd1 knockdown escort cells

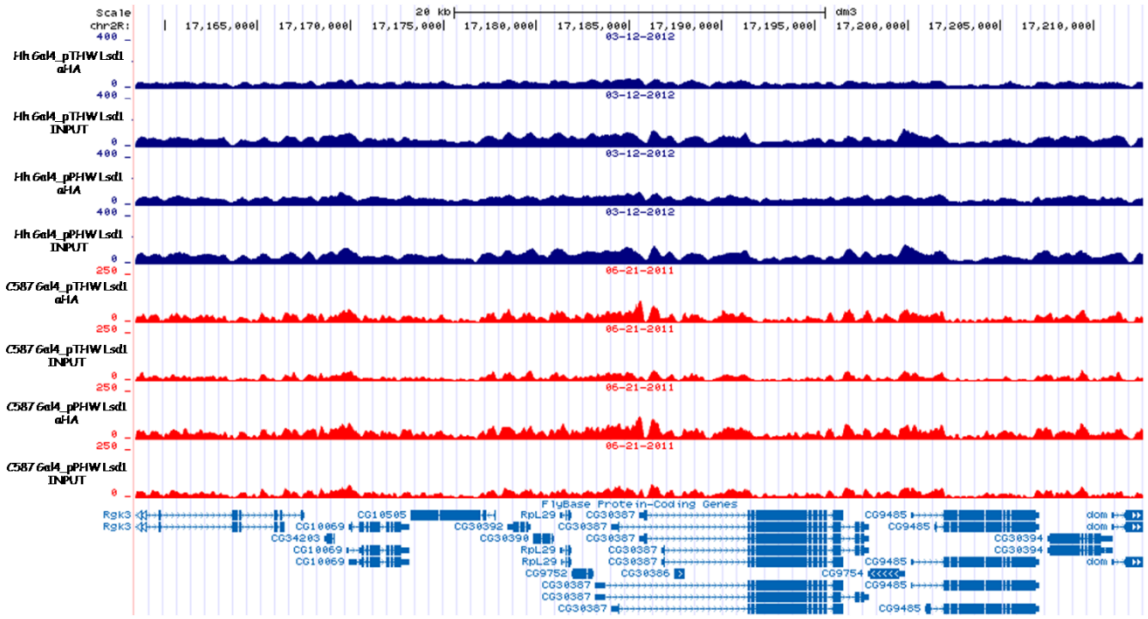

Figure 68. Screenshot of Lsd1 binding sites on coordinates chr2R:17,158,412-17,212,672

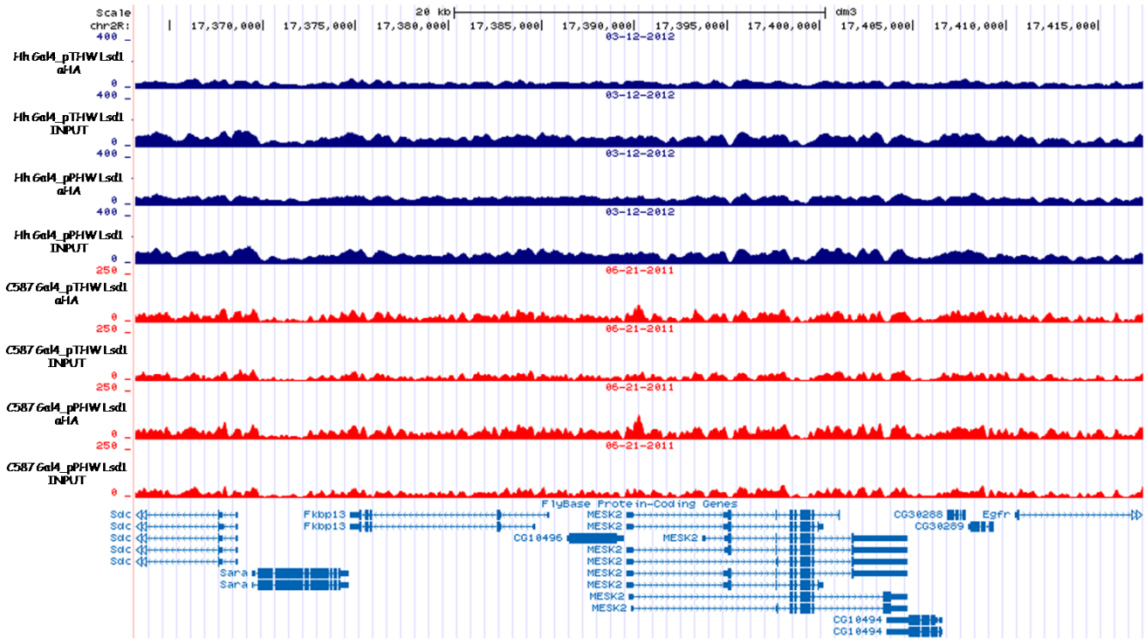

Gene	Locus	WT_EC	Lsd1 KD_EC	log2(fold_change)	significant
MESK2	chr2R:17389590-17406611	26.5327	46.4068	0.806562	yes

Figure 69. Screenshot of Lsd1 binding sites on coordinates chr2R:17,363,142-17,417,402 and RNA seq data for genes that exhibit significant difference between WT escort cells and Lsd1 knockdown escort cells

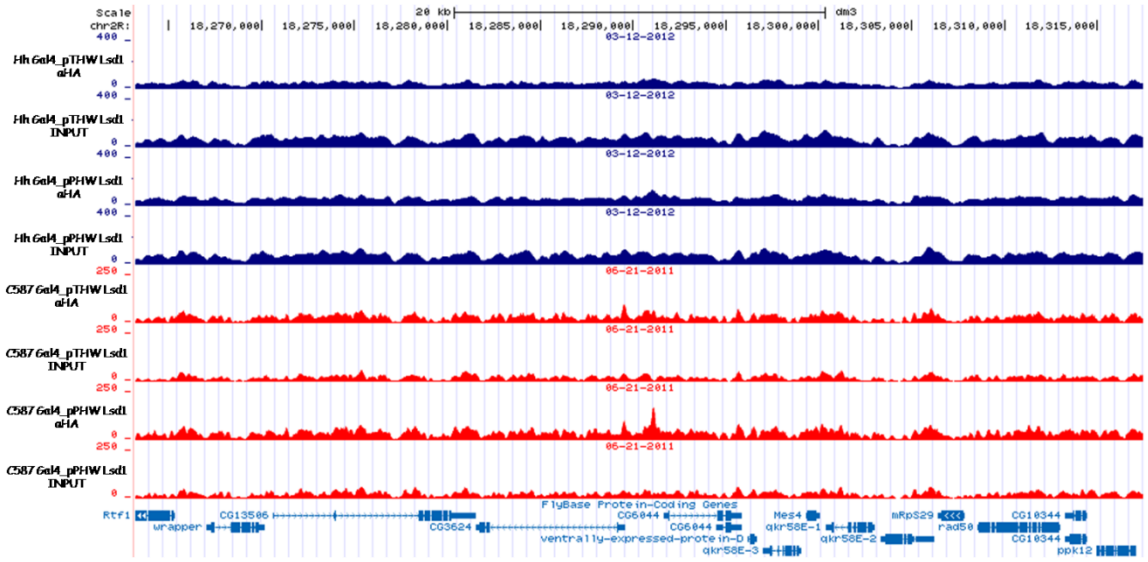

Figure 70. Screenshot of Lsd1 binding sites on coordinates chr2R:18,263,207-18,317,467

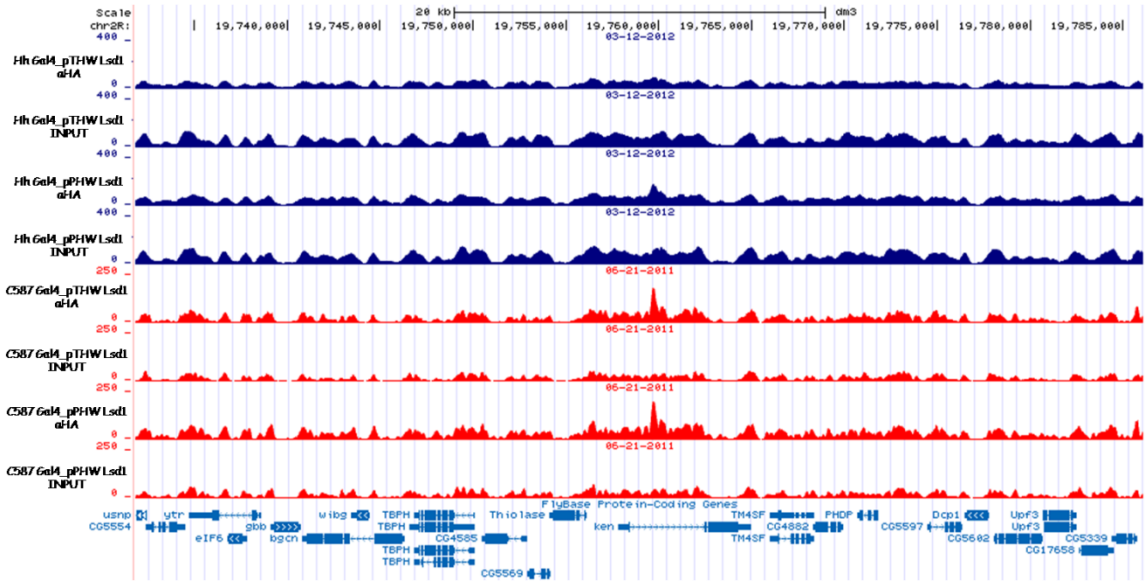

Figure 71. Screenshot of Lsd1 binding sites on coordinates chr2R:19,731,824-19,786,084

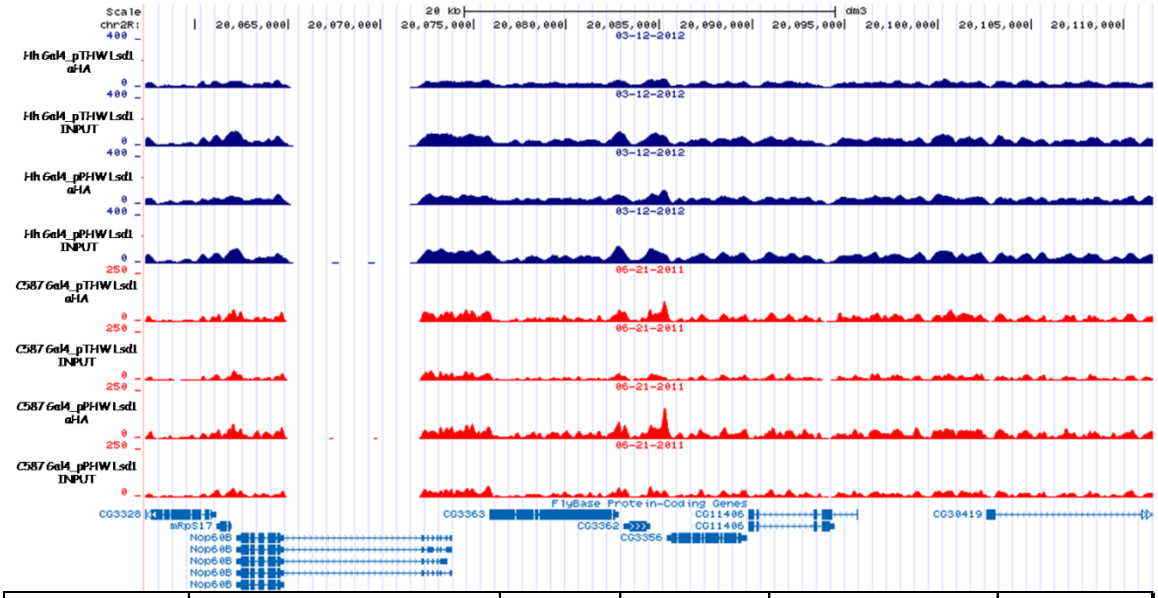

gene	locus	WT_EC	Lsd1 KD_EC	log2(fold_change)	significant
CG11406	chr2R:20085404-20095726	0.100868	0.886968	3.13641	yes

Figure 72. Screenshot of Lsd1 binding sites on coordinates chr2R:20,057,331-20,111,591 and RNA seq data for genes that exhibit significant difference between WT escort cells and Lsd1 knockdown escort cells

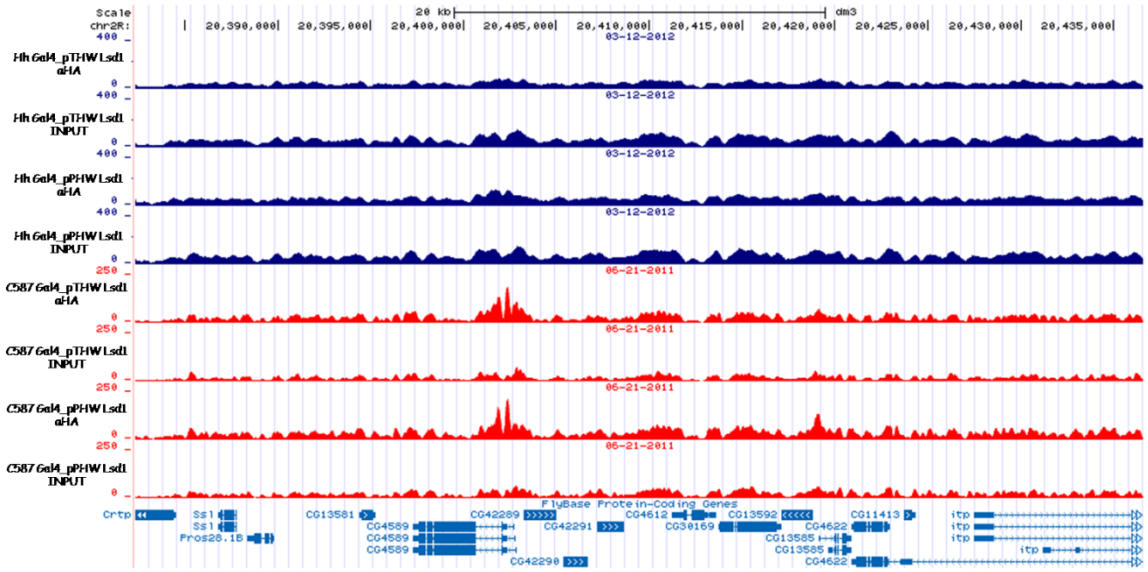

Figure 73. Screenshot of Lsd1 binding sites on coordinates chr2R:20,382,331-20,436,591

Binding Sites of Lsd1 on Chromosome 3L

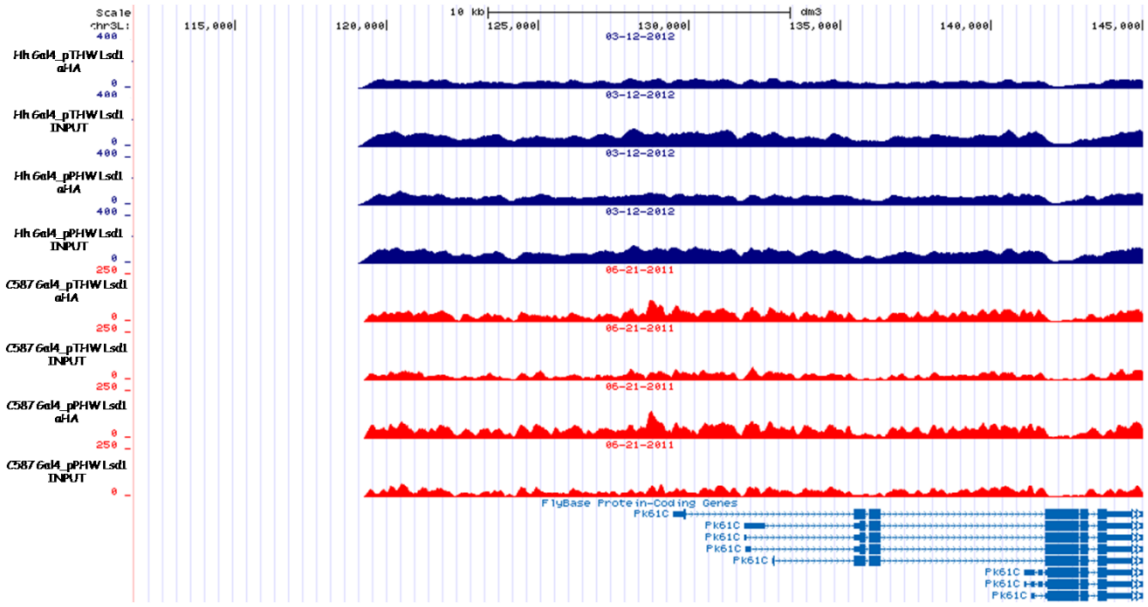

Figure 74. Screenshot of Lsd1 binding sites on coordinates chr3L:111,684-145,016

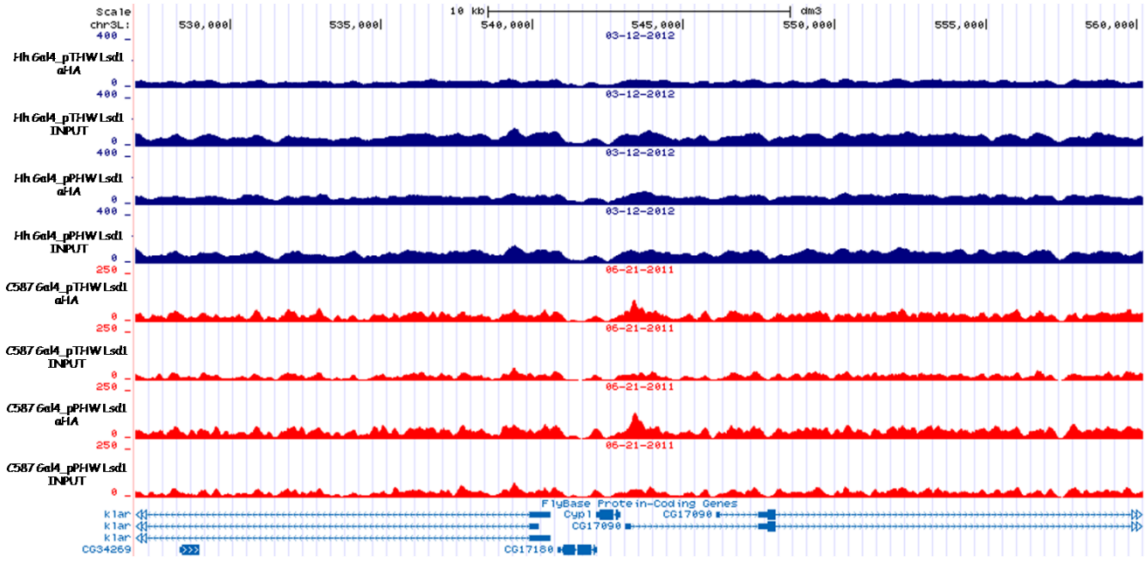

Figure 75. Screenshot of Lsd1 binding sites on coordinates chr3L:526,874-560,206

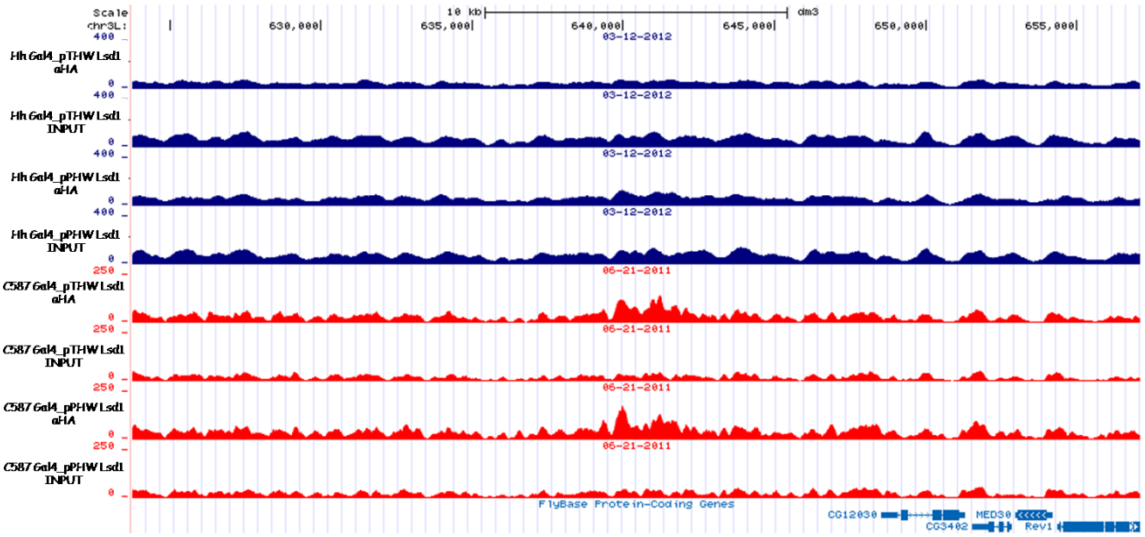

Figure 76. Screenshot of Lsd1 binding sites on coordinates chr3L:623,760-657,092

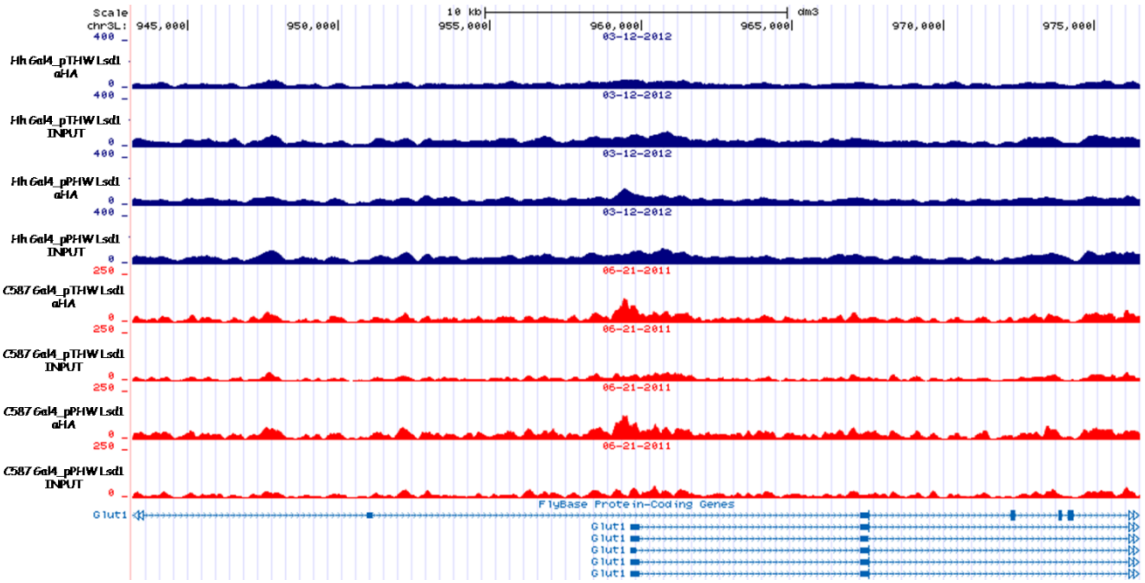

Figure 77. Screenshot of Lsd1 binding sites on coordinates chr3L:943,179-976,511

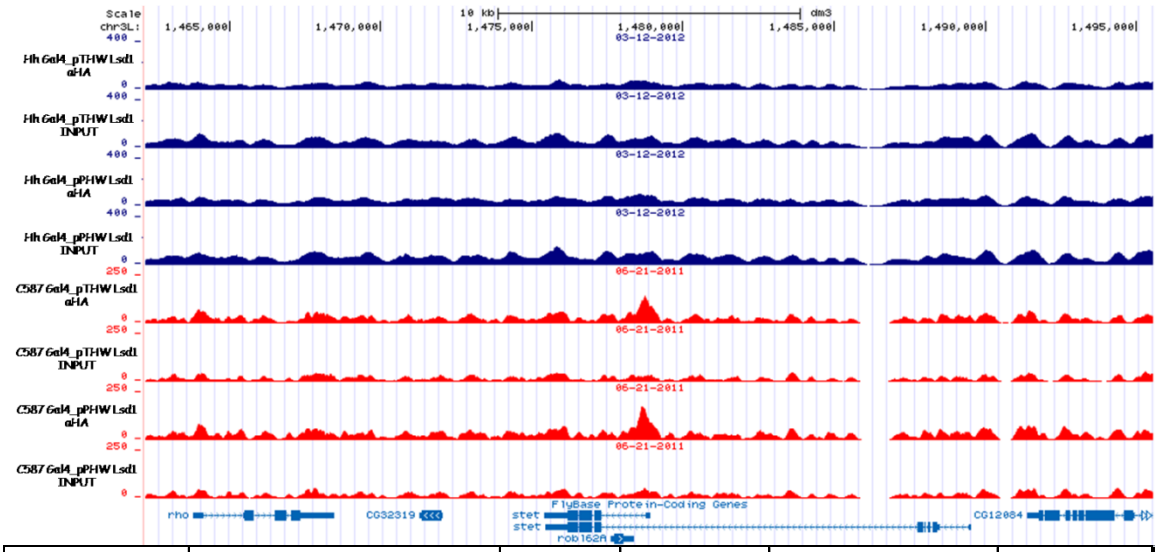

gene	locus	WT_EC	Lsd1 KD_EC	log2(fold_change)	significant
stet	chr3L:1475430-1489547	0.169522	2.29037	3.75604	yes

Figure 78. Screenshot of Lsd1 binding sites on coordinates chr3L:1,462,221-1,495,553 and RNA seq data for genes that exhibit significant difference between WT escort cells and Lsd1 knockdown escort cells

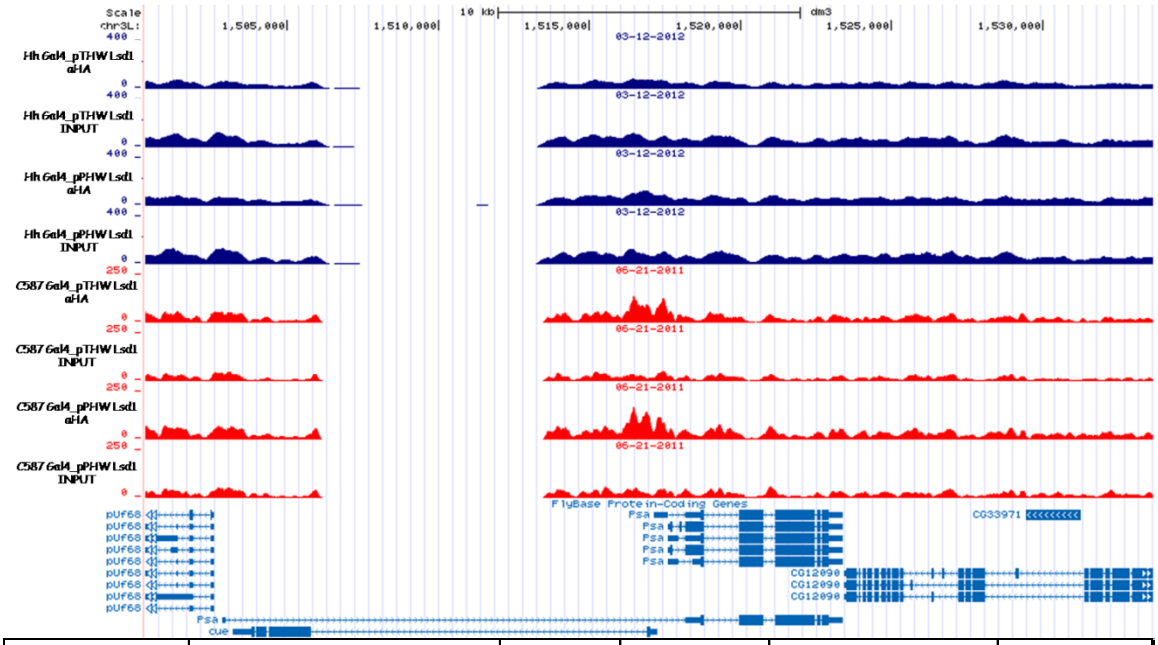

gene	locus	WT_EC	Lsd1 KD_EC	log2(fold_change)	significant
Psa	chr3L:1502842-1523380	23.5808	41.2166	0.80561	yes

Figure 79. Screenshot of Lsd1 binding sites on coordinates chr3L:1,500,315-1,533,647 and RNA seq data for genes that exhibit significant difference between WT escort cells and Lsd1 knockdown escort cells

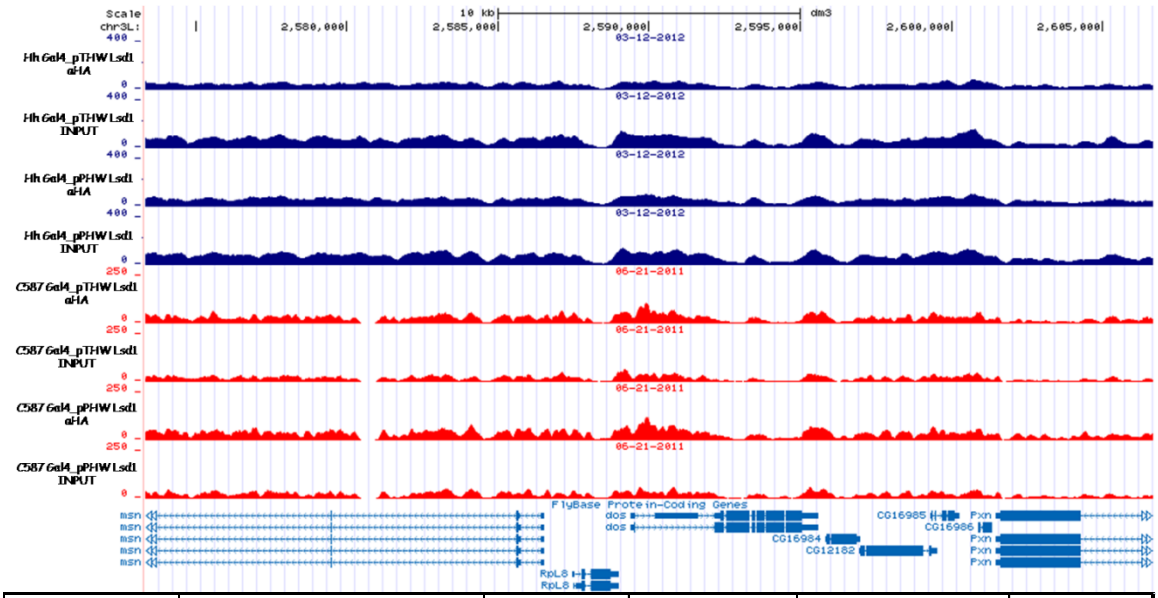

Gene	Locus	WT_EC	Lsd1 KD_EC	log2(fold_change)	significant
msn	chr3L:2555774-2586540	40.8525	66.9769	0.713239	yes

Figure 80. Screenshot of Lsd1 binding sites on coordinates chr3L:2,573,335-2,606,667 and RNA seq data for genes that exhibit significant difference between WT escort cells and Lsd1 knockdown escort cells

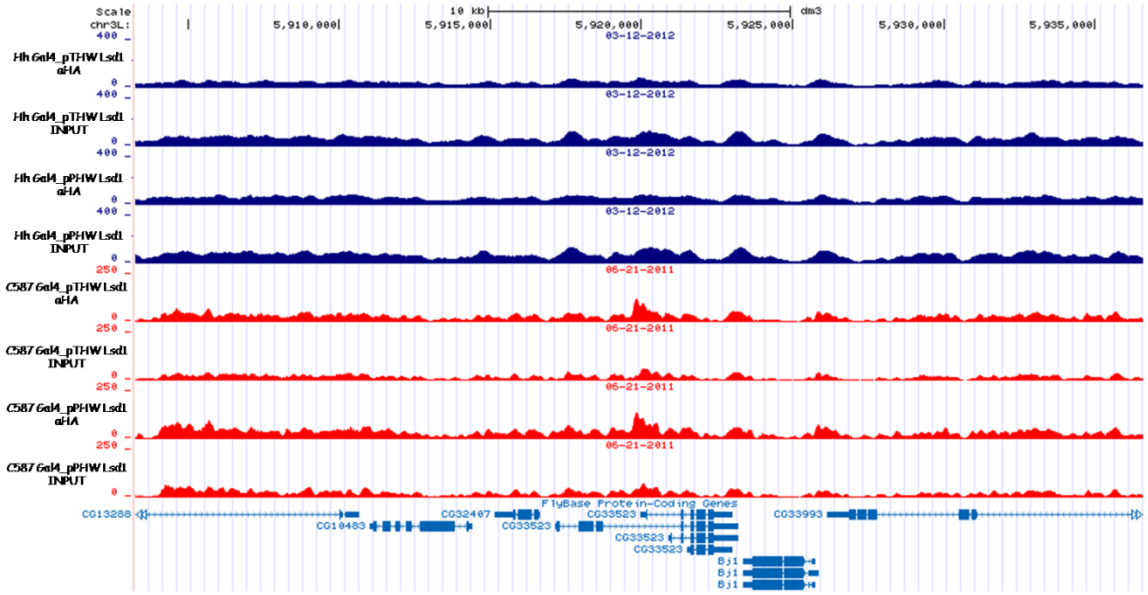

Figure 81. Screenshot of Lsd1 binding sites on coordinates chr3L:5,903,262-5,936,594

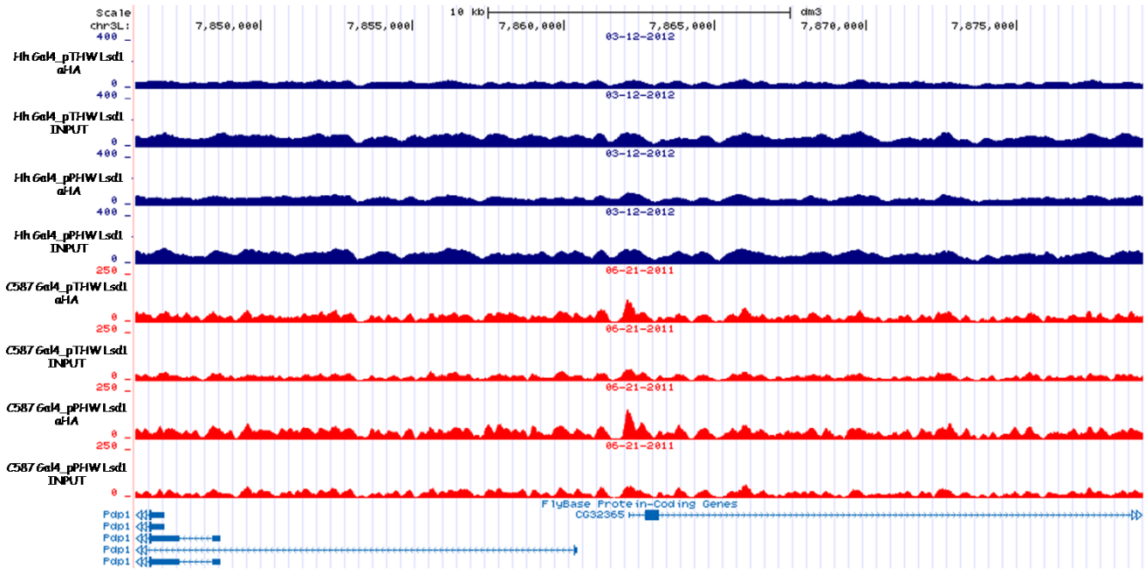

gene	locus	WT_EC	Lsd1 KD_EC	log2(fold_change)	significant
Pdp1	chr3L:7807436-7860472	12.4291	33.345	1.42374	yes

Figure 82. Screenshot of Lsd1 binding sites on coordinates chr3L:7,845,835-7,879,167 and RNA seq data for genes that exhibit significant difference between WT escort cells and Lsd1 knockdown escort cells

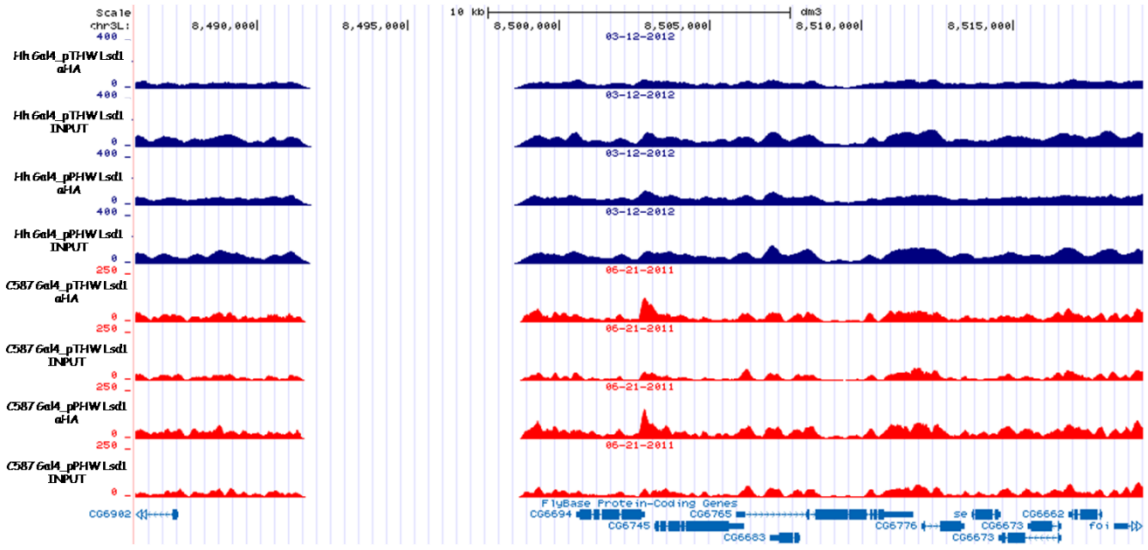

Figure 83. Screenshot of Lsd1 binding sites on coordinates chr3L:8,485,985-8,519,317

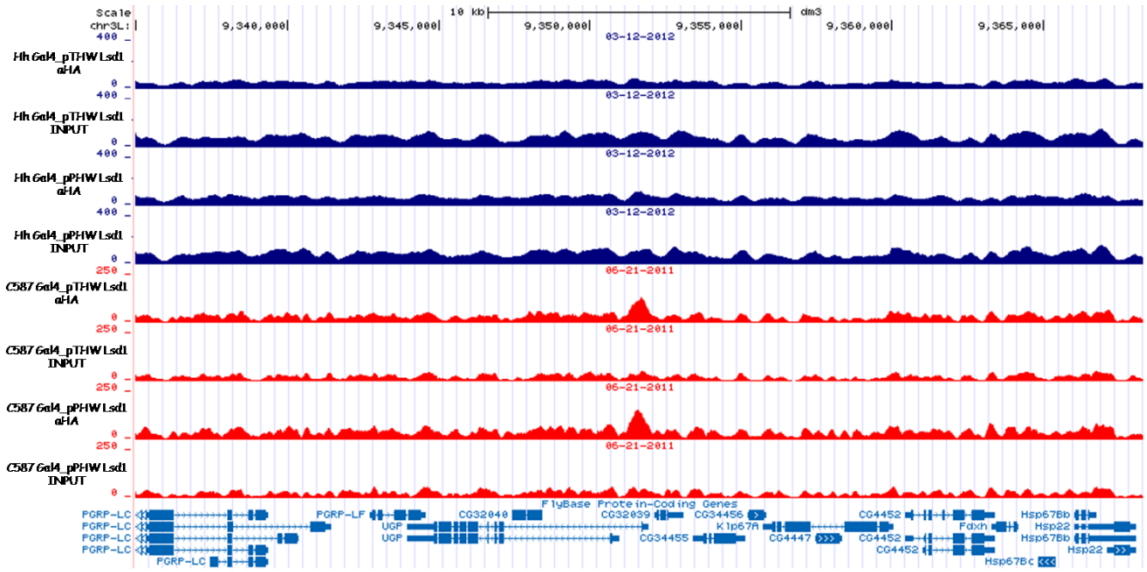

Figure 84. Screenshot of Lsd1 binding sites on coordinates chr3L:9,334,969-9,368,303

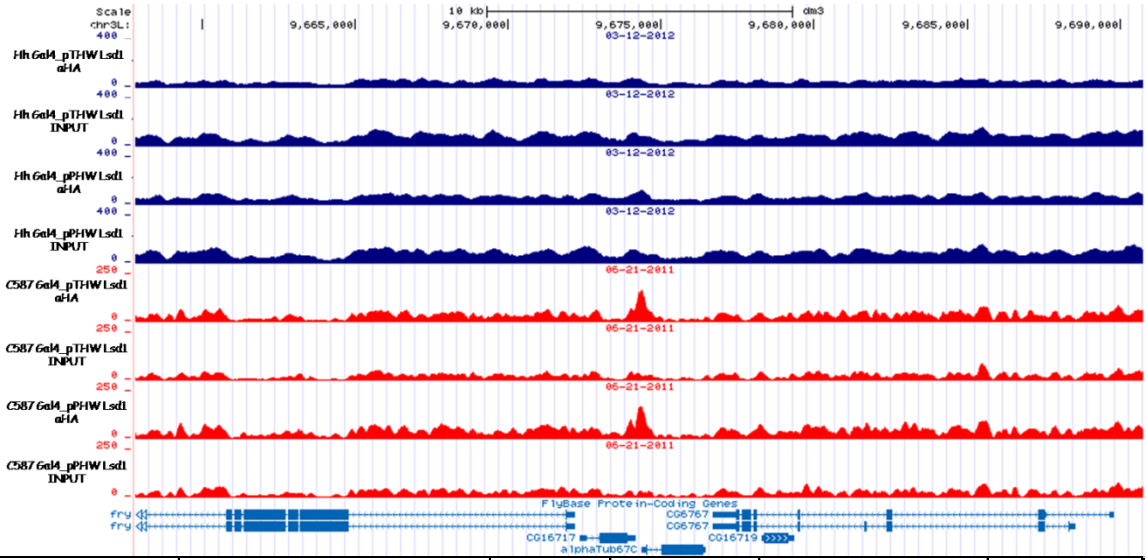

gene	locus	WT_EC	Lsd1 KD_EC	log2(fold_change)	significant
alphaTub67C	chr3L:9674378-9676470	1.08977	7.72599	2.82569	yes

Figure 85. Screenshot of Lsd1 binding sites on coordinates chr3L:9,657,818-9,690,751 and RNA seq data for genes that exhibit significant difference between WT escort cells and Lsd1 knockdown escort cells

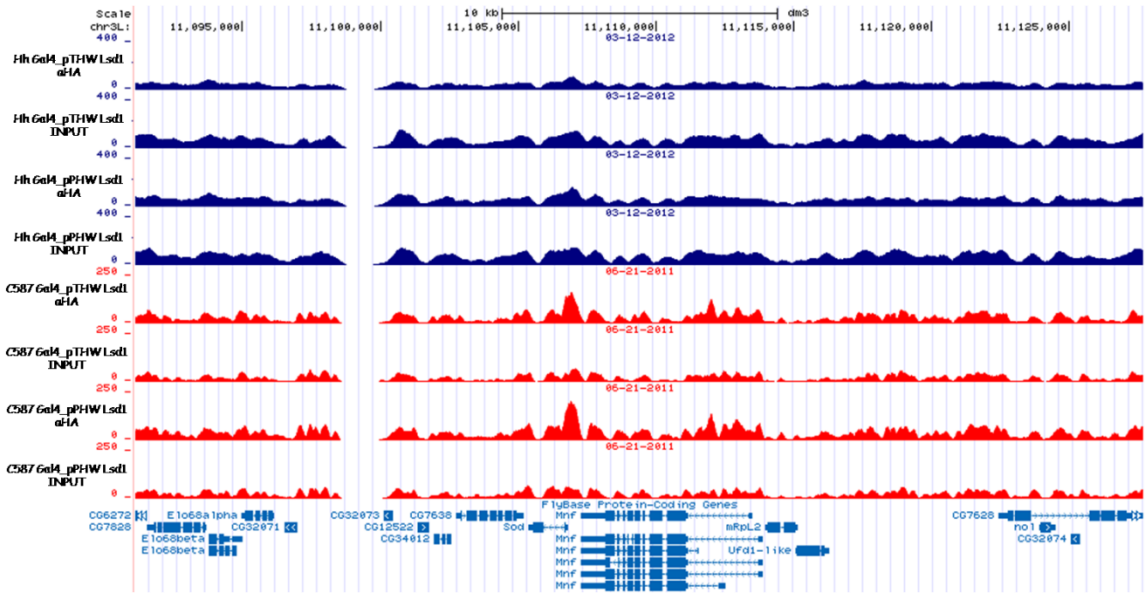

Figure 86. Screenshot of Lsd1 binding sites on coordinates chr3L:11,091,106-11,127,698

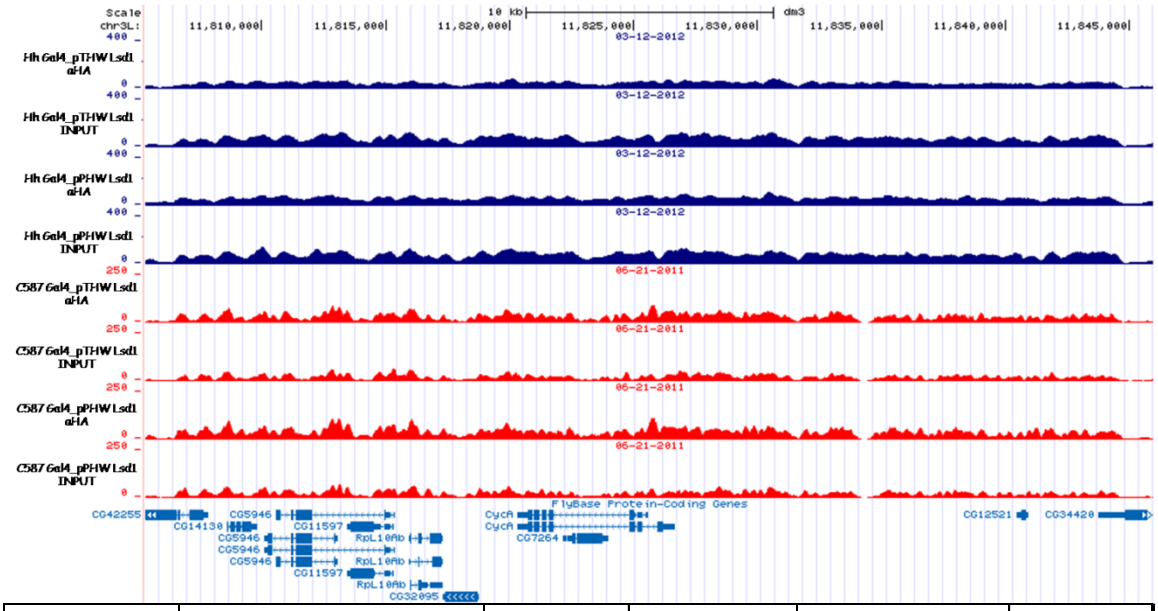

Gene	Locus	WT_EC	Lsd1 KD_EC	log2(fold_change)	significant
CycA	chr3L:11820296-11826677	3.96898	21.5491	2.44078	yes

Figure 87. Screenshot of Lsd1 binding sites on coordinates chr3L:11,805,297-11,845,954 and RNA seq data for genes that exhibit significant difference between WT escort cells and Lsd1 knockdown escort cells

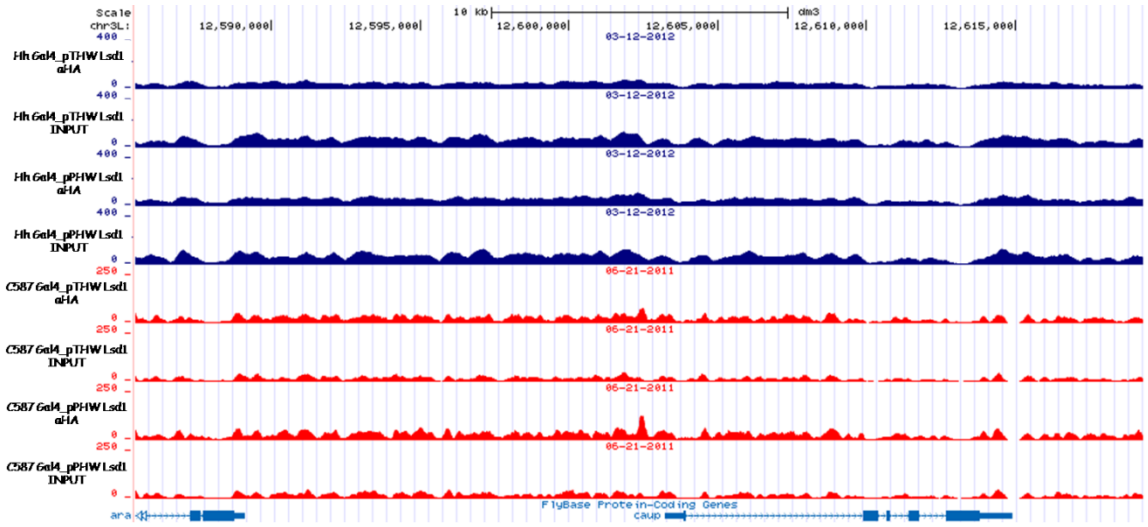

Figure 88. Screenshot of Lsd1 binding sites on coordinates chr3L:12,585,425-12,619,309

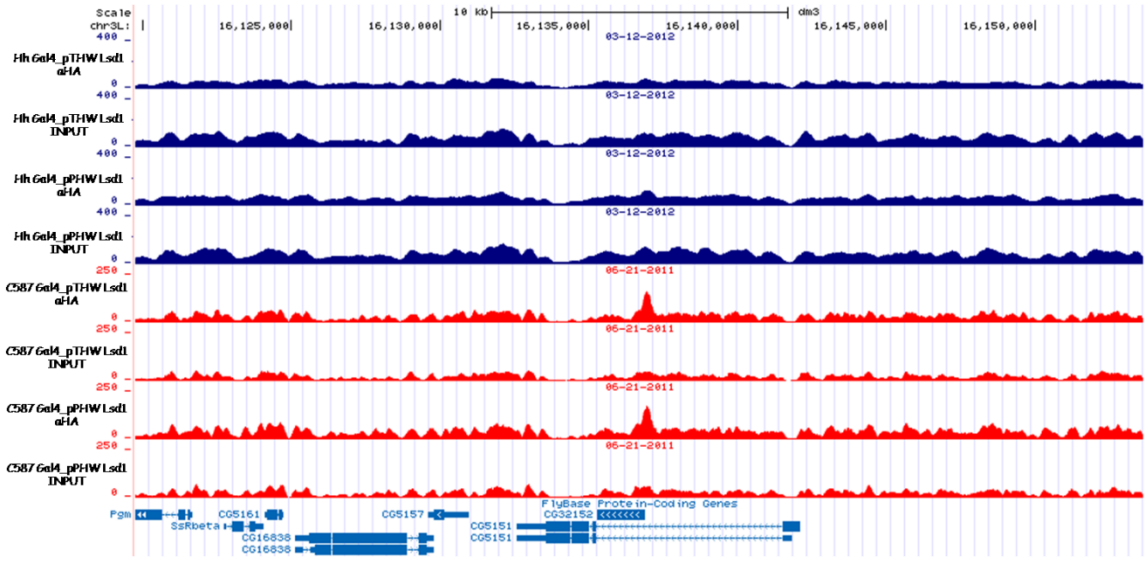

Figure 89. Screenshot of Lsd1 binding sites on coordinates chr3L:16,119,756-16,153,640

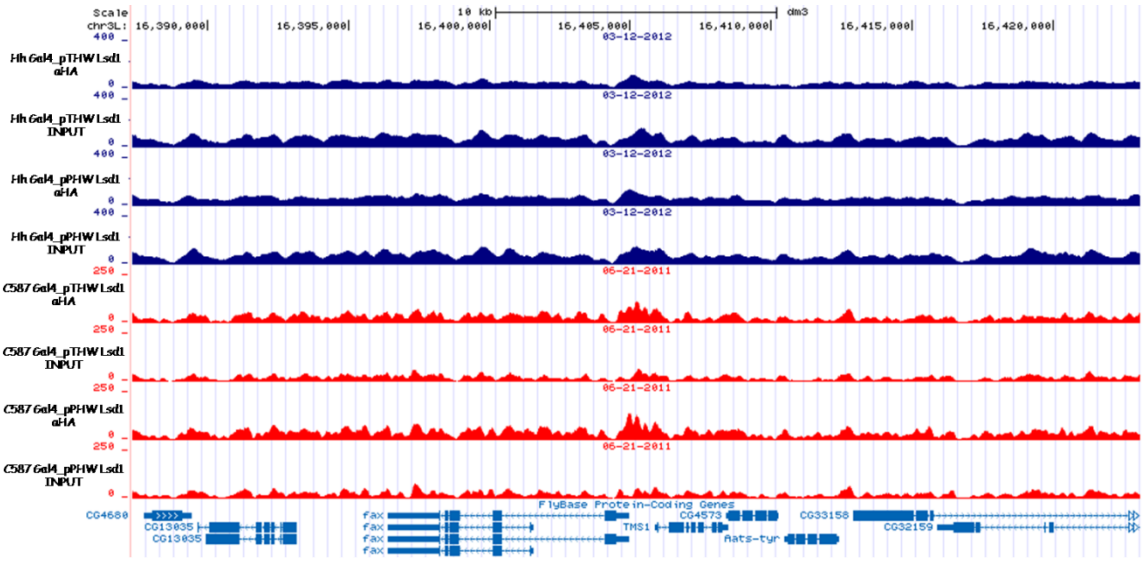

Figure 90. Screenshot of Lsd1 binding sites on coordinates chr3L:16,387,328-16,423,089

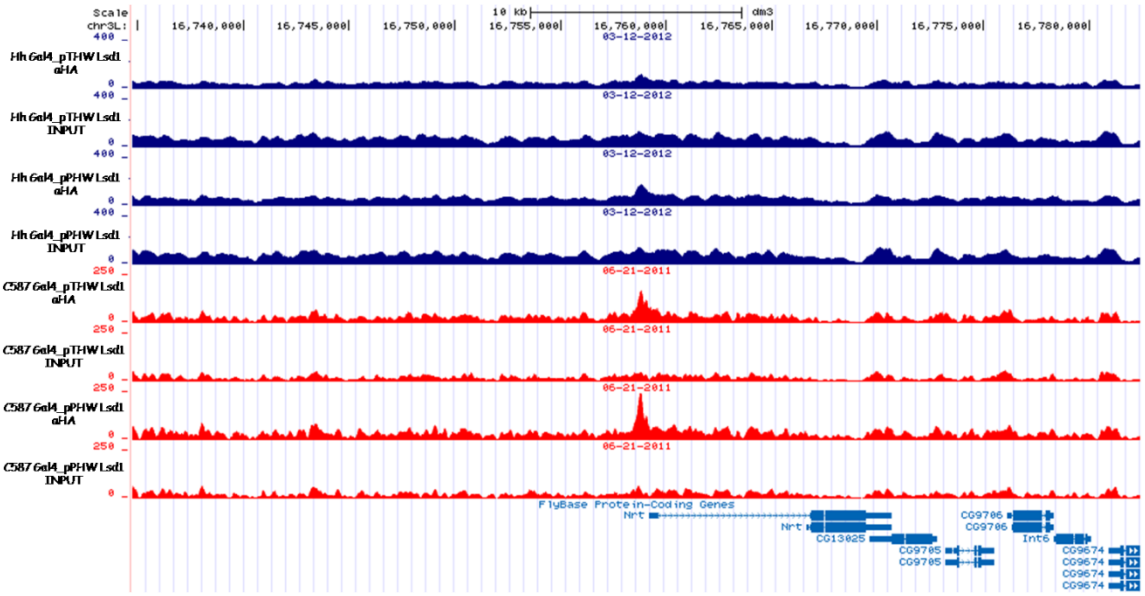

Figure 91. Screenshot of Lsd1 binding sites on coordinates chr3L:16,734,744-16,782,425

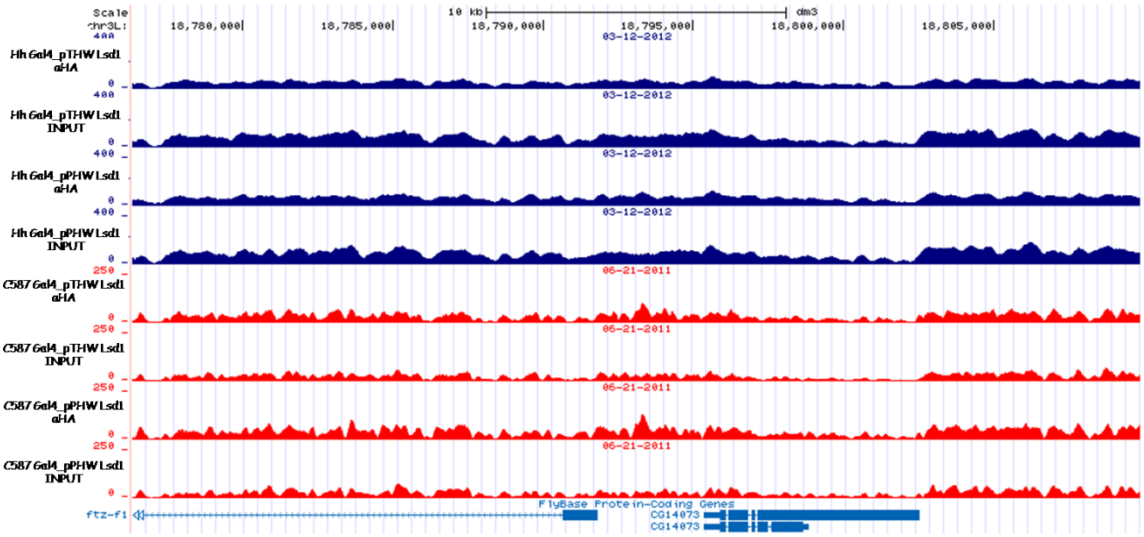

Figure 92. Screenshot of Lsd1 binding sites on coordinates chr3L:18,776,333-18,809,865

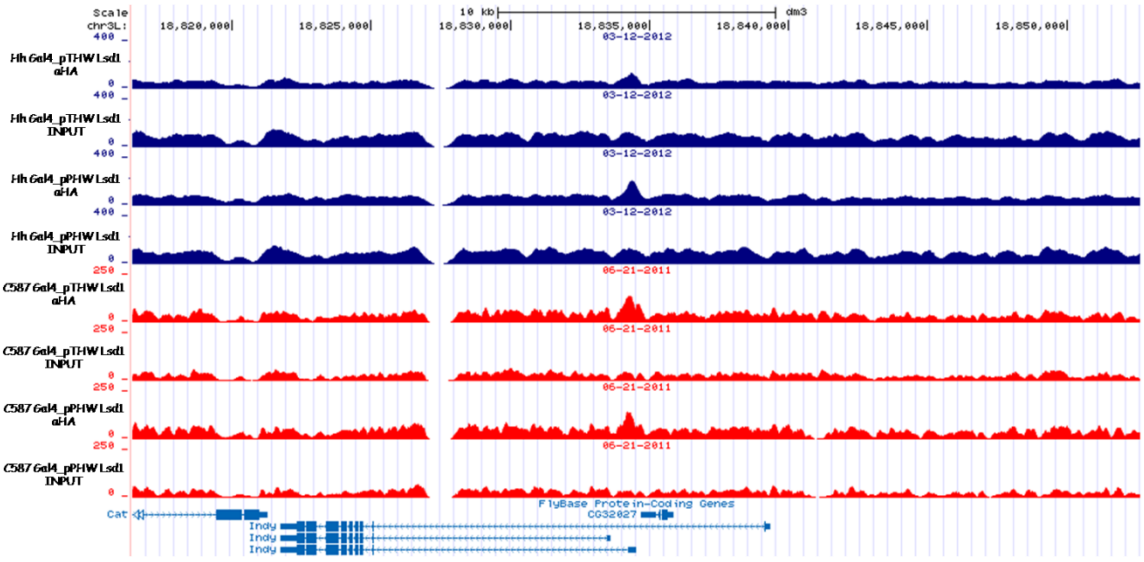

Figure 93. Screenshot of Lsd1 binding sites on coordinates chr3L:18,816,415-18,852,639

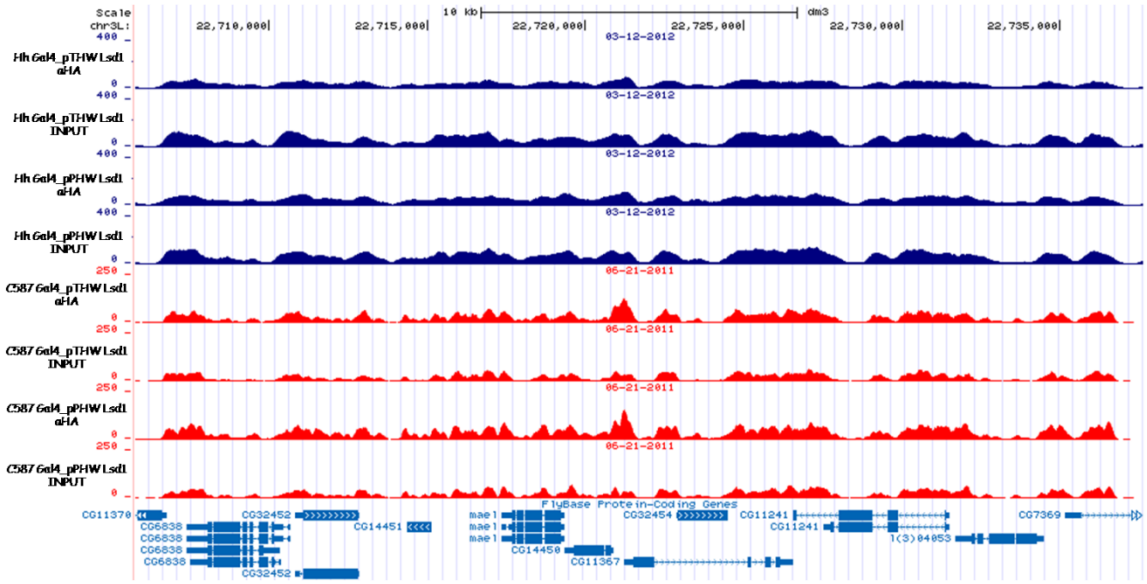

Figure 94. Screenshot of Lsd1 binding sites on coordinates chr3L:22,705,774-22,737,618

Binding Sites of Lsd1 on Chromosome 3R

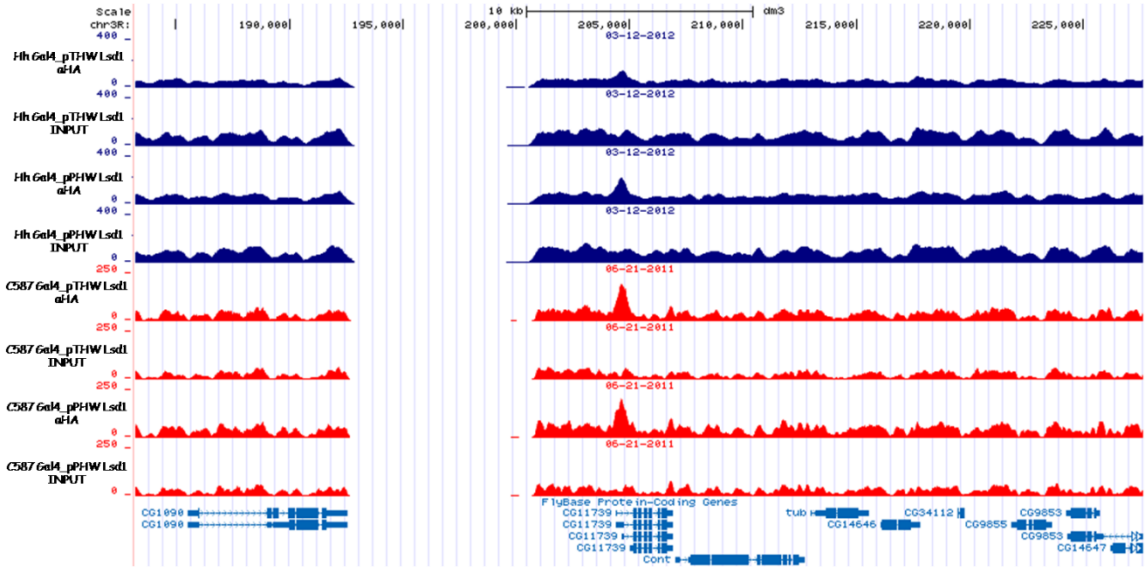

Figure 95. Screenshot of Lsd1 binding sites on coordinates chr3R:183,204-227,647

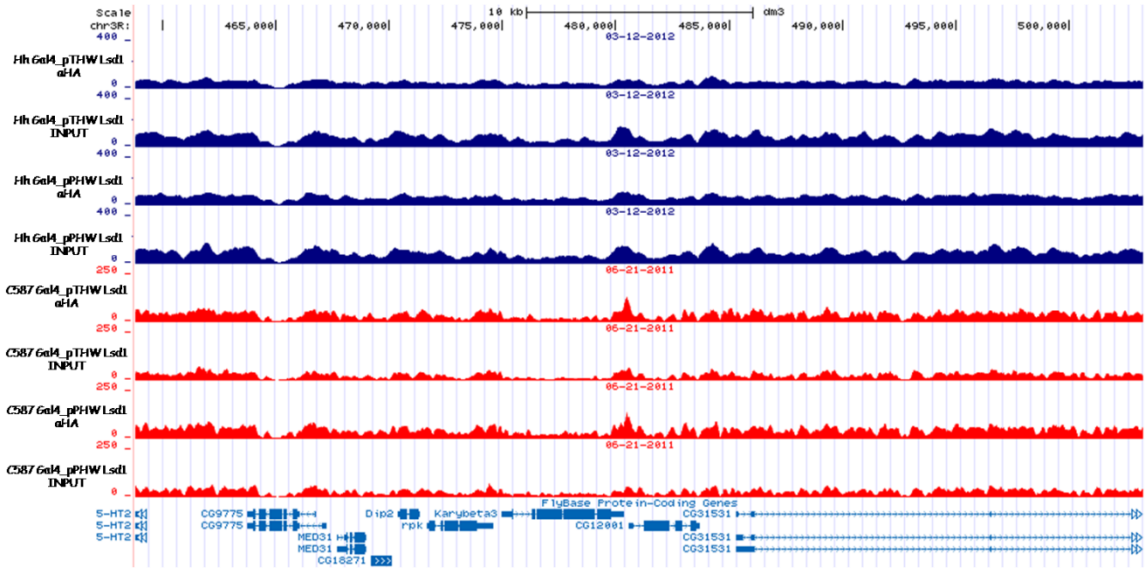

Figure 96. Screenshot of Lsd1 binding sites on coordinates chr3R:458,813-503,256

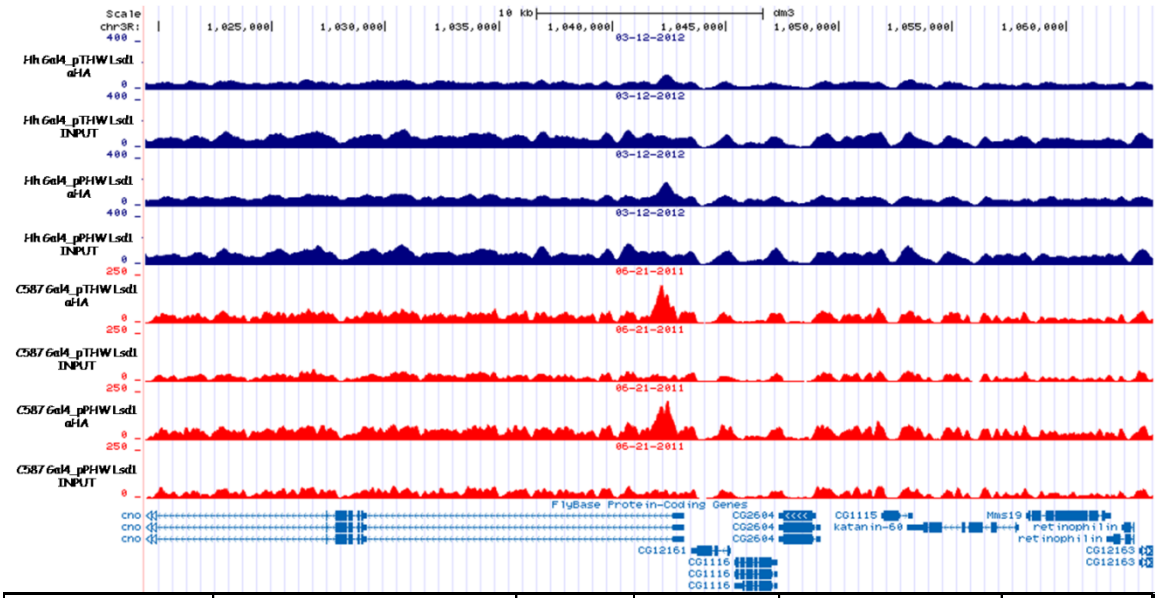

gene	locus	WT_EC	Lsd1 KD_EC	log2(fold_change)	significant
CG2604	chr3R:1047346-1049197	8.86245	26.0158	1.55361	yes

Figure 97. Screenshot of Lsd1 binding sites on coordinates chr3R:1,019,407-1,063,850 and RNA seq data for genes that exhibit significant difference between WT escort cells and Lsd1 knockdown escort cells

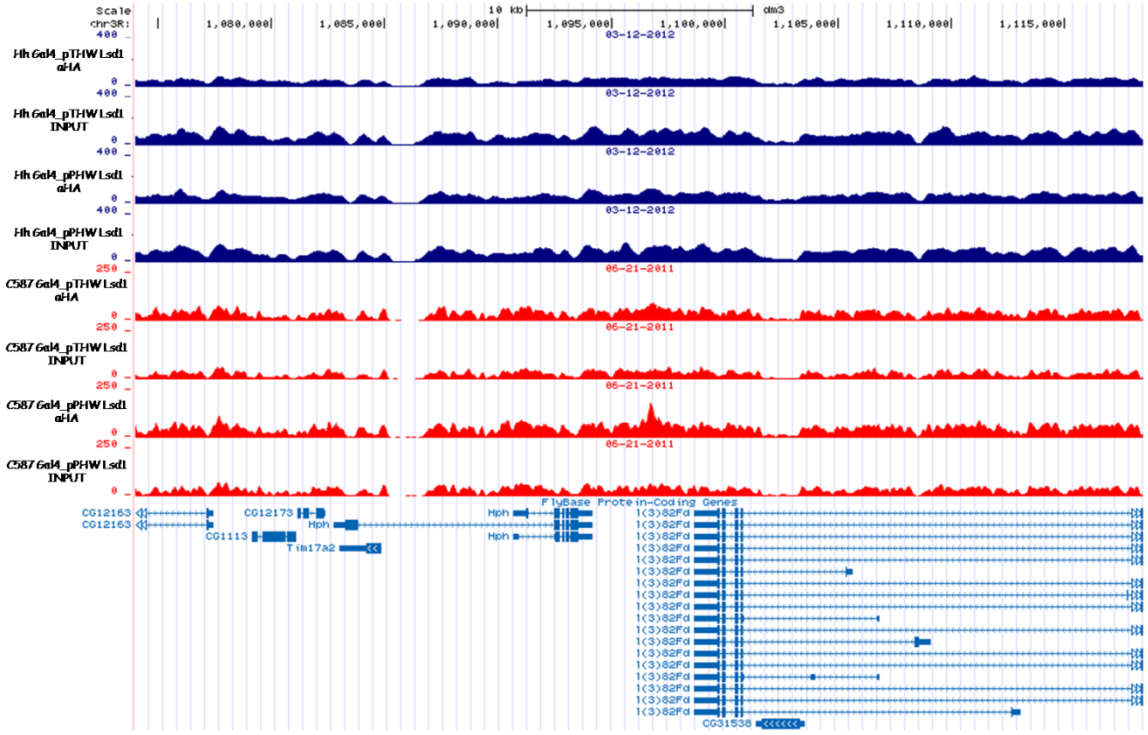

Figure 98. Screenshot of Lsd1 binding sites on coordinates chr3R:1,074,012-1,118,455

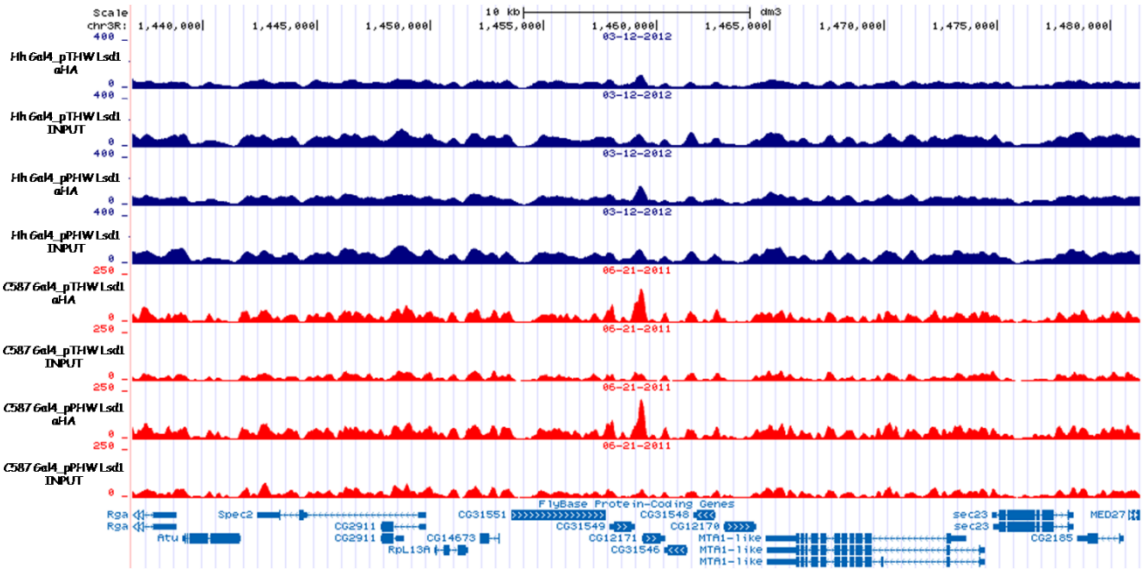

Figure 99. Screenshot of Lsd1 binding sites on coordinates chr3R:1,436,867-1,481,310

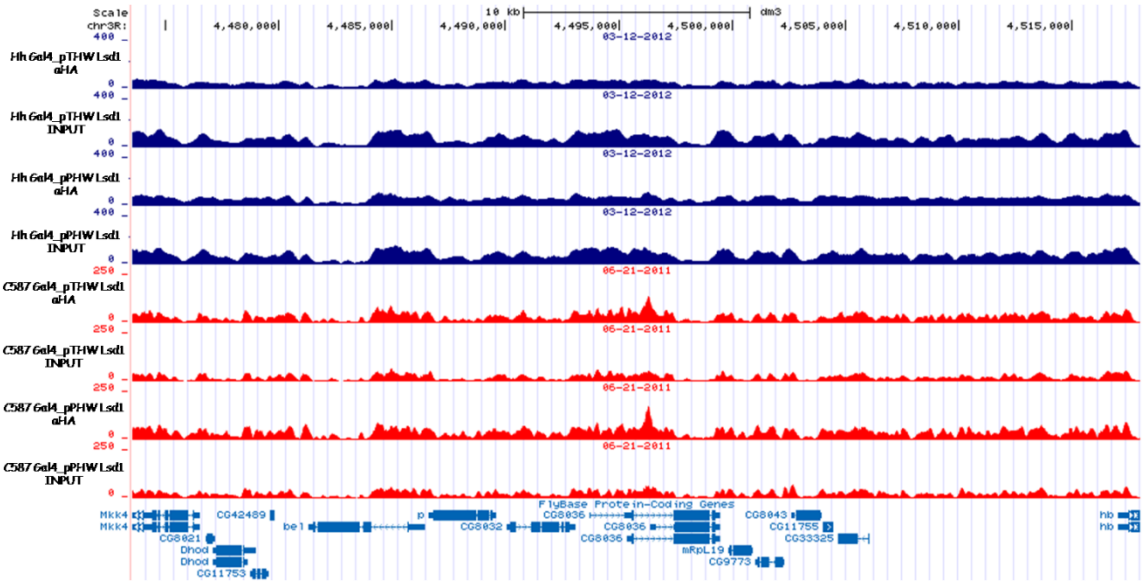

Figure 100. Screenshot of Lsd1 binding sites on coordinates chr3R:4,473,550-4,517,993

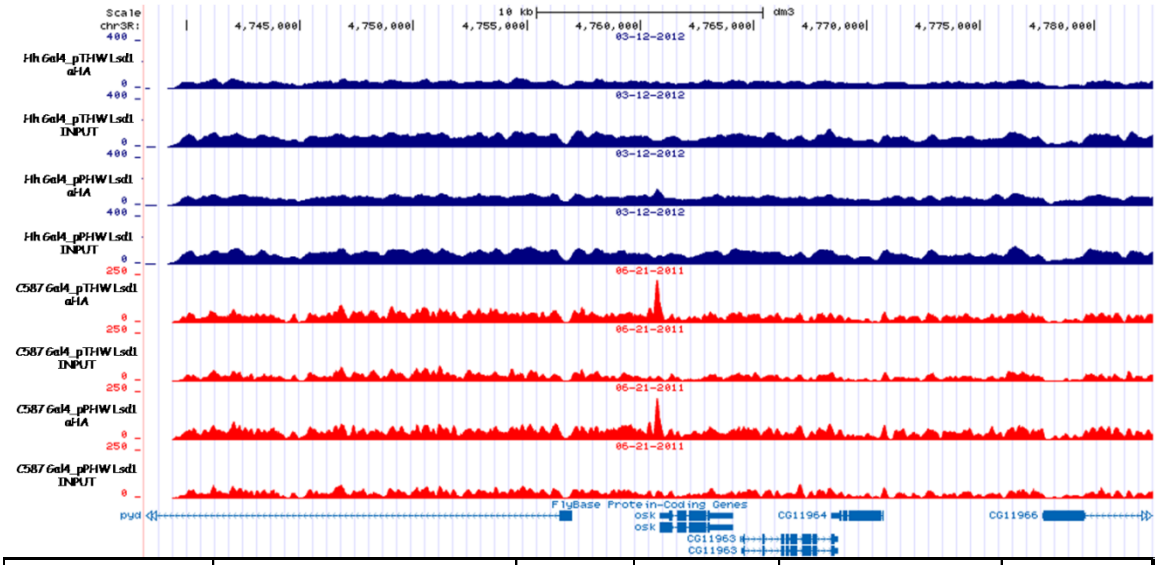

gene	locus	WT_EC	Lsd1 KD_EC	log2(fold_change)	significant
osk	chr3R:4760852-4764123	1.14619	10.4554	3.18933	yes

Figure 101. Screenshot of Lsd1 binding sites on coordinates chr3R:4,738,176-4,782,619 and RNA seq data for genes that exhibit significant difference between WT escort cells and Lsd1 knockdown escort cells

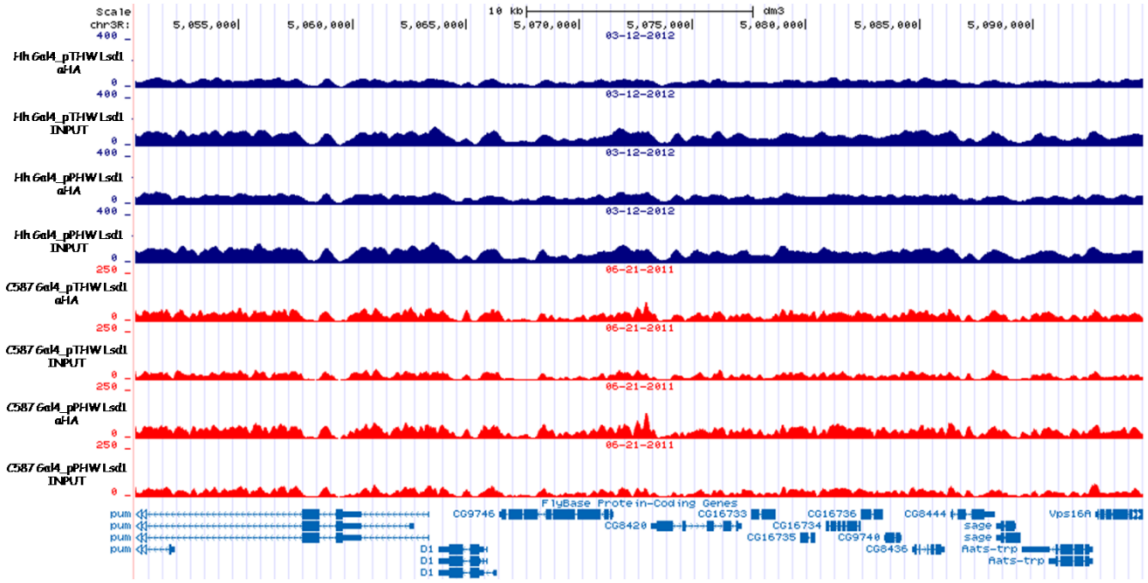

gene	locus	WT_EC	Lsd1 KD_EC	log2(fold_change)	significant
CG8420	chr3R:5073172-5077160	0.166233	1.44425	3.11904	yes

Figure 102. Screenshot of Lsd1 binding sites on coordinates chr3R:5,050,428-5,094,871 and RNA seq data for genes that exhibit significant difference between WT escort cells and Lsd1 knockdown escort cells

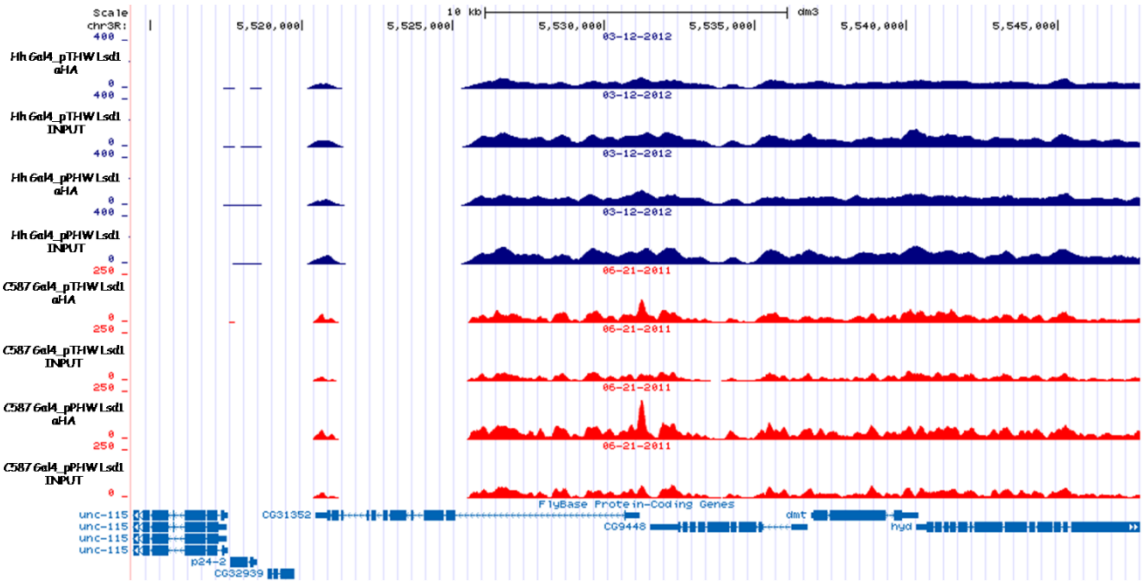

Figure 103. Screenshot of Lsd1 binding sites on coordinates chr3R:5,514,399-5,547,733

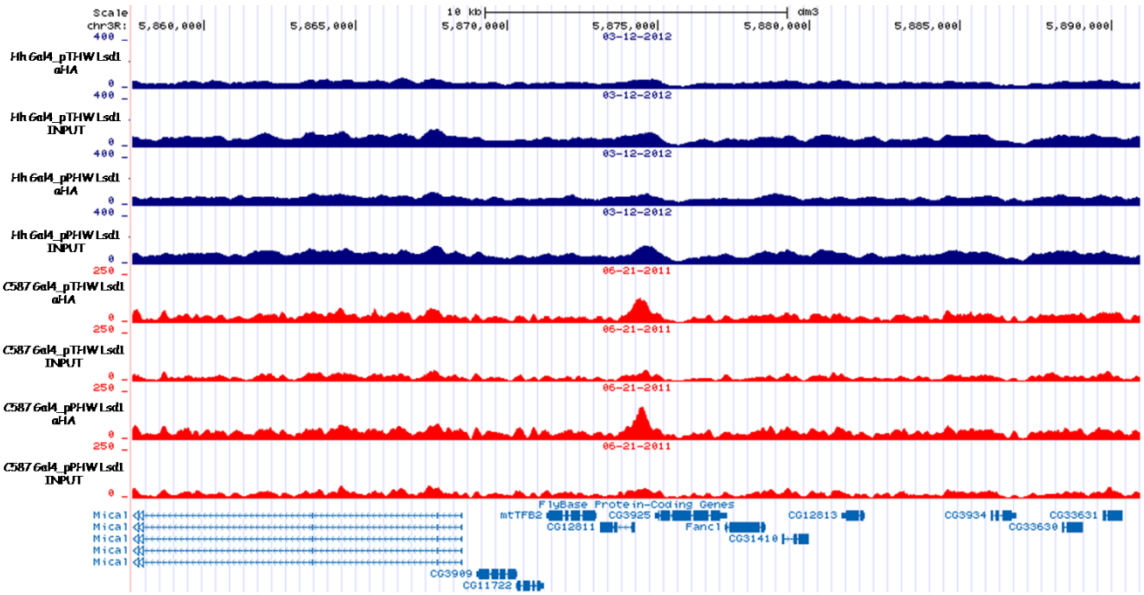

Figure 104. Screenshot of Lsd1 binding sites on coordinates chr3R:5,857,615-5,890,949

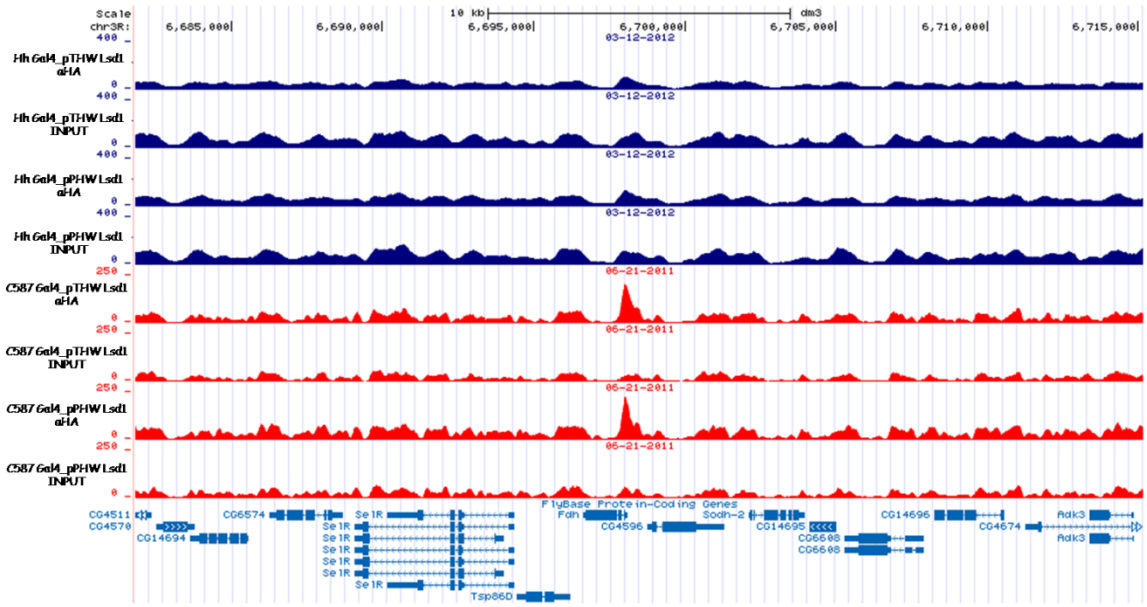

Gene	Locus	WT_EC	Lsd1 KD_EC	log2(fold_change)	significant
Fdh	chr3R:6696626-6698102	21.2892	63.2254	1.57038	yes

Figure 105. Screenshot of Lsd1 binding sites on coordinates chr3R:6,681,826-6,715,160 and RNA seq data for genes that exhibit significant difference between WT escort cells and Lsd1 knockdown escort cells

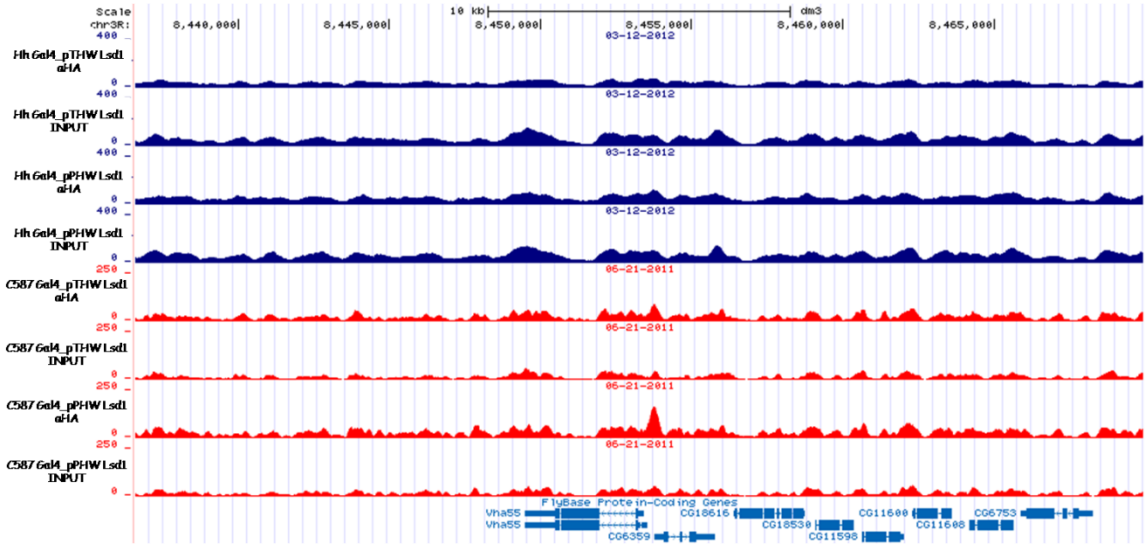

Figure 106. Screenshot of Lsd1 binding sites on coordinates chr3R:8,436,601-8,469,935

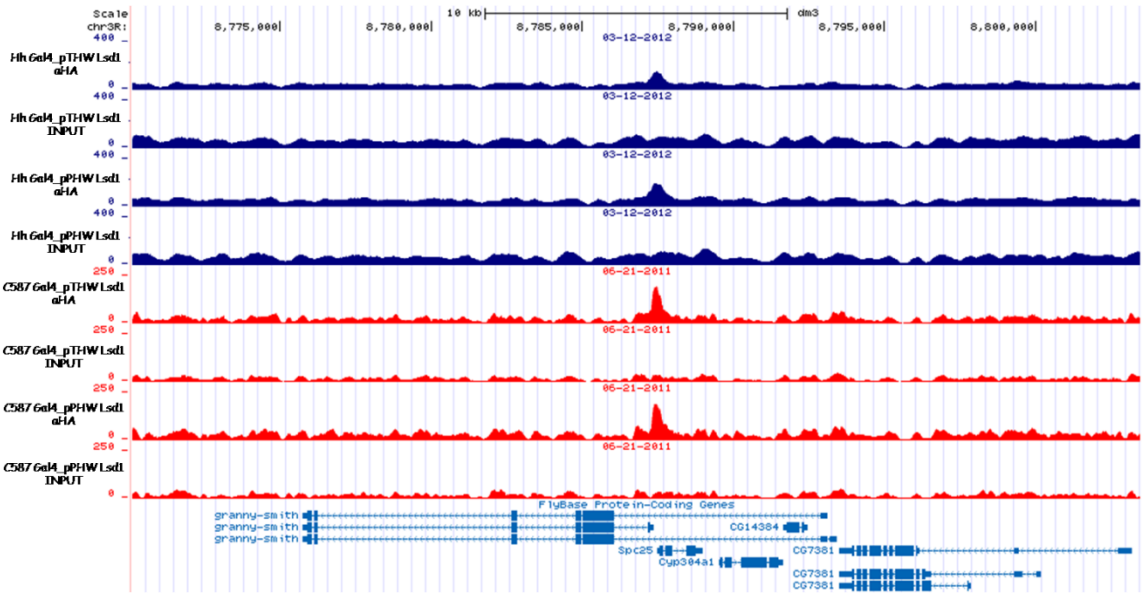

Figure 107. Screenshot of Lsd1 binding sites on coordinates chr3R:8,770,116-8,803,450

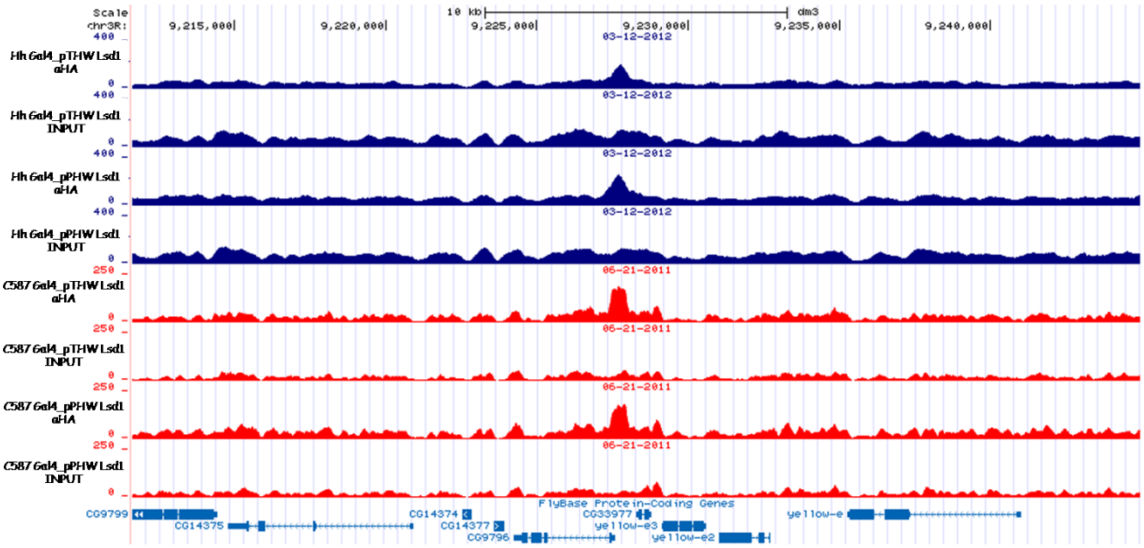

Figure 108. Screenshot of Lsd1 binding sites on coordinates chr3R:9,211,616-9,244,950

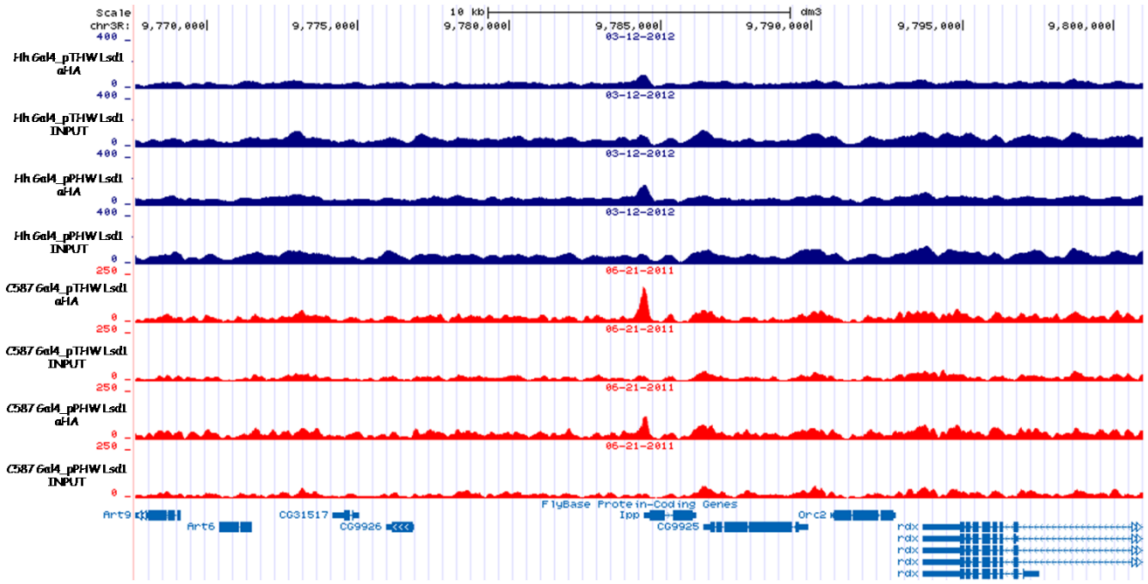

Figure 109. Screenshot of Lsd1 binding sites on coordinates chr3R:9,767,632-9,800,966

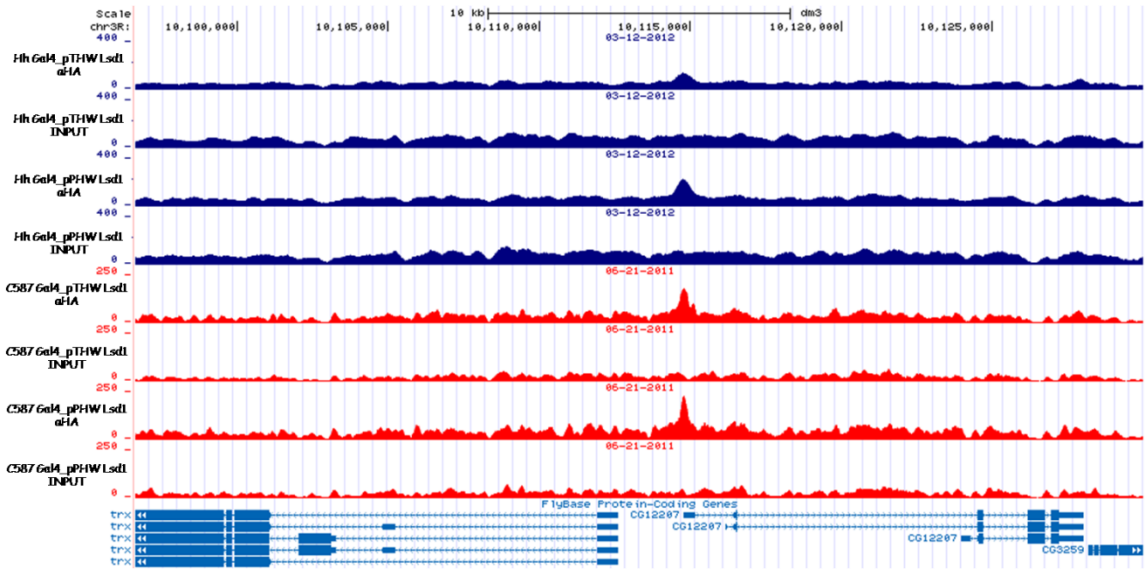

Figure 110. Screenshot of Lsd1 binding sites on coordinates chr3R:10,096,644-10,129,978

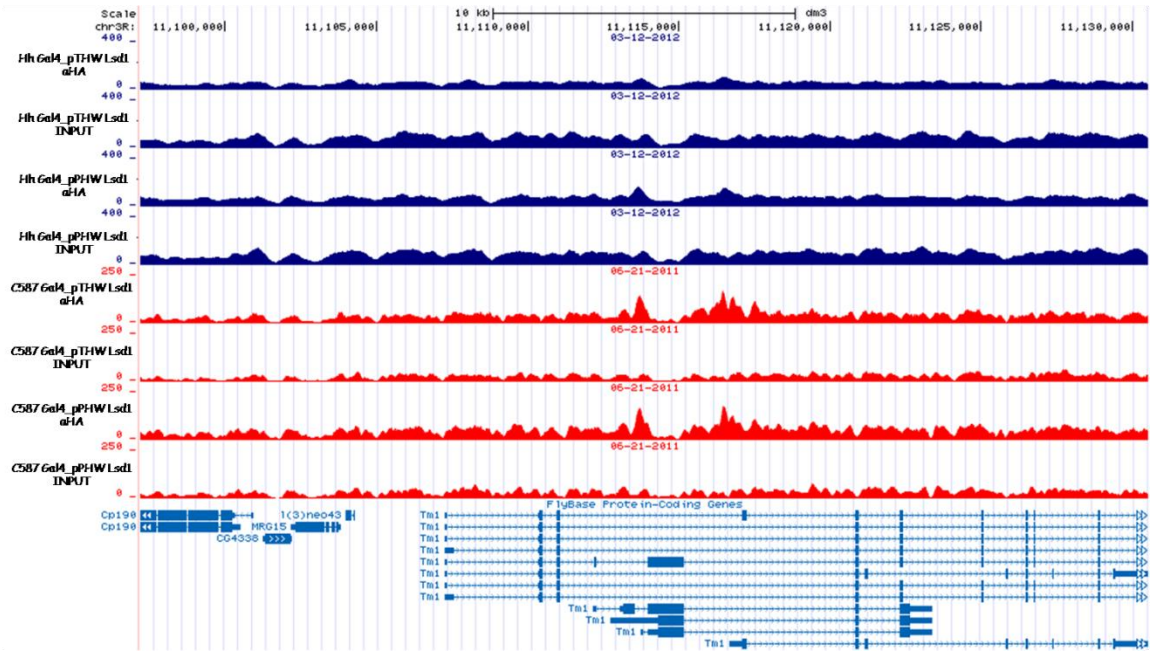

Figure 111. Screenshot of Lsd1 binding sites on coordinates chr3R:11,097,190-11,130,524

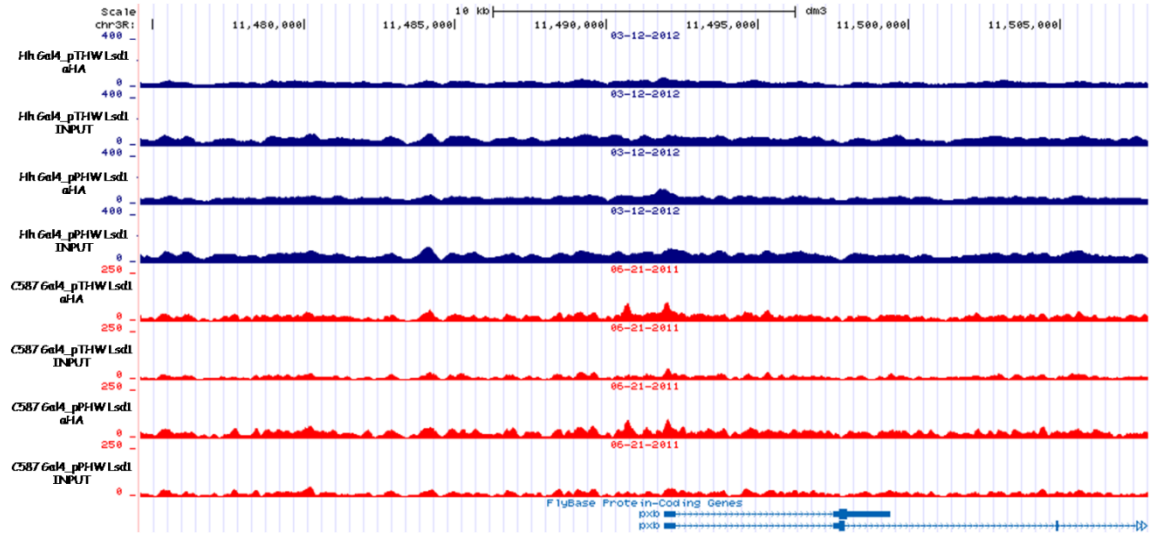

Figure 112. Screenshot of Lsd1 binding sites on coordinates chr3R:11,474,588-11,507,922

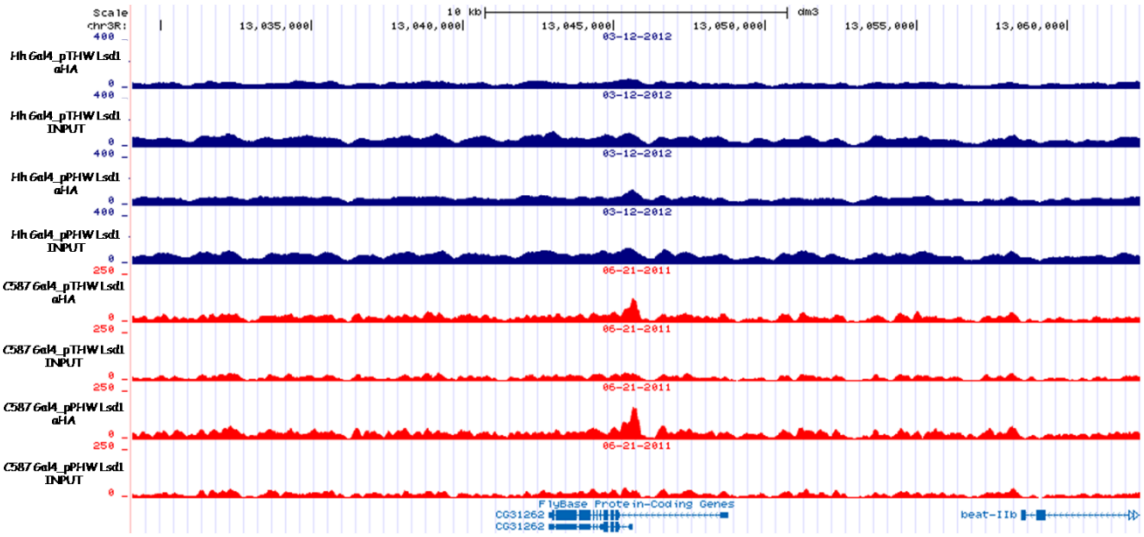

Figure 113. Screenshot of Lsd1 binding sites on coordinates chr3R:13,029,072-13,062,406

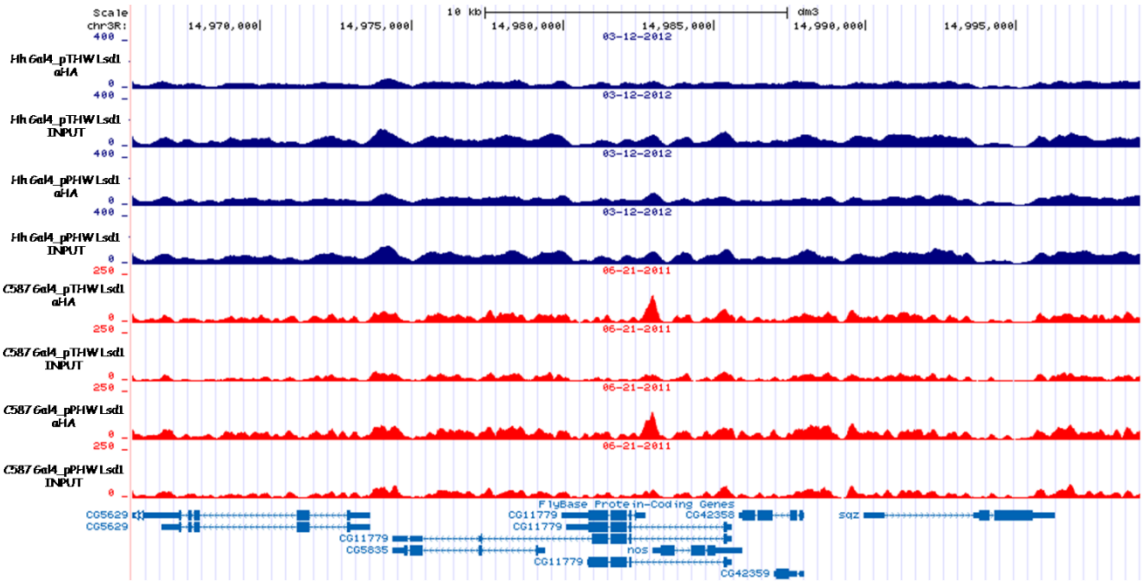

Figure 114. Screenshot of Lsd1 binding sites on coordinates chr3R:14,965,764-14,999,098

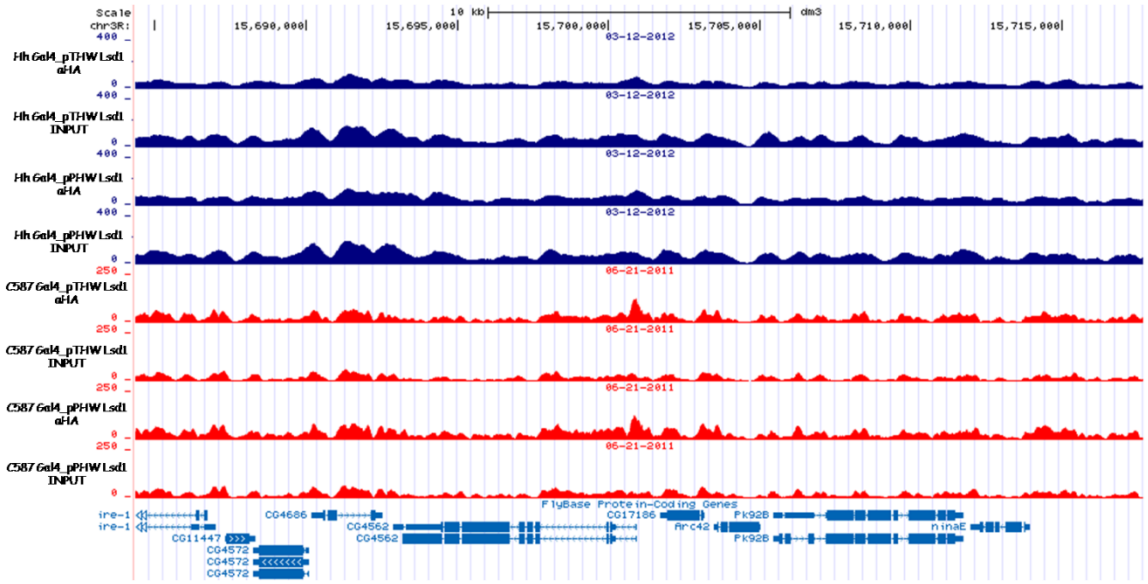

Figure 115. Screenshot of Lsd1 binding sites on coordinates chr3R:15,684,348-15,717,682

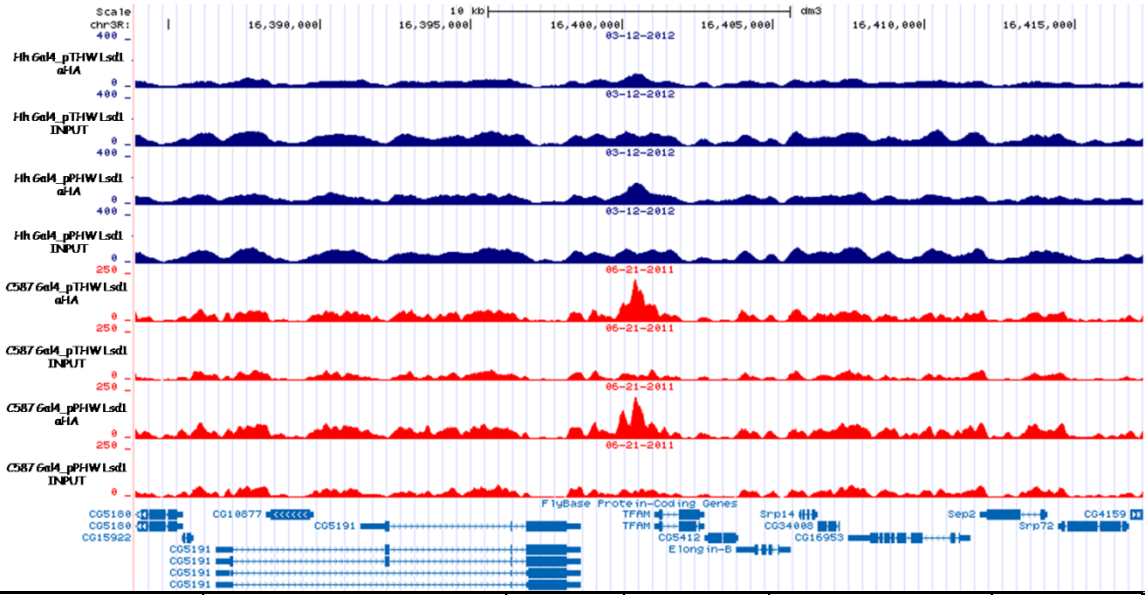

gene	locus	WT_EC	Lsd1 KD_EC	log2(fold_change)	significant
CG5191	chr3R:16386581-16398636	16.1975	42.0661	1.37688	yes

Figure 116. Screenshot of Lsd1 binding sites on coordinates chr3R:16,383,905-16,417,239 and RNA seq data for genes that exhibit significant difference between WT escort cells and Lsd1 knockdown escort cells

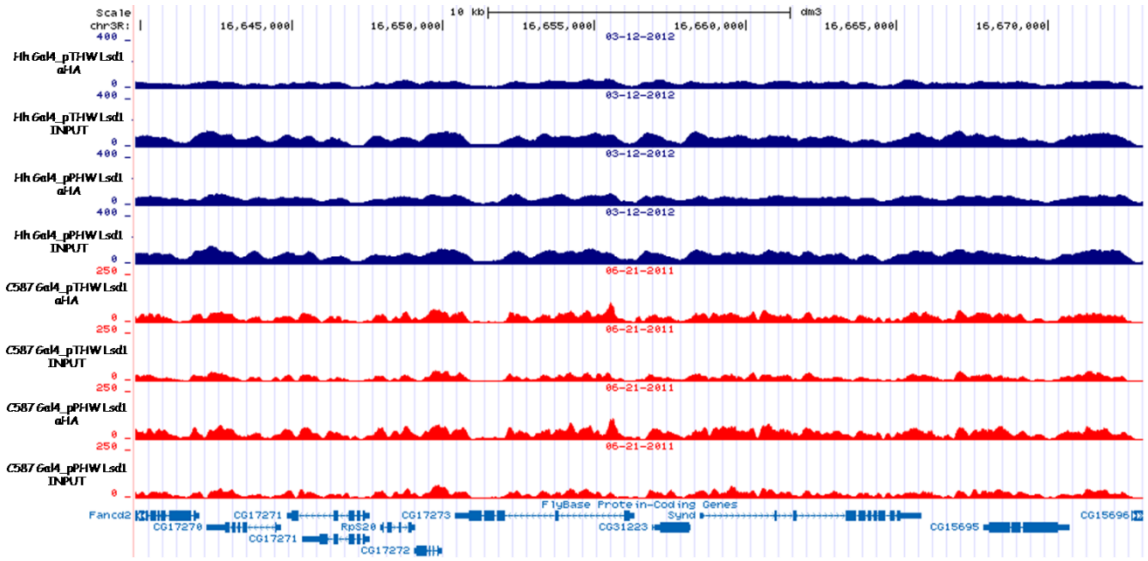

Figure 117. Screenshot of Lsd1 binding sites on coordinates chr3R:16,639,818-16,673,152

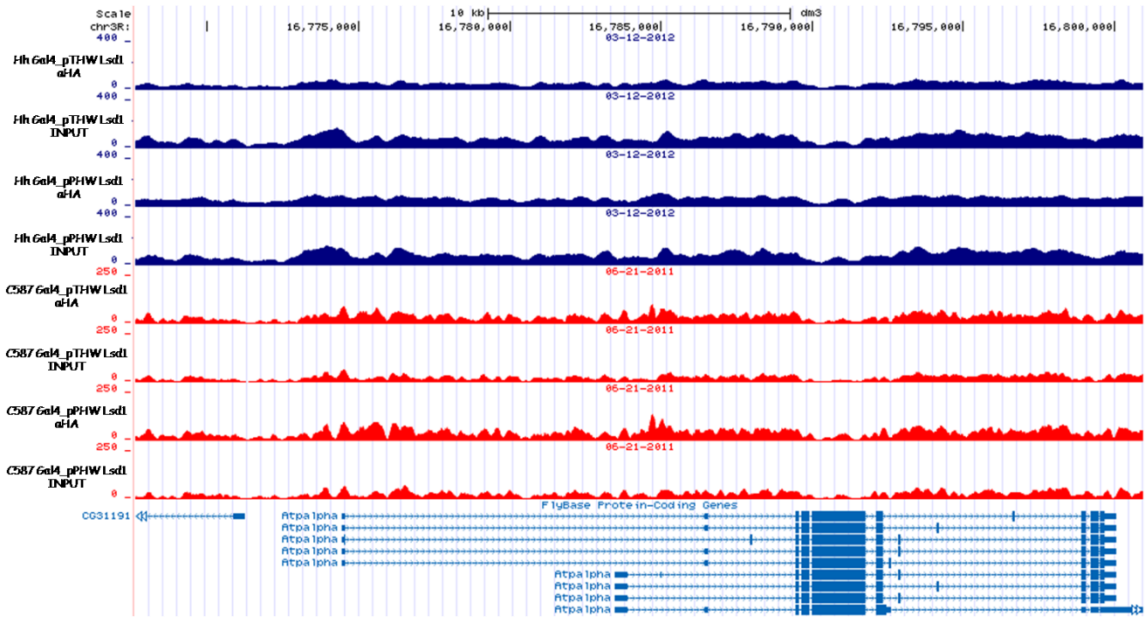

Figure 118. Screenshot of Lsd1 binding sites on coordinates chr3R:16,767,610-16,800,944

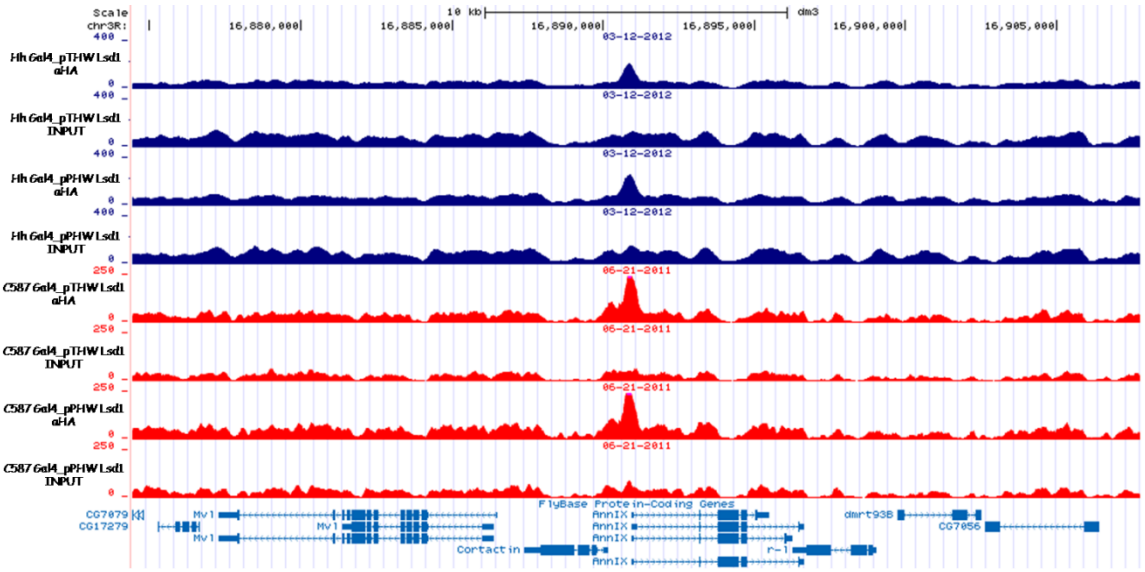

gene	locus	WT_EC	Lsd1 KD_EC	log2(fold_change)	significant
AnnIX	chr3R:16890950-16899039	303.244	490.122	0.69266	yes

Figure 119. Screenshot of Lsd1 binding sites on coordinates chr3R:16,874,428-16,907,762 and RNA seq data for genes that exhibit significant difference between WT escort cells and Lsd1 knockdown escort cells

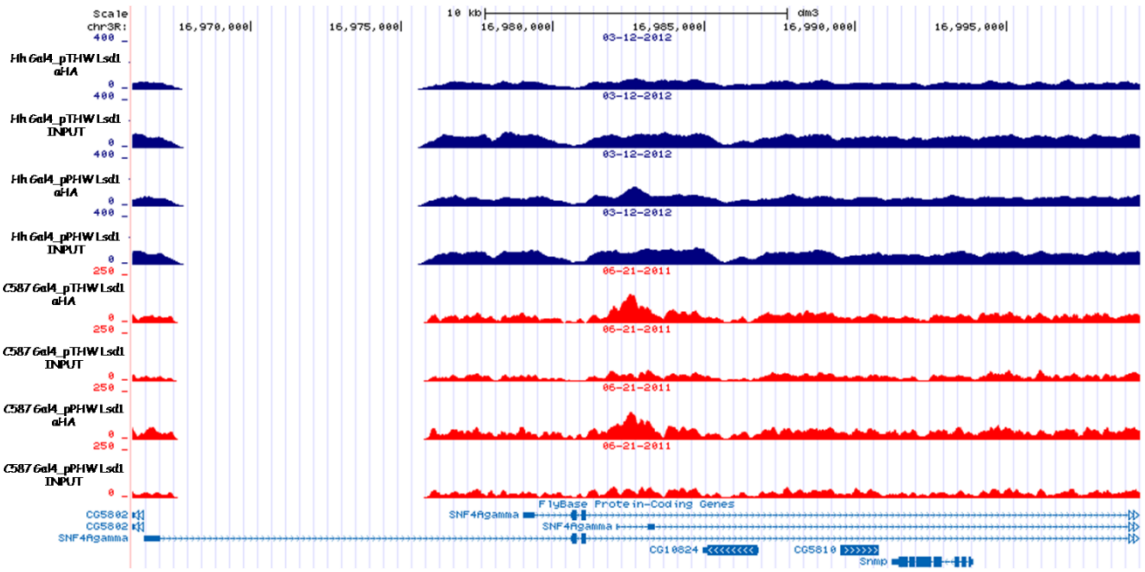

Figure 120. Screenshot of Lsd1 binding sites on coordinates chr3R:16,966,092-16,999,426

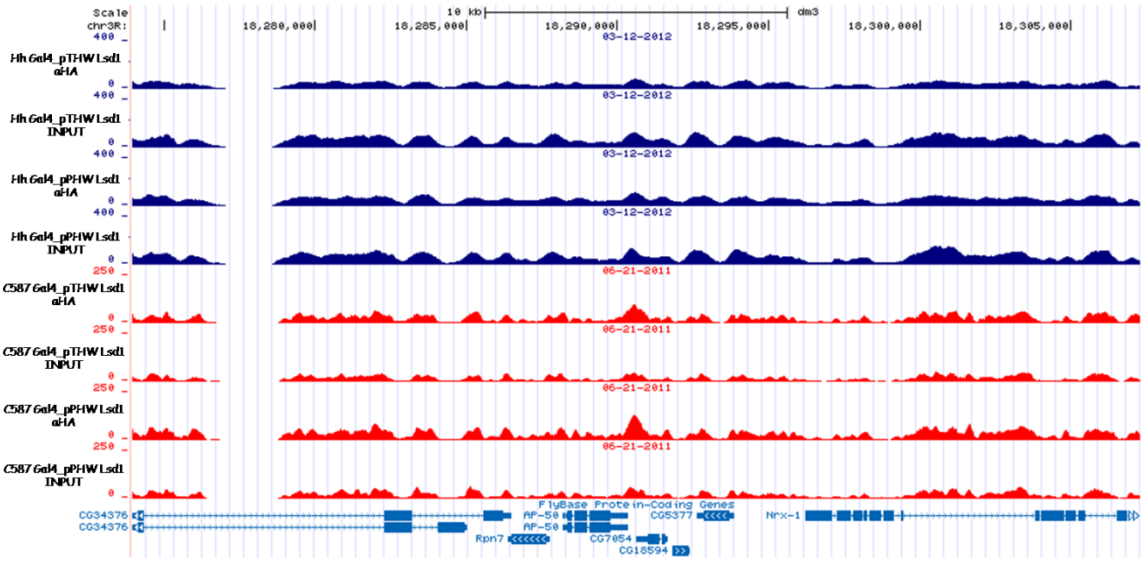

Figure 121. Screenshot of Lsd1 binding sites on coordinates chr3R:18,273,951-18,307,285

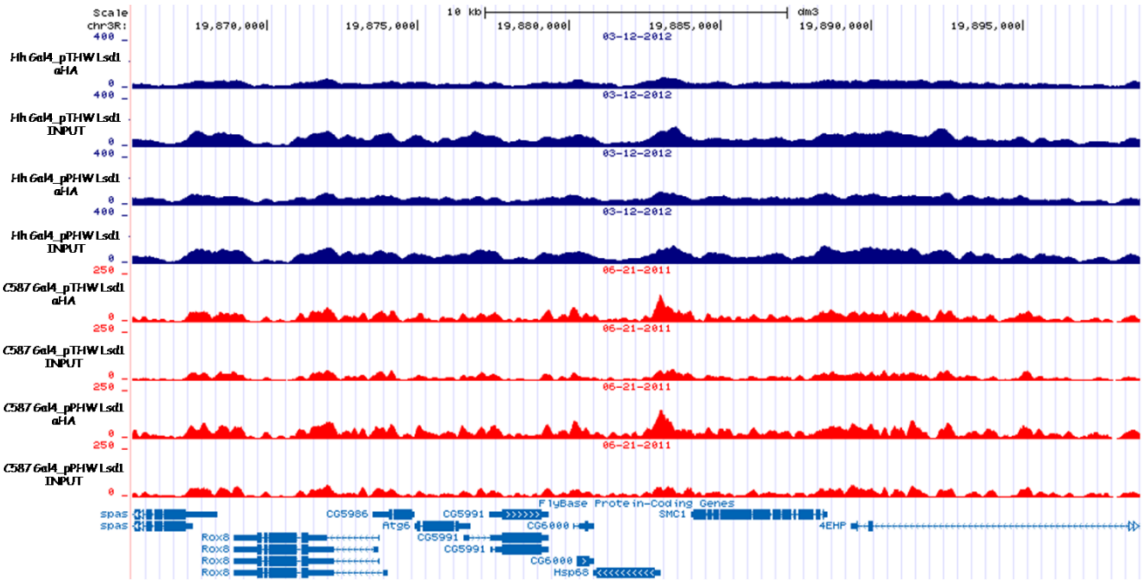

gene	locus	WT_EC	Lsd1 KD_EC	log2(fold_change)	significant
CG5991	chr3R:19874892-19879314	15.332	35.1087	1.19528	yes

Figure 122. Screenshot of Lsd1 binding sites on coordinates chr3R:19,865,553-19,898,887 and RNA seq data for genes that exhibit significant difference between WT escort cells and Lsd1 knockdown escort cells

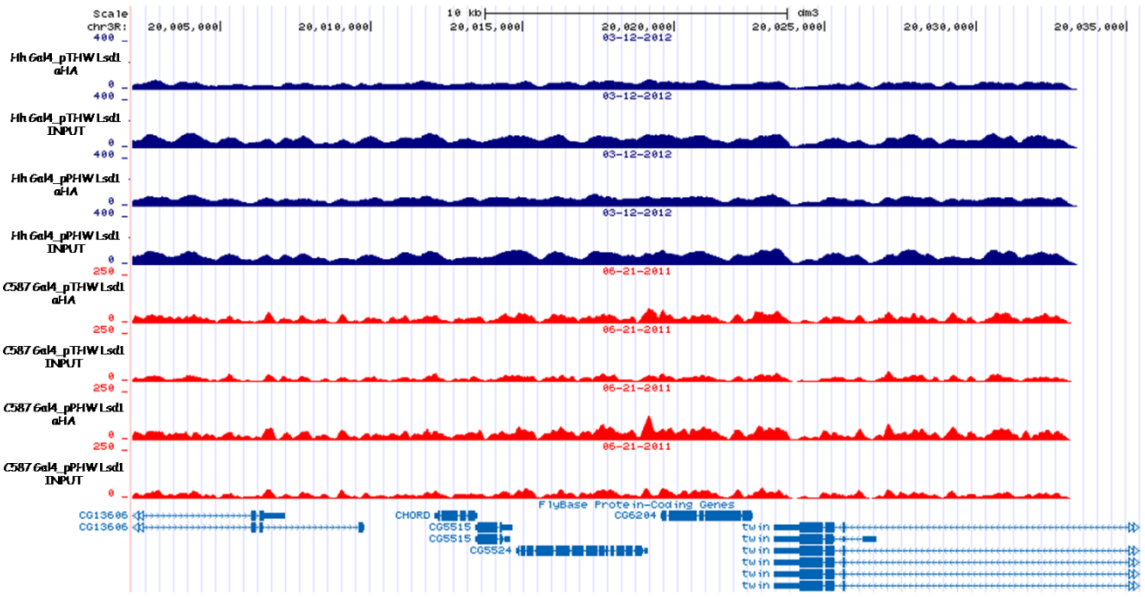

Figure 123. Screenshot of Lsd1 binding sites on coordinates chr3R:20,002,093-20,035,427

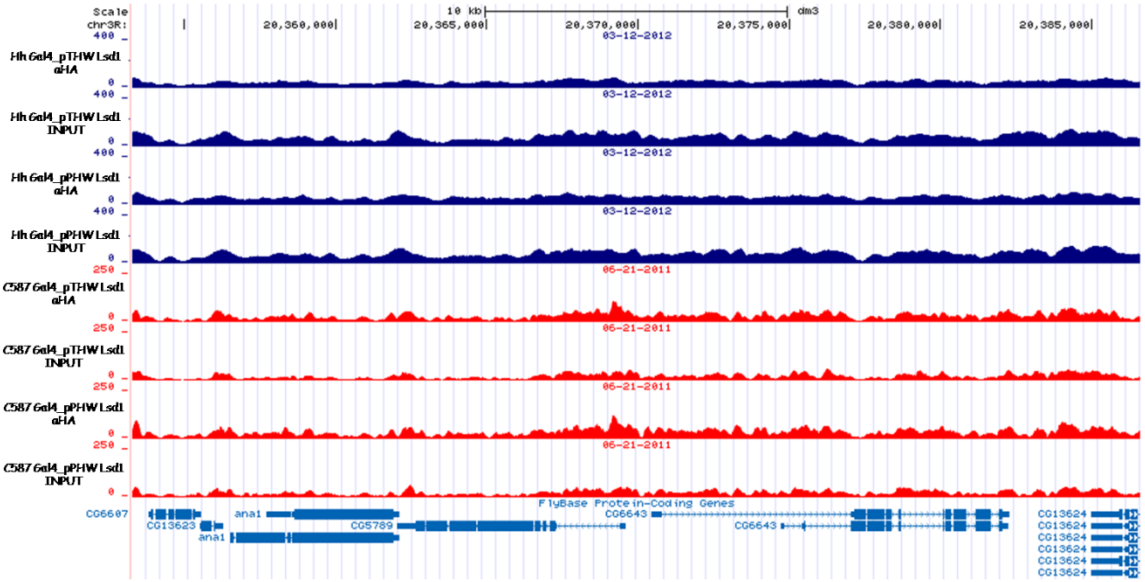

Gene	Locus	WT_EC	Lsd1 KD_EC	log2(fold_change)	significant
CG5789	chr3R:20356399-20369629	8.4419	30.7935	1.86699	yes

Figure 124. Screenshot of Lsd1 binding sites on coordinates chr3R:20,353,277-20,386,611 and RNA seq data for genes that exhibit significant difference between WT escort cells and Lsd1 knockdown escort cells

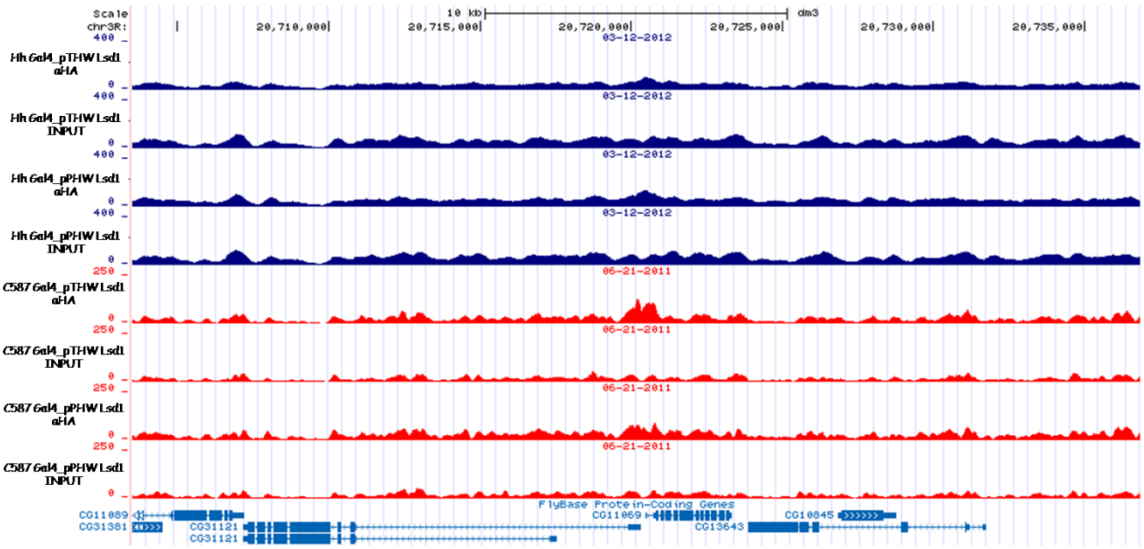

Figure 125. Screenshot of Lsd1 binding sites on coordinates chr3R:20,703,499-20,736,833

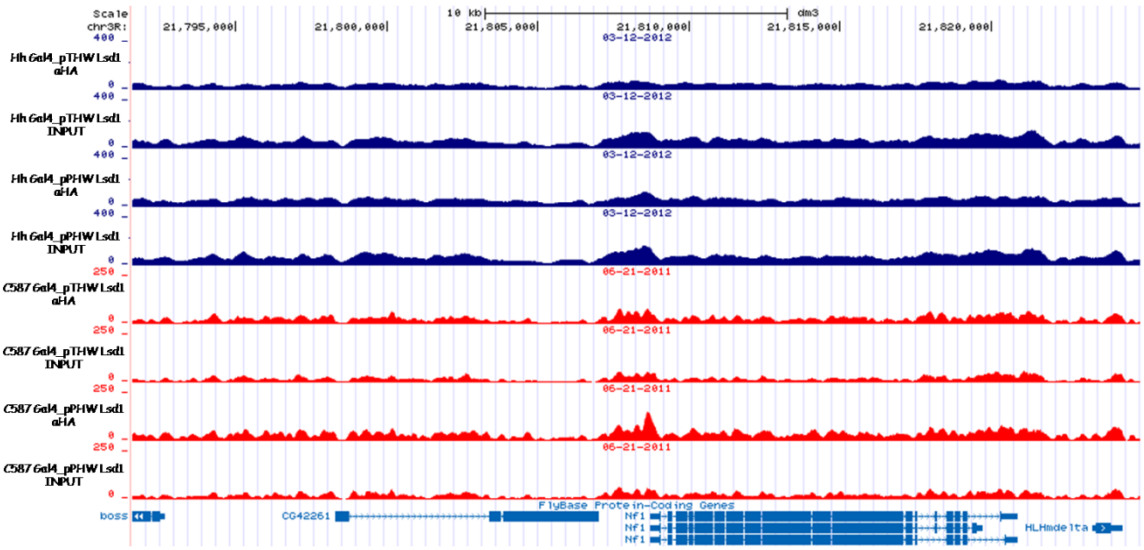

Figure 126. Screenshot of Lsd1 binding sites on coordinates chr3R:21,791,589-21,824,923

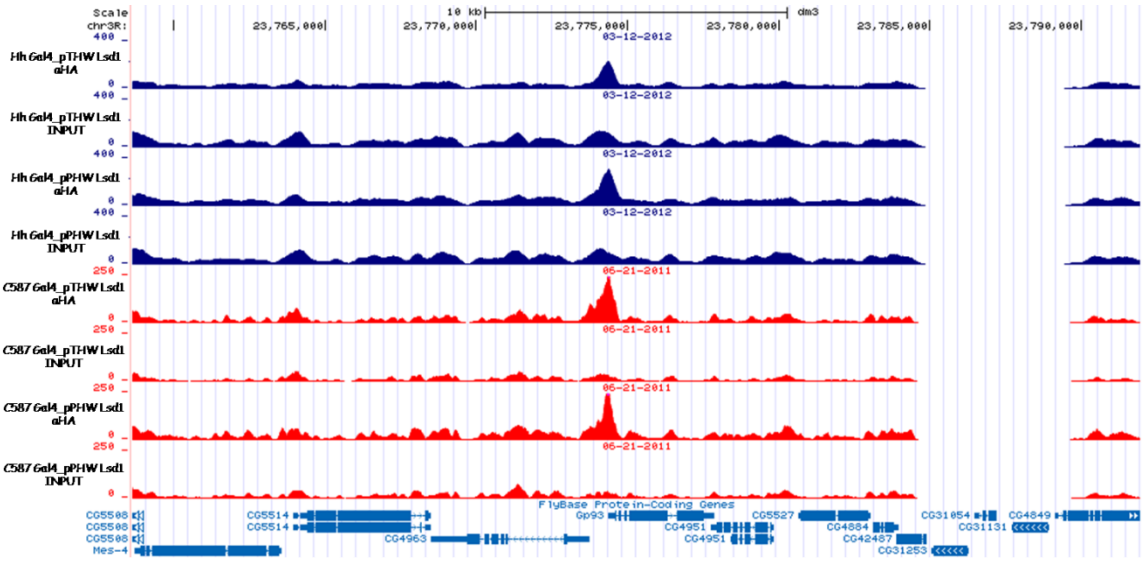

Figure 127. Screenshot of Lsd1 binding sites on coordinates chr3R:23,758,626-23,791,960

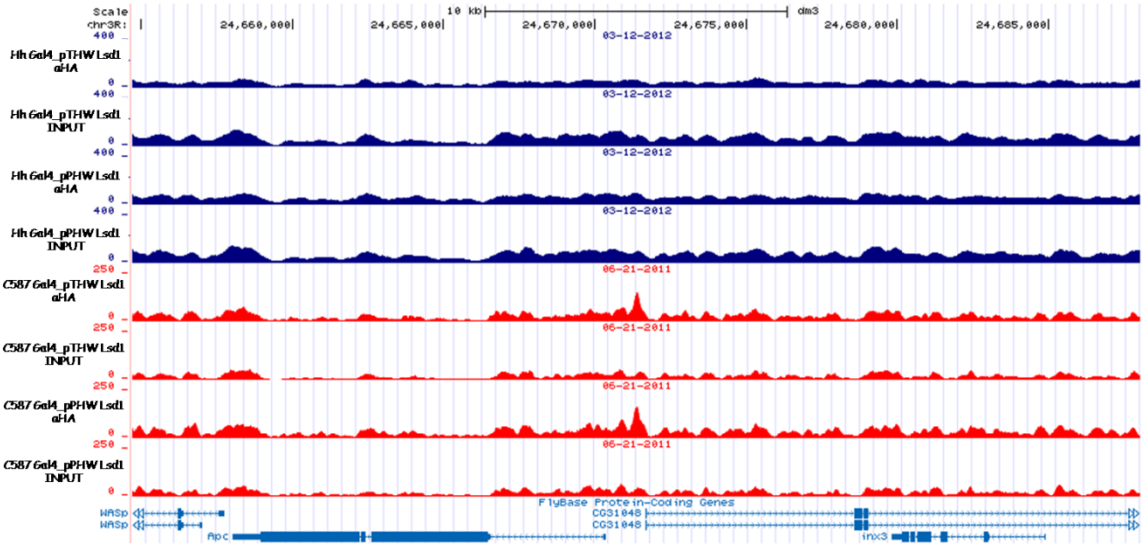

Figure 128. Screenshot of Lsd1 binding sites on coordinates chr3R:24,654,702-24,688,036

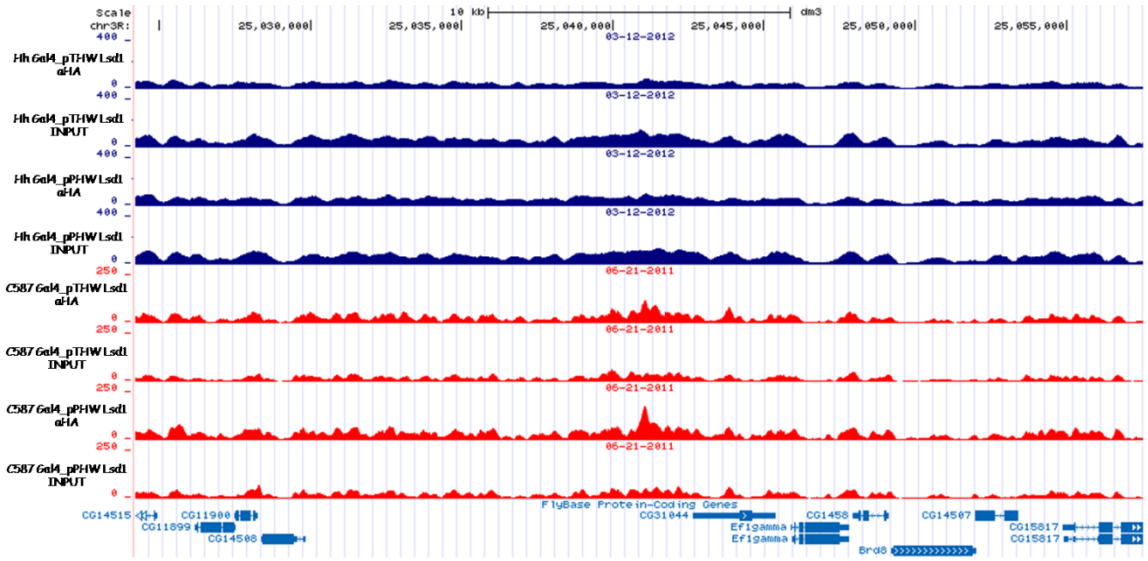

Figure 129. Screenshot of Lsd1 binding sites on coordinates chr3R:25,024,208-25,057,542

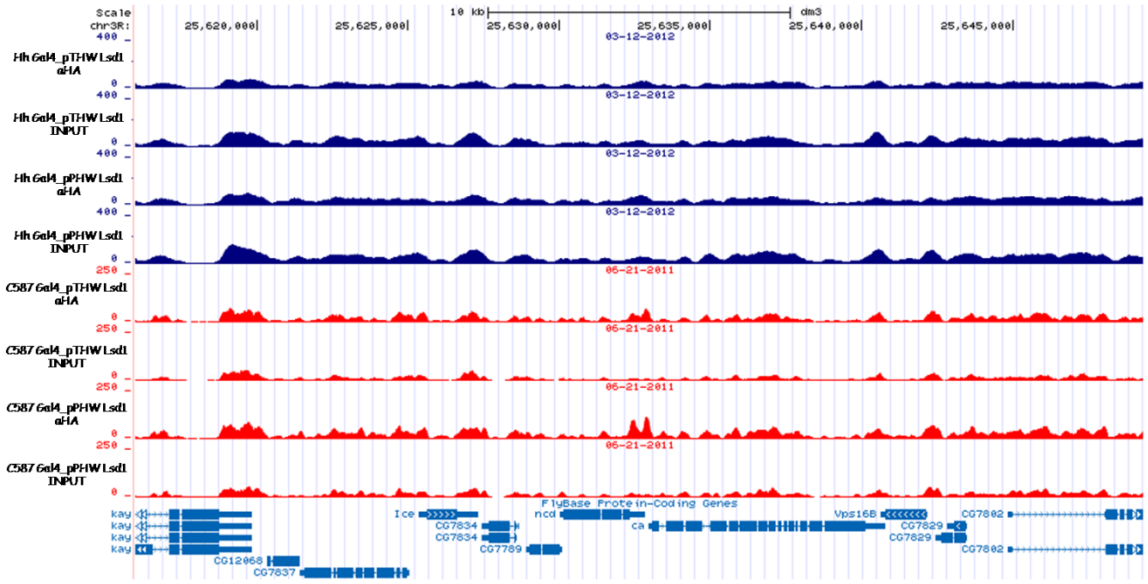

Figure 130. Screenshot of Lsd1 binding sites on coordinates chr3R:25,615,984-25,649,318

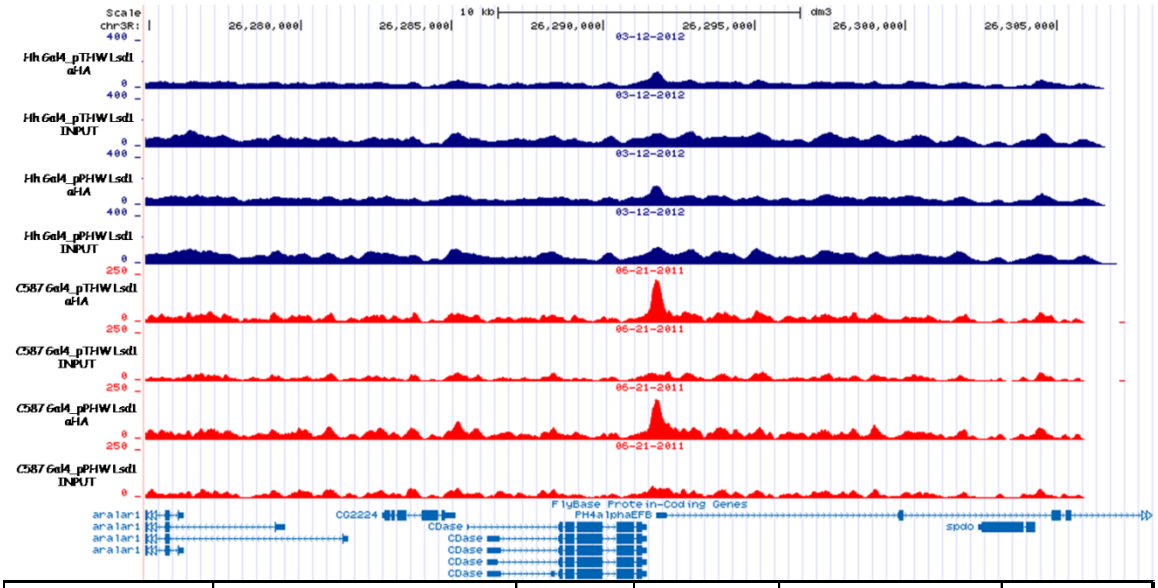

gene	locus	WT_EC	Lsd1 KD_EC	log2(fold_change)	significant
CDase	chr3R:26285510-26291458	4.9416	14.8028	1.58282	yes

Figure 131. Screenshot of Lsd1 binding sites on coordinates chr3R:26,274,861-26,308,195 and RNA seq data for genes that exhibit significant difference between WT escort cells and Lsd1 knockdown escort cells

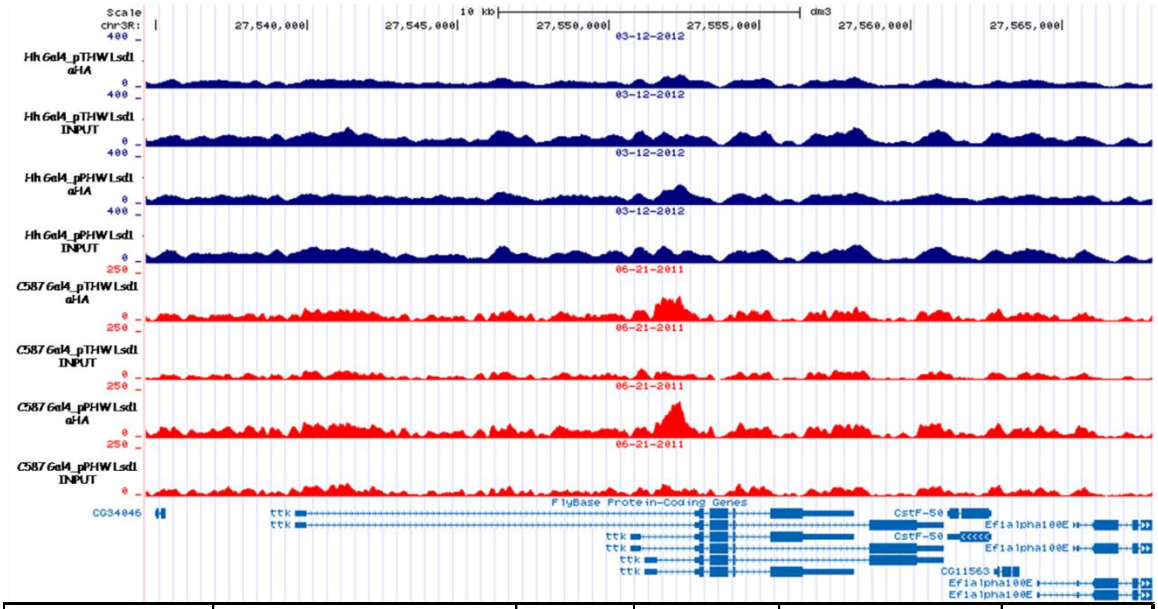

gene	locus	WT_EC	Lsd1 KD_EC	log2(fold_change)	significant
ttk	chr3R:27539590-27561114	300.53	186.229	-0.690431	yes

Figure 132. Screenshot of Lsd1 binding sites on coordinates chr3R:27,534,669-27,568,003 and RNA seq data for genes that exhibit significant difference between WT escort cells and Lsd1 knockdown escort cells

Binding Sites of Lsd1 on Chromosome 4

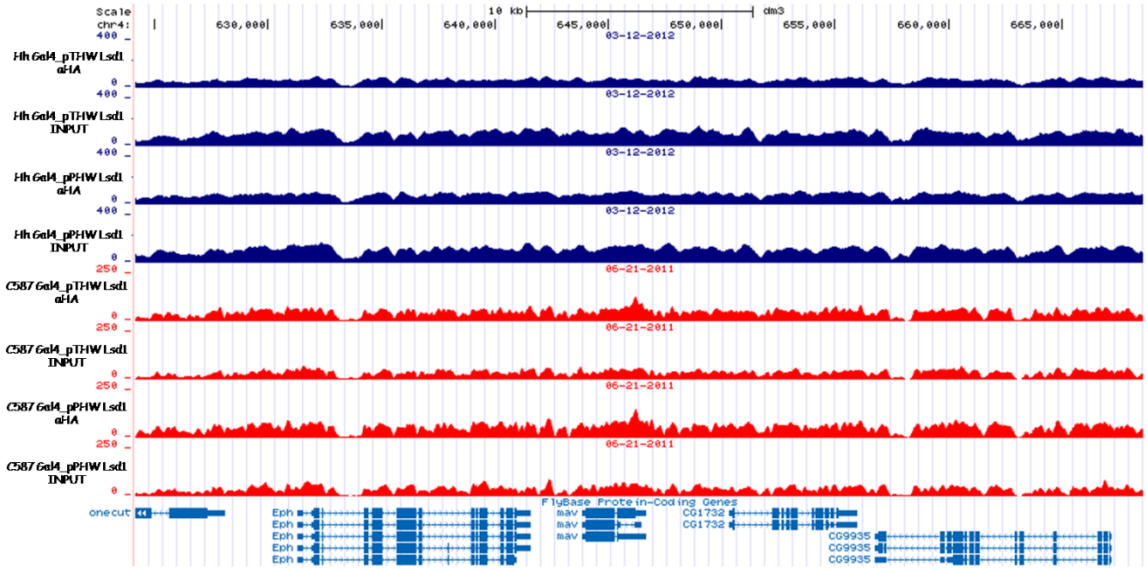

Figure 133. Screenshot of Lsd1 binding sites on coordinates chr4:624,141-668,585

BIBLIOGRAPHY

REFERENCES

Ables ET, Drummond-Barbosa D. 2010. The steroid hormone ecdysone functions with intrinsic chromatin remodeling factors to control female germline stem cells in Drosophila. *Cell Stem Cell* **7**: 581-592.

Adamo A, Sese B, Boue S, Castano J, Paramonov I, Barrero MJ, Izpisua Belmonte JC. 2011. LSD1 regulates the balance between self-renewal and differentiation in human embryonic stem cells. *Nat Cell Biol* **13**: 652-659.

Ades SE, Sauer RT. 1994. Differential DNA-binding specificity of the engrailed homeodomain: the role of residue 50. *Biochemistry* **33**: 9187-9194.

Akiyama T, Kamimura K, Firkus C, Takeo S, Shimmi O, Nakato H. 2008. Dally regulates Dpp morphogen gradient formation by stabilizing Dpp on the cell surface. *Dev Biol* **313**: 408-419.

Amente S, Bertoni A, Morano A, Lania L, Avvedimento EV, Majello B. 2010. LSD1-mediated demethylation of histone H3 lysine 4 triggers Myc-induced transcription. *Oncogene* **29**: 3691-3702.

Asaoka M, Lin H. 2004. Germline stem cells in the Drosophila ovary descend from pole cells in the anterior region of the embryonic gonad. *Development* **131**: 5079-5089.

Bednar J, Horowitz RA, Grigoryev SA, Carruthers LM, Hansen JC, Koster AJ, Woodcock CL. 1998. Nucleosomes, linker DNA, and linker histone form a unique structural motif that directs the higher-order folding and compaction of chromatin. *Proc Natl Acad Sci U S A* **95**: 14173-14178.

Binda C, Mattevi A, Edmondson DE. 2002. Structure-function relationships in flavoenzyme-dependent amine oxidations: a comparison of polyamine oxidase and monoamine oxidase. *J Biol Chem* **277**: 23973-23976.

Bolivar J, Pearson J, Lopez-Onieva L, Gonzalez-Reyes A. 2006. Genetic dissection of a stem cell niche: the case of the Drosophila ovary. *Dev Dyn* **235**: 2969-2979.

Bonnet D, Dick JE. 1997. Human acute myeloid leukemia is organized as a hierarchy that originates from a primitive hematopoietic cell. *Nat Med* **3**: 730-737.

Bose SK, Bullard RS, Donald CD. 2008. Oncogenic role of engrailed-2 (en-2) in prostate cancer cell growth and survival. *Translational oncogenomics* **3**: 37-43.

Brand AH, Perrimon N. 1993. Targeted gene expression as a means of altering cell fates and generating dominant phenotypes. *Development* **118**: 401-415.

Brennecke J, Malone CD, Aravin AA, Sachidanandam R, Stark A, Hannon GJ. 2008. An epigenetic role for maternally inherited piRNAs in transposon silencing. *Science* **322**: 1387-1392.

Bustin M, Catez F, Lim JH. 2005. The dynamics of histone H1 function in chromatin. *Mol Cell* **17**: 617-620.

Buszczak M, Paterno S, Lighthouse D, Bachman J, Planck J, Owen S, Skora AD, Nystul TG, Ohlstein B, Allen A et al. 2007. The carnegie protein trap library: a versatile tool for Drosophila developmental studies. *Genetics* **175**: 1505-1531.

Cao R, Wang L, Wang H, Xia L, Erdjument-Bromage H, Tempst P, Jones RS, Zhang Y. 2002. Role of histone H3 lysine 27 methylation in Polycomb-group silencing. *Science* **298**: 1039-1043.

Casanueva MO, Ferguson EL. 2004. Germline stem cell number in the Drosophila ovary is regulated by redundant mechanisms that control Dpp signaling. *Development* **131**: 1881-1890.

Chan CS, Rastelli L, Pirrotta V. 1994. A Polycomb response element in the Ubx gene that determines an epigenetically inherited state of repression. *EMBO J* **13**: 2553-2564.

Chanut F, Heberlein U. 1997. Role of decapentaplegic in initiation and progression of the morphogenetic furrow in the developing Drosophila retina. *Development* **124**: 559-567.

Chen D, McKearin D. 2003a. Dpp signaling silences bam transcription directly to establish asymmetric divisions of germline stem cells. *Curr Biol* **13**: 1786-1791.

Chen D, McKearin DM. 2003b. A discrete transcriptional silencer in the bam gene determines asymmetric division of the Drosophila germline stem cell. *Development* **130**: 1159-1170.

Chen J, Godt D, Gunsalus K, Kiss I, Goldberg M, Laski FA. 2001. Cofilin/ADF is required for cell motility during Drosophila ovary development and oogenesis. *Nat Cell Biol* **3**: 204-209.

Chen S, Birve A, Rasmuson-Lestander A. 2008. In vivo analysis of Drosophila SU(Z)12 function. *Molecular genetics and genomics : MGG* **279**: 159-170.

Chen S, Rasmuson-Lestander A. 2009. Regulation of the Drosophila engrailed gene by Polycomb repressor complex 2. *Mech Dev* **126**: 443-448.

Chen Y, Yang Y, Wang F, Wan K, Yamane K, Zhang Y, Lei M. 2006. Crystal structure of human histone lysine-specific demethylase 1 (LSD1). *Proc Natl Acad Sci U S A* **103**: 13956-13961.

Chosed R, Dent SY. 2007. A two-way street: LSD1 regulates chromatin boundary formation in S. pombe and Drosophila. *Mol Cell* **26**: 160-162.

Clayton AL, Hazzalin CA, Mahadevan LC. 2006. Enhanced histone acetylation and transcription: a dynamic perspective. *Mol Cell* **23**: 289-296.

Clough E, Moon W, Wang S, Smith K, Hazelrigg T. 2007. Histone methylation is required for oogenesis in Drosophila. *Development* **134**: 157-165.

Cooper MT, Bray SJ. 1999. Frizzled regulation of Notch signalling polarizes cell fate in the Drosophila eye. *Nature* **397**: 526-530.

Cox DN, Chao A, Baker J, Chang L, Qiao D, Lin H. 1998. A novel class of evolutionarily conserved genes defined by piwi are essential for stem cell self-renewal. *Genes Dev* **12**: 3715-3727.

Cox DN, Chao A, Lin H. 2000. piwi encodes a nucleoplasmic factor whose activity modulates the number and division rate of germline stem cells. *Development* **127**: 503-514.

Czermin B, Melfi R, McCabe D, Seitz V, Imhof A, Pirrotta V. 2002. Drosophila enhancer of Zeste/ESC complexes have a histone H3 methyltransferase activity that marks chromosomal Polycomb sites. *Cell* **111**: 185-196.

Davis PK, Brackmann RK. 2003. Chromatin remodeling and cancer. *Cancer biology & therapy* **2**: 22-29.

de Celis JF, Bray S. 1997. Feed-back mechanisms affecting Notch activation at the dorsoventral boundary in the Drosophila wing. *Development* **124**: 3241-3251.

de Cuevas M, Spradling AC. 1998. Morphogenesis of the Drosophila fusome and its implications for oocyte specification. *Development* **125**: 2781-2789.

De Koning L, Corpet A, Haber JE, Almouzni G. 2007. Histone chaperones: an escort network regulating histone traffic. *Nat Struct Mol Biol* **14**: 997-1007.

Decotto E, Spradling AC. 2005. The Drosophila ovarian and testis stem cell niches: similar somatic stem cells and signals. *Dev Cell* **9**: 501-510.

Deuring R, Fanti L, Armstrong JA, Sarte M, Papoulas O, Prestel M, Daubresse G, Verardo M, Moseley SL, Berloco M et al. 2000. The ISWI chromatin-remodeling protein is required for gene expression and the maintenance of higher order chromatin structure in vivo. *Mol Cell* **5**: 355-365.

DeVido SK, Kwon D, Brown JL, Kassis JA. 2008. The role of Polycomb-group response elements in regulation of engrailed transcription in Drosophila. *Development* **135**: 669-676.

Di Stefano L, Ji JY, Moon NS, Herr A, Dyson N. 2007. Mutation of Drosophila Lsd1 disrupts H3-K4 methylation, resulting in tissue-specific defects during development. *Curr Biol* **17**: 808-812.

Eimer S, Lakowski B, Donhauser R, Baumeister R. 2002. Loss of spr-5 bypasses the requirement for the C.elegans presenilin sel-12 by derepressing hop-1. *EMBO J* **21**: 5787-5796.

Eliazer S, Shalaby NA, Buszczak M. 2011. Loss of lysine-specific demethylase 1 nonautonomously causes stem cell tumors in the Drosophila ovary. *Proc Natl Acad Sci U S A* **108**: 7064-7069.

Emerald BS, Roy JK. 1998. Organising activities of engrailed, hedgehog, wingless and decapentaplegic in the genital discs of Drosophila melanogaster. *Dev Genes Evol* **208**: 504-516.

Feinberg AP, Ohlsson R, Henikoff S. 2006. The epigenetic progenitor origin of human cancer. *Nat Rev Genet* **7**: 21-33.

Feinberg AP, Tycko B. 2004. The history of cancer epigenetics. *Nature reviews Cancer* **4**: 143-153.

Forbes AJ, Lin H, Ingham PW, Spradling AC. 1996a. hedgehog is required for the proliferation and specification of ovarian somatic cells prior to egg chamber formation in Drosophila. *Development* **122**: 1125-1135.

Forbes AJ, Spradling AC, Ingham PW, Lin H. 1996b. The role of segment polarity genes during early oogenesis in Drosophila. *Development* **122**: 3283-3294.

Foster CT, Dovey OM, Lezina L, Luo JL, Gant TW, Barlev N, Bradley A, Cowley SM. 2010. Lysine-specific demethylase 1 regulates the embryonic transcriptome and CoREST stability. *Mol Cell Biol* **30**: 4851-4863.

Fraaije MW, Mattevi A. 2000. Flavoenzymes: diverse catalysts with recurrent features. *Trends Biochem Sci* **25**: 126-132.

Fraaije MW, Van Berkel WJ, Benen JA, Visser J, Mattevi A. 1998. A novel oxidoreductase family sharing a conserved FAD-binding domain. *Trends Biochem Sci* **23**: 206-207.

Gayther SA, Batley SJ, Linger L, Bannister A, Thorpe K, Chin SF, Daigo Y, Russell P, Wilson A, Sowter HM et al. 2000. Mutations truncating the EP300 acetylase in human cancers. *Nat Genet* **24**: 300-303.

Gilboa L, Lehmann R. 2004. Repression of primordial germ cell differentiation parallels germ line stem cell maintenance. *Curr Biol* **14**: 981-986.

-. 2006. Soma-germline interactions coordinate homeostasis and growth in the Drosophila gonad. *Nature* **443**: 97-100.

Godt D, Laski FA. 1995. Mechanisms of cell rearrangement and cell recruitment in Drosophila ovary morphogenesis and the requirement of bric a brac. *Development* **121**: 173-187.

Guo Z, Wang Z. 2009. The glypican Dally is required in the niche for the maintenance of germline stem cells and short-range BMP signaling in the Drosophila ovary. *Development* **136**: 3627-3635.

Hakimi MA, Bochar DA, Chenoweth J, Lane WS, Mandel G, Shiekhattar R. 2002. A core-BRAF35 complex containing histone deacetylase mediates repression of neuronal-specific genes. *Proc Natl Acad Sci U S A* **99**: 7420-7425.

Hama C, Ali Z, Kornberg TB. 1990. Region-specific recombination and expression are directed by portions of the Drosophila engrailed promoter. *Genes Dev* **4**: 1079-1093.

Han M, Grunstein M. 1988. Nucleosome loss activates yeast downstream promoters in vivo. *Cell* **55**: 1137-1145.

Harris RE, Pargett M, Sutcliffe C, Umulis D, Ashe HL. 2011. Brat promotes stem cell differentiation via control of a bistable switch that restricts BMP signaling. *Dev Cell* **20**: 72-83.

Hayami S, Kelly JD, Cho HS, Yoshimatsu M, Unoki M, Tsunoda T, Field HI, Neal DE, Yamaue H, Ponder BA et al. 2011. Overexpression of LSD1 contributes to human carcinogenesis through chromatin regulation in various cancers. *Int J Cancer* **128**: 574-586.

Hayashi Y, Kobayashi S, Nakato H. 2009. Drosophila glypicans regulate the germline stem cell niche. *J Cell Biol* **187**: 473-480.

Hepker J, Blackman RK, Holmgren R. 1999. Cubitus interruptus is necessary but not sufficient for direct activation of a wing-specific decapentaplegic enhancer. *Development* **126**: 3669-3677.

Hodin J, Riddiford LM. 1998. The ecdysone receptor and ultraspiracle regulate the timing and progression of ovarian morphogenesis during Drosophila metamorphosis. *Dev Genes Evol* **208**: 304-317.

Hsu HJ, Drummond-Barbosa D. 2009. Insulin levels control female germline stem cell maintenance via the niche in Drosophila. *Proc Natl Acad Sci U S A* **106**: 1117-1121.

-. 2011. Insulin signals control the competence of the Drosophila female germline stem cell niche to respond to Notch ligands. *Dev Biol* **350**: 290-300.

Hu X, Li X, Valverde K, Fu X, Noguchi C, Qiu Y, Huang S. 2009. LSD1-mediated epigenetic modification is required for TAL1 function and hematopoiesis. *Proc Natl Acad Sci U S A* **106**: 10141-10146.

Hudson JB, Podos SD, Keith K, Simpson SL, Ferguson EL. 1998. The Drosophila Medea gene is required downstream of dpp and encodes a functional homolog of human Smad4. *Development* **125**: 1407-1420.

Humphrey GW, Wang Y, Russanova VR, Hirai T, Qin J, Nakatani Y, Howard BH. 2001. Stable histone deacetylase complexes distinguished by the presence of SANT domain proteins CoREST/kiaa0071 and Mta-L1. *J Biol Chem* **276**: 6817-6824.

Iovino N, Pane A, Gaul U. 2009. miR-184 has multiple roles in Drosophila female germline development. *Dev Cell* **17**: 123-133.

Jenuwein T, Allis CD. 2001. Translating the histone code. *Science* **293**: 1074-1080.

Jin Z, Kirilly D, Weng C, Kawase E, Song X, Smith S, Schwartz J, Xie T. 2008. Differentiation-defective stem cells outcompete normal stem cells for niche occupancy in the Drosophila ovary. *Cell Stem Cell* **2**: 39-49.

Kai T, Spradling A. 2003. An empty Drosophila stem cell niche reactivates the proliferation of ectopic cells. *Proc Natl Acad Sci U S A* **100**: 4633-4638.

Katz DJ, Edwards TM, Reinke V, Kelly WG. 2009. A C. elegans LSD1 demethylase contributes to germline immortality by reprogramming epigenetic memory. *Cell* **137**: 308-320.

Kennison JA. 1995. The Polycomb and trithorax group proteins of Drosophila: trans-regulators of homeotic gene function. *Annual review of genetics* **29**: 289-303.

Kiger AA, Jones DL, Schulz C, Rogers MB, Fuller MT. 2001. Stem cell self-renewal specified by JAK-STAT activation in response to a support cell cue. *Science* **294**: 2542-2545.

Kimura H, Cook PR. 2001. Kinetics of core histones in living human cells: little exchange of H3 and H4 and some rapid exchange of H2B. *J Cell Biol* **153**: 1341-1353.

King FJ, Lin H. 1999. Somatic signaling mediated by fs(1)Yb is essential for germline stem cell maintenance during Drosophila oogenesis. *Development* **126**: 1833-1844.

King FJ, Szakmary A, Cox DN, Lin H. 2001. Yb modulates the divisions of both germline and somatic stem cells through piwi- and hh-mediated mechanisms in the Drosophila ovary. *Mol Cell* **7**: 497-508.

King RC, Aggarwal SK, Aggarwal U. 1968. The development of the female Drosophila reproductive system. *J Morphol* **124**: 143-166.

Kirilly D, Xie T. 2007. The Drosophila ovary: an active stem cell community. *Cell Res* **17**: 15-25.

Kirkpatrick CA, Selleck SB. 2007. Heparan sulfate proteoglycans at a glance. *J Cell Sci* **120**: 1829-1832.

Knezetic JA, Luse DS. 1986. The presence of nucleosomes on a DNA template prevents initiation by RNA polymerase II in vitro. *Cell* **45**: 95-104.

Koch CM, Andrews RM, Flicek P, Dillon SC, Karaoz U, Clelland GK, Wilcox S, Beare DM, Fowler JC, Couttet P et al. 2007. The landscape of histone modifications across 1% of the human genome in five human cell lines. *Genome research* **17**: 691-707.

Konig A, Yatsenko AS, Weiss M, Shcherbata HR. 2011. Ecdysteroids affect Drosophila ovarian stem cell niche formation and early germline differentiation. *EMBO J* **30**: 1549-1562.

Kornberg RD. 1974. Chromatin structure: a repeating unit of histones and DNA. *Science* **184**: 868-871.

-. 1977. Structure of chromatin. *Annu Rev Biochem* **46**: 931-954.

Kornberg RD, Thomas JO. 1974. Chromatin structure; oligomers of the histones. *Science* **184**: 865-868.
Kouzarides T. 2002. Histone methylation in transcriptional control. *Current opinion in genetics & development* **12**: 198-209.
-. 2007. Chromatin modifications and their function. *Cell* **128**: 693-705.
Li B, Carey M, Workman JL. 2007. The role of chromatin during transcription. *Cell* **128**: 707-719.
Li Y, Minor NT, Park JK, McKearin DM, Maines JZ. 2009. Bam and Bgcn antagonize Nanos-dependent germ-line stem cell maintenance. *Proc Natl Acad Sci U S A* **106**: 9304-9309.
Lim S, Janzer A, Becker A, Zimmer A, Schule R, Buettner R, Kirfel J. 2010. Lysine-specific demethylase 1 (LSD1) is highly expressed in ER-negative breast cancers and a biomarker predicting aggressive biology. *Carcinogenesis* **31**: 512-520.
Lin H, Spradling AC. 1995. Fusome asymmetry and oocyte determination in Drosophila. *Dev Genet* **16**: 6-12.
Lin H, Yin H. 2008. A novel epigenetic mechanism in Drosophila somatic cells mediated by Piwi and piRNAs. *Cold Spring Harb Symp Quant Biol* **73**: 273-281.
Lin H, Yue L, Spradling AC. 1994. The Drosophila fusome, a germline-specific organelle, contains membrane skeletal proteins and functions in cyst formation. *Development* **120**: 947-956.
Liu M, Lim TM, Cai Y. 2010. The Drosophila female germline stem cell lineage acts to spatially restrict DPP function within the niche. *Sci Signal* **3**: ra57.
Lopez-Onieva L, Fernandez-Minan A, Gonzalez-Reyes A. 2008. Jak/Stat signalling in niche support cells regulates dpp transcription to control germline stem cell maintenance in the Drosophila ovary. *Development* **135**: 533-540.
Lorch Y, LaPointe JW, Kornberg RD. 1987. Nucleosomes inhibit the initiation of transcription but allow chain elongation with the displacement of histones. *Cell* **49**: 203-210.
Luger K, Mader AW, Richmond RK, Sargent DF, Richmond TJ. 1997. Crystal structure of the nucleosome core particle at 2.8 A resolution. *Nature* **389**: 251-260.
Lusser A, Kadonaga JT. 2003. Chromatin remodeling by ATP-dependent molecular machines. *BioEssays : news and reviews in molecular, cellular and developmental biology* **25**: 1192-1200.
Martens JA, Winston F. 2003. Recent advances in understanding chromatin remodeling by Swi/Snf complexes. *Current opinion in genetics & development* **13**: 136-142.
McKearin D, Ohlstein B. 1995. A role for the Drosophila bag-of-marbles protein in the differentiation of cystoblasts from germline stem cells. *Development* **121**: 2937-2947.
McKearin DM, Spradling AC. 1990. bag-of-marbles: a Drosophila gene required to initiate both male and female gametogenesis. *Genes Dev* **4**: 2242-2251.
Metzger E, Wissmann M, Yin N, Muller JM, Schneider R, Peters AH, Gunther T, Buettner R, Schule R. 2005. LSD1 demethylates repressive histone marks to promote androgen-receptor-dependent transcription. *Nature* **437**: 436-439.
Morgan R, Boxall A, Bhatt A, Bailey M, Hindley R, Langley S, Whitaker HC, Neal DE, Ismail M, Whitaker H et al. 2011. Engrailed-2 (EN2): a tumor specific urinary

biomarker for the early diagnosis of prostate cancer. *Clin Cancer Res* **17**: 1090-1098.

Morris LX, Spradling AC. 2011. Long-term live imaging provides new insight into stem cell regulation and germline-soma coordination in the Drosophila ovary. *Development* **138**: 2207-2215.

Nakato H, Futch TA, Selleck SB. 1995. The division abnormally delayed (dally) gene: a putative integral membrane proteoglycan required for cell division patterning during postembryonic development of the nervous system in Drosophila. *Development* **121**: 3687-3702.

O'Brien CA, Kreso A, Jamieson CH. 2010. Cancer stem cells and self-renewal. *Clin Cancer Res* **16**: 3113-3120.

Ohlstein B, Kai T, Decotto E, Spradling A. 2004. The stem cell niche: theme and variations. *Curr Opin Cell Biol* **16**: 693-699.

Ohlstein B, Lavoie CA, Vef O, Gateff E, McKearin DM. 2000. The Drosophila cystoblast differentiation factor, benign gonial cell neoplasm, is related to DExH-box proteins and interacts genetically with bag-of-marbles. *Genetics* **155**: 1809-1819.

Ohlstein B, McKearin D. 1997. Ectopic expression of the Drosophila Bam protein eliminates oogenic germline stem cells. *Development* **124**: 3651-3662.

Pan L, Chen S, Weng C, Call G, Zhu D, Tang H, Zhang N, Xie T. 2007. Stem cell aging is controlled both intrinsically and extrinsically in the Drosophila ovary. *Cell Stem Cell* **1**: 458-469.

Peterson CL, Laniel MA. 2004. Histones and histone modifications. *Curr Biol* **14**: R546-551.

Peterson CL, Tamkun JW. 1995. The SWI-SNF complex: a chromatin remodeling machine? *Trends Biochem Sci* **20**: 143-146.

Petrij F, Giles RH, Dauwerse HG, Saris JJ, Hennekam RC, Masuno M, Tommerup N, van Ommen GJ, Goodman RH, Peters DJ et al. 1995. Rubinstein-Taybi syndrome caused by mutations in the transcriptional co-activator CBP. *Nature* **376**: 348-351.

Podos SD, Hanson KK, Wang YC, Ferguson EL. 2001. The DSmurf ubiquitin-protein ligase restricts BMP signaling spatially and temporally during Drosophila embryogenesis. *Dev Cell* **1**: 567-578.

Rangan P, Malone CD, Navarro C, Newbold SP, Hayes PS, Sachidanandam R, Hannon GJ, Lehmann R. 2011. piRNA production requires heterochromatin formation in Drosophila. *Curr Biol* **21**: 1373-1379.

Rastelli L, Chan CS, Pirrotta V. 1993. Related chromosome binding sites for zeste, suppressors of zeste and Polycomb group proteins in Drosophila and their dependence on Enhancer of zeste function. *EMBO J* **12**: 1513-1522.

Reik W. 2007. Stability and flexibility of epigenetic gene regulation in mammalian development. *Nature* **447**: 425-432.

Reinke H, Horz W. 2003. Histones are first hyperacetylated and then lose contact with the activated PHO5 promoter. *Mol Cell* **11**: 1599-1607.

Reuter G, Spierer P. 1992. Position effect variegation and chromatin proteins. *BioEssays : news and reviews in molecular, cellular and developmental biology* **14**: 605-612.

Rhiner C, Diaz B, Portela M, Poyatos JF, Fernandez-Ruiz I, Lopez-Gay JM, Gerlitz O, Moreno E. 2009. Persistent competition among stem cells and their daughters in the Drosophila ovary germline niche. *Development* **136**: 995-1006.

Ringrose L, Rehmsmeier M, Dura JM, Paro R. 2003. Genome-wide prediction of Polycomb/Trithorax response elements in Drosophila melanogaster. *Dev Cell* **5**: 759-771.

Rojas-Rios P, Guerrero I, Gonzalez-Reyes A. 2012. Cytoneme-mediated delivery of hedgehog regulates the expression of bone morphogenetic proteins to maintain germline stem cells in Drosophila. *PLoS biology* **10**: e1001298.

Rudolph T, Yonezawa M, Lein S, Heidrich K, Kubicek S, Schafer C, Phalke S, Walther M, Schmidt A, Jenuwein T et al. 2007. Heterochromatin formation in Drosophila is initiated through active removal of H3K4 methylation by the LSD1 homolog SU(VAR)3-3. *Mol Cell* **26**: 103-115.

Ruthenburg AJ, Li H, Patel DJ, Allis CD. 2007. Multivalent engagement of chromatin modifications by linked binding modules. *Nature reviews Molecular cell biology* **8**: 983-994.

Sahut-Barnola I, Godt D, Laski FA, Couderc JL. 1995. Drosophila ovary morphogenesis: analysis of terminal filament formation and identification of a gene required for this process. *Dev Biol* **170**: 127-135.

Satijn DP, Gunster MJ, van der Vlag J, Hamer KM, Schul W, Alkema MJ, Saurin AJ, Freemont PS, van Driel R, Otte AP. 1997. RING1 is associated with the polycomb group protein complex and acts as a transcriptional repressor. *Mol Cell Biol* **17**: 4105-4113.

Schofield R. 1978. The relationship between the spleen colony-forming cell and the haemopoietic stem cell. *Blood Cells* **4**: 7-25.

Schulte JH, Lim S, Schramm A, Friedrichs N, Koster J, Versteeg R, Ora I, Pajtler K, Klein-Hitpass L, Kuhfittig-Kulle S et al. 2009. Lysine-specific demethylase 1 is strongly expressed in poorly differentiated neuroblastoma: implications for therapy. *Cancer Res* **69**: 2065-2071.

Schulz C, Wood CG, Jones DL, Tazuke SI, Fuller MT. 2002. Signaling from germ cells mediated by the rhomboid homolog stet organizes encapsulation by somatic support cells. *Development* **129**: 4523-4534.

Sengupta AK, Kuhrs A, Muller J. 2004. General transcriptional silencing by a Polycomb response element in Drosophila. *Development* **131**: 1959-1965.

Shao Z, Raible F, Mollaaghababa R, Guyon JR, Wu CT, Bender W, Kingston RE. 1999. Stabilization of chromatin structure by PRC1, a Polycomb complex. *Cell* **98**: 37-46.

Shi Y, Lan F, Matson C, Mulligan P, Whetstine JR, Cole PA, Casero RA. 2004. Histone demethylation mediated by the nuclear amine oxidase homolog LSD1. *Cell* **119**: 941-953.

Shi Y, Sawada J, Sui G, Affar el B, Whetstine JR, Lan F, Ogawa H, Luke MP, Nakatani Y. 2003. Coordinated histone modifications mediated by a CtBP co-repressor complex. *Nature* **422**: 735-738.

Shi YJ, Matson C, Lan F, Iwase S, Baba T, Shi Y. 2005. Regulation of LSD1 histone demethylase activity by its associated factors. *Mol Cell* **19**: 857-864.

Shogren-Knaak M, Ishii H, Sun JM, Pazin MJ, Davie JR, Peterson CL. 2006. Histone H4-K16 acetylation controls chromatin structure and protein interactions. *Science* **311**: 844-847.

Smulders-Srinivasan TK, Szakmary A, Lin H. 2010. A Drosophila chromatin factor interacts with the Piwi-interacting RNA mechanism in niche cells to regulate germline stem cell self-renewal. *Genetics* **186**: 573-583.

Song X, Call GB, Kirilly D, Xie T. 2007. Notch signaling controls germline stem cell niche formation in the Drosophila ovary. *Development* **134**: 1071-1080.

Song X, Wong MD, Kawase E, Xi R, Ding BC, McCarthy JJ, Xie T. 2004. Bmp signals from niche cells directly repress transcription of a differentiation-promoting gene, bag of marbles, in germline stem cells in the Drosophila ovary. *Development* **131**: 1353-1364.

Song X, Xie T. 2002. DE-cadherin-mediated cell adhesion is essential for maintaining somatic stem cells in the Drosophila ovary. *Proc Natl Acad Sci U S A* **99**: 14813-14818.

Starz-Gaiano M, Lehmann R. 2001. Moving towards the next generation. *Mech Dev* **105**: 5-18.

Stavropoulos P, Blobel G, Hoelz A. 2006. Crystal structure and mechanism of human lysine-specific demethylase-1. *Nat Struct Mol Biol* **13**: 626-632.

Strahl BD, Allis CD. 2000. The language of covalent histone modifications. *Nature* **403**: 41-45.

Suikki HE, Kujala PM, Tammela TL, van Weerden WM, Vessella RL, Visakorpi T. 2010. Genetic alterations and changes in expression of histone demethylases in prostate cancer. *Prostate* **70**: 889-898.

Talbert PB, Henikoff S. 2006. Spreading of silent chromatin: inaction at a distance. *Nat Rev Genet* **7**: 793-803.

Tamkun JW, Deuring R, Scott MP, Kissinger M, Pattatucci AM, Kaufman TC, Kennison JA. 1992. brahma: a regulator of Drosophila homeotic genes structurally related to the yeast transcriptional activator SNF2/SWI2. *Cell* **68**: 561-572.

Tian X, Fang J. 2007. Current perspectives on histone demethylases. *Acta biochimica et biophysica Sinica* **39**: 81-88.

Tong JK, Hassig CA, Schnitzler GR, Kingston RE, Schreiber SL. 1998. Chromatin deacetylation by an ATP-dependent nucleosome remodelling complex. *Nature* **395**: 917-921.

Tsai MC, Manor O, Wan Y, Mosammaparast N, Wang JK, Lan F, Shi Y, Segal E, Chang HY. 2010. Long noncoding RNA as modular scaffold of histone modification complexes. *Science* **329**: 689-693.

Tsai WW, Nguyen TT, Shi Y, Barton MC. 2008. p53-targeted LSD1 functions in repression of chromatin structure and transcription in vivo. *Mol Cell Biol* **28**: 5139-5146.

Tsukiyama T, Wu C. 1995. Purification and properties of an ATP-dependent nucleosome remodeling factor. *Cell* **83**: 1011-1020.

Tulina N, Matunis E. 2001. Control of stem cell self-renewal in Drosophila spermatogenesis by JAK-STAT signaling. *Science* **294**: 2546-2549.

Wallrath LL, Elgin SC. 1995. Position effect variegation in Drosophila is associated with an altered chromatin structure. *Genes Dev* **9**: 1263-1277.

Wang J, Hevi S, Kurash JK, Lei H, Gay F, Bajko J, Su H, Sun W, Chang H, Xu G et al. 2009a. The lysine demethylase LSD1 (KDM1) is required for maintenance of global DNA methylation. *Nat Genet* **41**: 125-129.

Wang J, Scully K, Zhu X, Cai L, Zhang J, Prefontaine GG, Krones A, Ohgi KA, Zhu P, Garcia-Bassets I et al. 2007. Opposing LSD1 complexes function in developmental gene activation and repression programmes. *Nature* **446**: 882-887.

Wang L, Li Z, Cai Y. 2008a. The JAK/STAT pathway positively regulates DPP signaling in the Drosophila germline stem cell niche. *J Cell Biol* **180**: 721-728.

Wang X, Harris RE, Bayston LJ, Ashe HL. 2008b. Type IV collagens regulate BMP signalling in Drosophila. *Nature* **455**: 72-77.

Wang Y, Zhang H, Chen Y, Sun Y, Yang F, Yu W, Liang J, Sun L, Yang X, Shi L et al. 2009b. LSD1 is a subunit of the NuRD complex and targets the metastasis programs in breast cancer. *Cell* **138**: 660-672.

Ward EJ, Shcherbata HR, Reynolds SH, Fischer KA, Hatfield SD, Ruohola-Baker H. 2006a. Stem cells signal to the niche through the Notch pathway in the Drosophila ovary. *Curr Biol* **16**: 2352-2358.

Ward EJ, Zhou X, Riddiford LM, Berg CA, Ruohola-Baker H. 2006b. Border of Notch activity establishes a boundary between the two dorsal appendage tube cell types. *Dev Biol* **297**: 461-470.

Wharton KA, Thomsen GH, Gelbart WM. 1991. Drosophila 60A gene, another transforming growth factor beta family member, is closely related to human bone morphogenetic proteins. *Proc Natl Acad Sci U S A* **88**: 9214-9218.

Whyte WA, Bilodeau S, Orlando DA, Hoke HA, Frampton GM, Foster CT, Cowley SM, Young RA. 2012. Enhancer decommissioning by LSD1 during embryonic stem cell differentiation. *Nature* **482**: 221-225.

Wissmann M, Yin N, Muller JM, Greschik H, Fodor BD, Jenuwein T, Vogler C, Schneider R, Gunther T, Buettner R et al. 2007. Cooperative demethylation by JMJD2C and LSD1 promotes androgen receptor-dependent gene expression. *Nat Cell Biol* **9**: 347-353.

Wurst W, Auerbach AB, Joyner AL. 1994. Multiple developmental defects in Engrailed-1 mutant mice: an early mid-hindbrain deletion and patterning defects in forelimbs and sternum. *Development* **120**: 2065-2075.

Xia L, Jia S, Huang S, Wang H, Zhu Y, Mu Y, Kan L, Zheng W, Wu D, Li X et al. 2010. The Fused/Smurf complex controls the fate of Drosophila germline stem cells by generating a gradient BMP response. *Cell* **143**: 978-990.

Xie T, Spradling AC. 1998. decapentaplegic is essential for the maintenance and division of germline stem cells in the Drosophila ovary. *Cell* **94**: 251-260.

-. 2000. A niche maintaining germ line stem cells in the Drosophila ovary. *Science* **290**: 328-330.

Yin H, Lin H. 2007. An epigenetic activation role of Piwi and a Piwi-associated piRNA in Drosophila melanogaster. *Nature* **450**: 304-308.

You A, Tong JK, Grozinger CM, Schreiber SL. 2001. CoREST is an integral component of the CoREST- human histone deacetylase complex. *Proc Natl Acad Sci U S A* **98**: 1454-1458.

Yu X, Hoppler S, Eresh S, Bienz M. 1996. decapentaplegic, a target gene of the wingless signalling pathway in the Drosophila midgut. *Development* **122**: 849-858.

Zecca M, Basler K, Struhl G. 1995. Sequential organizing activities of engrailed, hedgehog and decapentaplegic in the Drosophila wing. *Development* **121**: 2265-2278.

Zhang J, Niu C, Ye L, Huang H, He X, Tong WG, Ross J, Haug J, Johnson T, Feng JQ et al. 2003. Identification of the haematopoietic stem cell niche and control of the niche size. *Nature* **425**: 836-841.

Zhang Y, Liu T, Meyer CA, Eeckhoute J, Johnson DS, Bernstein BE, Nusbaum C, Myers RM, Brown M, Li W et al. 2008. Model-based analysis of ChIP-Seq (MACS). *Genome biology* **9**: R137.

Zhu CH, Xie T. 2003. Clonal expansion of ovarian germline stem cells during niche formation in Drosophila. *Development* **130**: 2579-2588.